Erding formula and bioactive markers in hyperuricemia: towards rational scientific approaches for the modernization of Traditional Chinese Medicine

by

Jieyu Zuo

A thesis submitted in partial fulfillment of the requirements for the degree of

Doctor of Philosophy

In

Pharmaceutical Sciences

Faculty of Pharmacy and Pharmaceutical Sciences
University of Alberta

Abstract

Introduction: Traditional Chinese Medicine (TCM) represents one of the first holistic approaches in the world to treat and prevent disease. Herbal medicine is one of the major therapeutic remedy in TCM. It often involves multi-herb therapies instead of single herb preparations. Parallel to western medicine, hundreds of herbal formulas have been made available as finished products. Currently, the use of herbal products is popular as treatment option or to complement western medicine. Indications of the herbal formulas were established by TCM terms such as "heat-clearing and/or detoxifying" which lack modern pharmacological meanings. It is difficult for people without relevant background to understand such terms and their implications for treatments. Furthermore, due to the quality control issues of herbal medicines which contain multiple constituents, consumers may be confronted with the risk of using unstandardized products. Hence, in this thesis, the modernization of TCM is discussed through employing scientific pharmaceutical approaches to a traditional formula, called Erding formula (EF). The aim was to investigate if a new indication, hyperuricemia, can be assigned to a heat-clearing and detoxifying formula. Our hypothesis was: Can Erding formula be used for hyperuricemia treatment and is esculetin a bioactive marker for this new indication?

Methods: A hypoxanthine and potassium oxonate-induced hyperuricemic mouse model, a xylene-induced inflammatory mouse model, and an acetic acid-induced pain model were used to investigate EF and its constituent herbs. The quantity of esculetin was measured by

high-performance liquid chromatography. The therapeutic effect of esculetin was assessed using potassium oxonate induced hyperuricemic mouse model, and esculetin and its metabolites were characterized in serum via ultra-performance liquid chromatography-quadrupole time-of-flight mass spectrometry. To develop a modern dosage form, a laboratory-scale wet bead milling approach was employed to prepare esculetin nanocrystals. The formulation was further optimized by design of experiment, and an optimized formulation was then characterized for its saturation solubility and short-term stability.

Results: The study showed that EF and Viola yedoensis Makino (Viola) lowered uric acid (UA) levels, while EF and all four individual herbs had anti-inflammatory and analgesic activities. These findings revealed that EF was able to treat hyperuricemia and suggested that Viola was the main herb in EF on reducing UA levels. The study showed that esculetin significantly reduced UA levels and six metabolites of esculetin were identified in serum. This confirms that esculetin was absorbed and is a suitable bioactive and quality control marker for EF in hyperuricemia treatment. An esculetin-Povacoat nanocrystal formulation with a 200 nm particle size was successfully prepared. The formulation presented up to a 1.5-fold increase in saturation solubility compared to the bulk esculetin and it was stable for 180 days.

Conclusion: The studies proved that Erding formula can be used for hyperuricemia treatment with esculetin as bioactive quality control marker. As well, a new nano-sized

formulation of the bioactive marker, esculetin, was created. This presented the possibility to develop an innovative nanotechnological product of the active substances derived from herbal medicine. The findings facilitated a better understanding of TCM terms and concept through mechanistic scientific experiments. This study revealed a potential pathway and an idea to modernize TCM without setting aside its unique concepts. This might increase the global acceptance of TCM products. Furthermore, the TCM concept might be useful in the development of multi-component drug products.

Resumo

Medicina Tradicional Chinesa (MTC) representa uma das primeiras abordagens holísticas em âmbito global para tratar e prevenir doenças. A fitoterapia consiste na principal terapia na MTC. Frequentemente, envolve terapias com múltiplas ervas em vez de preparações individuais. Paralelamente à medicina ocidental, centenas de fórmulas herbais foram disponibilizadas como produtos acabados. Atualmente, o uso de produtos fitoterápicos é popular como opção de tratamento ou para complementar a medicina ocidental. As indicações das fórmulas fitoterápicas foram estabelecidas pelos termos da MTC, tais como "limpeza pelo calor e / ou desintoxicante", que não têm significados farmacológicos modernos. É difícil para a população em geral e mesmo para profissionais sem histórico relevante na área entender tais termos e suas implicações para os tratamentos. Além disso, devido às questões de controle de qualidade dos medicamentos fitoterápicos que contêm múltiplos constituintes, os pacientes podem ser confrontados com o risco de usar produtos não padronizados. Assim, nessa tese, a modernização da MTC é discutida por meio da utilização de abordagens farmacêuticas científicas para uma fórmula tradicional, denominada fórmula de Erding (FE). O objetivo foi o de investigar se uma nova indicação, a hiperuricemia, pode ser atribuída a uma fórmula desintoxicante e de compensação de calor. Nossa hipótese foi: a fórmula de Erding pode ser usada para tratamento de hiperuricemia e a esculetina é um marcador bioativo para essa nova indicação? Foi empregado modelo de camundongo

hiperuricêmico induzido por hipoxantina e oxonato de potássio, outro modelo de camundongo inflamatório induzido por xileno e, adicionalmente, modelo de dor induzida por ácido acético. Esses modelos foram usados para investigar a FE e suas ervas constituintes. A quantidade de esculetina foi determinada por cromatografia líquida de alta eficiência. O efeito terapêutico da esculetina foi avaliado utilizando modelo de camundongo hiperuricêmico induzido por oxonato de potássio, e a esculetina e seus metabólitos foram caracterizados no soro por cromatografia líquida de alto desempenho - espectrometria de massa. Para desenvolver forma farmacêutica moderna, uma abordagem de moagem em escala úmida reduzida foi empregada tendo em vista a preparação de nanocristais de esculetina. A formulação foi ainda otimizada empregado planejamento experimental. Essa fórmula foi caracterizada quanto à sua solubilidade de saturação e estabilidade a curto prazo. O estudo mostrou que a FE e a Viola *yedoensis* Makino (Viola) reduziram os níveis de ácido úrico (AU), enquanto a FE e as quatro plantas individuais apresentaram atividades antiinflamatória e analgésica. Esses resultados revelaram que a FE foi capaz de tratar a hiperuricemia e sugeriu que a viola foi a principal erva da FE na redução dos níveis de AU. O estudo mostrou também que a esculetina reduziu significativamente os níveis de AU e os seis metabólitos da esculetina foram identificados no soro. Tal resultado confirma que a esculetina foi absorvida e pode ser usada como marcador de controle bioativo e de qualidade para FE, no tratamento da hiperuricemia. A formulação de nanocristais de esculetin-povacoat® apresentou tamanho

de partícula de 200 nm. A formulação apresentou aumento de 1,5 vezes na solubilidade de saturação em comparação com a esculetina em escala micrométrica e manteve-se estável durante 180 dias. Os estudos comprovaram que a fórmula de Erding pode ser utilizada no tratamento da hiperuricemia empregando a esculetina como marcador bioativo de controle de qualidade. Além disso, foi desenvolvida formulação inovadora, em escala nanométrica, do marcador bioativo, a esculetina. Esse resultado permitiu desenvolver produto com base nanotecnológica das substâncias ativas derivadas do fitoterápico, assim comol permitiram melhor compreensão dos termos e dos conceitos da MTC por meio de experimentos científicos mecanicistas. Esse estudo revelou potencial para a modernização da MTC sem excluir seus conceitos únicos. Isso pode aumentar a aceitação global dos produtos MTC. Além disso, o conceito de MTC pode ser útil no desenvolvimento de medicamentos de múltiplos componentes.

Preface

This thesis is an original work completed by Jieyu Zuo under the supervision of Prof. Dr. Raimar Löbenberg at the University of Alberta and Prof. Dr. Nádia Bou-Chacra at the University of São Paulo.

Chapter 2 "Traditional Chinese Medicine for Managing Inflammatory Pain of Arthritis with Herbal Medicines" is a review article has been published as: Jieyu Zuo, Qin Zheng, Hui Jian, Tasha Porttin, Chanelle Willson, Fiona Misquita, Jordan Capicio, Raimar Löbenberg. **Current Traditional Medicine**. 2016;2(2):80-93.

Chapter 3 "Erding Formula in hyperuricemia treatment: unfolding traditional Chinese herbal compatibility using modern pharmaceutical approaches" has been published as: Jieyu Zuo, Hongming He, Zhengyun Zuo, Nadia Araci Bou Chacra, Raimar Löbenberg. **Journal of Pharmacy and Pharmacology.** 2018; 70: 124-132.

Chapter 4 "Esculetin as bioactive marker: towards a rational scientific approach for the treatment of hyperuricemia using Traditional Chinese Medicine" has been accepted by Brazilian Journal of Pharmaceutcal Sciences, as Jieyu Zuo, Wugang Zhang, Hui Jian, Nadia Araci Bou Chacra, Raimar Löbenberg.

Chapter 5 "Development of esculetin nanocrystals using wet media milling, DOE and subsequent solidification approaches." The research of this study was performed in University of Sao Paulo, Brazil under the supervision of Dr. Nádia Bou-Chacra. Jieyu Zuo was responsible for data collection, analysis and writing. The analysis of design of

experiment was performed in the help with Dr. Nádia Bou-Chacra. The experiments and data analysis of thermo analysis and X-ray powder diffraction (XRPD) of esculetin nanocrystals was performed in help with Dr. Gabriel Lima Barros de Araujo. A patent (BR 10 2018 069511 8) was approved in Brazil based on the results of this study.

The articles in **Appendix** is the work completed by Jieyu Zuo under the supervision of Prof. Dr. Raimar Löbenberg at the University of Alberta during the time before transferring from a master student to a PhD student.

Appendix 1 "Evaluation of the DDSolver Software Applications," is published in **BioMed Research International**, vol. 2014, Article ID 204925, 9 pages, 2014, by Jieyu Zuo, Yuan Gao, Nadia Bou-Chacra, and Raimar Löbenberg.

Appendix 2 "Challenges and Opportunities to Use Biowaivers to Compare Generics in China" is published in **AAPS PharmSciTech**. 2014;15(5):1070-5. Jieyu Zuo, Yuan Gao, Nadia Bou Chacra, Raimar Löbenberg.

Appendix 3

"In Vitro Release Kinetics of Antituberculosis Drugs from Nanoparticles Assessed Using a Modified Dissolution Apparatus" is a collaborated project with Dr. Yuan Gao under the supervision of Prof. Dr. Raimar Löbenberg. Jieyu Zuo is a co-first author who contribute in performing dissolution test and data analysis. The article is published in **BioMed Research International**, vol. 2013, Article ID 136590, 9 pages, 2013 by Yuan Gao, Jieyu

Zuo, Nadia Bou-Chacra, Terezinha de Jesus Andreoli Pinto, Sophie-Dorothee Clas, Roderick B. Walker, and Raimar Löbenberg.

Appendix 4 "Investigation of the Disintegration Behavior of Dietary Supplements in Different Beverages" is published in **Dissolution Technologies.** 2013; 20(4):6-9. Jieyu Zuo, Yuan Gao, May Almukainzi, Raimar Löbenberg.

Acknowledgements

I would like to express my sincere appreciation to my supervisor, Dr. Raimar Löbenberg and Dr. Nádia Bou-Chacra for their excellent professional supervision, highly encouragement and invaluable guidance throughout the research project. Working with them is an amazing experience.

Sincere thanks are extended to my supervisory committee members, Dr. Afsaneh Lavasanifar and Dr. Sharon Marsh for their kind suggestions and feedbacks.

I wish to thank for International Scientific Collaboration Grant of Jiangxi Province, China for the financial support for research.

I would like to thank my lab colleagues in University of Alberta, Canada, Jiangxi University of Traditional Chinese Medicine, China and University of Sao Paulo, Brazil for their help and advices. I would like to express my gratitude to Dr. Yuan Gao, Dr. Vijay Somayaji, Dr. Yulin Feng, Dr. Wugang Zhang, Dr. Marco Antonio Stephano and Dr. Gabriel Lima Barros de Araujo, who taught me several techniques and provided me valuable advices.

Words cannot ever express my thanks to my parents for their endless love, patience, support and encouragement throughout my whole life.

Last but not least, I wish to thank all the administrative and support staff in the Faulty of Pharmacy and Pharmaceutical Sciences for their kindness throughout the years. Special thanks go to Mrs. Joyce Johnson and Ms. Diseray Schamehorn.

Table of Content

List of Tables

List of Figures

List of abbreviation

adj-R^2	Adjusted coefficient of determination
AIC	Akaike information criterion
ANOVA	Analysis of variances
API	Active pharmaceutical ingredient
AS	Radix Angelicae Sinensis
BCS	Biopharmaceutical classification system
B-L model	Baker-Lonsdale model
CFDA	China Food and Drug Administration
ChP	Chinese Pharmacopeia
CMC-Na	Sodium carboxymethyl cellulose
COX	Cyclooxygenase
CPP	Comparator pharmaceutical product
CT	Cycle threshold
CV	Coefficient variation
ddH2O	Double distilled water
DHJST	Du Huo Ji Sheng Tang
DLS	Dynamic light scattering
DoE	Design of experiments
DSC	Differential scanning calorimetry

EF	Erding formula
EMA	European Medicines Agency
Exp.	Expiry
F0	Initial burst effect
f_2	Similarity factor
FD	Freeze-dried
FDA	Food and Drug Administration
H-C model	Hixson-Crowell model
HPLC	High performance liquid chromatography
IFN	Interferon
IL	Interleukin
iNOS	Inducible nitric oxide
IR	Immediate release
Isatidis	Isatis indigotica Fort.
K-P model	Korsmeyer-Peppas model
LD	Laser diffraction
Lobelia	Lobelia chinensis Lour.
LPS	Lipopolysaccharide
MAPKs	Mitogen-activated protein kinases

MMPs	Matrix metalloproteinases
MSC	Model selection criterion
MX	Moxifloxacin hydrochloride
MX-Gel-NPs	Moxifloxacin loaded gelatin nanoparticles
MX-PBCA-NPs	Moxifloxacin loaded polybutyl cyanoacrylate nanoparticles
NHP	Natural Health Products
NO	Nitric oxide
NPs	Nanoparticles
NSAID	Non-steroidal anti-inflammatory drugs
OA	Osteoarthritis
PA	Radix Paeonia Alba
PBCA	Polybutyl cyanoacrylate
PBS	Phosphate buffer solution
PD	Pharmacodynamic
PdI	Polydispersity index
Pepsi	Pepsi cola
PGE2	Prostaglandin E2
PK	Pharmacokinetic
Plantacare® 2000	Alkyl polyglucoside C8-C10

PNS	Panax Notoginseng saponins
Povacoat™	A polyvinyl alcohol copolymer
pred-R^2	Predicted coefficient of determination
QC	Quality control
Q-marker	Quality marker
R^2	Coefficient of determination
R2adjusted	Adjusted coefficient of determination
RA	Rheumatoid
RC	Rhizoma Chuanxiong
RIF	Rifampicin
RIF-Gel-NPs	Rifampicin loaded gelatin nanoparticles
RIF-PBCA-NPs	Rifampicin loaded polybutyl cyanoacrylate nanoparticles
RPM	Revolutions per minute
RSD	Relative standard deviation
RSM	Response surface methodology
RT	Real-time
SD	Standard deviation
SD	Spray-dried
SDS	Sodium dodecyl sulfate

SEM	Scanning electron microscopy
SGF	Simulated gastric fluid
SIF	Simulated intestinal fluid
Soluplus®	Polyvinyl caprolactam–polyvinyl acetate–polyethylene glycol graft copolymer
Taraxacum	Taraxacum mongolicum Hand.- Mazz.
TCHM	Traditional Chinese herbal medicines
TCM	Traditional Chinese Medicine
TEM	Transmission electron microscopy
TG	Thermogravimetric
TGP	Total glucosides of peony
Tlag	Lag time
TNF-α	Tumor necrosis factor-alpha
TPGS	Vitamin E polyethylene glycol succinate
TwHF	Tripterygium wilfordii Hook. f.
UA	Uric acid
UHPLC/Q-TOF-MS/MS	Ultra-high performance liquid chromatography-quadrupole time-of-flight mass Spectrometry
USP	United State Pharmacopeia

Viola	Viola yedoensis Makino
WHO	World Health Organization
XOIs	Xanthine oxidase inhibitors
XRPD	X-ray powder diffraction

Chapter 1 General Introduction

1.1 Traditional Chinese Medicine (TCM)

Ancient Chinese people believed the universe and all natural phenomena could be classified into two opposite, complementary, interdependent aspects, Yin and Yang (阴阳) (Figure 1.1). They believed that the universe was made up of five basic elements (五行) (wood, fire, earth, metal, and water, Figure 1.1), and the universe was constantly changing to maintain and restore harmony between these elements. TCM is derived from these philosophies and they have been applied to understand, prevent, and cure disease (1, 2).

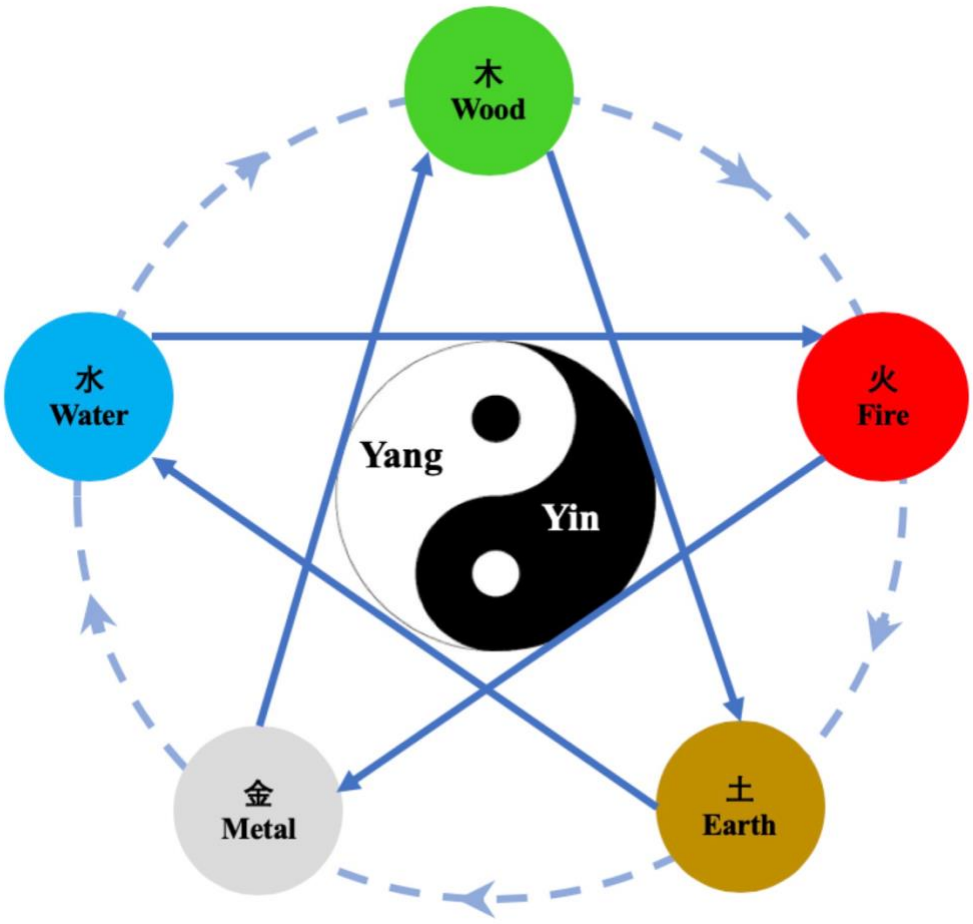

Figure 1.1 The schematic diagram of the laws of promotion and restriction among five

elements. Dotted arrow: promotion (one of five elements promotes and helps another one), solid arrow: restriction (one of five element restricts or restrains another one), further details can be found in reference (2).

As one of the mainstream medical practices in the Chinese healthcare system, TCM was developed and used to treat and prevent diseases (3, 4). The history of TCM dates back more than 2,500 years to the Warring States period (475-221 B.C.) when the first written work on the subject, Huang Di Nei Jing (黄帝内经, Yellow Emperor's Inner Canon), was compiled (5). Before English missionaries entered the country in the 19th century, TCM was the only medicinal method used in China. (6).

As a holistic and complex medical approach, TCM reflects traditional Chinese culture and philosophy; TCM uses dialectical thought to address the human body and focuses on bringing people back into balance to restore their health (7). The fundamentals of TCM, namely, the Qi system, Yin-Yang balance and five element theories, guide the therapeutic principles and goals of TCM and cause TCM to focus mainly on the integrity of the human body and the relationship between the body and the environment (8). TCM regards Qi as the root of life, and its motion and change reflect the activity of the body. In TCM, optimal health is achieved when the systems are balanced, since the human body is regarded as a holistic and endlessly changeable progression (9). Diseases occur when the harmony is disrupted by the invasion of pathogens and is cured when the dynamic balance is re-established (3).

To restore harmony, the therapeutic goals and principles of TCM concentrate on the overall state of the patient and patterns that reflect multi-system changes (7). TCM practitioners diagnose diseases based on the patient symptoms via four examinations: wang (望), inspection of skin complexion, physique and tongue condition; wen (闻), listening to the patient's voice and sniffs and noting body odors that can indicate illnesses; wen (问), asking how the patient feels; and qie (切), palpation to feel the patient's pulse and assess overall health. After these examinations, the practitioners prescribe one or several therapeutic remedies to cure the diagnosed disease (6).

TCM comprises a series of therapeutic remedies including acupuncture, Chinese Material Medica (medical material), moxibustion (the burning of herbs on acupuncture points), tui na (therapeutic massage), tai chi and qi gong (movement and breathing exercises), dietary therapy, cupping (local suction on the skin using a heated cup) and gua sha (scraping the skin to produce light bruising) (6).

Among the therapeutic remedies discussed above, Chinese Material Medica is the most related to modern pharmaceuticals. Material medica has been used in China for more than 3,000 years, as relevant documents were written starting at least as far back as 1,100 BC (10). Chinese Material Medica consists of herbs, minerals and animal parts, and herbs make up the majority (90%) of the more than 10,000 known medicinal species (11). In this thesis, the studies focused on the herbal medicines.

1.2 Herbal medicine

Herbal medicines (phytomedicine) are used worldwide as home remedies, dietary supplements, over-the-counter drug products and pharmaceutical products. They constitute a substantial proportion of the global market of medicines. In recent years, the use of herbal medicines has increased markedly, and as many as 80% of people throughout the world have been exposed to herbal medicines (12). As well, the use of herbal medicine is well established in European countries (13). However, in those countries, herbal medicines are typically standardized extracts of single herbs for particular conditions (14).

1.3 Traditional Chinese Herbal medicine

More than 8,000 medicinal herbs are known in TCM, and 500 of those are commonly used. TCM uses four properties and five tastes to describe and classify the characteristics of medicinal herbs. Raw materials of herbs must be processed using different methods to enhance their therapeutic effects, eliminate toxicity, modify their efficacy, change their properties and remove any impurities before they can be used. Processing methods are chosen according to the features of plants and the requirements of the therapy, prescription and preparations (15).

With thousands of years of accumulated therapeutic experience, TCM practitioners gradually realized that many diseases are regulated by multiple pathogenesis. Single herbs

are not sufficient to address the complex symptoms of severe diseases. To achieve better treatment results with fewer side effects and/or to broaden the scope of treatments, traditional Chinese herbal medicines (TCHMs) often involve herbal formulas (fufang, 复方) with a combination of up to 50 herbs (thousands of compounds). During the past centuries, more than 100,000 multi-herb formulas have been described. (16-21)

The selection of the herbal formula composition follows the rules of "compatibility" (peiwu, 配伍). Rather than a random list of herbs in formulations, the compatibility in the formulation is guided by the properties of the herbs and treatment required for the diseases. The principle that governs multi-herb formulas is based on the basic structure of the formula of "Jun-Chen-Zuo-Shi". The herbs in multi-herb formulas are classified and described by these four categories according to their functions in specific formulas. "Jun" (emperor) is/are the herb(s) that perform major pharmacological functions and is/are the essential herb(s) in the formula. "Chen" (minister) herb(s) aid the action of emperor herbs and/or have additive effects. In general, "Zuo" (assistant) herb(s) present detoxifying effects for both emperor and minister herbs or are used to treat accompanying symptoms. "Shi" (guide) herb(s) mainly work to help other herbs reach their targets (22-24).

TCHMs are traditionally administered orally or percutaneously. The sublingual. inhalation, mucosal absorption or rectal administrations are alternative administration routes. Recently, because of the influence of western medicine, more administration routes have been

adopted, such as subcutaneous, intramuscular, intravenous and acupuncture point injection (15, 25).

TCHMs are typically taken in forms such as decoctions, pills, powders, ointments, medicinal wines, dan (a preparation made of precious or marked effects drugs or different crystals made by firming certain types of minerals in high temperature), medicinal teas, distillates, troches, medicinal sticks, medicinal threads and suppositories (15, 25).

1.4 TCM Modernization

TCM and herbal medicines have attracted the attention of researchers and have become popular throughout the world. However, it is still difficult for people without relevant background to accept TCM as a scientific based medicine, because of its unique theories, diagnose, and treatment system. To address TCM scientifically, efforts to modernize TCM were started in the 1950s (26). Since then, the Chinese government has begun to establish its national network of TCM universities, hospitals, and research institutions. In the early years (1950s-1980), researchers mainly attempted to isolate active compounds from TCM remedies to treat diseases. Numerous promising compounds were discovered, such as artemisinin from *Artemisia annua* L. for malaria and camptothecin from Camptotheca acuminate Decne for cancer. (27-31) In the following decades (1980-present), the regulation, standardization, quality control and globalization of Chinese herbal medicine represent the main efforts and achievements. Instead of isolating individual active

compounds to treat diseases, researchers became interested in the synergistic effects among the active compounds isolated from herbs and/or formulas, such as realgar-indigo to treat promyelocytic leukemia (32-34). In order to the globalize TCM and elucidate complex components of herbal medicines, studies of commonly used herbs and formulas mainly focused on clarifying the chemical composition, structures, and functions. Modern analytical separation methods have been developed to identify herbs and characterize their components (35-37).

However, TCM modernization not only involves combining TCM with modern technologies, modern concepts, and modern scientific approaches but also involves advancing its traditional advantages and characters (38). It is important to use modern scientific technologies to test if TCM works as intended by its principles.

1.5 Tested herbal formula

The well-established formula of Erding granules is listed in the Chinese Pharmacopeia (ChP) and is commercially available in Chinese markets. This formula is made of four individual herbs (*Viola yedoensis* Makino, *Taraxacum mongolicum* Hand.-Mazz., *Lobelia chinensis* Lour., and the root of *Isatis indigotica* Fort.) in equal quantities (Figure 1.2) (39). Due to its heat-clearing and detoxifying properties, this formula was originally used to treat furuncle, carbuncle, sore throat, and wind burn-related eye inflammation.

Figure 1.2 The consist of the herbal formula, Erding granules.

Recently, several TCM practitioners have used this product to treat the patients with gout. Gout is a painful inflammatory form of arthritis which is caused by hyperuricemia and deposition of monosodium urate crystals into joints (40). Therapeutically, the actions of heat clearing and detoxifying can be considered as antipyretic and anti-inflammatory (41, 42).

Therefore, at the beginning of the study, we focused on how herbal medicines are used in managing inflammatory pain of arthritis, which is presented in Chapter 2.

However, after further investigating the formula under the TCM framework, we recognized that TCM considers the root cause of the gout, hyperuricemia, as the major treatment focus. The inflammation and pain of gout are considered as accompany symptoms in TCM. TCM practitioners will therefore treat and prevent high uric acid (UA) levels together with controlling pain and inflammation. Hence, in Chapter 3, we investigated the urate lowering, anti-inflammatory and analgesic activity of Erding formula (EF) using mouse models.

1.6 Hyperuricemia in TCM

As far as TCM is concerned, hyperuricemia is a modern disease because the UA levels in blood can be only determined by analytical techniques. The ancient written records of TCM relevant to hyperuricemia are more about gout, which is a type of arthromyodynia (bi syndrome, 痹症). TCM practitioners believe that hyperuricemia is caused by a "turbid toxin" (浊毒). The pathogenesis of simple hyperuricemia is deficiency of Qi in the kidney and the dysfunction of spleen and kidney. Qi stagnation, blood stasis, and phlegm obstruction imply that turbid phlegm and blood stasis are at the root of the problem. Finally, the stasis becomes toxic and obstructs the channel, leading to the disease. If the toxin stays in the kidney, it can damage the vital essence of the kidney and become dysfunction. Blocking of the channel by toxin can lead to acute swelling and joint pain. (43, 44)

1.7 Scientific view of hyperuricemia

UA is the final oxidation product of human and hominoid purine metabolism, during which xanthine oxidase catalyzes the hypoxanthine and/or xanthine into UA, as shown in Figure 1.3. In other mammals, the enzyme uricase can further oxidize UA to a more soluble compound, allantoin, which can be excreted in urine (Figure 1.3). Mammals with uricase do not develop hyperuricemia (45). Hyperuricemia is an abnormally high level of UA in the blood caused by either overgeneration of UA from hepatic metabolism, renal

underexcretion, or a combination of the two. Hyperuricemia observed in most patients (80-90%) is due to renal underexcretion. A serum UA level of 6.8 mg/dL or 7.0 mg/dL is considered the threshold for hyperuricemia (46-49). Hyperuricemia is a result of age, gender, race, genetic factors, environmental factors and dietary habits (45, 50-51). The global prevalence of hyperuricemia has rapidly increased from 8.5% (2005) to 21.0% (2017) in the western world and13.3% in mainland China in 2014 (52, 53). Long-term hyperuricemia has been identified as a risk factor for gout, nephrolithiasis and chronic nephropathy and is known to be associated with metabolic syndromes such as hypertension, obesity, diabetes and cardiovascular diseases (54, 55). Long-term hyperuricemia is also predicted to become the second most common metabolic disease after diabetes (56).

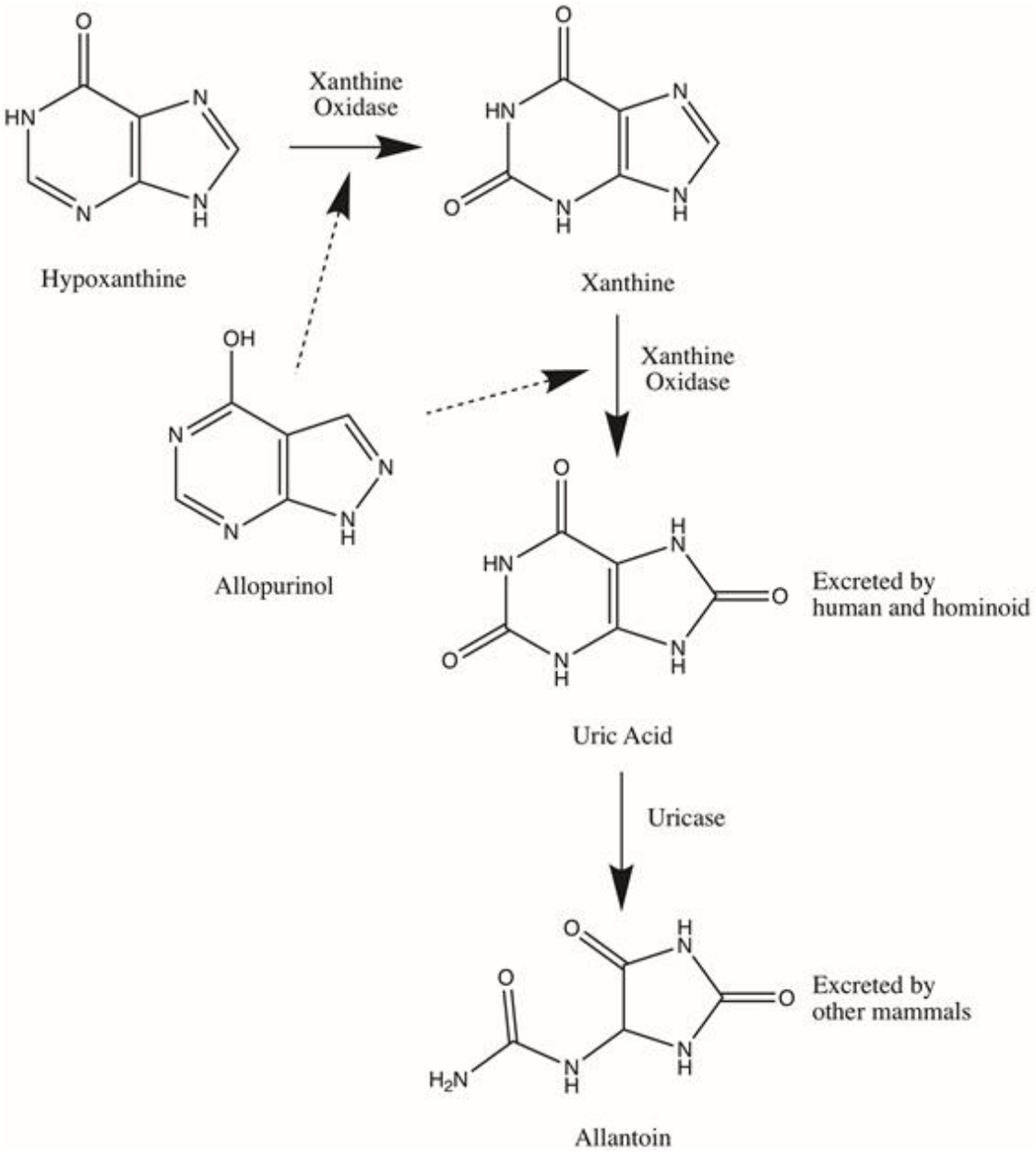

Figure 1.3 The production and excretion of uric acid in human and other mammals. Allopurinol inhibits xanthine oxidase activity to block the conversion of hypoxanthine to xanthine and xanthine to uric acid.

1.8 Hyperuricemia treatment

Currently, the therapies for managing hyperuricemia are mainly aimed at modulating the enzymes involved in the metabolism and excretion of UA. Due to the pathological condition, treatments for hyperuricemia can be divided into two main classes: xanthine oxidase inhibitors (XOIs) and uricosurics (57, 58). According to the British, American and European guidelines for the management of gout, XOIs, which reduce UA production through competitive xanthine oxidase inhibition in the liver, are the most commonly used type of UA treatment (40, 58-59). Due to its efficacy, availability, and low cost, allopurinol, a structural isomer of hypoxanthine (Figure 1.2), is the most commonly prescribed XOI. However, allopurinol has side effects including gastrointestinal intolerance, rashes, and allopurinol hypersensitivity syndrome (60). The guidelines advised to be careful when prescribing allopurinol to Asians and Blacks because their high risk of allopurinol-related skin reactions (40, 61). Uricosurics (probenecid and benzbromarone) are the other major class of compounds used to lower UA levels and function via the blocking of renal tubular reabsorption to enhance urinary UA excretion through the kidneys (Figure 1.4) (62). This type of agent is used for patients who are intolerant to allopurinol or cannot reach the target serum UA level in monotherapy with XOIs. The use of probenecid increases the risk of the development of kidney stones and urate nephropathy. Although benzbromarone is more potent than probenecid and equally as effective as allopurinol, the approval of benzbromarone has been withdrawn in several countries due to its liver toxicity (63, 64). Another group of UA-lowering agents available other than XOIs and uricosurics are

uricases, comprised of a group of enzymes lost during human evolution. Uricases are enzymes that break down UA into more water-soluble allantoin (Figure 1.3). Pegloticase is a porcine recombinant polyethylene glycol-conjugated uricase that was approved by the Food and Drug Administration (FDA) in 2010 for patients for whom conventional therapy was ineffective (40, 57, 65). The use of pegloticase is limited because of the side effects that accompany with rapid UA reduction including higher frequency of cardiovascular events, formation of antipegloticase antibodies, and acute gout flares (66-68).

In general, modern mono-chemical drug products are successful in curing diseases in the short term due to the fast and accurate targeting actions of these products. When long-term and indefinite therapies are needed for chronic conditions, those treatments may cause serious side effects. If the disease is complex, each drug component may be able to solve only one specific aspect of the disease. Therefore, researchers are gaining interest in identifying potential herbal medicines that can act as alternative agents to improve the efficacy and reduce the side effects of drugs.

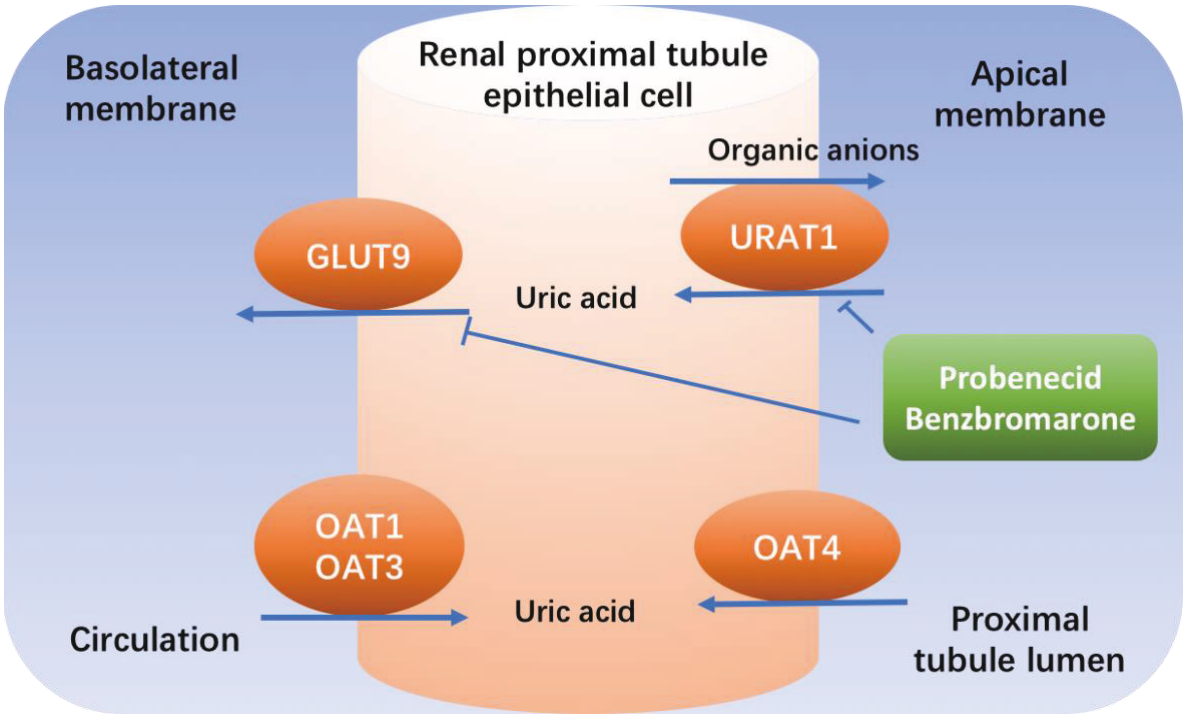

Figure 1.4 Simplified schema of the mechanism of uricosuric drugs on renal anion transporters involved in urate reabsorption and excretion in the proximal tubules of the kidney.

1.9 Quality control of herbal medicine

Controlling the consistency and quality of the material is a key issue for TCM modernization and the worldwide growth of the herbal medicine industry due to the multiple constituents. Until now, a universal quality control system of TCM has not been established. The ChP is the main reflection of TCM quality standards. However, in the ChP, the integral quality standards for the majority of crude herbs are still lacking, and some of them miss specific markers (69). According to Liu et al, the quality marker (Q-marker) of

TCM should be defined by following features: 1) they are the natural chemical compounds in herbs, decoction slices, extracts, and finished formulations, or they are resultant during the processing; 2) they could be determined and characterized through either qualitative or quantitative approaches; 3) they are chemical substances, which have definite structure and functional properties; 4) For the herbal formula, Q-marker could be the representative substances of the emperor herb or selected following the compatibility theory (69, 70). The traditional and simple identification and quantitative analysis techniques for chemical markers in herbal medicines, such as thin layer chromatography is not sufficient to determine the quality of the product (71). In this case, comprehensive analytical methods are recommended to ensure the quality and proper concentration of the herbal medicines. These methods include fingerprint hyphenated techniques, such as HPLC-MS and HPLC-diode array detection, UPLC-ESI-MS/MS (72-74). However, the ideal quality control markers should be characteristic constituents that not only can be used for quantification but are also responsible for the biological or even therapeutic effects of the herbal medicine (75). The traditional method for screening bioactive compound is to isolate them and then evaluate their activity through animal, organ, tissue, cellular, and receptor models (76). Other methods that can be used to screen bioactivity are affinity chromatography, biofingerprint analysis, and metabolic fingerprint analysis (76-78). Another important aspect is that TCM practitioners frequently use the same herbal formula to treat different diseases. Instead of using a generic marker for analytical purposes only, determining an

appropriate marker for each indications of the formula will ensure the therapeutic efficacy for the treatment. A new indication of EF was verified in Chapter 3. Now the question was if the original quality control marker, esculetin, is still a suitable bioactive marker. This aspect was assessed in Chapter 4.

1.10 TCM dosage form development

With the development of pharmaceutical techniques, TCM dosage forms evolved from decoctions, pills, powders, ointments and pellets into tablets, capsules, emulsion, liposomes, and nanoparticles (79). Some of the herbal formulas are difficult to be absorbed effectively in the body due to their large size and/or poor solubility (80,81). This may limit their oral bioavailability and impact negatively the treatment. Most herbal medicines are made as decoction. Modern formulation processes such as salt formation, co-solvents, emulsion and solid dispersion technology can improve solubility problems (82-86). Hence, in order to improve the therapeutic effect and increase patient's compliance, developing new dosage form for herbal formula is another important direction in TCM modernization. Nano-size milling technology is a new approach that reduces the particle size into the nanometer scale. The particle size of a drug substance or a colloidal dispersion, which are no more than 1000 nm, can be defined as nanoparticles according to recent FDA guidelines (87, 88). Nanotechnology can change the properties of matter, such as electrical, reactivity, and behavior characteristics, *in vivo*, due to an increased surface area (38). The application

of nanotechnology in TCM is an important part of TCM modernization because nanotechnology might enhance the bioavailability, achieve sustained release, enabels target drug delivery, increases the pharmacological effects, and enables new routes of administration (38). The term nanotechnology in the context of TCM includes processing the bioactive ingredients, bioactive components, and herbal formulations of TCM into the nanoscale (89). There are eleven different types of nano-based drug delivery systems (90): 1) nanocrystals and nanosuspensions, 2) nanotubes and nanowires, 3) ceramic nanoparticles, 4) liposomes, 5) solid lipid nanoparticles, 6) polymeric nanoparticles, 7) hydrogel nanoparticles, 8) copolymerized peptide nanoparticles, 9) polymeric micelles, 10) dendrimers, and 11) functionalized nanocarriers. Most systems consist of at least two components, and one of these should be the drug substance (91, 92).

Compared with other nanotechnologies, drug nanocrystals, which are composed purely of the drug substance, have the advantage of high drug loading with no other carrier materials. Drug nanocrystals require only a small quantity of surface-active agent for stabilization and a dispersion media (usually water) (93). The typical size at which a drug powder is considered a nanocrystal is in the 200-600 nm range (94). Stabilizers (polymers and/or surfactants) are used to prevent aggregation and agglomeration of the nanocrystals through ionic and/or steric stabilization by covering the surface of the nanoparticles in certain systems (95). In cases such as these, there are two categories of stabilizers that are commonly used. One is electrostatic repulsion stabilizers such as sodium dodecyl sulfate;

the other is steric stabilizers such as polyvidone and polyvinyl alcohol. Combinations of these two types are often used for the preparation of nanocrystals for their synergistic stabilizing effects (96, 97). Nanocrystals can be prepared in three ways: bottom-up methods (precipitation), top-down methods (media-milling and high-pressure homogenization), and combination methods (98-101). In general, the top-down approaches are the most commonly used industrial methods because they avoid the use of organic solvents, they are easy to scale up, and they allow high drug loading (102, 103). However, they are energy intensive. For screening formulations, characterizing the crystals, and investigating stability, a small-scale wet milling approach is desirable due to its low cost and high efficiency.

Because some herbs within the herbal formula, such as rhizomatic and fibrous root herbs may be difficult to be milled, the property of active ingredients may change during the production, and the difficulty in quality control and characterization of multi-components, nano-system for herbal medicine still remains challenges (38). Poor solubility of compounds is also an issue when manufacturing medicine products from isolated and purified single active constituents. In order to investigate the possibility of nanocrystals to be applied to herbal medicine, a nanocrystal formulation of esculetin, a poorly water-soluble compound in EF was developed and described in Chapter 5.

1.11 Hypothesis

In this thesis, the modernization of TCM is discussed through employing modern pharmaceutical approaches to investigate if a new indication can be assigned to an existing TCM formula. We preserved the TCM information of the herbal formula and scientific experiments were used to confirm or reject the TCM concept.

Our hypothesis was: Can Erding formula be used for hyperuricemia treatment and is esculetin a bioactive marker for the new indication?

1.12 Objectives

The study covers the following objectives:

(1) To evaluate the effects of Erding formula on hyperuricemic mice model.

(2) To determine whether the experimental data of a herbal formula can be used to advance and understand TCM characters in hyperuricemia treatment.

(3) To investigate if the original quality control marker of Erding formula, esculetin, is still an appropriate bioactive marker for the new indication of formula.

(4) To develop a nanocrystal formula for esculetin, a bioactive and poor water-soluble compound in the Erding formula.

1.13 Study Details

Because the content of chapter 2, 3, 4 has been published, some details and explanations were not included in the manuscripts. The following paragraphs present several details beyond the content of the publications.

1.13.1 Dose calculation

Safety and efficacy are the guiding tenets in drug development. Erding granules is a commercially available product. The initial dose for the animal studies should be a clinically equivalent dose used in humans. The daily dose of Erding granules is 12 g, which is equivalent to 60 g of raw materials per day if the manufacturing protocol in ChP is followed (39). According to the FDA guideline (104), in general, the clinically equivalent doses for mice can be calculated based on the human dose using Equation 1:

Human dose mg/kg = Animal dose mg/kg * (animal weight in kg / human weight in kg)$^{0.33}$

Equation (1)

However, body weight is not the only important factor for calculating the dose. The correction factor (Km), a constant for each species, is estimated by dividing the average body weight (kg) of species by its body surface area (m^2) (105). This gives the following equation:

Human dose mg/kg = Animal dose mg/kg * (animal Km / human Km) = Animal dose mg/kg * Km ratio Equation (2)

In this thesis, the animal study was conducted using a mouse model. The Km ratio used in Equation 2 to convert the human dose to the mouse dose was 0.081 (104, 105). Hence, the clinical equivalent dose of Erding granules for mice is 12 g raw material/kg. After several tests, the results showed the dose of 12g is not efficient in the hyperuricemia mouse model in this study. Therefore, the experimental determined dose of Erding extract for hyperuricemia treatment was set to 24 g raw material/kg.

1.13.2 Sample size determination

The sample size in an animal study should be determined before the experiment to avoid bias in the interpretation of results, such as not properly representing the size of the target and/or not detecting differences between test groups (106). The sample size for a study impacts the confidence criteria, power of the study, size of the expected effect, and standard deviation in the population.

Generally, for most studies, the power should be larger than 80%, and for animal tests, 90% is desirable (107). In this study, the sample size was calculated by a statistics software, Minitab 17 (State College, PA, USA), and the sample size for the animal study with a power of 90% was determined to be 6 to 9. To improve the statistical power the sample size of the animals using in this thesis was 10 per treatment group.

Chapter 2 Traditional Chinese Medicine for Managing Inflammatory Pain of Arthritis with Herbal Medicines

This study has been published as Jieyu Zuo, Qin Zheng, Hui Jian, Tasha Porttin, Chanelle Willson, Fiona Misquita, Jordan Capicio, Raimar Löbenberg. Traditional Chinese Medicine for Managing Inflammatory Pain of Arthritis with Herbal Medicines in Current Traditional Medicine. 2016;2(2):80-93. Reference (108)

2.1 Introduction

This review focuses on traditional Chinese herbal treatment of Osteoarthritis (OA) and Rheumatoid (RA) published before July 2015 were identified using computer-based searches of the Scopus database, PubMed database and CNKI database (in Chinese). The following combination of keywords was used: “Traditional Chinese Medicine (中医) [Title/Abstract] and arthritis (关节炎) [Title/abstract] and/or (osteoarthritis (骨性关节炎) [All fields] or rheumatoid arthritis (类风湿性关节炎) [All fields]”. Publication titles were initially reviewed for suitability, and relevant abstracts were then obtained and reviewed for retrieving suitable full-text articles. Finally, data were extracted from suitable articles; they are described here in relevant sections. Ethical approval was not necessary because the pooled data from individual studies had received ethics approval.

2.2 Traditional Chinese Medicine

Traditional Chinese Medicine (TCM) comprises a series of therapeutic remedies developed and used in China to cure illnesses in the population (2). The history of TCM dates back to the Warring States period (475-221 B.C.), when the first surviving written work on Chinese medicine, Huang Di Nei Jing (黄帝内经, Yellow Emperor’s Inner Canon), was compiled (5). Over time, the underlying principles of TCM have remained consistent, whereas Western Medicine has evolved from folk medicine to a focus on scientific breakthroughs

(109). TCM maintains that vital energy (Qi) is the root of life and that its motion and change explain the life activity of the human body (110). In addition to Qi, Chinese philosophy uses Yin-Yang, five phases, visceral organs and channel systems to de- scribe our life and health: optimal health is achieved when the systems are balanced. TCM maintains that a human being is an organic entity and that life is an endlessly changeable progression. Pathogens invade and cause disease by disrupting harmony; therefore, TCM cures disease by re- establishing the dynamic balance of harmony (2).

Diagnosis and treatment in TCM require advanced skill, with an emphasis on logical thinking with a deep understanding of the factors that differentiate syndromes (111). With the growing popularity of TCM, the need for standardized education is increasingly important. For example, in Canada, numerous regulatory bodies have established training programs to qualify those who practice TCM (112). Although a regulatory examination is required at the end of a training program to ensure that patients receive standardized, safe and reliable care, considerable heterogeneity exists in training programs, and few programs have achieved full autonomy (112).

2.3 Use of herbs in TCM

In TCM, more than 8000 herbs are believed to have medicinal value; however, only 500 are commonly used (15). The basic medicinal properties of herbs are characterized by their nature, flavor, and meridian tropism (15). This means that herbs with different properties

and functions can have specific effects on certain diseases to reestablish the Yin-Yang harmony in the body (2).

To achieve better curative efficacies with fewer side effects, the herbs in TCM are commonly combined as a formulation to produce synergistic effects in the body (25). According to the TCM concept, the composition of an herb formulation may include four types of herbs according to their properties and the stage of the disease: [1] a primary (emperor) herb is the main therapeutic agent and the essential component in each formula; [2] a secondary (minister) herb will work to reinforce the primary one or to act on an accompanying disease; [3] an adjuvant herb may reinforce the primary or secondary herb as well as reduce side effects; [4] a guide herb is employed to facilitate the action of all of the other herbs, increasing the overall effect and helping to deliver the herbs to their site of action (25, 113). Due to the complexity of the chemical constituents in herbs and formulas, the active compounds and their exact therapeutic mechanisms of action remain largely unknown. Traditional Chinese Herbal Medicine is increasingly used to manage inflammatory pain for chronic diseases, such as arthritis (114-117).

2.4 Arthritis

Arthritis is one of the leading chronic conditions causing disability and work limitations among the general population. In 2010-2012, 22.7% (52.5 million) US adults were estimated to suffer from arthritis, and 43.2% of these individuals reported limitations to

activity (118). Similarly, 16.6% of Canadians (4.3 million) 15 years and older were reported to be affected by arthritis in 2010-11 (119). Individuals suffering from arthritis may experience a poorer quality of life compared to those suffering from other chronic diseases because they are likely to require more assistance in daily activities. These patients experience relatively more pain and have poorer health (120). In addition, the economic bur- den of medical expenditures and lost earnings attributed to arthritis is large: estimated to be $6.4 billion in Canada in 2000, with medical expenditures estimated to be $2.1 billion (121). In the US, medical expenditures among arthritis patients totaled $353 billion in 2005, a $100 billion increase compared to 1997 (122).

This type of disease can affect anyone at any age; however, the most frequent onset is in the elderly, particularly in women (123). Arthritis represents more than 100 conditions that involve the joints, and the disease can be classified as OA, RA, childhood arthritis, and systemic lupus erythematosus (124). This report focuses on two major forms of arthritis, OA and RA.

2.5 Osteoarthritis

OA is the most common type of joint disease and, for the most part, affects weight-bearing joints, such as the knees and hips, as well as the Traditional Chinese Medicine for Managing Inflammatory Pain hands (125). The characteristic feature of OA is progressive cartilage breakdown with concomitant joint space narrowing, osteophyte formation,

subchondral sclerosis and synovitis (126). This condition causes bones to rub against each other, eventually resulting in joint stiffness, pain, tenderness, loss of movement, crepitus, variable degrees of inflammation, and physical disability (127). The disease is characterized by progressive loss of articular cartilage. Due to the debilitating degenerative nature of arthropathy, current clinical treatment modalities for OA can only slow disease progression but cannot provide a cure (128). Risk factors contributing to the development and onset of OA include gender, genetics, obesity, cartilage injuries, repetitive movements, and muscle weakness (129, 130).

OA results from cartilage degradation, which is characterized by degeneration of the extracellular matrix and cell death, processes that are controlled by catabolism and anabolism in chondrocytes. Both synovial cells and chondrocytes within joints can secrete specific enzymes termed matrix metalloproteinases (MMPs), which can degrade all of the components of the extracellular matrix (127, 131). The levels of these enzymes are normally tightly regulated to ensure balance; however, this homeostasis can be compromised by interleukin-1 (IL-1) and tumor necrosis factor-alpha (TNF-α), which ultimately leads to the loss of joint cartilage. As powerful pro-inflammatory cytokines, IL-1 and TNF-α stimulate synovial cells and chondrocytes to secrete excess MMPs. Additionally, during pro- inflammatory states in articular cartilage, prostaglandin E2 (PGE2), the major contributor to arthritic inflammatory pain, is produced and released from OA chondrocytes stimulated by IL-1β (131). Each of the above mediators stimulates the

degenerative and nociceptive pathways associated with OA progression. Other cytokines, such as IL-6, which drives persistent inflammation and joint destruction, fibroblast growth factor 2, and nitric oxide (NO), may also contribute to this inflammatory and degradative disease (131).

2.6 Rheumatoid arthritis

RA is a systemic autoimmune disease accompanied by recurrent inflammatory flares. The painful inflammatory episodes are characterized by robust infiltration of inflammatory cells, resulting in hyperplasia of the synovial lining, edema, long-term cartilage erosion, articular destruction and pain (132, 133). RA can also affect extra-articular organs (125). RA afflicts 0.5-1.0% of the world's population and occurs most commonly in women and elderly individuals (134). Although the exact cause of RA is unknown (135), genetic and environmental factors have been identified as risk factors for its development (136).

Interactions between T and B lymphocytes, synovial-like fibroblasts, and macrophages can lead to overproduction of pro-inflammatory cytokines (TNF-α, IL-1, and IL-6) via overexpression of TNF, thus contributing to synovial inflammation and joint destruction during the development and onset of RA (136). In response to inflammatory stimuli, mitogen-activated protein kinases (MAPKs) are expressed in the synovial tissues of patients with RA. Activated MAPKs increase secretion of MMPs and pro-inflammatory cytokines (137, 138). NF-κB, another transcription factor associated with cytokines, MMP,

cyclooxygenase (COX)-2 and inducible nitric oxide (iNOS) are also overexpressed in RA (139).

The cytokines IL-1 and TNF-α play a major role in early joint swelling as well as in inflammation and are therefore key players in joint inflammation and cartilage and bone destruction (140). IL- 6 is a pro-inflammatory cytokine responsible for the presence of many rheumatoid factors (141). NO, a mediator in RA synthesized by iNOS, plays a major regulatory role in inflammation (142). COX- 2, which is commonly expressed in response to inflammatory signals, is involved in the production of another important mediator of RA: PGE2 (143).

Accordingly, suppression of COX-2, NO production, and TNF-α, PGE2, NF-κB and MAPK expression may be important in treating RA.

In Western Medicine, RA is currently treated with non-biological, disease-modifying, anti-rheumatic drugs (DMARDs), such as methotrexate, to reduce synovitis and inflammation instead of the previously used non-steroidal anti-inflammatory drugs. Biologic DMARDs, such as TNF-α inhibitors, are used in cases of uncontrolled disease (144).

2.7 The TCM view of arthritis

In TCM, arthritis belongs to the category ‘bi syndrome,’ which is attributed to the obstruction of qi and blood in the meridians following invasion of climatic pathogens ‘wind,’ ‘damp,’ ‘cold,’ and ‘heat’ (145, 146). The characteristics of bi disease are pain,

soreness and numbness of the muscles and tendons; swelling, stiffness, and deformity of joints; and limitations of movement (147). According to TCM theory, 'wind,' 'damp,' 'heat,' and 'cold' belong to 'six evils', or the exogenous pathogen. Under normal conditions, they represent climatic changes in nature and do not cause disease, becoming pathogens only in instances of severe weather change and decreased immunity. Each pathogen may cause disease alone or together with other pathogens. Therefore, 'bi syndrome' can be classified as the 'wind-cold-damp' type or the 'wind-damp-heat' type. 'Wind-cold- damp' bi is also denoted 'wind' bi, 'cold' bi and 'damp' bi depending on which pathogen predominates. 'Bi syndrome' is diagnosed by differentiating its principal symptoms. 'Wind' bi is the sudden and acute onset of disease; its symptoms are wandering, erratic and variable. 'Wind' is a Yang pathogen; thus, it prominently affects the upper body and occurs primarily in the early stage of arthritis. 'Damp' is a Yin pathogen and easily blocks the activity and movement of Yang. Symptoms of 'damp' bi are heaviness and swelling of the joints or even the entire body as well as fluid retention. Instead of the sharp and sudden appearance of pain, patients experience pain that is deeper and progressively worsens. 'Damp' bi can be initiated or aggravated by wet weather and the environment, for example, rainy weather or damp localities. 'Cold' is a Yin pathogen and relates to the worsening of symptoms, especially severe pain. 'Wind-damp-heat' bi can simply result from an attack of exterior wind-damp-heat and can be transformed by invasion of wind-cold-damp with signs of interior heat (2, 145). The principal symptoms of 'wind-damp-

heat' bi are predominantly heat, such as fever, irritability, restlessness, painful swollen joints, redness, heat sensation and difficulty moving, which are different from the symptoms of 'wind-damp-cold' bi (145). Therefore, according to TCM theory, if qi and blood are circulating normally without obstructions in the meridians, there will be no pain (146).

2.8 Herbs for arthritis

The fundamental principle of TCM is to treat the disease by applying treatment according to syndrome differentiation (2). Selected herbs work together or alone to restore balance according to the requirements of different syndromes and diseases. In TCM, these herbs can be used to treat certain syndromes due to their specific properties (15). Table 2.1 list the herbs that could be used for the treatment of RA and OA. The following paragraphs discuss key herbs that are traditionally and most frequently employed for treating RA and OA. The scientific evidence is discussed in addition to the traditional basis for use in TCM. Based on the characteristics of arthritis in TCM and the intended effects of the herbs, commonly used herbs can be divided into the following types: promoting blood circulation and removing stasis, dispelling wind and eliminating dampness, nourishing blood, invigorating Qi, and dispersing wind and cold.

Table 2. 1 Key herbs that are most frequently employed in the treatment of RA and OA in TCM

Latin Name	Chinese Name	Medicinal use	Dose/day	TCM Nature	TCM Flavor	Collected season	Reference
Myrrh	Mo Yao (没药)	Blood-activating and stasis-resolving	3-10g	Neutral	Pungent, Bitter	Winter	148-151
Rhizoma Chuanxiong	Chuan Xiong（川芎）		3-10g	Warm	Pungent	Summer	152-159
Olibanum	Ru Xiang (乳香)		3-10g	Warm	Pungent, Bitter	Spring,Summer	160-163
Radix Clematidis	Wei Ling Xian（威灵仙)	Wind-dampness-dispelling	6-9g	Warm	Pungent, Salty	Autumn	164-167
Tripterygium Wilfordii Hook. f.	Lei Gong Teng (雷公藤)		1-5g	Cool	Pungent, Bitter	Late autumn, Early Winter	168-184
Radix Angelicae Sinensis	Dang Gui（当归）	Blood tonic	3-15g	Warm	Pungent, Sweet	Late autumn	185-194
Radix Paeonia Alba	Bai Shao（白芍）		6-15g	Slightly cold	Bitter, Sour	Summer, autumn	195-207
Licorice	Gan Cao（甘草）	Qi tonic	1.5-9g	Neutral	Sweet	Autumn, Spring	208-215
Radix Saposhnikovia	Fang Feng (防风)	Wind-cold-effusing	5-10g	Slightly warm	Pungent, Sweet	Spring, Autumn	216-222

2.8.1 Blood-activating and Stasis-resolving Herbs

Blood-activating and stasis-resolving herbs are used to promote blood flow and eliminate blood stasis.

Myrrh - Mo Yao

Myrrh is the dried resinous exudate of Commiphora myrrha Engl. It is known to Chinese practitioners as 'Mo Yao' (148). In TCM, myrrh was first used in the Tang Dynasty in 600 AD. Traditionally, myrrh is used for skin ulcers, wounds, pain, tumors, arthritis, inflammatory diseases, and diseases caused by blood stagnation, such as rheumatism, hemiplegia, and acroanesthesia. Clinically, myrrh is generally prescribed in combination with Ru Xiang to treat arthritis. The common dose of myrrh raw material is 3-10 g per day. Scientific studies have shown that extracts of myrrh have anti-tumor, anti-inflammatory, analgesic and anti-oxidant pharmacological activities (149-151). The anti-inflammatory mechanism of myrrh involves decreasing PEG2 levels, inhibiting NO production and suppressing COX expression (150).

Rhizoma Chuanxiong - Chuan Xiong

Rhizoma Chuanxiong (RC), called 'Chuan Xiong' in China, is the dried rhizome of Ligusticum chuanxiong Hort. from the Umbelliferae family (15). It was first listed in Shen

Nong Ben Cao Jing (神农本草经), the oldest Materia Medica book in China. In TCM, RC is generally used to stimulate blood circulation and remove blood stasis. It is frequently combined with Dang Gui as an herbal formula to treat OA and RA (152). This herb is commonly administered at a dose of 3-10 g as a decoction (15).

One study reported that RC exerts anti- inflammatory effects by inhibiting NO production in lipopolysaccharide (LPS)- and interferon γ (IFNγ)-stimulated RAW264.7 cells (153). Three of the major bioactive constituents of RC are phenols and organic acids, phthalides, and alkaloids (154). One of the primary compounds, also used as a quality control marker, is ferulic acid, which exerts anti-inflammatory activity by suppressing IL-8 production (155-157). Two phthalides, Z-ligustilide and senkyunolide A, have been demonstrated to have an anti-inflammatory effect by inhibiting TNF-α production and NF-κB activation in vitro (158, 159).

Olibanum - Ru Xiang

Olibanum, called "Ru Xiang" in China, is the dried resin of Boswellia carterii Birdw; it was first used as a TCM herb in the Han Dynasty in 498 AD (15). Olibanum is commonly used in China to reduce swelling, alleviate inflammatory pain and invigorate blood circulation (160). The typical dose is 3-10 g of raw material per day (15). This herb is frequently combined with myrrh to treat diseases associated with inflammatory pain. The anti-inflammatory mechanism of action of Olibanum may be related to

suppressing the overproduction of inflammatory mediators, such as PEG2 and NO (160). Boswellic acids in Olibanum are believed to act on the immune system (161). Boswellia is used as an anti-arthritic agent in Indian Ayurveda Medicine (162) and as a dietary supplement in the US for patients with arthritis and inflammatory pain disorders (163).

2.8.2 Wind-dampness-dispelling (anti-rheumatic) herbs

Wind-dampness-dispelling herbs can expel wind and remove dampness from muscles, tendons and joints to treat bi syndrome resulting from wind-damp invasion.

Radix Clematidis - Wei Ling Xian

Radix Clematidis, which is called "Wei Ling Xian" in Chinese, is the root and rhizome of Clematis chinensis Osbeck (15). It is primarily distributed in southern China and is widely used in TCM for treating rheumatic disease and alleviating pain (164,165). This herb is generally used either alone as Weilingxian powder or as an ingredient in a formulation (166). Raw herbal material is available at an oral dose of approximately 6-9 g per day or at an appropriate dose for external use (15).

Triterpenoid saponins are the major active components in Clematidis. AR-6, a triterpene saponin, can be isolated from this herb and is thought to possess numerous biological activities (167). Studies conducted on this compound have demonstrated its ability to inhibit production of IL- 1β, IL-6, and TNF-α in rats with adjuvant arthritis and to

significantly suppress serum inflammatory mediators (IL-1β and TNF-α) in rats with collagen-induced arthritis. The anti-inflammatory mechanism of action occurs via inhibition of NF- κB p65 subunit, TNF-α and COX-2 expression. These characteristics render AR-6 a potential agent for the treatment of RA.

Another study concluded that the saponin fraction from Clematidis exerts preventative effects with regard to extracellular matrix degradation and chondrocyte injury in rats with monosodium iodoacetate-induced OA. This fraction represents a potential agent for treating osteoarthritis by inhibiting inflammation and protecting articular cartilage (164).

Tripterygium Wilfordii - Lei Gong Teng

The dried root of Tripterygium wilfordii Hook. f. (TwHF), which is known to TCM practitioners as "lei gong teng" or "thunder god vine," is abundant in southern China (168). It has been used medicinally in China for approximately 400 years to treat autoimmune and inflammatory conditions, including RA, ankylosing spondylitis, systemic lupus erythematosus, psoriasis, and idiopathic IgA nephropathy (169, 170).

Triptolide, tripdiolide, and triptonide are the three most abundant components in TwHF extracts, and several studies have reported that these three components contribute to the majority of the herb's immunosuppressive and anti-inflammatory effects. Among these components, triptolide is the major biologically active constituent in RA treatment (171, 172).

Extracts of TwHF and triptolide inhibit expression of pro-inflammatory genes, such as those that result in PGE2, NO and TNF-α production, to significantly lower concentrations of inflammatory mediators (173, 174). However, the herbal components only suppress COX-2-regulated PGE2 production (175). An additional proposed mechanism of action of TwHF extracts and triptolide is inhibition of T cell proliferation and suppression of MMP production, thereby alleviating RA symptoms (173, 176). Another proposed mechanism of action of TwHF is suppressing antibody formation. In RA, B cell activity is increased due to secretion of numerous autoantibodies, whereas inhibiting autoantibody generation decreases the symptoms of RA (177, 178).

TwHF is a toxic herb, and it should be carefully administered orally. The suggested dose of raw material is 1-5 g per day (15). The side effects of this plant include GI discomfort, hair loss, headache, skin rash, myelosuppression, decreased bone density in women (with prolonged use), decreased male fertility and even death (168-169, 179). To minimize toxicity and maximize the therapeutic benefits, several preparations have been developed and are commercially available in China (180-182). Clinical trials of TwHF extracts for RA treatment report that daily doses greater than 360 mg and up to 570 mg appear to be safe and elicit a better clinical benefit (183, 184).

2.8.3 Blood Tonic Herbs

The function of blood tonic herbs is to replenish the blood and treat blood deficiency syndromes.

Radix Angelicae Sinensis - Dang Gui

Radix Angelicae Sinensis (AS) is the dried root of Angelica sinensis (Oliv.) Diels. AS, which is also known as 'dang gui' in China, has been commonly used by TCM practitioners since 200 B.C (15). AS is from the Umbelliferae family, as is RC. The usual daily oral dose varies from 3 g to 15 g as a decoction (15). Due to its ability to enrich the blood, invigorate blood circulation and harmonize vital energy, this herb is also known as "female ginseng" in China and is used to treat female reproductive problems, such as menstrual disorders and the need to recover from blood loss after childbirth or surgery (139, 185). This herb can be used as a medicinal food cooked with meat or prepared in soup (185). In TCM, AS can be used alone or together with other herbs for inflammatory-related diseases, nerve pain and bone injuries (186, 187). It is also well known for its beneficial therapeutic effects regarding RA and OA (188, 189).

Studies have found that an ethyl acetate fraction of AS decreases inflammation by inhibiting IL-1β-induced cell proliferation, COX-2 expression, PGE2 production and NO secretion via suppression of MAPK phosphorylation and NF-κB path- way activation in

both LPS/IFN-γ-induced murine peritoneal macrophages and synovial fibroblasts from RA patients (189, 190). The ethyl acetate extract inhibits the production of cytokines, including TNF-α and IL-6, in LPS/IFN-γ-simulated RAW 264.7 cells, (191) and similar anti-inflammatory mechanisms of action were also demonstrated in mice (191).

Phthalides, ferulic acid, and polysaccharides are believed to be the major groups of active compounds in AS (185). Ferulic acid is the functional compound contributing to the herb's therapeutic properties, (192) exerting anti-arthritic effects by inhibiting hydrogen peroxide-induced pro-inflammatory cytokine (IL-1β and TNF-α) and metalloproteinase (MMP-1 and MMP-13) gene expression in chondrocytes (186).

It should be noted that many scientists are concerned about the potential risk of bleeding when this herb is used concurrently with anti-coagulant agents, such as warfarin (193, 194).

Radix Paeonia Alba - Bai Shao

Radix Paeonia Alba (PA), the dried root without bark of Paeonia lactiflora Pall, is a common medicinal herb used in TCM for centuries (15). The decoction has long been used to treat pain or inflammatory disorders and autoimmune diseases, including headache, spasmodic pain, fever, anemia, menstrual disorders, RA, systemic lupus erythematosus, and hepatitis (195, 196). The common dosage of this herb is a decoction of 6-15 g raw material per day (15).

Total glucosides of peony (TGP), the active compound extracted from PA, comprises more than 15 components. In 1998, a preparation of TGP was approved by the China Food and Drug Administration to enter the market as a disease- modifying agent for RA. Paeoniflorin, a water-soluble glucoside, is the standardization for PA because it constitutes more than 90% of TGP and 0.05-6.01% of PA. This glucoside also accounts for the pharmacological effects observed for TGP (195-197).

Considering the above mentioned symptoms and pathological changes associated with RA, numerous studies have reported potential therapeutic effects of PA in RA by demonstrating analgesic, anti-inflammatory, immunomodulatory and protective cartilage effects of TGP or paeoniflorin. The analgesic effect of paeoniflorin, inhibition of the extracellular signal-regulated protein kinase pathway, is mediated through the adenosine A1 receptor (198).

It is now believed that PA suppresses both acute and chronic inflammation as follows: by inhibiting production of chemokines; suppressing production of pro-inflammatory cytokines and inflammatory mediators PGE2, leukotriene B4, NO, and reactive oxygen species; decreasing microvascular permeability; inhibiting proliferation of lymphocytes; suppressing activation of neutrophils; and inducing apoptosis of lymphocytes (195, 199-205).

Several studies have reported that TGP effectively inhibits synovial hypertrophy and neovascularization and protects against joint destruction by suppressing synoviocyte proliferation, inflammatory cell infiltration, new blood vessel formation, and cartilage-

degrading enzyme production (195, 206-207). Nonetheless, the protective activity of PA against joint destruction requires clinical support involving RA patients.

2.8.4 Qi Tonic Herb

This type of herb, for the most part, functions by replenishing Qi.

Licorice - Gan Cao

Licorice, or 'Gan Cao', as it is known in Chinese to TCM practitioners, is derived from the root of Glycyrrhiza uralensis Fisch (15). The first recorded medicinal use of licorice in China is in 200 B.C. in the earliest Materia Medica book called Shen Nong Ben Cao Jing (208). In TCM, licorice is a widely used herb that appears in approximately 60% of herbal formulas (209). Historically, it has been used not only as a sweetening and flavoring agent but also as a treatment for various health ailments, such as asthma, cough, fever, spasms, and pain (210). In both traditional and modern TCM formulations, licorice is most commonly used as a guide agent to harmonize the characteristics of other herbs, such as to decrease toxicity and reduce side effects (208). Among the 300 compounds isolated from licorice, triterpenoid saponins and flavonoids are the primary constituents (211).

Licorice has traditionally been indicated for the treatment of arthritis, and it is the most commonly used herb in herbal formulas for the treatment of both RA and OA (212, 213). Patients are prescribed 1.5-9 g daily as a decoction (15).

One study demonstrated that licorice extract has anti-inflammatory activity against collagen-induced arthritis in mice (214). Licorice functions by blocking production of the inflammatory cytokines TNF-α and IL-1β.

The anti-inflammatory activities of the flavonoids isolated from licorice have been tested (210, 215). These flavonoids suppressed production of inflammatory cytokines, such as NO, IL-1β IL-6 and PGE2, by down-regulating iNOS and improving COX-2 expression in LPS-induced macrophages.

2.8.5 Wind-cold Effusing Herbs

Wind-cold effusing herbs primarily disperse wind-cold to treat the exterior syndrome of wind- cold.

Radix Saposhnikovia - Fang Feng

Radix Saposhnikovia is the dried root of Saposhnikovia divaricata (Turcz.) Schischk and is known to Chinese practitioners as 'Fang Feng.' Traditionally, the herb induces diaphoresis to expel wind, dispel damp, stop pain and relieve spasms (15). According to Chinese Pharmacopeia, the suggested daily dose of Radix Saposhnikovia is 5-10 g (216). Radix Saposhnikovia can be combined with other herbs to treat bi syndrome due to wind-cold-damp (15, 216). This herb possesses analgesic, anti-pyretic, anti-inflammatory, anti-oxidant and anti-platelet aggregation properties (217, 218). Studies have shown that the

active ingredients of Radix Saposhnikovia include essential oils, mannitol, glycosides, chromones, natural coumarins, polyacetylenes, and polysaccharides, of which chromones are considered to be the major bioactive constituents (219-221). One study reported that the chromone extract of Saposhnikovia divaricate suppressed secretion of cytokines (TNFα, IL-1, and IL-6) and production of mediators (PGE2); furthermore, this suppression was demonstrated to be, at least in part, due to inhibition of NF-κB and MAPK activities (222). This scientific evidence to date provides support for the traditional use of this herb in the treatment of RA.

2.9 Multi-ingredient formulations

To generate synergistic therapeutic effects and neutralize potential side effects of individual substances, formulas are commonly used in traditional Chinese herbal practice (25). Herbal formulas have been well documented in both ancient and modern Chinese literature (223). The ingredients, dose, and dosage can be modified according to the individual patient. In TCM, an herbal formula is selected according to the different type of bi syndrome. For 'wind-cold-damp' bi, the typical formulas are Du Huo Ji Sheng Tang (独活寄生汤), Fang Feng Tang (防风汤), Wu Tou Tang (乌头汤), and Yi Yi Ren Tang (薏苡仁汤). For 'wind-damp-heat' bi, Bai Hu Jia Gui Zhi Tang (白虎加桂枝汤) is used for the syndrome caused by 'wind-damp-heat', and Gui Zhi Shao Yao Zhi Mu Tang (桂枝芍药知母汤) is selected for 'wind- damp-heat' bi syndrome transformed by invasion of

'wind-damp-cold.' (224). In the following section, a description of Du Huo Ji Sheng Tang is presented as a representative herbal formula.

Du Huo Ji Sheng Tang (DHJST)

A famous formulation in TCM for the treatment of arthritis is DHJST, also known as Du Huo Ji Sheng Wan in another dosage form. DHJST is an herbal formula first described by the Chinese physician Sun Simiao to treat lower back and knee pain in Essential Recipes for Emergent Use Worth a Thousand Gold (Bei Ji Qian Jin Yao Fang) in the Tang Dynasty (652 AD). DHJST formulations contain 15 main ingredients: Du Huo (Radix An- gelica Pubescentis), 9 g; Sang Ji Sheng (Ramulus Loranthi), 6 g; Qin Jiao (Radix Gentiana Macrophylla), 6 g; Fu Ling (Poria), 6 g; Gan Di Huang (Radix Rehmannia), 6 g; Gan Cao (Radix Glycyr- rhiza), 6 g; Rou Gui (Cortex Cinnamon), 6 g; Xixin (Herba Asari), 6 g; Fang Feng (Radix Lede- bouriella), 6 g; Du Zhong (Cortex Eucommia), 6 g; Bai Shao (Radix Paeonia Alba), 6 g; Huai Niu Xi (Radix Achyranthes Bidentata), 6 g; Chuan Xiong (Rhizoma Ligusticum Chuanxiong), 6 g; Ren Shen (Radix Ginseng), 6 g; and Dang Gui (Radix Angelica Sinensis), 6 g. The combination of these herbs is prescribed in TCM to dispel wind and eliminate dampness to treat lingering arthralgia syndrome and to relieve joint pain, stiffness and lethargy (25).

Due to actions of expelling wind and damp, stopping numbness and pain due to bi syndrome, nourishing the liver and kidney, invigorating Qi and blood, and clearing

channels and collaterals, this formulation is commonly used in TCM to treat OA and RA caused by 'wind-damp-cold' with deficiencies of the liver, kidney, Qi and blood (225, 226). Furthermore, Du Huo is the emperor herb in the formula when it is used to dispel wind, cold and damp for relieving pain. The minister herbs are Fang Feng, Qin Jiao, Rou Gui, and Xi Xin, which free and warm the meridians to reduce pain. Nine herbs, Sang Ji Sheng, Du Zhong, Niu Xi, Dang Gui, Chuan Xiong, Gan Di Huang, Shaoyao, Ren Shen, and Fu Ling, act as assistant herbs to nourish the liver, kidney, Qi and blood. Gan Cao functions as the guide herb to harmonize the properties of all of the herbs. In DHJST therapy, the ingredients and/or dosages are altered as necessary (25).

One study tested the effectiveness of DHJST and reported significant reductions in patient scores for pain, stiffness, and physical functioning (227). In a study evaluating the safety of DHJST for treating OA, no cases of severe adverse events or adverse drug reactions were reported (228). During the four-week treatment, liver and kidney function was not significantly affected, and there was no renal tubular damage. Both research and clinical studies have proven that DHJST plays a significant role in regulating pro-inflammatory factors (TNFα, MMP-3, IL-1, IL-6, and NO) in the treatment of OA (128, 229-332). Similar to most TCM formulations, more research and clinical studies must be performed. When treating patients with a particular herbal formula, restriction according to the initial formulation is not necessary. Indeed, the herbs and their dosages in the formula can be modified in accordance with the requirements of the disease.

2.10 Safety and efficacy of TCM herbs

In general, herbs are considered to be safe because they are 'natural' products and because their use has been verified by anecdotal experience. However, due to a lack of consistent manufacturing practices, such as collecting, processing and storage, quality standards, scientific validation and well-designed clinical trials, the use of herbs may put consumers at risk for adverse or toxic effects (233).

TCM herbal formulas are gaining popularity in the Western world as a basis for the professional development of new medications. However, acceptance by Western mainstream health care remains minimal due to concerns regarding the safety and efficacy of herbs (234).

To recognize the growing concern over the regulation of herbal medicinal products, Health Canada released Natural Health Product Regulations in 2004 (235), the purpose of which was to standardize natural health products. According to these regulations, all natural health products recognized by Health Canada will be assigned a natural health product number and will require a license prior to sale in Canada. In the US, the US Pharmacopeial Convention publishes raw material and product monographs (236). Such monographs can help make herbal medicines safer and more standardized, thus supporting the ability of consumers to make decisions regarding products for health self-management. In the US, herbal products are commonly sold as dietary supplements, which are regarded as special

foods instead of medications; as such, these products do not require regulatory approval before they are marketed unless they contain a new dietary ingredient (237).

Additionally, single-active-ingredient therapeutics are representative of Western chemical medicine, and pharmaceutical industries and regulatory institutions are skeptical of natural product mixtures (233). Therefore, single-ingredient products derived from herbs, supported by adequate phytochemical, pharmacological and safety data, are at present more widely acceptable and available than multi-herb formulas. This is troublesome because multiple-ingredient formulations take advantage of synergistic and additive properties to improve the overall therapeutic effect.

2.11 Conclusion

When considering the use of TCM herbals for the treatment of arthritis, it is important to focus on individualized results because the efficacy of herbs varies from patient to patient. Clearly, more research on the safety and efficacy of TCM herbs is necessary to generate a more accurate and safe list of alternative treatments for inflammatory pain accompanying arthritis. Future studies should identify additional drug-herb and disease-herb interactions in clinical settings. Finally, additional research is needed to provide patients with the opportunity of utilizing a holistic treatment plan that incorporates alternative and Western Medicine to optimally manage arthritis.

Chapter 3 Erding Formula in hyperuricemia treatment: unfolding traditional Chinese herbal compatibility using modern pharmaceutical approaches

This study has been published as Jieyu Zuo, Hongming He, Zhengyun Zuo, Nadia Araci Bou Chacra, Raimar Löbenberg, in Journal of pharmacy and pharmacology. 2018;70(1):124-132. Reference (238)

3.1 Introduction

As an integral part of Chinese culture, Traditional Chinese Medicine (TCM) has been used as a holistic medical system for the diagnosis, prevention and treatment of diseases over thousands of years. (26) Rather than a monotherapy, TCM frequently creates multi-herb formulas based on the symptoms and characteristics of patients. The combination is guided by TCM theories to produce synergistic effects or modulate pharmacological outcomes. (239, 240) Herbal compatibility (Peiwu, 配伍), in which two or more herbs are prescribed in combination according to clinical experience and herb properties, is one of the fundamental principles in traditional Chinese herbal formula. (17, 20, 22) Over the past 2,000 years, more than 100,000 multi-herb formulas have been described. (21, 241) Most of these formulas are based on long-term clinical practice and are described by TCM theories, such as Yin-Yang balance and Five phases. (17, 25) However, understanding the composition is difficult for researchers without knowledge of the Chinese language and an appropriate TCM and cultural background. (22) Over several decades scientists tried to modernize TCM by isolating active compounds from TCM plants. This approach had several successes but could not explain how TCM works and if TCM treatments are scientifically justified.

In present study, we took an alternative new approach to TCM. The Erding formula (EF) is a traditional Chinese formula containing Viola yedoensis Makino (Viola), Taraxacum

mongolicum Hand.-Mazz. (Taraxacum), Lobelia chinensis Lour. (Lobelia), and Isatis indigotica Fort. (Isatidis) root in the same quantities. The formula has been officially listed in the Chinese Pharmacopoeia (ChP) since 2005. (39) The EF is commonly used to treat sore throats, carbuncles and boils. However, according to modern TCM practitioners, the formula should be able to treat gout due to its herbal combination.

Hyperuricemia is an abnormally high concentration of uric acid (UA) in the body. This disease appears to be rapidly increasing worldwide. It is also regarded as a risk factor of several chronic diseases, such as hypertension, diabetes, kidney disease, and cardiovascular diseases (242, 243). UA is the final product in the metabolism of endogenous and dietary purine. High levels of UA mainly occur due to insufficient UA excretion via the kidneys (244, 245). The protein responsible for tubular reabsorption of urate, URAT1, and organic anion transporter, OAT3, are kidney located transporters that are involved to UA excretion. Additionally, the long-term continually high UA levels may promote inflammation and pain in joints such as gout. (245-248).

Animal models for hyperuricemia, inflammation and analgesia were used to evaluate the effects of individual herbs and EF. In addition, their effects on the expression of URAT1 and OAT3 were measured by real-time (RT) PCR.

In this study, we focused on the potential hypouricemic effect of the formula and the individual herbs instead of isolating individual actives. Our study investigated herbal

compatibility of the formula when used to treat hyperuricemia which is a new indication for this formula.

3.2 Materials and methods

3.2.1 Reagents and materials

Oxonic acid potassium salt (Lot: BCBN6836V) and hypoxanthine (Lot: SLBH5921V) were purchased from Sigma-Aldrich (St. Louis, MO, USA). Benzbromarone tablets (Lot: 150313) and indomethacin tablets (Lot: 140901) were obtained from Excella GmbH (Feucht, Germany) and Guangzhou Huanan Pharmaceutical Group Co. Ltd. (Guangzhou, China), respectively. The UA assay kit was obtained from Nanjing Jiancheng Bioengineering Institute (Nanjing, China). Standards for esculetin (BCTG-0523), chicoric acid (BCTG-0328), caffeic acid (BCTG-0353) and epigoitrin (BCTG-0042) were received from Jiangxi Herbfine Co. Ltd. (Nanchang, China). Lobeline reference standard (001852) was purchased from European Pharmacopiea (Strasbourg, France). Other reagents were of analytical grade and synthesized in China. All primers (Table 3.1) used in this study were designed following Zhou's paper (249) and were synthesized by Genscript Co. Ltd. (Nanjing, China).

3.2.2 Plant materials

The commercially available dry matter of EF, Huizhongtang®, [whole plants of Viola yedoensis Makino (Viola, lot: 150309), whole plants of Taraxacum mongolicum Hand.-Mazz. (Taraxacum, lot: 150420), whole plants of Lobelia chinensis Lour. (Lobelia, lot: 150417), and Isatis indigotica Fort. roots (Isatidis, lot: 150317)] were obtained from Jiangxi Provincial Hospital of Traditional Chinese Medicine, Nanchang, China. The voucher specimens of four herb materials were deposited at the Herbarium of Jiangxi University of Traditional Chinese Medicine under number 150705.

3.2.3 Preparation of EF aqueous extracts and individual plant extracts

EF extract was prepared according to the Chinese Pharmacopoeia (39). The raw materials of all four herbs were mixed at equal quantities. The mixed raw materials were decocted with distilled water (1:10, w/v) under reflux for 2h. The supernatant was filtered and collected. The residue material was immediately extracted for another 1.5h using the same quantity of menstruum followed by filtering. The two filtrates were combined and concentrated under vacuum to half of the volume. The remaining solution was spray-dried. The yield of EF extract was 32.20%. The aqueous extracts of the individual herbs were prepared using the same process as the EF extract and presented yields of 21.30% for Viola,

25.10% for Taraxacum, 26.80% for Lobelia and 35.60% for Isatidis. The extracts were characterized according to the ChP and complied with the pharmacopeial specifications.

3.2.4 Analytical methods

3.2.4.1 High performance liquid chromatography (HPLC) condition

A Waters E2695 HPLC system with Welch Ultimate® XB-C18 column (4.6mm*250mm, 5μm) was used for analyze of Erding extract. The mobile phase consisted of buffer A (water containing 0.1% phosphoric acid) and buffer B (methanol) and the elution gradient was set as follows: 2% B (10min), 15% B (25 min), 24% B (40 min), 100% B (60 min), 2% B (65 min), 2%B (70min). The flow rate was 1.0 mL/min and the column temperature was 30 ℃. The wavelength of detection was set at 245 nm. All data were acquired and processed using Waters Empower3 software (Milford, MA, USA).

3.2.4.2 Standards and sample preparation

Stock solutions of esculetin, chicoric acid, caffeic acid, epigoitrin, and lobeline, was prepared in methanol. Aliquots of the standards were combined at 19.6 μg /mL, 12.0 μg/mL, 9.6 μg /mL, 9.6 μg /mL and 8.0 μg /mL, respectively. Erding extract was dissolved in water at the concentration of 6.21 mg/mL. All sample solutions were filtered through 0.45μm filters (Merck Millipore, Germany) and transferred into auto-sampler vials. A 10 μl aliquot was injected into system for analysis.

3.2.5 Animals

All studies were performed in accordance with the Regulations of Experimental Animal Administration issued by the State Committee of Science and Technology of the People's Republic of China, and they were approved by the University Committee on the Use and Care of Animals, Jiangxi University of Traditional Chinese Medicine (No: JXUTCM-20140311). Male Kunming mice (16±2 g) were purchased from the Shanghai Slac Laboratory Animal Co. Ltd. (Shanghai, China). These animals were housed in an air-conditioned room at a temperature of 22±2°C and relative humidity of 50%±20%. They were provided standard chow and water under a natural light-dark cycle and were allowed to acclimate to their environment prior to the experiments.

3.2.6 Treatment

All of the extracts were re-dissolved in distilled water, and the doses were expressed as grams of raw material per kilogram of body weight. The dose of EF extract was determined by pilot dose selection study. The doses of the individual plants were equal to their corresponding dose in the EF extract. Therefore, in the present study, the dose for each group was as follows: EF extract, 24 g raw materials/kg; Viola, 6 g raw material/kg; Taraxacum, 6 g raw material/kg; Lobelia, 6 g raw material/kg; and Isatidis, 6 g raw material/kg. Briefly, mice were administered with a volume of 20 mL/kg by gavage once

daily for five consecutive days. Food (but not water) was withdrawn from the mice 1 h prior to the administration except on the last day, when food was withdrawn 12 h before administration.

3.2.7 Evaluating the anti-inflammatory and analgesic effects of EF extract.

3.2.7.1 Effects on xylene-induced auricle inflammation in mice

Xylene-induced ear edema was performed with modifications to assess the anti-inflammatory effects in the mouse model. (250) Seventy male Kunming mice were randomly divided into seven groups (n=10): untreated disease, positive control (indomethacin 5 mg/kg) (251), EF extract, Viola extract, Taraxacum extract, Lobelia extract and Isatidis extract. Except for the untreated disease group, all of the mice were administered their respective dose by gavage once daily for five consecutive days. One hour after the final administration, 50 μL of xylene was applied on the posterior and anterior surface of the right ear of each mouse to induce inflammation while maintaining the left ear as a control. Thirty minutes after xylene application, all of the mice were sacrificed by cervical dislocation. Both the left and right ears were removed, and earplugs (diameter 8 mm) were obtained by circular section from the ears by a cork borer. Then, the degree of edema was assessed by the weight difference between the left and right ears of the same mouse and the data are presented with a boxplot. One-way ANOVA followed by

a Dunnett's test (Minitab 17, State College, PA, USA) was performed, and a p value<0.05 under α=0.05 considered to be a significantly difference compared with untreated disease mice. The anti-inflammatory ratio was evaluated as follows:

Anti-inflammatory ratio (%) = (1-edema degree of each group/edema degree of untreated disease group) *100%

3.2.7.2 Effects on acetic acid-induced writhing response in mice

The mice were treated according to the method described by Collier's et al. (252) with minor modifications. Seventy Kunming male mice were randomly divided into seven groups of ten each. The mice were orally administered the substances described above once daily for five consecutive days. One hour after the final dose, 0.2 mL of 0.75% acetic acid in saline was injected intraperitoneally into all mice. During the next 20 minutes, the number of writhing responses that occurred in each mouse was recorded to calculate the analgesic ratio. Compared with the writhing response of the untreated disease control group, a significant reduction in the writhing response of each treatment group was considered to be a positive analgesic effect. The writhing response times are presented in a boxplot. A t-test was performed to evaluate the differences between positive control group and untreated group. Statistically significant differences of writhing response among residual treated groups versus untreated group were tested by one-way ANOVA followed by Dunnett's

test. The differences with a p value<0.05 under α=0.05 were considered significant. The following formula was used to calculate the analgesic ratio:

Analgesic ratio (%)=(1-number of writhing response of each group/number of writhing response of untreated disease group)*100%

3.2.8 Hyperuricemic mouse model

A hyperuricemic animal model was induced by hypoxanthine combined with potassium oxonate with modification. (253) The mice were randomly divided into eight groups (n=10): untreated (healthy), untreated disease, positive control (Benzbromarone, 20 mg/kg) (254), EF extract, and four individual plant extract groups (Viola, Taraxacum, Lobelia, and Isatidis). Both hypoxanthine and potassium oxonate were freshly suspended in 0.5% w/v CMC-Na before use. The mice were intraperitoneally injected with hypoxanthine (375 mg/kg) and subcutaneously administered with potassium oxonate (62.5 mg/kg) 1 h before gavage administration once daily for five consecutive days to enhance the serum UA levels.

3.2.8.1 Blood and kidney sample collection of hyperuricemic mouse model

The blood samples were collected 1 h after the final dose and then allowed to clot at room temperature for 1 h before centrifugation at 1,400 x g for 10 min to obtain the serum, which was collected and stored at -20°C until analysis. After the blood sample collection, all of the mice were sacrificed by cervical dislocation. The kidneys were rapidly and carefully

separated on an ice plate, immediately frozen in liquid nitrogen, and stored at -80°C until assayed.

3.2.8.2 Determination of UA in serum of hyperuricemic mouse model

The UA levels in serum were determined by the phosphotungstic acid method (255) as described in the manufacturer's protocol. The UA levels of all the tested groups are illustrated in a boxplot. Statistically significant differences of the UA levels between the untreated disease group and treated groups were evaluated by one-way ANOVA followed by a Dunnett's test. Differences were considered to be statistically significant with an α equal to 5% ($p < 0.05$).

3.2.8.3 Assessing the expression of mRNA for URAT1 and OAT3 by real-time PCR in hyperuricemic mouse model

Real-time (RT) PCR was performed to evaluate the effects of the extracts on mRNA levels. Total RNA was extracted from homogenized mouse kidney using TRIzol® Reagent (Life Technologies, CA, USA) according to the manufacturer's protocol. The RNA concentration was determined by measuring the absorbance at a wavelength of 260 nm. Two micrograms of total RNA was used to synthesize cDNA by using SuperScript™ III Reverse Transcriptase (Invitrogen, CA, USA) following the manufacturer's recommendation. URAT1 and OAT3 mRNA levels were measured on a 7500 RT-PCR

system (Applied Biosystems®, CA, USA) with SYBR® Green PCR Master Mix (Life Technologies, CA, USA). The endogenous housekeeping gene GAPDH was used as a control for normalization. The primer sequences used in the PCR amplification are listed in Table 3.1. The cycle threshold (CT) levels of mRNA were measured and normalized with the individual GAPDH control CT values which presented as ΔCT. Each primer template for the individual samples was measured three times (n=3). The data of ΔCT are presented in scatterplots, and power of the sample size was calculated. Statistically difference between treated group to untreated disease group was evaluated by one-way ANOVA followed by a Dunnett's test. P-values lower than 0.05 were considered to be significant with α=0.05.

Table 3.1 Summary of the gene-specific real-time PCR primer sequences used in the experiments

Description	Gene bank	Forward primer (5′-3′)	Reverse primer (5′-3′)	Product size (bp)
mURAT1	NM_001 012 363.3	CCATGGCCTCCA GATTACCAC	TGCTGAGTCACAGC CAGTCAAG	93
mOAT3	NM_031 194.5	GCCAGGACACTC AGCTTGGA	GCAGTCATTAGCTCT GTGGTTGATA	120
mGAPDH	NM_008 084.2	TGTGTCCGTCGT GGATCTGA	TTGCTGTTGAAGTCG CAGGAG	150

3.3 Results

3.3.1 HPLC profile of Erding extracts and standards

The ChP only specifies esculetin as quality control marker for Erding Formula (39). Chicoric acid is another published compound found in EF (256) and is present in Taraxacum and Viola. Caffeic acid and epigoitrin, are markers for Taraxacum and Isatidis as per ChP monographs (39). Esculetin and lobeline are markers for Viola and Lobelia respectively (257-259).

Figure 3.1 shows chromatograms of the five standard solutions and Erding extract. As seen the five markers are well separated. Each marker can be found in the Erding Extract: epigoitrin (peak 1), esculetin (peak 2), caffeic acid (peak 3), chicoric acid (peak 4) and lobeline (peak 5).

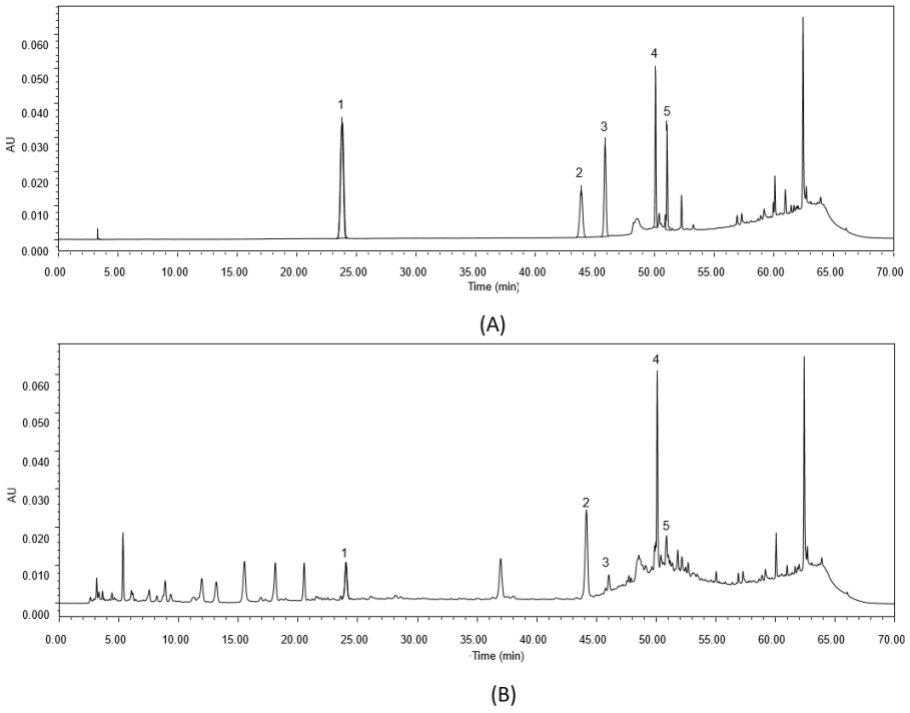

Figure 3.1 Chromatograms of five chemical marker compounds in reference mixture (a) and Erding extract (b) at detection wavelength (245 nm). 1, epigoitrin; 2, esculetin; 3, caffeic acid; 4, chicoric acid; 5, lobeline.

3.3.2 Effects on xylene-induced auricle inflammation in mice

The resulting ear edema of each group are presented in Figure 3.2. Compared with the untreated disease group, EF, Viola, Taraxacum, Lobelia and Isatidis extracts significantly inhibited the ear swelling caused by xylene ($P<0.05$) with inhibition ratios (%) of 52.0, 45.3, 45.3, 38.0, and 53.2, respectively. The positive control group (indomethacin) also exhibited a reducing ear swelling with an inhibition ratio of 28.3% but did not show a statistically significant difference from the untreated disease group.

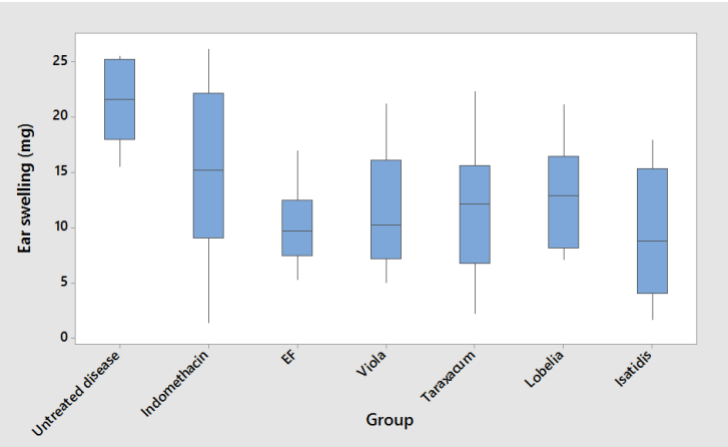

Figure 3.2 Effects of the EF extract and associated herbs on mice ear swelling induced by xylene (n = 10). The box represents the data from the 25th to 75th percentiles, and the line in the middle of box is the median. The end of bars represents the minimum and maximum values. EF, Erding Formula; Viola, Viola yedoensis Makino; Taraxacum, Taraxacum mongolicum Hand.-Mazz.; Lobelia, Lobelia chinensis Lour.; Isatidis, Root of Isatis indigotica Fort.

3.3.3 Effects on acetic acid-induced writhing responses in mice

The numbers of body writhing were recorded for 20 min after diluted acetic acid injection. The results are presented in Figure 3.3. Statistical analysis revealed that all treated groups (positive, EF, Viola, Taraxacum, Lobelia, Isatidis) significantly decreased the body writhing times caused by acetic acid ($P<0.05$) compared to the untreated disease group. The observed analgesic ratios (%) were 92.3, 61.3, 72.0, 58.7, 67.6, and 86.1, respectively.

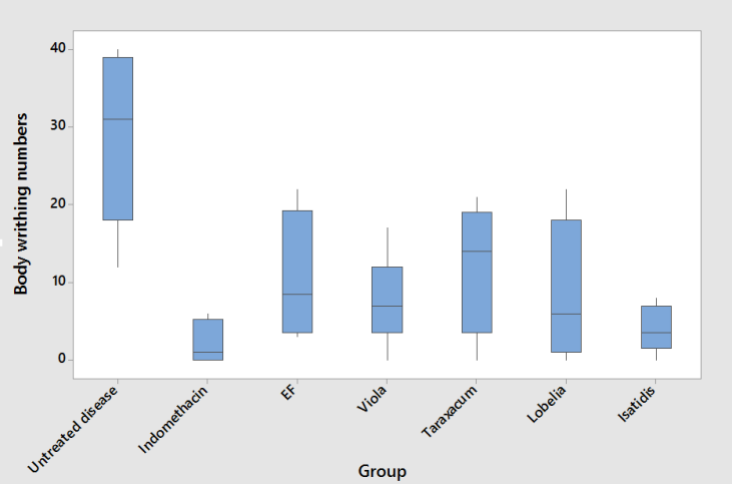

Figure 3.3 Effects of EF and associated herb extracts on the mouse acetic acid writhing model of pain (n = 10). The box represents the data from the 25th to 75th percentiles, and the line in the middle of box is the median. The end of bars represents the minimum and maximum values. EF, Erding Formula; Viola, Viola yedoensis Makino; Tarax- acum, Taraxacum mongolicum Hand.-Mazz.; Lobelia, Lobelia chinensis Lour.; Isatidis, Root of Isatis indigotica Fort.

3.3.4 Effects of the EF extract and the constituent herb extracts on the serum UA levels in the hypoxanthine and potassium oxonate-induced hyperuricemic mice

The effects of each extract group on the serum UA levels in hypoxanthine and potassium oxonate-induced hyperuricemic mice are shown in Figure 3.4. Statistical analysis showed that intraperitoneally injected hypoxanthine and subcutaneously administered potassium oxonate significantly enhanced the serum UA levels in the untreated disease group compared with the untreated mice. The EF and Viola groups significant decreased UA

levels ($P<0.05$) compared with untreated disease mice. The other treatments (positive control, Taraxacum, Lobelia, and Isatidis) did not reveal statistically significant differences from the untreated disease mice.

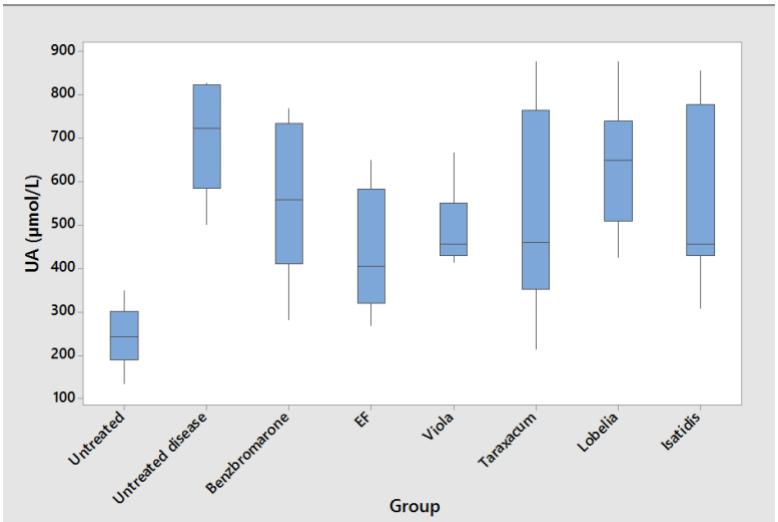

Figure 3.4 Effects of the EF extract and associated herbs on the serum UA levels in hypoxanthine and potassium oxonate-induced consecutive hyperuricemic mice (n = 10). The box represents the data from the 25th to 75th percentiles, and the line in the middle of box is the median. The end of bars represents the minimum and maximum values. EF, Erding Formula; Viola, Viola yedoensis Makino; Taraxacum, Taraxacum mongolicum Hand.-Mazz.; Lobelia, Lobelia chinensis Lour.; Isatidis, Root of Isatis indigotica Fort.

3.3.5 Effects of the extracts on mURAT1 and mOAT3 mRNA levels in hyperuricemic mice

The effects of the EF extract and associated individual herb extracts on the renal URAT1 and OAT3 mRNA levels in hyperuricemic mice are shown in Figure 3.5. Hypoxanthine

and potassium oxonate significantly inhibited the OAT3 ($P<0.05$) mRNA expression but did not show a significant effect on the URAT1 mRNA expression when untreated mice were compared to untreated disease mice. The positive control was benzbromarone, which significantly inhibited the URAT1 mRNA levels ($P<0.05$) but did not alter the OAT3 mRNA levels compared with those of the untreated disease group. EF and Viola down-regulated the expression of renal URAT1 mRNA ($P<0.05$) in hyperuricemic mice. Furthermore, EF, Taraxacum, and Isatidis significantly up-regulated the OAT3 mRNA levels ($P<0.05$) in hyperuricemic mice.

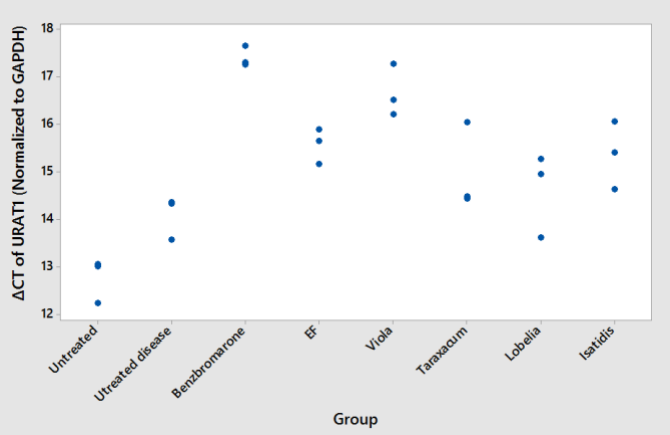

(A)

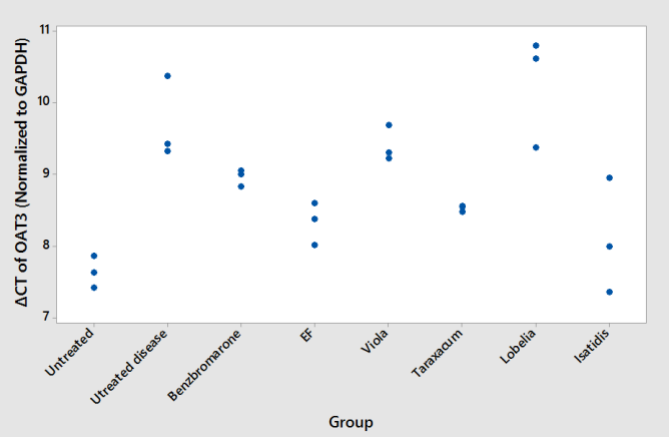

(B)

Figure 3.5 Effect of the EF extract and associated herbs on the mURAT1 (a) and mOAT3 (b) mRNA expression normalized to GAPDH in hyper- uricemic mice (n = 3). Abbreviation in the figure: EF, Erding Formula; Viola, Viola yedoensis Makino; Taraxacum, Taraxacum mongolicum Hand.-Mazz.; Lobelia, Lobelia chinensis Lour.; Isatidis, Root of Isatis indig-otica Fort.

3.4 Discussion

Inflammation is a potent symptom accompanied hyperuricemia. Long-term continually high UA levels will lead to inflammatory arthritis in joints, which called gout. Generally, non-steroidal anti-inflammatory drugs (NSAID) are the first choice for the treatment of the pain and inflammation caused by gout. Hence, one NSAID, indomethacin, was chosen as the positive control in the study of anti-inflammatory and pain controlling effects. In our study, the anti-inflammatory effect of indomethacin was not statistically different from the untreated disease group. However, it had a statistically significant effect on relieving pain. From TCM view, all four herbs (Viola, Taraxacum, Lobelia, and Isatidis) have heat-clearing properties. The original indication of EF mentioned in ChP is also heat clearing. The main actions of heat clearing are clearing away interior heat, purging fire, drying dampness, cooling blood and relieving toxic material. Thus, therapeutically, they can be considered as antipyretics (41, 42). According to these properties, both EF and four tested herbs should have the anti-inflammatory and analgesic effects. Hence, our results confirm the TCM properties with modern pharmacological experiments.

In rodents, the presence of uricase, which is not found in humans, maintains blood urate at a low level. (260) A high-purine diet can be another reason for hyperuricemic condition in humans. To simulated human's hyperuricemia condition in an experimental mouse model, the uricase inhibitor potassium oxonate was administered. The sole use of an inhibitor as a

model agent cannot completely simulate high purine uptake and induce a consistently high UA levels in mice. (261, 262) Therefore, in this study, we induced hyperuricemia in mice by administering the precursor of UA, hypoxanthine, together with potassium oxonate.

This study was primarily focused on the effects of the extracts on the urinary excretion of UA. Therefore, we selected benzbromarone, a uricosuric agent and an inhibitor of the URAT1 transporter as positive control (263). In Figure 3.4, the benzbromarone only exhibited a trend towards reduced UA levels, but a statistically significant compared to untreated disease group was not observed. This finding may be due to the effects of potassium oxonate which exceeded the hypouricemic effect of benzbromarone. A similar finding was reported by Kou et al. (264).

URAT1 and OAT3 are transporters relevant to uric acid reabsorption and excretion, which occur in the renal proximal tubule. Uric acid precursor, hypoxathine, and uricase inhibitor, potassium oxonate might not have an effect on UA reabsorption, this might be the reason why there was no difference in the URAT1 expression between the untreated mice and untreated disease mice, as shown in Figure 3.5A. However, the inhibition of uricase by postassium oxonate is relevant to UA excretion, which explained the detected OAT3 expression difference between untreated mice and untreated disease mice (Figure 3.5B). The positive control agent, benzbromarone, is an inhibitor of URAT1. Hence, it inhibited URAT1 expression but had no impact on OAT3 (Figure 3.5A and 3.5B). However, EF

reduced UA levels by inhibiting the UA reabsorption and enhancing the excretion of UA, which revealed a synergistic effect.

Our findings (Figures 3.2 to 3.5) indicated that the EF extract was the only treatment to show effects on all tested aspects: reducing serum UA levels, suppressing inflammation and pain, inhibiting URAT1 mRNA expression and enhancing OAT3 mRNA expression using modern pharmacological tests. In contrast, the individual herbs, Viola, Taraxacum, Lobelia and Isatidis, only showed partial effects. Similarly, the positive control drug, benzbromarone and indomethacin only work as uricosuric and NSAIDs, respectively. In addition, the findings of EF show the potential to treat gout through controlling the inflammation, pain and down-regulate the uric acid level at the same time.

Jun–Chen–Zuo–Shi is the basic theory of the properties of each medicinal herb, and it is used to guide the compatibility of traditional herbal formulas originating from Huang Di Nei Jing (Yellow Emperor's Classic). (23) Jun (emperor) herbs represent the principal component that targets the main cause or major symptom of a disease. The Chen (minister) herbs can enhance the therapeutic effects of Jun herb(s) and may be used to treat secondary symptoms. The possible adverse or toxic effects of Jun and Chen herbs can be reduced by Zuo (assistant) herbs, which can enhance the pharmacological effects of Jun and Chen herb(s) and may be used to treat accompanying symptoms. Shi (courier) herbs facilitate the delivery of the principal components to the target sites and harmonize the properties of other components in the formula. (23, 265)

Jun herbs are often easy to be identified because they present in a larger dose. In the tested EF, identifying the Jun herb is difficult because all four herbs are used in the same quantity. When EF is used to treat hyperuricemia, TCM practitioners regard Viola as the Jun herb, Taraxacum and Lobelia as the Chen herbs and Isatidis as the Zuo herb based on their properties and the patterns of the disease. In this study, Viola was the only herb that shows a significant effect on reducing UA levels. Thus, Viola may be regarded as the main herb of the formula in hyperuricemic treatment. Inflammation and pain are potent accompanying symptom of hyperuricemia, and all four herbs showed anti-inflammatory and analgesic effects. Therefore, Taraxacum, Lobelia and Isatidis could belong to the Chen and/or Zuo and/or Shi herb categories. For their classification, additional studies are needed.

3.5 Conclusion

TCM frequently uses complex herbal formulations (Fufang, 复方) to maximize treatment efficacy. Our study confirmed herbal compatibility of EF when used to treat hyperuricemia which is a new indication for this formula. These findings provide pharmacological insights into the effects of EF and the individual herbs on the excretion of UA. This study facilitates better understanding of TCM principles and theories using modern pharmaceutical approaches.

Chapter 4 Esculetin as bioactive marker: towards a rational scientific approach for the treatment of hyperuricemia using Traditional Chinese Medicine.

This study has been accepted as Jieyu Zuo, Wugang Zhang, Hui Jian, Nadia Araci Bou Chacra, Raimar Löbenberg. Esculetin as bioactive marker: towards a rational scientific approach for the treatment of hyperuricemia using Traditional Chinese Medicine in Brazilian journal of Pharmaceutical Sciences.

4.1 Introduction

Traditional Chinese Herbal Medicine (TCHM) has been used in China for centuries to prevent and cure disease (266). TCHM generally uses several medicinal herbs together, which is quite different from the monotherapies used in Western medicine (266, 267). As herbal medicines are gaining popularity worldwide, medicines of consistent and controllable quality are required (71). However, because the composition of herbal products is complex, defining appropriate markers for herbal products remains a challenge for scientists, regulators, and manufacturers (268). Markers are chemically defined constituents of herbal products used for quality control (QC) purposes. Accordingly, there are two categories of markers; active markers, which are accepted to contribute to the therapeutic effect; and analytical markers, which only serve analytical purposes (269). The use of bioactive markers in an herbal product is recommended for QC purposes (270). Therefore, for orally administered TCHMs, the components that are absorbed into the systemic circulation and contribute to the therapeutic effect should be considered QC markers (271).

Erding granules are an herbal formula containing *Viola yedoensis* Makino (Viola), *Taraxacum mongolicum* Hand.-Mazz. (Taraxacum), *Lobelia chinensis* Lour. (Lobelia), and root of *Isatis indigotica* Fort. (Isatidis) in equal quantities. According to the Chinese Pharmacopeia (ChP), the Erding formula is used to treat sore throat, carbuncles and boils

due to its heat-clearing and detoxifying properties. Esculetin is a QC marker for the original Erding granule indications listed above, based on content (39). This substance is a coumarin that exhibits antibacterial, anti-inflammatory, sedative, anticonvulsive, analgesic, antitussive, expectorant, and antiasthmatic effects (272). Hence, for the original indication of the Erding formula, esculetin could be regarded as an active marker. Previous studies found that this formula has the potential for treating hyperuricemia (273, 238). Hyperuricemia is an abnormally high concentration of uric acid (UA) in the body caused by a purine metabolic disorder. This disease is a risk factor for gout, hypertension, diabetes mellitus, stroke, kidney failure and cardiovascular events (53). Population-based studies have estimated a prevalence of up to 21.0% for hyperuricemia in Western countries, and the prevalence of hyperuricemia in mainland China is 13.3% (52, 53). In treating hyperuricemia, esculetin might only be an analytical marker instead of a relevant marker of *in vivo* activity.

Ultra-high performance liquid chromatography-quadrupole time-of-flight mass spectrometry (UHPLC/Q-TOF-MS/MS) is a very rapid, sensitive, powerful and reliable analytical method for characterizing the absorbed constituents and metabolites of TCHMs. This method can provide excellent chromatography separation with accurate mass measurements of precursor and metabolite ions to identify the main and/or trace substances in herbal formulas (274, 275).

Therefore, in this study, we aimed to identify whether the pre-existing marker esculetin is a potential bioactive and QC marker for the Erding formula when used to treat hyperuricemia by investigating its therapeutic effects in an animal model and identifying its metabolites in serum.

4.2 Materials and methods

4.2.1 Reagents

Oxonic acid potassium salt (Lot: BCBN6836V) was purchased from Sigma Aldrich (St. Louis, MO, USA). Allopurinol tablets (Lot: 05150603) were purchased from Shanghai SINE Pharm Co., Ltd. (Shanghai, China). The UA assay kit was obtained from Nanjing Jiancheng Bioengineering Institute (Nanjing, China). The esculetin (Figure 4.1) (BCTG-0523) standard was obtained from the Jiangxi Herbfine Co., Ltd. (Nanchang, China). Methanol and acetonitrile used in the experiments were of high-performance liquid chromatography (HPLC) grade and were obtained from Fisher Scientific (Pittsburgh, PA, USA). Other reagents were of analytical grade.

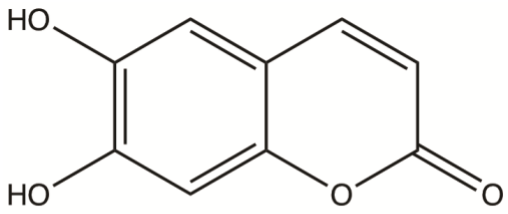

Esculetin

Figure 4. 1 Chemical structure of esculetin.

4.2.2 Plant materials

The commercial available dry components of Erding granules including Viola (lot: 150309), Taraxacum (lot: 150420), Lobelia (lot: 150417), and Isatidis (lot: 150317) were obtained from the Jiangxi Provincial Hospital of Traditional Chinese Medicine, Nanchang, China. The voucher specimens of the four herb materials were deposited at the Herbarium of the Jiangxi University of Traditional Chinese Medicine with the number 150705.

4.2.3 Preparation of the Erding aqueous extract

The Erding extract composition was based on the recipe in the ChP (39). All four herbs were mixed in equal quantities. The mixtures were decocted with distilled water (1:10, w/v) under reflux for 2 h, and the supernatant was filtered. The extraction process was immediately repeated with the residue material for another 1.5 h with the same quantity of menstruum and was followed by filtering. The combined two filtrates were concentrated under vacuum, and the remaining solution was spray-dried. The extract yield was 32.20% (w/w).

4.2.4 HPLC assessment of esculetin content in the Erding extract

The HPLC assay was performed with a slight modification in accordance with the ChP chapter on Erding granules (39). The esculetin content in the Erding extract was determined using a Shimadzu LC-20ADXR HPLC instrument (Kyoto, Japan) with a Welch Ultimate® (Shanghai, China) XB-C18 column (4.6 mm*250 mm, 5 μm). The mobile phase consisted of acetic acid: water: methanol (0.4:70:30, v/v). The flow rate was 1.0 mL/min, the column temperature was 25°C, and the injection volume was 10 μL. The UV detector wavelength was set to 353 nm according to the ChP (39). The run time for each sample was 20 min, and the retention time of esculetin was approximate 10.8 min. The standard esculetin solutions were prepared in methanol at concentrations ranging from 0.0042 to 0.042 μg/μL. The Erding extract was completely dissolved and prepared in water at 9.98 μg/μL. Then, all the solutions were filtered (0.45 μm) and transferred into auto-sampler vials. A 10-μL aliquot was injected into the system for analysis. Three replicates were performed on independent samples (n=3). The peak area was used to quantify the esculetin content in the Erding extract. All the data were acquired and processed using Lab Solution software (Shimadzu, Kyoto, Japan).

4.2.5 Animals

All the studies were performed in accordance with the Regulations of the Experimental Animal Administration issued by the State Committee of Science and Technology of the People's Republic of China and were approved by the University Committee on the Use and Care of Animals, Jiangxi University of Traditional Chinese Medicine. Specific pathogen-free male Kunming mice (body weight 14-16 g) were obtained from the Shanghai Slac Laboratory Animal Co., Ltd. (Shanghai, China). These animals were housed in an air-conditioned room at 22±2°C with a relative humidity of 50±20%. Standard food and water were provided under a natural light-dark cycle for 3 days to allow the animals to adapt to their environment before the experiment.

4.2.6 Hyperuricemic mouse model

The hyperuricemic animal model was induced by a uricase inhibitor, potassium oxonate (276). The mice were randomly divided into 5 groups (n=10): the untreated (healthy mice), untreated disease, positive control (allopurinol), Erding extract, and esculetin groups. Potassium oxonate was freshly suspended in 0.5% (w/v) sodium carboxymethyl cellulose (CMC-Na) solution before use. Except for the normal control mice, which received a 0.5% (w/v) CMC-Na solution, the mice were intraperitoneally injected with potassium oxonate (450 mg/kg) 1 h before the last dose to enhance the serum UA level.

4.2.7 Treatment

The extract was dissolved in distilled water, and the administered volume to mice was 20mL /kg body weight. The dose to mice was expressed as gram of extract per kilogram of body weight. In this study, the Erding extract dose was 7.73 g/kg body weight. The esculetin dose was equal to its content in the Erding extract. The esculetin was freshly suspended in water before use. The extract and esculetin were administered to the mice for five consecutive days by gavage. Simultaneously, allopurinol was administered orally at 15 mg/kg body weight as a positive control. The untreated and untreated disease groups were orally administered water for five consecutive days. Food but not water was withdrawn from the mice 1 h prior to administration except for the last day, on which the food was withdrawn 12 h before administration.

4.2.8 Blood sample collection and UA assay of hyperuricemic mice

Blood samples were obtained from eyes and collected in 1.5mL Eppendorf tubes 1 h after the last dose. All blood samples were allowed to clot at room temperature for 1 h before centrifugation at 1,400 x g for 10 min to obtain serum. The serum was collected and stored at -20°C until analysis. After blood sample collection, all the mice were sacrificed by cervical dislocation. The serum UA level was determined using the phosphotungstic acid method following the manufacturer's protocol (255). Except for the untreated and the

positive control groups, residual serum (untreated disease, Erding extract, and esculetin groups) were stored at -80°C until metabolite analysis.

4.2.9 Assessing Erding extract metabolites by UPLC/Q-TOF-MS/MS

4.2.9.1 UHPLC/Q-TOF-MS/MS system conditions

The esculetin metabolites of both Erding extract group and esculetin group were identified using a Shimadzu UHPLC LC-30AD system (Kyoto, Japan) coupled with an AB Sciex Triple TOF^{TM} 5600^{+} mass spectrometer (Foster City, CA, USA) with a DuoSpray^{TM} ion source. The serum samples were separated using a Waters ACQUITY® UPLC BEH C18 column (2.1 mm×100 mm, 1.7 μm, Milford, MA, USA) with an acetonitrile gradient at room temperature. The mobile phase consisted of phase A (water containing 0.1% formic acid) and phase B (acetonitrile), and the elution gradient was set as follows: 5%-65% B at 0.1-15.0 min, 65-100% B at 15.1-37.0 min, and 5% B at 37.1-40.0 min. The flow rate was 0.3 mL/min, and the injected sample size was 5 μL. The mass spectra were acquired in negative ion mode with the following parameters: ion spray voltage: -4500 V (negative ion), nebulizer gas: 50 psi, turbo gas: 50 psi, curtain gas (nitrogen): 25 psi, mass range: *m*/*z* 50-1250, accumulation time: 300.0 ms. The obtained data were analyzed using PeakView® Software 1.2 (Foster City, CA, USA).

4.2.9.2 UHPLC/Q-TOF-MS/MS sample preparation

The serum samples (100 μL each) from untreated disease, Erding extract, and esculetin groups were mixed with 500 μL of methanol in a 1.5-mL Eppendorf tube. The mixture was vortexed for 5 min and then centrifuged at 16,000 x g for 10 min. The supernatant was transferred to a new 1.5-mL Eppendorf tube and evaporated to dryness under nitrogen. The dry residue was re-dissolved in 100 μL of acetonitrile: water (50:50, v/v) and vortexed for 5 min. Finally, the resulting solution was filtered (0.45 μm) and transferred to an auto-sampler vial. A 5-μL aliquot was injected into the system for analysis. Three independent replicates were performed for each group (n=3).

4.2.10 Statistical analysis

All data are expressed as the mean ± standard deviation of the mean from 10 mice per group. Statistical comparisons were performed by a t-test with α=0.05 using Minitab 15 (State College, PA, USA).

4.3 Results and discussion

4.3.1 HPLC profile of the Erding extract

The correlation coefficient of the calibration curve (y=50054193.1217x-6563.9444, n=6) was 0.9999 over the 0.0042-0.042 μg/μL concentration range, with a coefficient variation

of 0.27%. The HPLC profile of the esculetin in the Erding extract is shown in Figure 4.2. The esculetin content in the Erding extract was 0.26±0.05% (w/w). For the QC of the Erding formula in the ChP, the content of esculetin should be no less than 0.09% (w/w) (39). In the present study, the esculetin quantity is sufficient for the QC of the Erding formula. As such, the extract could be used to evaluate therapeutic efficacy in a hyperuricemic animal model.

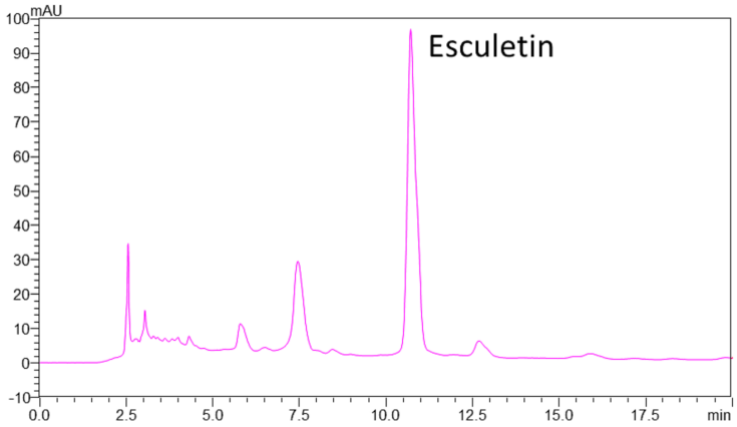

Figure 4. 2 Chromatogram of the esculetin (retention time: 10.8 min) in the Erding extract at the detected wavelength, 353 nm.

4.3.2 Effects of esculetin and the Erding extract in mice with potassium oxonate-induced hyperuricemic mice

The oxonate-induced hyperuricemic mouse model was used to investigate the hypouricemic effect of esculetin and Erding extract. This model has been used for decades to evaluate potentially medicinal substances that influence UA levels (242, 277).

Throughout evolution, humans have lost uricase, an enzyme that breaks down UA to allantoin, while other mammals, such as rodents, have not. To mimic this human condition in a rodent model, a uricase inhibitor, such as potassium oxonate, which blocks the conversion of UA to allantoin, was chosen to accumulate and increase UA levels in rodents (264). In this study, we used a colorimetric method in which a phosphotungstic reagent oxidized the UA to allantoin (255) to determine the UA levels. This method was used because other existing methods for measuring UA may be impacted by potassium oxonate, as it is used to determine the concentration of hydrogen peroxide formed by oxidizing UA to allantoin under the catalysis of uricase (278, 279).

According to the dose of Erding (7.73 g/kg body weight) and the content of esculetin in the Erding extract (0.26±0.05% w/w), the esculetin dose administered to mice was 20 mg/kg body weight. The effects of esculetin on the UA levels are shown in Figure 4.3. Examination of the results demonstrates that intraperitoneally injected potassium oxonate significantly elevated the serum UA levels (p-value<0.01, α=0.05). However, allopurinol and the Erding extract significantly decreased the UA levels in hyperuricemic mice (p-value<0.01, α=0.05). The orally administered esculetin suspension also reduced the UA levels compared with the untreated disease group (p-value<0.05, α=0.05). The results showed the treatment with either the Erding formula or esculetin was determined to exert hypouricemic effects by measuring the UA levels. The effect of Erding formula on

reducing UA levels has been shown in previous study (238). Esculetin can be one of the active compounds when Erding formula was used to treat hyperuricemia.

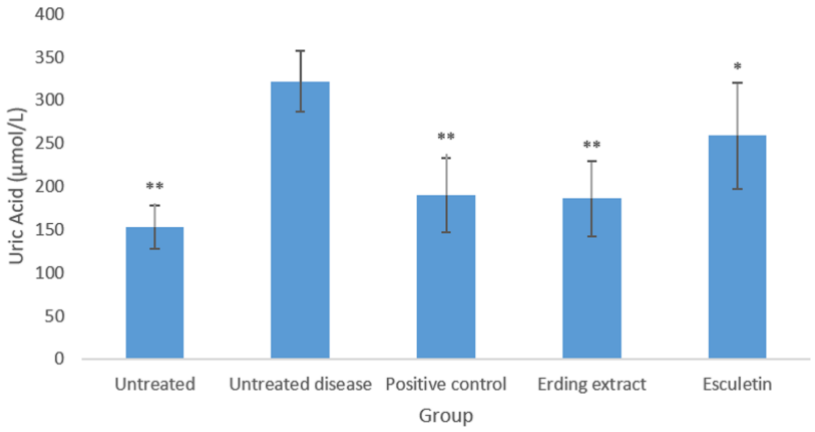

Figure 4.3 Effects of esculetin and the Erding extract on the serum UA levels in mice with potassium oxonate-induced hyperuricemia. *p-value<0.05 and **p-value <0.01 compared with the untreated disease group.

4.3.3 Identification of esculetin and its metabolites in serum using UPLC/Q-TOF-MS/MS

UHPLC/Q-TOF-MS/MS was employed to identify the metabolites of esculetin in dosed serum of mice. It is a very reliable analytical method for identifying trace amounts of absorbed constituents and metabolites of TCHM formulas. The method can provide excellent chromatography separation with accurate mass measurements of precursor and metabolite ions to identify the main and/or trace substances of herbal formulas. The

electrospray ionization-MS and collision-induced dissociation-MS/MS conditions were optimized to obtain suitable fragment ions for the identification of esculetin and its metabolites in serum. Welch UHPLC C18 (100 mm x 2.1 mm, 1.8 μm) and Waters ACQUITY UPLC BEH C18 (100 mm x 2.1 mm, 1.7 μm) columns were investigated to obtain a better resolution and peak shape from the substances. Finally, the negative ion mode and Waters ACQUITY UPLC BEH C18 column were selected according to the higher MS response of esculetin and its metabolites and the better separation efficacy. Formic acid was added to the mobile phase to inhibit insufficient substance ionization.

The full-scan mass spectrum of fragment ions in mouse serum after administration of the Erding extract or esculetin was compared with the spectra obtained from untreated disease serum samples to identify esculetin and its possible metabolites. As shown in Figure 4.4, the peaks detectable in the serum of Erding extract- and esculetin-treated hyperuricemic mice, but not in the serum of mice in the untreated disease control group, could be as attributed to esculetin and its metabolites. Using the PeakView 1.2 software EIC function, we obtained the relative peak areas (Figure 4.4) of esculetin and possible metabolites (M1-M6).

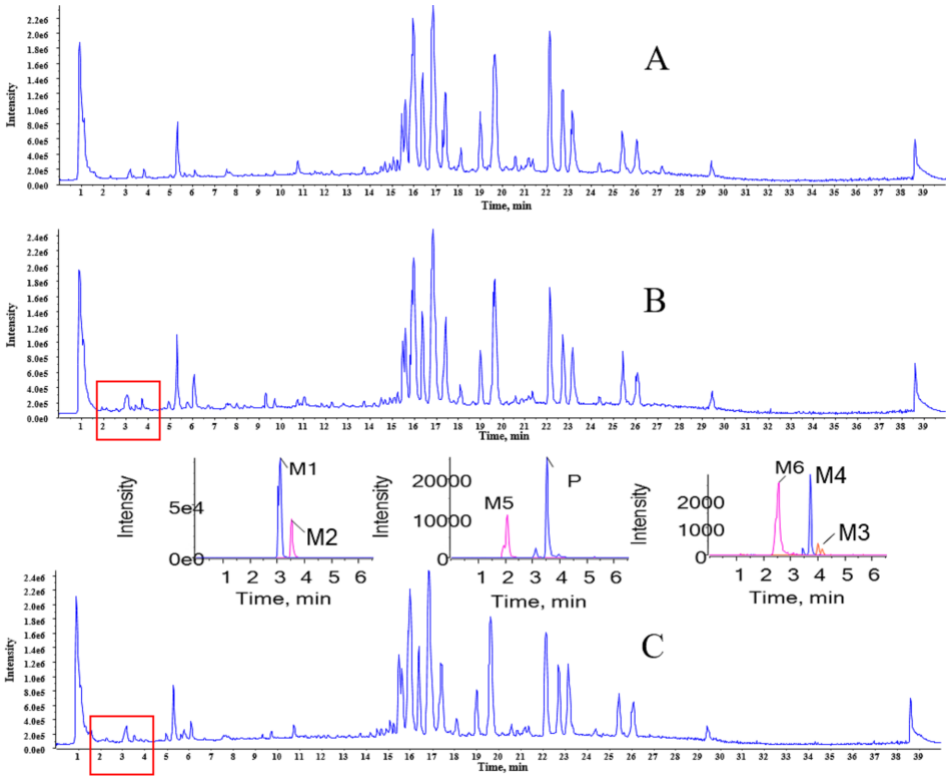

Figure 4.4 Total ion chromatogram and extract ion chromatogram of esculetin and metabolites from mice serum samples in negative ion mode. (A) Untreated hyperuricemic mice; (B) Erding extract-treated hyperuricemic mice; (C) esculetin-treated hyperuricemic mice. P: parent esculetin C9H6O4; M1: glucuronide metabolite C15H14O10, M2: sulfation metabolite C9H6O7S; M3: sulfation and methylation metabolite C10H8O7S; M4: glucuronide and methylation metabolite C16H16O10; M5: diglucuronide metabolite C21H22O16; M6: glucuronide and sulfation metabolite C15H14O13S.

The spectra of esculetin and its metabolites (M1-M6) exhibited $[M-H]^-$ at m/z 177.019, 353.051, 256.976, 270.992, 367.067, 529.084, and 433.008, respectively, which indicated the formulas were $C_9H_6O_4$ (esculetin), $C_{15}H_{14}O_{10}$ (M1), $C_9H_6O_7S$ (M2), $C_{16}H_{16}O_{10}$ (M3),

$C_{21}H_{22}O_{16}$ (M4), $C_{21}H_{22}O_{16}$ (M5) and $C_{15}H_{14}O_{13}S$ (M6), as shown in Table 4.1 and Figure 4.5.

Table 4. 1 Accurate mass measurement of protonated metabolites in mouse serum samples in negative ion mode.

No.	Formula	T_R (min)	Ion mode	Measured mass	Error (ppm)	Metabolite description
P	C9H6O4	3.52	$[M-H]^-$	177.019	-1.4	Parent esculetin
M1	C15H14O10	3.10	$[M-H]^-$	353.051	-0.4	Glucuronide
M2	C9H6O7S	3.52	$[M-H]^-$	256.976	-1.0	Sulfation
M3	C10H8O7S	4.01	$[M-H]^-$	270.992	-3.2	Sulfation and methylation
M4	C16H16O10	3.72	$[M-H]^-$	367.067	-0.9	Glucuronide and methylation
M5	C21H22O16	2.07	$[M-H]^-$	529.084	0.8	Diglucuronide
M6	C15H14O13S	2.54	$[M-H]^-$	433.008	-0.6	Glucuronide and sulfation

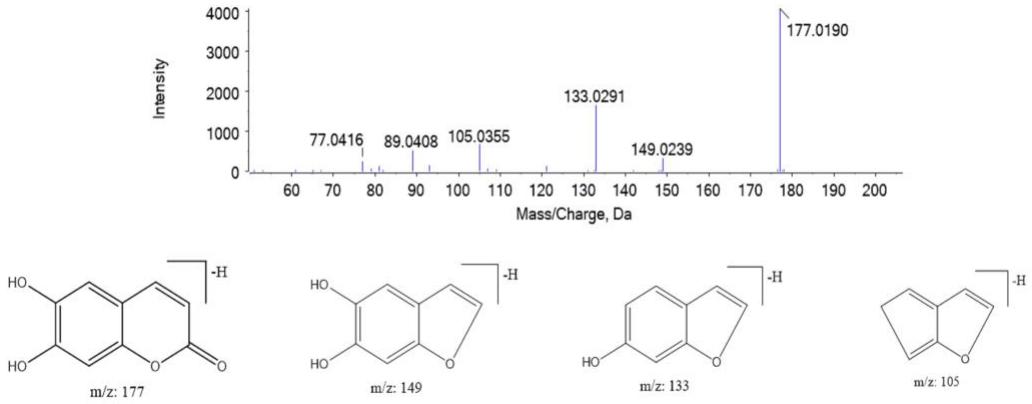
Intensity
4000
3000
2000
1000
0
177.0190
133.0291
77.0416
89.0408
105.0355
149.0239
60 70 80 90 100 110 120 130 140 150 160 170 180 190 200
Mass/Charge, Da
HO
HO
O
O
-H
m/z: 177
HO
O
-H
m/z: 149
HO
O
-H
m/z: 133
O
-H
m/z: 105

(A)

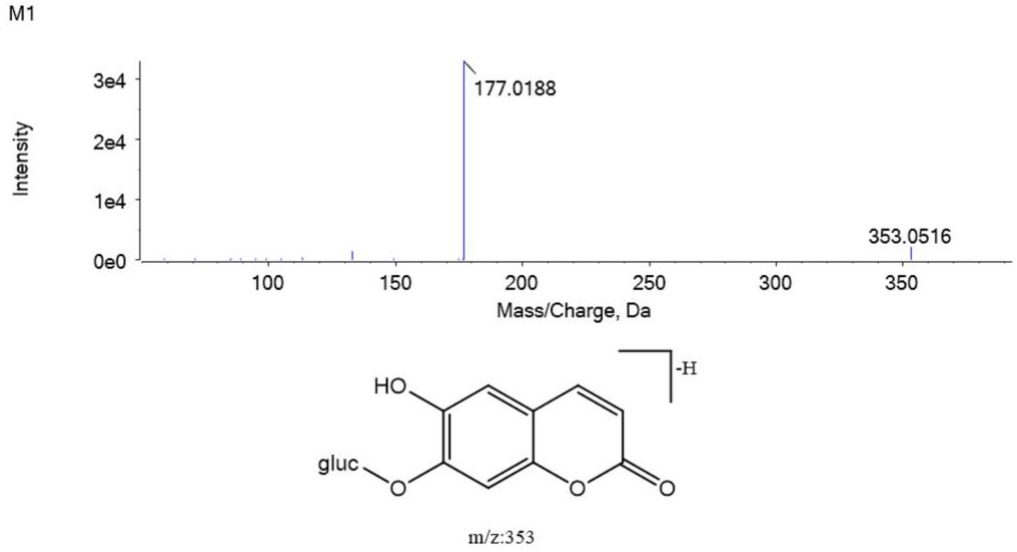
M1
Intensity
3e4
2e4
1e4
0e0
177.0188
353.0516
100 150 200 250 300 350
Mass/Charge, Da
HO
gluc
O
O
O
-H
m/z:353

(B)

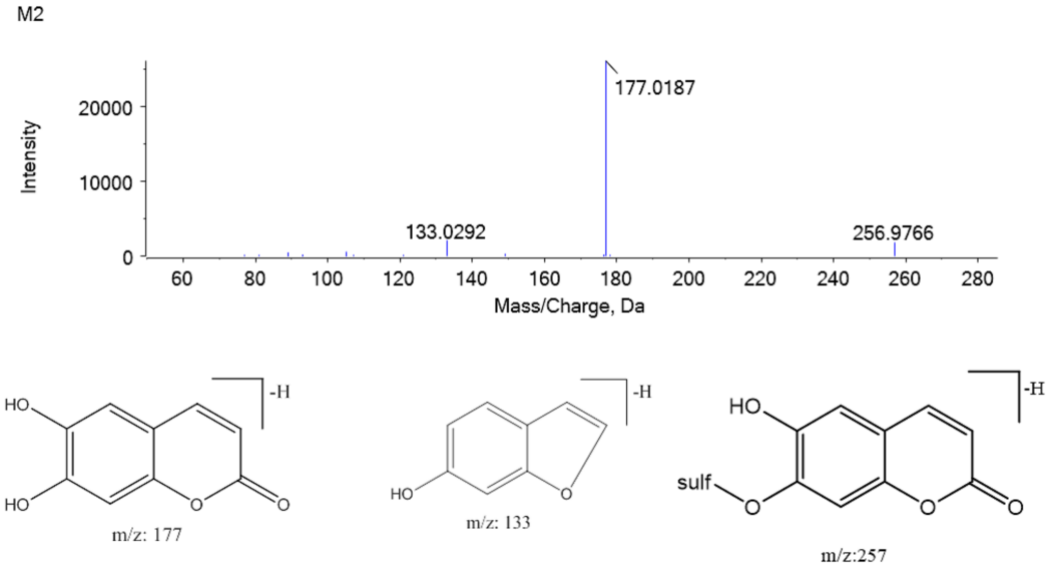
M2
Intensity
20000
10000
0
177.0187
133.0292
256.9766
60
80
100
120
140
160
180
200
220
240
260
280
Mass/Charge, Da
HO
HO
O
O
-H
m/z: 177
HO
O
-H
m/z: 133
HO
sulf
O
O
O
-H
m/z:257

(C)

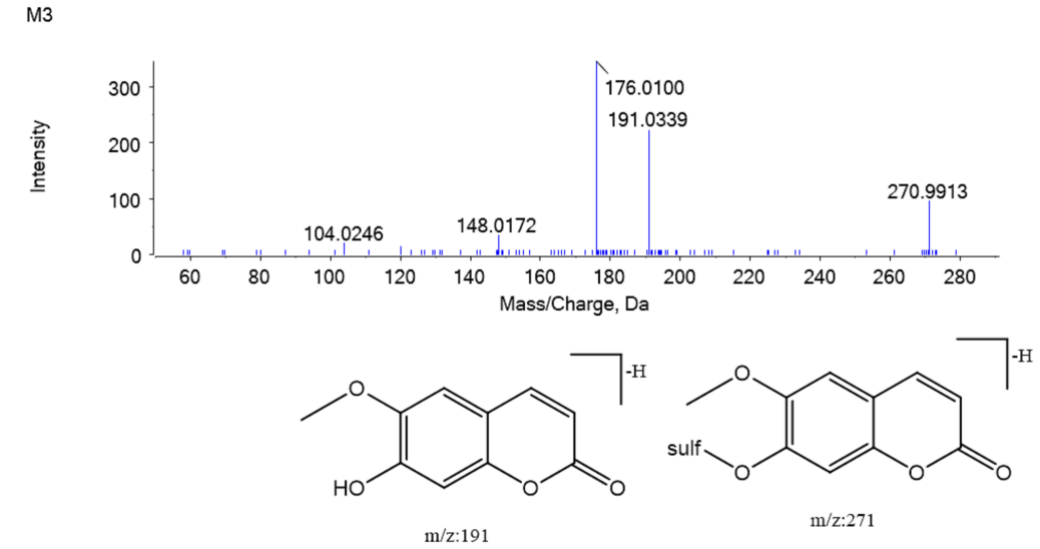
M3
Intensity
300
200
100
0
176.0100
191.0339
270.9913
104.0246
148.0172
60
80
100
120
140
160
180
200
220
240
260
280
Mass/Charge, Da
O
HO
O
O
-H
m/z:191
O
sulf
O
O
O
-H
m/z:271

(D)

M4

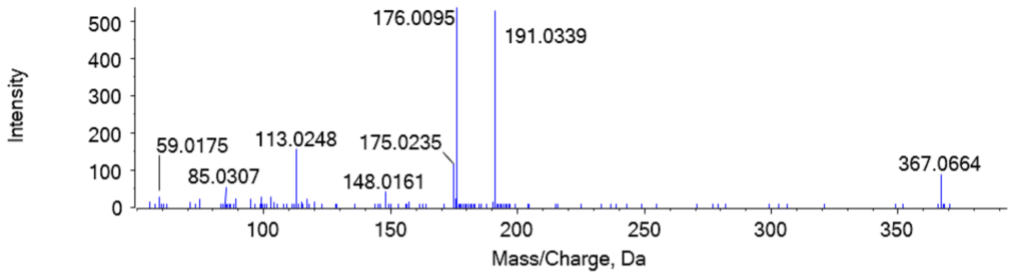

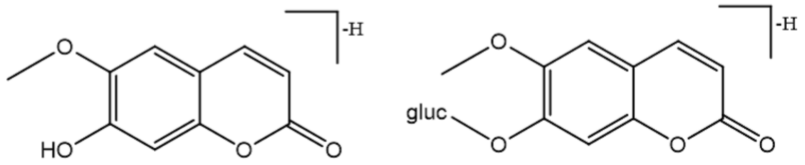

m/z:191 m/z:367

(E)

M5

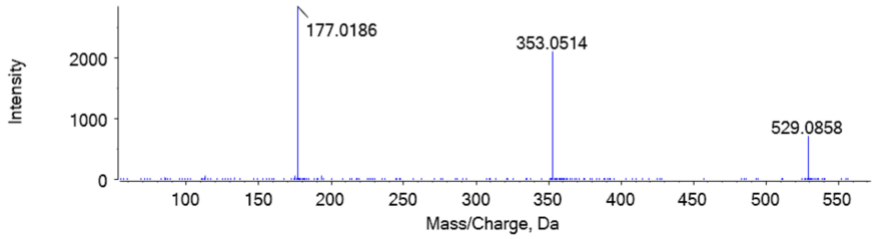

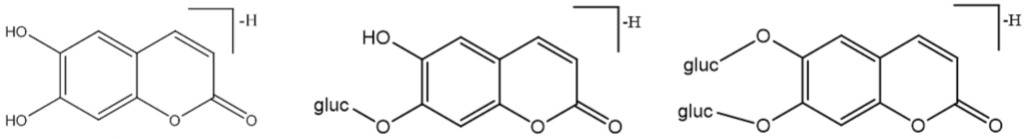

m/z: 177 m/z:353 m/z:529

(F)

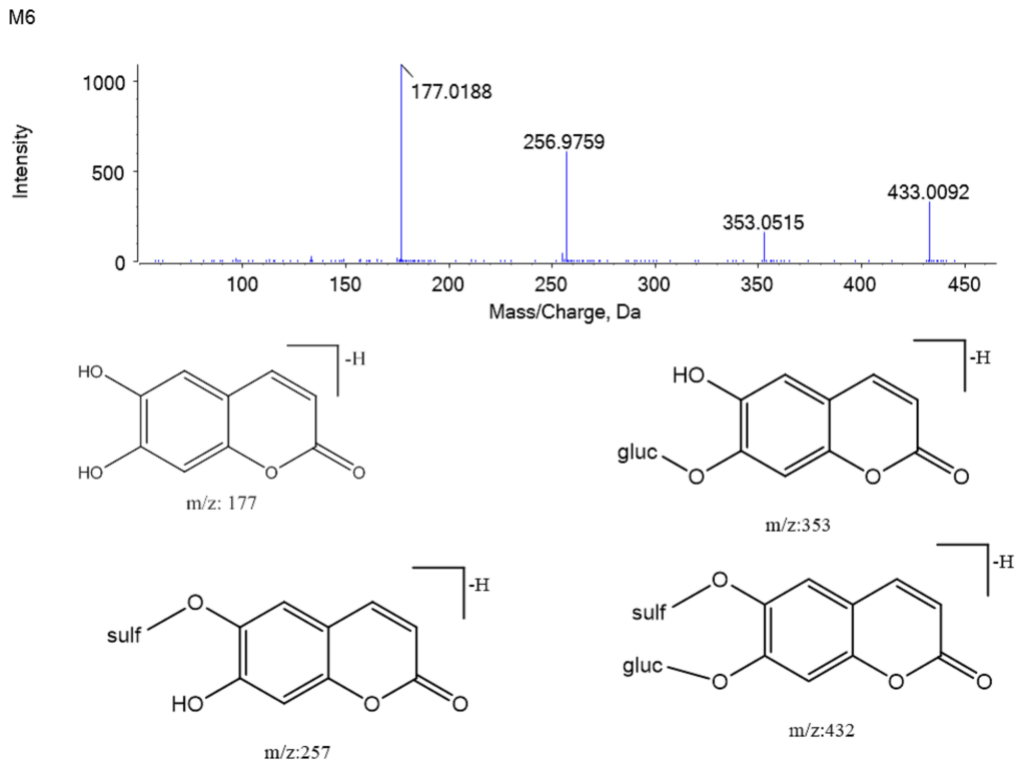

(G)

Figure 4.5 Mass spectra (MS/MS) of esculetin and its possible metabolites. (A) Esculetin, (B) M1, (C) M2, (D) M3, (E) M4, (F) M5, and (G) M6.

When a substance is absorbed into the circulation, enzymes cause further metabolization. Generally, the metabolism can be divided into two phases. Phase I reactions mainly include modification via oxidation, reduction, hydrolysis, cyclization, and decyclization, as well as oxygen addition or hydrogen removal. Phase II reactions mainly occur at carboxyl, hydroxyl, amino, and sulfhydryl groups via conjugation with such molecules as glutathione, sulfate, glycine, and glucuronic acid. (275)

Esculetin is the simplest coumarin, with two hydroxyl groups at carbons 6 and 7 (as shown in Figure 4.1), which suggests that the metabolism of esculetin *in vivo* is probably mainly

a phase II reaction because the hydroxyl groups may be easily substituted. In the MS/MS spectra (Figure 4.5), M1, M4, and M6 lost 176 Da to produce fragments at m/z 177, 191, and 257, respectively. M5 could lose 176 Da twice to produce fragments at m/z 353 and 177. These results indicate that one or two glucuronic acids were dissociated with metabolites. For M2, M3, and M6, the loss of SO3 (80 Da) suggests sulfate group conjugation. The loss of 14 Da (CH2) in M3 and M4 suggests the occurrence of methylation. Therefore, each or both of the hydroxyl groups of esculetin were modified by glycosylation, sulfation and/or methylation after drug administration and absorption from the gastrointestinal tract. The identification and characterization of M1-M5, as shown in Figure 4.5, is consistent with previously reported data from Ding et al. (280). We hypothesized that the glucuronide (M1) and sulfation (M2) metabolites of esculetin observed in serum may be the major metabolites in the circulation, depending on the intensity of the responses, as shown in Figure 4.4. These findings demonstrate that esculetin is one of the compounds within the Erding extract that is absorbed into the systemic circulation.

As the use of herbs and natural-origin products becomes more common not only in Asia but also in Western countries, proper product identification and QC is becoming increasingly necessary (281). For TCHMs, an ideal QC marker should not only be a high-content analytical marker but also a constituent responsible for the biological and/or therapeutic effects of the treatment (71). When a new therapeutic use for a formula is added,

whether the original marker is still a suitable bioactive marker or a new marker is required should be investigated. For the treatment of hyperuricemia, flavonoids are a group of phytochemicals that are potent alternatives to allopurinol (282-284). However, for the Erding formula, the content of flavonoids and/or a specific representative flavonoid are not clear. Additionally, according to the ChP and a previous study, esculetin is a pre-existing and relatively high-content QC marker for the Erding formula (39, 256). In this case, esculetin is an appropriate bioactive and QC marker for the Erding extract in treating hyperuricemia.

Most herbal products are orally administered; however, phytoequivalence is somewhat theoretical when herbs and their products are developed or compared with other products. In addition to the lack of established reference products, some specific issues should also be considered. Unlike conventional/orthodox Western medicines containing one or a few combinations of defined active pharmaceutical ingredients, herbal formulas are more complex, and most of the ingredients are unknown. Herbal extracts can contain constituents solely responsible for the therapeutic activity, chemically defined constituents possessing active markers, or chemical markers only. Hence, it is valuable to confirm that the most appropriate biomarker is chosen to ensure the quality of herbal products upon the addition of a new indication (268).

4.4 Conclusion

In this study, a rational scientific approach based on UHPLC/Q-TOF-MS/MS revealed that esculetin is an appropriate bioactive QC marker for Erding formula in hyperuricemia treatment. These findings will not only contribute to improve the modern TCHM preparations quality but also will help to ensure therapeutic efficacy for patients.

Chapter 5 Development of esculetin nanocrystals using wet media milling, DoE and subsequent solidification approaches

Partial of this study has been deposited in a patent (BR1020180695118) approved in Brazil.

5.1 Introduction

Over the last decade, nearly half of potential drug candidates have shown poor aqueous solubility (285). For the same reason, many active molecules originating from medicinal plants have not entered the drug development pipelines. The study in Chapter 4 proved that esculetin is a bioactive compound in an herbal formulation for the treatment of hyperuricemia. In addition, it has been shown to present antibacterial, anti-inflammatory, sedative, anticonvulsive, analgesic, antitussive, expectorant, and anti-asthmatic effects (272). However, to the best of our knowledge, esculetin has not been developed into novel drug products.

Nanosizing is a promising approach to improve the bioavailability of drug substances by increasing the surface area, reducing the diffusion layer thickness, and enhancing the saturation solubility (286-288). In recent years, among various nanosized drug delivery systems, nanocrystals have become recognized as an attractive approach due to their considerably simple components (drug substance, stabilizer and dispersion medium), easy production and high drug loading (97, 289). However, the smaller the particles are, the higher the surface free energy will be, leading to an increasing tendency for aggregation, which is a risk to the solubility and the dissolution rate (290). As reported by Ochi et al., the interaction between the drug and stabilizer molecules on the surface of the particles can

prevent aggregation (291). However, finding a suitable stabilizer is a challenging and critical step in the development of nanocrystals (292, 293).

In developing a new formulation, the process parameters and the interactions among them play an important role. Design of experiments (DoE) is a structured and organized statistical tool for providing in-depth knowledge of the relationships among the independent and dependent variables affecting the process and the output of that process (294). These relationships can be expressed by a mathematical and statistical equation, allowing the definition of a process and/or a product that consistently meets its quality characteristics with a high degree of assurance. The designed experiments and predictive equations are required to achieve a design space, which is defined by International Council for Harmonization (295).

Typically, the nanocrystal formulation is obtained in its liquid form, a nanosuspension. However, dried particulates are more stable and convenient for shipping and dispensing than liquids. To achieve a product with long-term stability, the production of powders via water elimination from the resulting suspension is a promising strategy. This solidification can prevent Ostwald ripening, subsequent agglomeration and/or chemical changes by hydrolysis (296). Spray-drying and freeze-drying are two commonly used solidification approaches to prepare ready-to-dissolve powders.

The aim of this study was to develop esculetin nanocrystals through stabilizer screening using laboratory-scale wet bead milling. The formulation and selected stabilizer was optimized by DoE and further characterized.

5.2 Materials and Methods

5.2.1 Materials

Esculetin (purity>98%) was purchased from Chengdu Herbpurify Co., Ltd. (Chengdu, China). Vitamin E polyethylene glycol succinate (trade name Kolliphor® TPGS), alkyl polyglucoside C8-C10 (trade name Plantacare® 2000 UP), poloxamer 407 (trade name Kolliphor® P407), poloxamer 188 (trade name Kolliphor® P188) and polyvinyl caprolactam–polyvinyl acetate–polyethylene glycol graft copolymer (trade name Soluplus®, MW=90,000-140,000) were kindly provided by BASF, Brazil (Sao Paulo, Brazil). A polyvinyl alcohol copolymer (Povacoat™, Type F, MW=40,000) was supplied by Daido Chemical Corporation (Osaka, Japan). Polysorbate 80 and sodium dodecyl sulfate (SDS) were purchased from Synth (Sao Paulo, Brazil). Ultrapurified water was obtained from a Milli-Q Millipore water apparatus (Sao Paulo, Brazil). All other reagents were analytical grade.

5.2.2 Methods

5.2.2.1 Nanocrystal preparation by small-scale wet milling

The esculetin nanocrystals were produced by a wet bead milling method using 3 cross stirring bars (Big Science, Inc., USA) layered vertically one over the other in a 10 mL glass vial (Figure 5.1) on a magnetic stirring plate (IKA-Werke GmbH & Co. KG, Germany) at 800 rpm at room temperature. The total suspension before milling was 7 g and consisted of esculetin, stabilizer and water. The milling beads were 0.1mm yttria-stabilized zirconium oxide balls, and the proportion of beads to suspension was 1.0:2.3 (v/v).

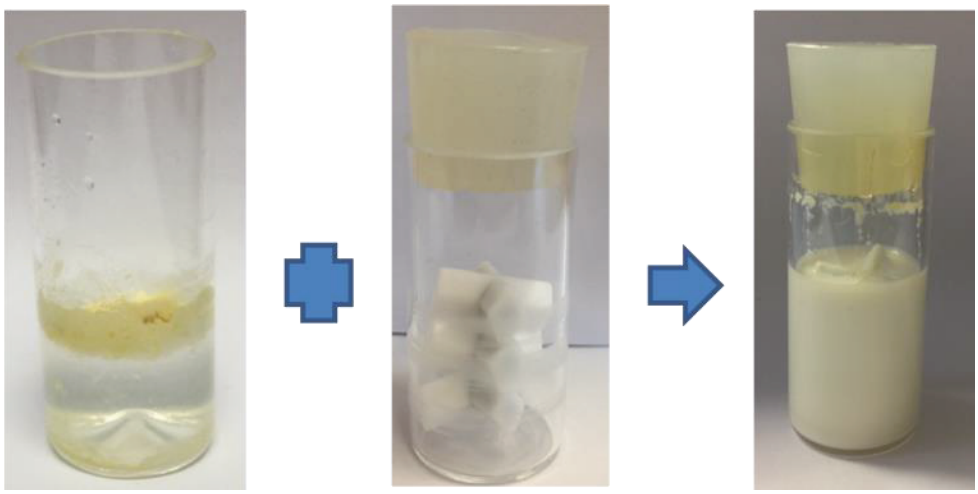

Figure 5.1 Picture of the device used for small-scale wet media milling and resulted nanosuspension.

5.2.2.2 Stabilizer screening

To select the most suitable stabilizer for esculetin nanocrystals, different surfactants and polymeric stabilizers were screened. The components of the different suspensions were 3.0% w/w esculetin, 3.0% w/w different stabilizers (0.2% w/w for SDS) and purified water added to a total of 7 g. The samples were withdrawn after 3 days of processing. The particle size and polydispersity index (PdI) were measured using a Zetasizer Nano ZS90 (Malvern Instruments, Malvern, UK). All samples were stored at 4°C for 7 days in capped glass vials to investigate stability.

5.2.2.3 Optimization of formulation parameters for esculetin-Povacoat™ nanocrystals

DoE was employed to investigate the influence variables on the response (particle size) and their relationships to obtain an optimized esculetin nanosuspension. The three independent variables selected were the esculetin content (% w/w), the Povacoat™ content (% w/w), and the milling time (days). The variables were studied at two levels, and the actual values for each level are shown in Table 5.1. A total of 14 experiments including 6 center points were conducted independently using a factorial design. Minitab 17 software (State College, PA, USA) was used for the regression and graphical analysis of the data and to estimate regression equation coefficients. For estimation of the quadratic terms, 6

axial points were added to the experiment, yielding a total of 20 formulations. The obtained regression equation was further verified by two independent confirmatory experiments. Multiple linear regression analysis and ANOVA were employed to develop a mathematical model. The general form of the model is represented by Equation (1):

$$Y = b_0 + b_1X_1 + b_2X_2 + b_3X_3 + b_4X_1^2 + b5X_2^2 + b_6X_3^2 + b_7X_1X_2 + b_8X_1X_3 + b_9X_2X_3 + b_{10}X_1X_2X_3 \quad (1)$$

where Y is the response (particle size), b_0 is the mean response (intercept), and $b_{1\text{-}10}$ are the regression coefficients derived from the experimental values. X_1, X_2, and X_3 are individual independent variables. X_1^2, X_2^2 and X_3^2 are quadratic effects indicating nonlinear correlations. X_1X_2, X_2X_3, X_1X_3 and $X_1X_2X_3$ are interaction effects revealing variations in the responses when 2 or more factors change simultaneously (297).

Table 5.1 Independent variables used for the experimental design of esculetin-Povacoat™ nanosuspensions.

Variables	**Levels**		
	−1	**0**	**1**
Esculetin (% w/w)	1.5	3.0	4.5
Povacoat™ (% w/w)	1.5	3.0	4.5
Milling time (days)	2.0	3.0	4.0

5.2.2.3 Solidification of optimized esculetin nanosuspensions

5.2.2.3.1 Spray-drying

A B-190 mini spray-dryer (Buchi, Flawil, Switzerland) was employed to spray-dry 40 mL of nanosuspension containing 5.0% w/w mannitol. The conditions were set as follows: inlet temperature, 120°C; feed rate, 3.5 mL/min; and air flow rate, 800 L/h. The resulting outlet temperature was 80°C. The nanosuspension was under constant stirring during the spray-drying process (298).

5.2.2.3.2 Freeze-drying

Approximately 1.5 mL of the final nanosuspension was immediately transferred into 10 mL glass flasks after preparation by wet milling. The bulking agent mannitol (5.0%, w/w) was added to prevent aggregation, and the flasks were partially closed with rubber stoppers. Then, samples were placed in a Dura-Stop MP & Dura-Top MP Tray Dryer MNL-031-A system (FTS system, New York, USA) individually for slow freezing (1°C/min) until the product temperature reached -40°C, where it was held for 5 min. The annealing heat treatment was applied with heating to -10°C and a 5-min hold at this temperature. Then, the primary drying was conducted at a product temperature of -25°C and a pressure of 100 mTorr for 24 h. In the secondary drying stage, the product was held at 10°C and the same pressure for 8 h.

5.2.2.4. Characterization

5.2.2.4.1 Particle size and size distribution analysis

5.2.2.4.1.1 Dynamic light scattering (DLS)

The particle size of the freshly prepared nanosuspension, spray-dried (SD) powder, and freeze-dried (FD) powder was measured in triplicate by photon correlation spectroscopy using a Zetasizer Nano ZS90 (Malvern Instruments, Malvern, UK). The SD and FD powders were redispersed in Milli-Q water to the same detected concentration of the fresh suspension. The z-average diameter and size distribution in terms of PdI were measured in triplicate for each sample.

5.2.2.4.1.2 Particle distribution of nanocrystals using laser diffraction (LD)

The initial size distribution of the drug substance, esculetin, and nanosuspension was measured by the LD method using a Cilas 1090 granulometer (Cilas, Orleans, France). The saturated esculetin solution was used as the dispersing medium, and insoluble esculetin was filtered prior to the measurements.

5.2.2.4.2 Morphological study of nanocrystals using transmission electron microscopy (TEM) and scanning electron microscopy (SEM)

The morphology and particle size of the SD and FD nanocrystals was observed using TEM (FEI Tecnai™ G2 Spirit Twin, Thermo Scientific, Hillsboro, OR, US) at 120 kV. After the powders were resuspended in water, one drop was placed on a 300-mesh ultrathin Formvar film grid. The grid was left to dry at room temperature before the test.

The morphology of the raw materials, SD and FD powder were observed respectively using SEM (FEI Quanta™ 250, Thermo Scientific, Hillsboro, OR, US). Samples were measured at an acceleration voltage of 15 kV, and images were acquired at a magnification of 400-6000x.

5.2.2.4.3 Thermal analysis

The crystallinity of solid-state of the esculetin, Povacoat™, mannitol, FD nanocrystal powder and SD nanocrystal powder was measured by differential scanning calorimetry (DSC) and thermogravimetric (TG).

5.2.2.4.3.1 DSC

DSC curves were obtained using a DSC-50 cell (Shimadzu, Kyoto, Japan). Approximately 2 mg of sample was weighed into an aluminum pan and hermetically sealed. The samples were heated to 350°C from 25°C at a rate of 10°C/min under nitrogen flow (100 mL/min).

5.2.2.4.3.2 TG

TG was performed using a TGA-51H model thermobalance (Shimadzu, Kyoto, Japan) in the temperature range 25-600°C at a heating rate of 10°C/min. Approximately 5 mg of sample was weighed into a platinum pan. The test was conducted under nitrogen flow (50 mL/min).

5.2.2.4.4 X-ray powder diffraction (XRPD)

The XRPD patterns of the esculetin, Povacoat, mannitol, FD nanocrystal powder and SD nanocrystal powder were measured using a Siemens/Bruker D5000 diffractometer (Billerica, MA, USA) to further investigate crystallinity (299). The radiation was generated by a Cu Kα filter with a wavelength of 1.54 Å at 40 kV and 40 mA. The diffraction angle range was set to $4° < (2°\theta) < 40°$ with a step time of 5 s and a step size of 0.02° per second.

5.2.2.5 Determination of saturation solubility

The saturation solubility of the esculetin, physical mixture (esculetin, Povacoat^{TM} and mannitol at the same nanocrystal concentration), and dried nanocrystal powders was analyzed in different media (simulated gastric fluid (SGF), acetate buffer (pH 4.5 USP), and simulated intestinal fluid (SIF)) by the shake-flask method (300). The buffers were prepared without enzyme following the United State Pharmacopeia procedure (301). The excess quantity of sample powder was added into 10 mL of aqueous medium and then

shaken at room temperature and 200 rpm for 72 h. The test for each medium was performed in triplicate. Then, the supernatant was obtained after centrifugation at 100,000 * g using an Airfuge® Air-Driven ultracentrifuge (Beckman Coulter, Brea, CA, USA) for 15 min and filtered through a 0.22 μm syringe filter (Millex GM, Millipore, Billerica, MA, USA). Finally, the content of esculetin in the samples was detected by high-performance liquid chromatography (HPLC) using a slightly modified Chinese Pharmacopeia HPLC method for esculetin (39). The mobile phase was methanol: water: acetic acid (30:70:0.4). The flow rate was 1 mL/min, and the injected sample size was 10 μL. UV detection was performed at 353 nm. The run time was 6.0 min, and the retention time was 3.5 min. A LiChrospher® 100 RP-18 column (12.5 × 5 mm, Merck, Darmstadt, Germany) with a guard column was used. The saturation solubility of each tested group is expressed as the mean ± standard deviation of the mean, respectively. A t-test was performed to evaluate the differences between nanocrystal group and raw material group of the same media using Minitab 18 (State College, PA, USA). The differences with a p value<0.05 under α=0.05 were considered significant.

5.2.2.6 Stability

The stability of the esculetin suspension, FD powder and SD powder was assessed in a short-term storage study. The samples were stored in capped glass vials at 4°C for a period of 6 months. The dried powders were redispersed in Milli-Q water before each

measurement. The particle size and PdI of the samples were measured on the day after preparation and after 30, 90 and 180 days.

5.3 Results

5.3.1 Stabilizer selection

Table 5.2 shows the mean particle size and PdI of all freshly produced suspensions prepared with Polysorbate 80, Poloxamer 188, Poloxamer 407, TPGS, Soluplus®, Plantacare® 2000, Povacoat™ or SDS as a stabilizer. Povacoat™ (size: 187.7±1.4 nm, PdI: 0.179±0.029) was selected as the stabilizer for use in the preparation of esculetin nanocrystals.

Table 5. 2 Formulation, preparation parameters, particle size and PdI of tested formulas, mean±standard deviation (n=3). (Tested aliquots withdrawn immediately after preparation).

Stabilizer type	Esculetin (% w/w)	Stabilizer (% w/w)	Milling time (days)	Particle size (nm)	PdI	After 7 days
Polysorbate 80	3.0	3.0	3.0	228.5±2.3	0.185±0.008	Precipitation
Poloxamer 188	3.0	3.0	3.0	249.1±6.1	0.248±0.041	Precipitation
Poloxamer 407	3.0	3.0	3.0	185.7±0.7	0.180±0.020	Precipitation
TPGS	3.0	3.0	3.0	193.5±3.3	0.177±0.013	Precipitation
Soluplus®	3.0	3.0	3.0	197.4±4.6	0.305±0.009	Precipitation
Plantacare® 2000	3.0	3.0	3.0	161.5±1.9	0.203±0.007	Precipitation
Povacoat™	3.0	3.0	3.0	187.7±1.4	0.179±0.029	195.3±1.6
SDS	3.0	0.2	3.0	259.6±2.4	0.241±0.010	Precipitation

TPGS: vitamin E polyethylene glycol succinate; SDS: sodium dodecyl sulfate

5.3.2 Experimental design for esculetin-Povacoat™ nanocrystals

The influence of the esculetin concentration (% w/w), Povacoat™ concentration (%w/w) and milling time (days) on the particle size was evaluated using 14 independent experiments. The experimental particle size (nm) values at the design points are shown in Table 5.3. The average particle sizes for the nanocrystal formulations varied from 183.9 to 337.3 nm, and all PdIs were <0.3 (data not shown).

ANOVA (Table 5.4) revealed both linear and nonlinear significance ($p<0.001$, $\alpha=0.05$). Thus, the existing factorial design was modified into a response surface methodology

(RSM) by adding face-centered axial points (Table 5.5) in order to analyze a model with quadratic terms.

Table 5.3 Composition and particle size of esculetin-Povacoat™ nanocrystals. The sizes are presented as the mean±standard deviation (n=3).

Formulation	Esculetin (% w/w)	Povacoat™ (%w/w)	Milling time (days)	Experimental particle size (nm)
1	4.5	4.5	2.0	308.4±1.3
2	3.0	3.0	3.0	190.4±0.9
3	3.0	3.0	3.0	189.3±1.2
4	4.5	4.5	4.0	224.2±4.0
5	4.5	1.5	4.0	295.2±4.3
6	3.0	3.0	3.0	183.9±1.7
7	1.5	1.5	4.0	195.4±1.3
8	3.0	3.0	3.0	178.9±2.6
9	3.0	3.0	3.0	192.5±1.3
10	4.5	1.5	2.0	337.3±6.4
11	1.5	1.5	2.0	233.7±0.9
12	3.0	3.0	3.0	189.6±1.7
13	1.5	4.5	2.0	309.0±5.5
14	1.5	4.5	4.0	203.9±1.9

Table 5.4 ANOVA test for significance in the evaluation of esculetin nanocrystal particle size containing the esculetin concentration (% w/w), Povacoat™ concentration (% w/w) and milling time (days) as variables in a factorial design.

Source	DF	SS (adj)	MS (adj)	F-value	*p*-value
Model	6	40826.5	6804.4	197.8	<0.001
Linear	3	15346.4	5115.5	148.7	<0.001
Esculetin (% w/w)	1	6221.7	6221.7	180.9	<0.001
Povacoat™ (% w/w)	1	32.4	32.4	0.9	0.364
Milling time (days)	1	9092.3	9092.3	264.4	<0.001
2-Way interactions	2	5700.6	2850.3	82.9	<0.001
Esculetin (% w/w) * Povacoat™ (% w/w)	1	4218.2	4218.2	122.6	<0.001
Povacoat™ (% w/w) * Milling time (days)	1	1482.4	1482.4	43.1	<0.001
Curvature	1	19779.6	19779.6	575.1	<0.001
Error	7	240.8	34.4		
Lack-of-fit	2	112.8	56.4	2.2	0.206
Pure error	5	128.0	25.6		
Total	13	41067.3			

DF: degrees of freedom; SS (adj): adjusted sum of squares; MS (aj): adjusted mean square; F-value: statistics F-test; *p*-value: level of significance.

Table 5.5 Added face-centered axial points in the existing factorial design: composition and particle size of esculetin-Povacoat™ nanocrystals.

Formulation	Esculetin (% w/w)	Povacoat™ (%w/w)	Milling time (days)	Experimental particle size (nm)
15	1.5	3.0	3.0	209.7±0.7
16	4.5	3.0	3.0	260.8±1.0
17	3.0	1.5	3.0	188.5±1.3
18	3.0	4.5	3.0	189.6±1.2
19	3.0	3.0	2.0	207.0±1.5
20	3.0	3.0	4.0	163.4±0.6

The average particle size for the nanocrystal formulations varied from 163.4 to 337.3 nm, and the PdIs were <0.3 (data not shown). An outline of ANOVA for the response surface model of the esculetin nanocrystals is shown in Table 5.6. The *p*-value of 0.058 (α=0.05) indicated that the lack-of-fit is non-significant compared to the pure error. As shown in Table 5.6, the esculetin concentration, milling time and their quadratic terms showed the significant effect on the response ($p<0.05$, α=0.05), while the impact of the Povacoat™ concentration was not significant ($p=0.596$, α=0.05) in the studied range (1.5 to 4.5% w/w). Both the interaction of esculetin with Povacoat™ and Povacoat™ with milling time illustrated significant effects ($p<0.05$, α=0.05) on particle size. The residual analysis in ANOVA revealed constant variances, random variables and normal distributions (data not shown).

The best-fitting model was selected from the regression analysis according to a comparison of the following statistical parameters: the coefficient of determination (R^2), adjusted

coefficient of determination (adj-R^2), and predicted coefficient of determination (pred-R^2). The R^2 shows how well the terms fit a curve or line. The adj-R^2 not only indicates how well terms fit a curve or line but also adjusts for the number of terms in a model. The pred-R^2 indicates the probability of the experimental value being close to that calculated from the model (302). The R^2 (98.33%), adj-R^2 (97.11%), and pred-R^2 (92.86%) values indicated that the model was suitable (Table 5.7). Thus, this model was selected for the response surface analysis.

Table 5.6 ANOVA to test for significance in the evaluation of esculetin nanocrystal particle size containing the esculetin concentration (% w/w), Povacoat™ concentration (% w/w) and milling time (days) as variables in the response surface design.

Source	DF	SS (adj)	MS (adj)	F-value	*p*-value
Model	8	48812.1	6101.5	80.85	<0.001
Blocks	1	418.5	418.5	5.55	0.038
Linear	3	17356.8	5785.6	76.66	<0.001
Esculetin (% w/w)	1	7518.6	7518.6	99.63	<0.001
Povacoat™ (% w/w)	1	22.5	22.5	0.30	0.596
Milling time (days)	1	9815.7	9815.7	130.07	<0.001
Square	2	22539.3	11269.7	149.33	<0.001
Esculetin (% w/w) * Esculetin (% w/w)	1	11957.1	11957.1	158.44	<0.001
Milling time (days) * Milling time (days)	1	415.2	415.2	5.50	0.039
2-Way interactions	2	5700.6	2850.3	37.77	<0.001
Esculetin (% w/w) * Povacoat™ (% w/w)	1	4218.2	4218.2	55.90	<0.001
Povacoat™ (% w/w) * Milling time (days)	1	1482.4	1482.4	19.64	0.001
Error	11	830.1	75.5		
Lack-of-fit	6	702.2	117.0	4.57	0.058
Pure error	5	128.0	25.6		
Total	19	49642.2			

DF: degrees of freedom; SS (adj): adjusted sum of squares; MS (aj): adjusted mean square; F-value: statistics F-test; *p*-value: level of significance.

Table 5.7 Test for significance of the coded regression coefficients and fit indices of the selected model in the assessment of esculetin nanocrystal particle size containing the esculetin concentration (% w/w), Povacoat™ concentration (% w/w) and milling time (days) as variables in the response surface model.

Term	Coefficient	C-SD	T-value	*p*-value	VIF
Constant	183.99	2.93	62.75	<0.001	
Blocks					
1	5.15	2.19	2.36	0.038	1.06
Esculetin (% w/w)	27.42	2.75	9.98	<0.001	1.00
Povacoat™ (% w/w)	-1.50	2.75	-0.55	0.596	1.00
Milling time (days)	-31.33	2.75	-11.40	<0.001	1.00
Esculetin (% w/w) * Esculetin (% w/w)	61.51	4.89	12.59	<0.01	1.58
Milling time (days) * Milling time (days)	11.46	4.89	2.35	0.039	1.58
Esculetin (% w/w) * Povacoat™ (% w/w)	-22.96	3.07	-7.48	<0.001	1.00
Povacoat™ (% w/w) * Milling time (days)	-13.61	3.07	-4.43	<0.001	1.00

C-SD: coefficient of standard deviation; *p*-value: level of significance. Standard deviation (SD)=8.69; coefficient of determination (R^2)=98.33%; adjusted coefficient of determination (adj-R^2)=97.11%; predicted coefficient of determination of the adjusted model (pred-R^2)=92.86%.

Equation (2), the regression equation for the particle size in terms of uncoded variables, was derived as follows:

$$\text{Particle size} = 411.8 - 115.1\ X_1 + 56.8\ X_2 - 72.9\ X_3 + 27.3\ X_1^2 + 11.5\ X_3^2 - 10.2\ X_1X_2 - 9.1\ X_2X_3 \quad (2)$$

Where X_1 is the concentration of esculetin (% w/w), X_2 is the concentration of Povacoat™ (% w/w), and X_3 is the milling time (days).

From the contour plot of the regression model, as well as the surface plot (Figures 5.2 and 5.3), when the milling time was set to 3 days, particles smaller than 200 nm were revealed using esculetin concentration between 1.5 and 3.5% w/w, while the Povacoat™ concentration in the tested range did not have an influence. When the Povacoat™ concentration was held at 3.0% w/w and the esculetin concentration was within 1.5-3.5% w/w, particles smaller than 200 nm were obtained with 2.5-4.0 days of milling. When the esculetin concentration was kept at 3.0% w/w, within the tested range, only the milling time (more than 2.5 days) affected the particle size.

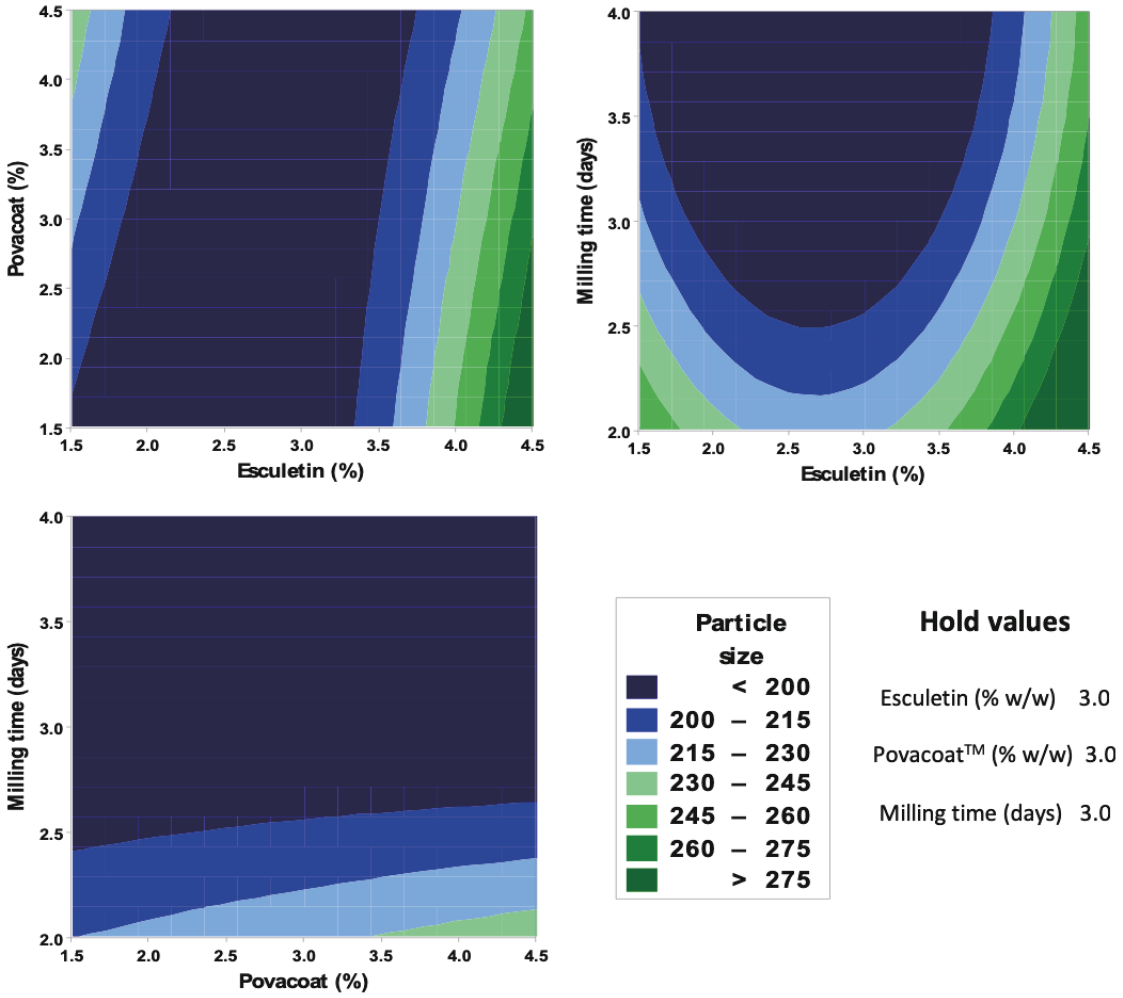

Figure 5.2 Contour plot of the regression model for particle size (nm) containing the following three variables: esculetin concentration (% w/w), Povacoat™ concentration (% w/w) and milling time (days). Each figure illustrates two of three variables, with the other variable fixed at 3.0.

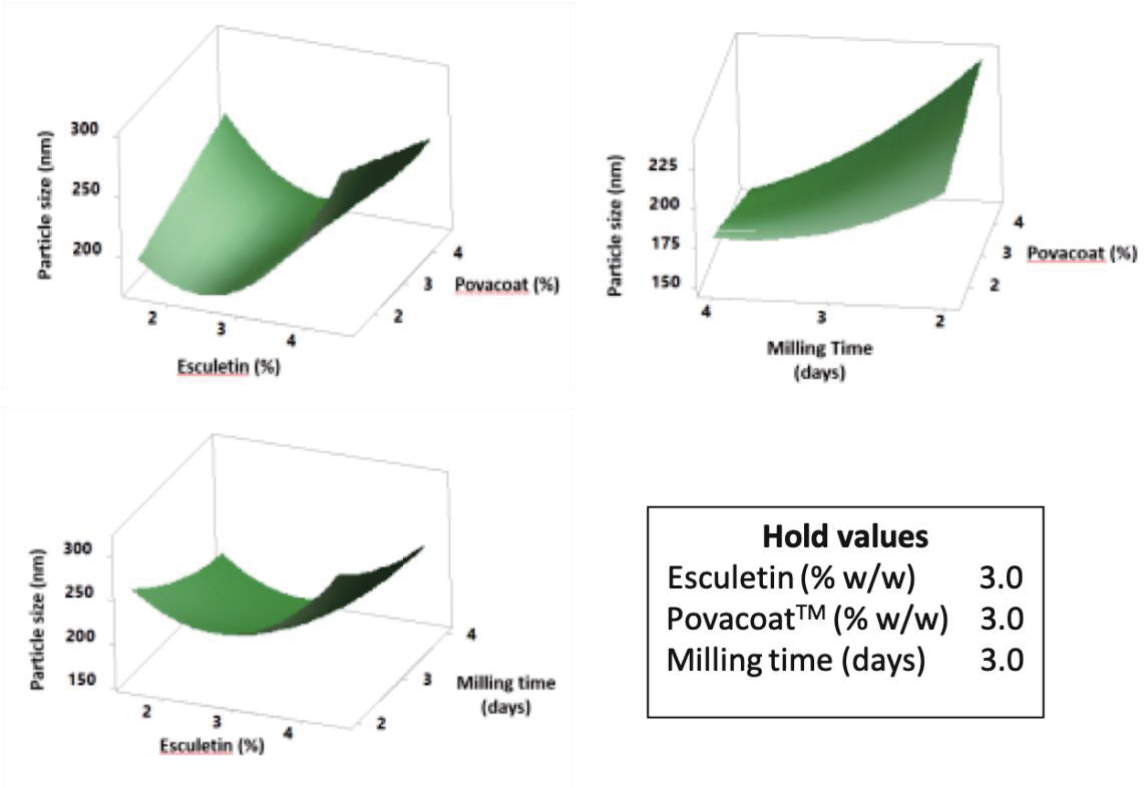

Figure 5.3 Three-dimensional surface plots of the regression model for particle size (nm) containing the following three variables: esculetin concentration (% w/w), Povacoat™ concentration (% w/w) and milling time (days). Each figure illustrates two of three variables, with the other variable fixed at 3.0.

The experimental and predicted values of particle size of the two independent experiments used to verify equation (2) are shown in Table 5.8. The values predicted from the equation are similar to the experimental values. From the tested ranges of the three variables, 3.0% w/w esculetin, 3.0% w/w Povacoat™ and 3.0 days of milling time were selected for further characterization.

Table 5. 8 Independent confirmatory experiments used to verify the model equation.

Esculetin (% w/w)	Povacoat™ (% w/w)	Milling time (days)	Particle size (nm)	
			Experimental	Predicted
4.5	4.5	3.0	261.4±1.4	258.4
1.5	1.5	3.0	210.0±3.7	206.4

5.3.3 Characterization of optimized esculetin nanocrystals

5.3.3.1 Particle size and size distribution

The mean particle size of the freshly prepared esculetin nanosuspension was 191.9±1.6 nm (PdI: 0.162±0.008), as determined by DLS. LD revealed that the diameter at 10, 50 and 90% of the cumulative population distribution was 60.0±0.0 nm, 220.0±10.0 nm and 500.0±70.0 nm, respectively.

The particle size and PdI of the esculetin nanosuspension before and immediately after spraying-drying and freeze-drying are shown in Table 5.9. The results show that the particle size remained similar after the solidification process.

Table 5.9 Particle size and PdI of nanocrystals before and immediately after spray-drying and freeze-drying, respectively.

Sample	Before drying		Immediately after drying	
	Size (nm)	PdI	Size (nm)	PdI
Spray-drying	199.1±2.8	0.172±0.035	213.7±4.0	0.174±0.033
Freeze-drying	194.4±1.2	0.178±0.006	194.5±0.7	0.164±0.008

PdI: polydispersity index.

5.3.3.2 Morphological study

Particles within the range from 100-500 nm were observed in both redispersed SD and FD powder under TEM (Figure 5.4). The particles were uniform, and no agglomeration was observed in either redispersed powder. Figure 5.5 illustrates SEM images of esculetin raw material (Figure 5.5A), SD nanocrystal agglomerates (Figure 5.5B), and FD nanocrystal agglomerates (Figure 5.5C). From the particle morphology, SD yielded nearly spherical agglomerates with depressions evident on the external surface, while the FD particles were flat, angular and irregularly shaped.

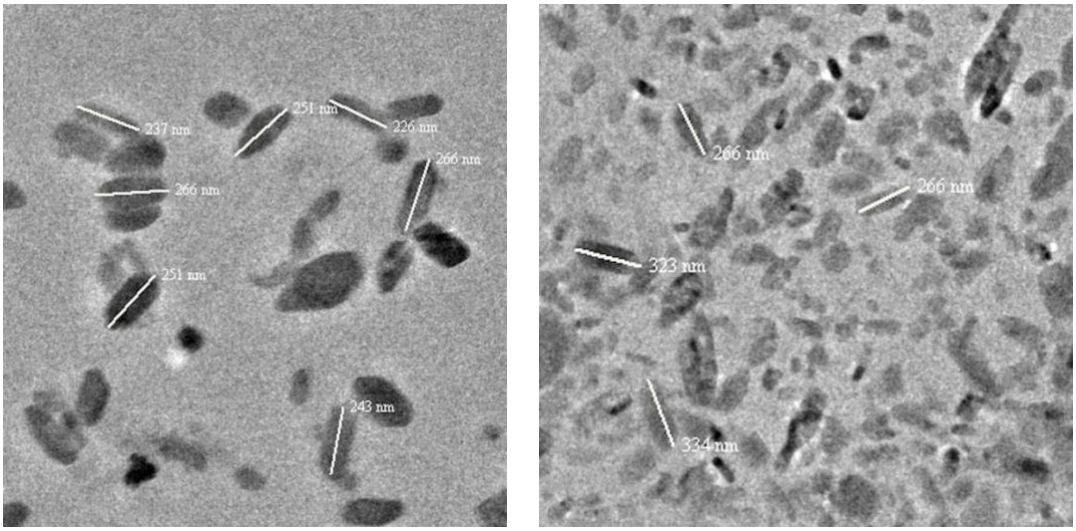

(A) (B)

Figure 5. 4 Transmission electrons micrograph of spray-drying nanocrystal (A) and freeze-drying esculetin nanocrystal (B).

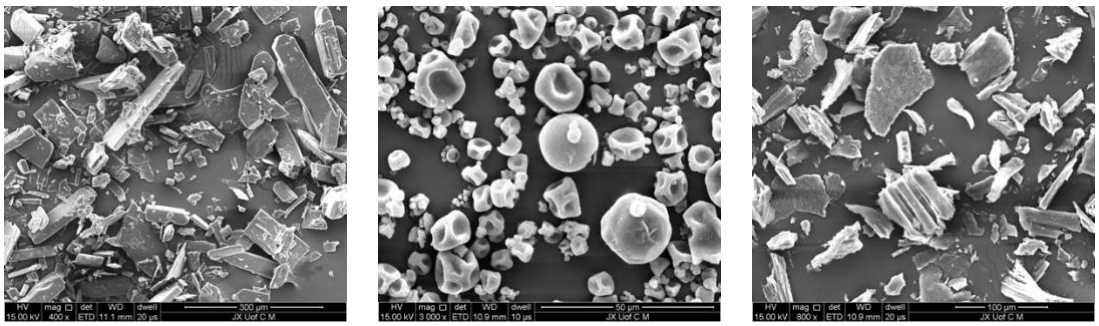

(A) (B) (C)

Figure 5. 5 Scan electron micrograph of esculetin raw material (A), spray-drying nanocrystal powder (B), and freeze-drying nanocrystal powder (C).

5.3.3.3 Thermal analysis

The thermal properties of the esculetin raw material, excipients, and formulations were evaluated by TG and DSC, and the curves are shown in Figures 5.6 and 5.7. From the DSC curves, the melting temperature (T_{onset}) of esculetin and mannitol were detected at 270°C and 165°C, respectively. The DSC curve of Povacoat^{TM} presented a broad endothermic event in the range of 50 to 100°C, which was associated with a mass loss of approximately 2.0% observed by TG. An additional endothermic event was observed between 160 and 211°C.

Similar thermal behavior was observed for both SD and FD powders, with two endothermic events in the DSC curves; the first was between 133°C and 160°C (T_{peak}=154°C), and the latter was in the range from 160-170°C (T_{peak}=164°C). In both samples, the characteristic melting peak of esculetin was not observed. However, the loss of residual moisture in the

range from 25-70° (~2.0%) was revealed by TG for the FD powder, and it was not observed in the TG curve of the SD sample. The thermal decomposition process of the esculetin raw material occurs in two stages in the following temperature ranges with the respective weight losses: 200-360°C (Δm_1=70%) and 360-600°C (Δm_2=30%). The thermal decomposition process of SD nanocrystals occurs as follows: 200-330°C (Δm_1=60%) and 330-600°C (Δm_2=30%). For the FD nanocrystals, the thermal decomposition process also occurs in two weight loss steps: 200-330°C (Δm_1=60%) and 330-600°C (Δm_2=40%).

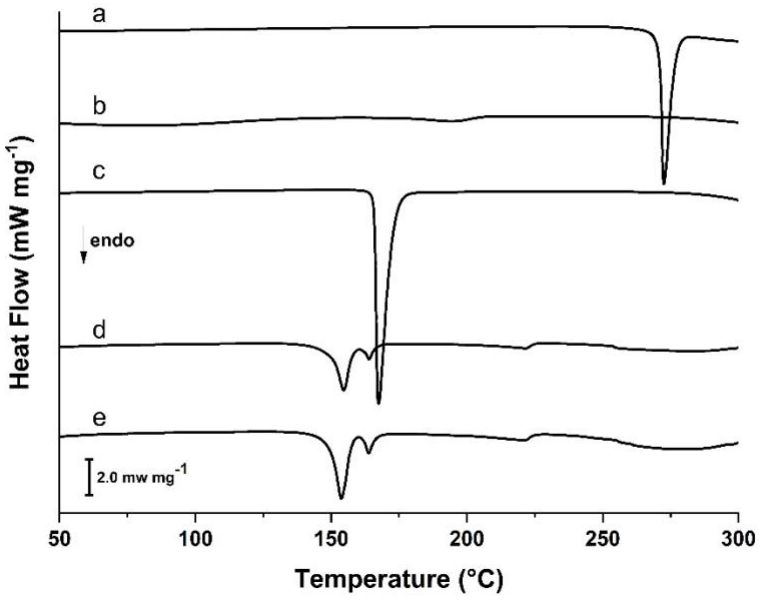

Figure 5. 6 Differential scanning calorimetry curves for esculetin (a), Povacoat^{TM} (b), mannitol (c), spray-dried nanocrystals (d) and freeze-dried nanocrystals (e).

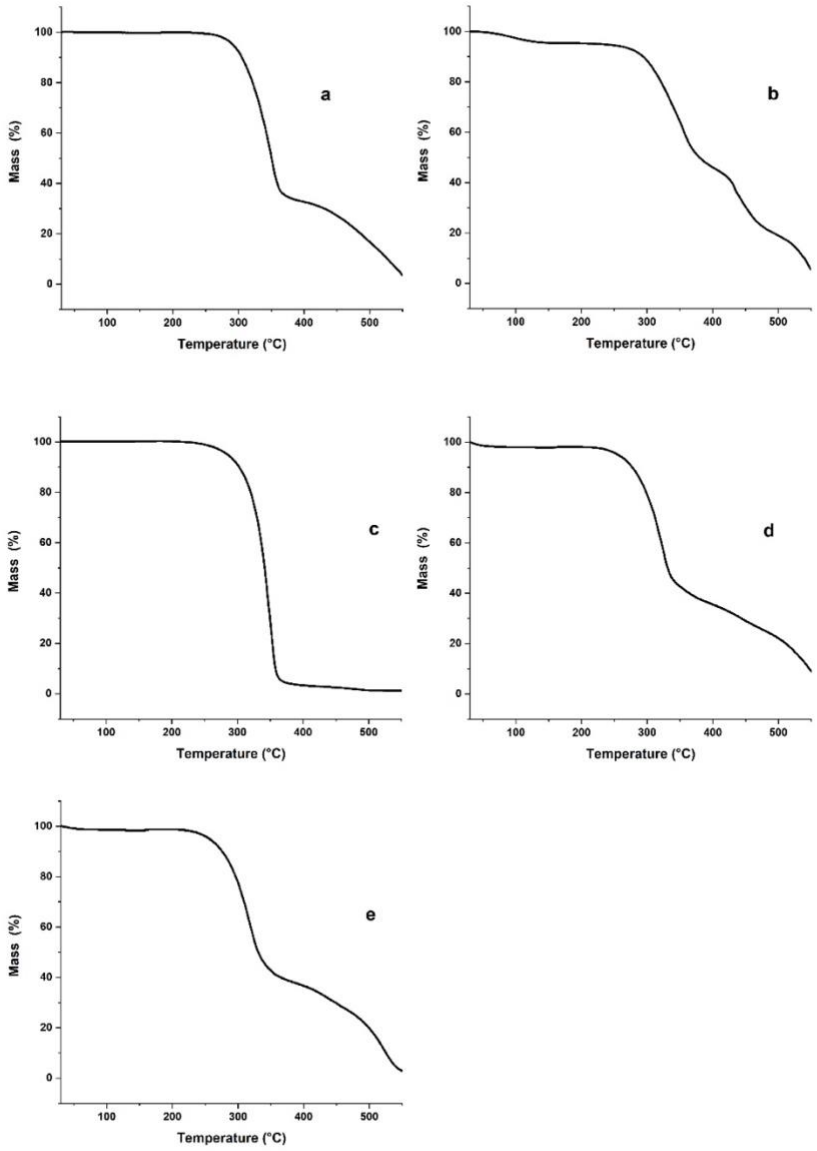

Figure 5. 7 Thermogravimetric curves for esculetin (a), Povacoat^{TM} (b), mannitol (c), freeze-dried nanocrystals (d), and spray-dried nanocrystals (e) obtained under dynamic nitrogen (50 mL/min) at a heating rate of 10°C/min.

5.3.3.4 XRPD

The XRPD patterns are shown in Figure 5.8. The normalized diffractogram of crystalline esculetin exhibited characteristic peaks at 2θ values of 10.8, 13.5°, 15.2°, 17.2°, 28.0° and 29.8°. Several esculetin peaks were reduced, shifted or not observable in the patterns of either the FD or SD nanocrystals.

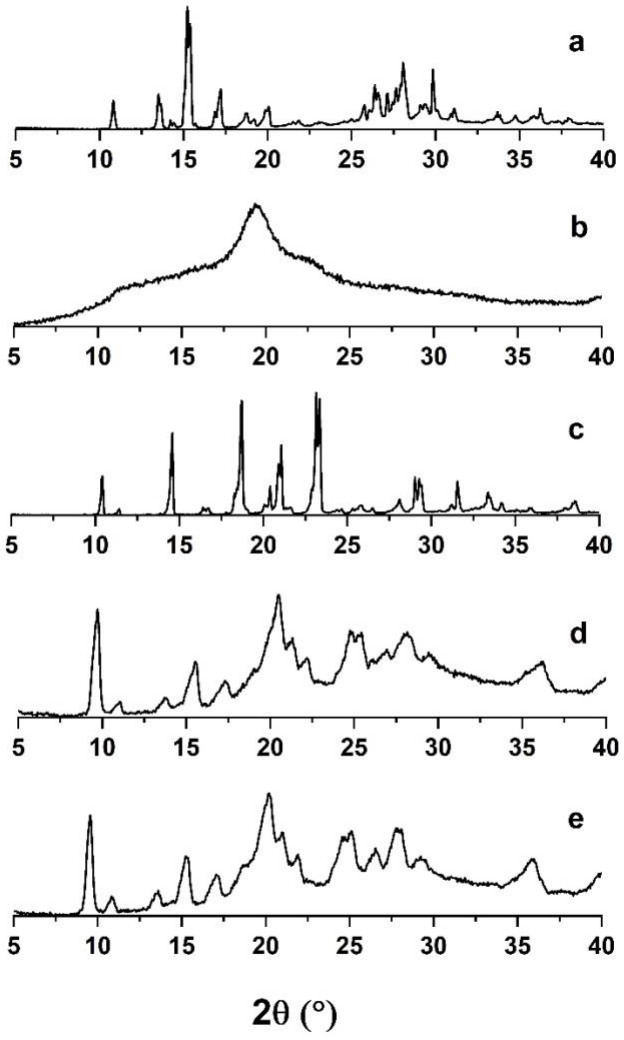

Figure 5. 8 Normalized X-ray powder diffractograms of esculetin (a), Povacoat^{TM} (b), mannitol (c), freeze-dried nanocrystals (d), and spray-dried nanocrystals (e).

5.3.4 Saturation solubility

The saturation solubility of the esculetin raw material, physical mixture, and nanocrystal powders in different media (SGF without enzyme, pH 4.5, and SIF without enzyme) are listed in Table 5.10. Compared with the esculetin raw material, no increased was observed

in the saturation solubility of the physical mixture. In different media (SGF, pH 4.5, and SIF), the saturation solubility of esculetin in the nanocrystals significantly increased (*p-value<0.05, α=0.05) by 1.2-fold, 1.4-fold and 1.5-fold, respectively, compared with the esculetin raw material.

Table 5. 10 Saturation solubility of the esculetin raw material, physical mixture and nanocrystals in different media (mean±standard deviation, n=3).

Media	Esculetin solubility (μg/mL)			
	Raw material	Physical mixture	Esculetin nanocrystals	Fold increase (nanocrystal-raw material)
SGF	140.0±3.3	140.4±4.2	172.3±7.4*	1.2
pH 4.5	146.3±7.4	142.8±3.1	203.6±2.6*	1.4
SIF	184.5±3.6	180.2±5.0	270.6±2.6*	1.5

SGF: simulated gastric fluid, pH 4.5: acetate buffer, SIF: simulated intestinal fluid. *p-value<0.05 under α=0.05 when compared with the raw material group in the same media.

5.3.5 Stability

The particle size and PdI of the nanosuspension, SD powder and FD powder stored at 4°C were assessed over a period of 180 days. Samples were collected after preparation and after 30, 90 and 180 days, and the results are summarized in Table 5.11. Both the particle size and PdI were similar for the nanosuspension, SD powder and FD powder stored at 4°C throughout the testing period.

Table 5.11 Short-term physical stability study of the esculetin nanosuspension, spray-drying powder and freeze-drying powder at 4°C over 180 days.

Sample	0 days		30 days		90 days		180 days	
	Size (nm)	PdI	Size (nm)	PdI	Size (nm)	PdI	Size (nm)	PdI
Nanosuspension	188.9±1.7	0.185±0.020	192.0±3.9	0.219±0.015	184.0±3.8	0.213±0.005	188.0±1.4	0.199±0.024
Spray-drying	213.7±4.0	0.174±0.033	209.3±2.1	0.176±0.022	203.4±1.8	0.202±0.010	197.0±3.9	0.218±0.012
Freeze-drying	205.8±2.1	0.183±0.025	208.6±2.8	0.174±0.014	211.1±3.9	0.187±0.026	210.4±3.5	0.210±0.028

PdI: polydispersity index.

5.4 Discussion

The stabilizer type and concentration play an important role in nanocrystal preparations, which contain only the drug substance and stabilizer. A stabilizer can provide a steric and/or ionic barrier to form a physically stable formulation. Surfactants and/or polymers are frequently used stabilizers. Ionic surfactants (e.g., SDS) stabilize drug nanocrystals electrostatically, while nonionic surfactants (e.g., Polysorbate 80, Poloxamer 188, Poloxamer 407, TPGS, and Plantacare®) and polymeric stabilizers (e.g., Soluplus® and Povacoat™) facilitate steric stability through both their molecular length and molecular weight.

However, compared to surfactants, polymeric stabilizers are adsorbed on particles and/or form a thick surface layer to prevent Ostwald ripening, and they will not affect the crystal

structure (303-305). Hence, different types of stabilizers were evaluated in this study to select the most suitable stabilizer for esculetin nanocrystals.

The particle size and PdI are relevant not only to the stability of the system but also to the rate and extent of drug release. The PdI is an indication of the size distribution, and generally a small PdI (<0.2) illustrates the uniformity and homogeneity of a nanosized system (306).

As shown in Table 5.2, all tested stabilizers yielded nanoscale particles smaller than 300 nm. The esculetin nanosuspensions prepared with Polysorbate 80 (PdI=0.185±0.008), Poloxamer 407 (PdI=0.180±0.020), TPGS (PdI=0.177±0.013), Plantacare® (PdI=0.203±0.007) and Povacoat™ (PdI=0.179±0.029) all exhibited PdI values less than 0.2. However, except for the esculetin nanosuspension prepared with Povacoat™, which presented a monomodal distribution, all other nanosuspensions showed precipitation within 7 days after sample collection. Thus, Povacoat™ was chosen as the most suitable stabilizer for esculetin nanocrystal preparation.

Povacoat™ is an aqueous polymer comprising polyvinyl alcohol, polyacrylic acid and polymethyl methacrylate groups. As mentioned by Yuminoki et al., Povacoat™ has high dispersion and redispersion stability for preventing the aggregation of nanoparticles in nanocrystal formulations of several poorly water-soluble compounds (e.g., griseofulvin, hydrochlorothiazide, and tolbutamide) prepared via wet milling (307).

In this study, the RSM allowed the identification and characterization of a design space in which the esculetin concentration and milling time were optimized to provide the lowest particle size (Figures 5.2 and 5.3). A second-order polynomial equation described the relationships among the independent variables (esculetin concentration, Povacoat™ concentration, and milling time) and the response (particle size). As the R^2 (98.33%), adj-R^2 (97.11%), and pred-R^2 (92.86%) values were all greater than 90%, it showed that the predicted (theoretical) data estimated by the model were close to the practical values. In this way, the mathematical model can be used to optimize the process. The coefficients indicate the direction and magnitude by which each independent variable impacts the response (297). In equation 2, the esculetin concentration and milling time have negative coefficients, meaning that increases in these two variables will decrease the particle size. However, the quadratic coefficients of the parameters (esculetin concentration and milling time) revealed positive values. The milling time, the interaction of esculetin with Povacoat™, and the interaction of Povacoat™ with the milling time could reduce the particle size because of their negative coefficients. Optimized formulation and processing time to yield the smallest mean particle size were identified within the design space. A similar DoE approach was performed in the development of a meloxicam nanosuspension prepared by high-pressure homogenization (297).

For the solid preparations, both approaches, spray-drying and freeze-drying, have their own advantages. Spray-drying is a conventional industrial process and preferred over freeze-

drying because of the simple operation and cost and time effectiveness (308). Freeze-drying is suitable for heat-sensitive and delicate materials because of the low processing temperatures compared to the hot air (above 80°C) needed in spray-drying (308). The melting point of esculetin is 278°C; thus, it was theoretically possible to apply an SD approach to solidify the esculetin nanosuspension in this study.

In this study, mannitol was added in both processes as a supporting agent to inhibit particle aggregation and achieve adequate redispersion. In order to facilitate the crystallization of mannitol during the freeze-drying process, a thermal treatment called annealing should be incorporated into the freeze-drying process. The annealing step recrystallizes smaller ice crystals to form larger ice crystals and shorten the primary drying time (309).

As observed by TEM (Figure 5.4), similar particle morphology was detected in the redispersed SD and FD powders. Both samples exhibited a uniform particle size (100-500 nm), and no agglomeration was observed. However, when comparing the morphology (Figure 5.5) of the raw material with the SD and FD nanocrystals by SEM, the SD technique yielded nearly spherical and microsized agglomerates of nanocrystals (Figure 5.5B), while FD (Figure 5.5C) yielded irregularly shaped nanocrystals. The dissimilarities observed in the shape and surface morphology of the SD and FD powders have also been reported by Toziopoulou et al. and Fini et al. (292, 310). As mentioned by Fini et al., the depressions in the external surface of SD particles are because of the rapid evaporation of the solvent during the spray-drying process (310). Additionally, the spherical shape of the

SD particles enables flowability (292, 310). In this case, the spray-drying technique resulted in particles with better particle performance than freeze-drying in the preparation of dry esculetin-Povacoat™ nanocrystals.

The broad endothermic event observed in the DSC and TG curves of Povacoat™ (Figures 5.6 and 5.7) was assigned to the moisture content. This broad peak may also have contributed to the glass transition event, as previously reported, at 82°C (311). Furthermore, as confirmed by XRPD (Figure 5.8), this polymer is completely amorphous. The additional endothermic event between 160 and 211°C was associated with intramolecular ester condensation (cyclic anhydride formation) induced by the heating, as reported by Lin et al. (311).

When nanocrystals are prepared, a change in the crystalline state can occur during both the milling and drying processes (312). The XRPD (Figure 5.8) results showed a suggestive broad peak associated with an increase in the background, indicating an increase in the degree of disorder due to amorphization and a reduction in the crystallite size. As shown in Figure 5.6, the melting temperature of the dried nanocrystal formulations was shifted and reduced compared with that of bulk esculetin and mannitol. This melting point depression for the nanocrystals is expected according to the Gibbs–Thomson relationship and has been previously reported (313); the melting point of a substance is proportional to its cohesive energy, and physical milling and drying can reduce the cohesive energy and introduce crystalline defects (312, 314). Therefore, the esculetin nanocrystals need less

energy to be melted than bulk esculetin. The results of all three characterization methods (DSC, TG, and XRPD) showed no significant differences between the FD and SD samples, indicating that both processes resulted in formulations with a similar solid-state structure.

In this study, the saturation solubility of the esculetin nanocrystals was 1.2- to 1.5-times higher than that of the esculetin raw material (Table 5.10) which revealed statistic significantly differences (*p-value<0.05, α=0.05). The highest increase occurred in SIF. No increase in the saturation solubility of esculetin was observed in physical mixtures, which revealed that the increase observed for the nanocrystals was not relevant to the addition of the stabilizer, Povacoat^{TM}. A similar finding was reported by Barbosa et al. (315). The increase in the saturation solubility of the nanocrystal powders was relevant to the particle size reduction, as the nanocrystals were approximately 700-times smaller than the raw esculetin particles (150.1 μm).

Dry powders should be shelf-stable, pharmaceutically elegant and able to instantly re-dispersed into a suspension (316). In this study, the powders produced by both drying processes re-dispersed instantly in water. According to Tables 5.9 and 5.11, the particle size remained unchanged after drying and was stable for 6 months at 4°C. Hence, stable esculetin nanocrystals were prepared in this study.

5.5 Conclusion

An esculetin-Povacoat™ nanocrystal formulation with a particle size of 200 nm was successfully prepared by a reduced-scale wet milling process. The design space approach allowed the description of the particle size performance of the formulation as a mathematical function of the stabilizer and esculetin concentrations and the milling time. Furthermore, it was possible to identify the critical components, factors and the limits within which variations in the component concentrations have minimal or no effects on the particle size. The formula containing 3.0% (w/w) esculetin and 3.0% (w/w) Povacoat™ presented up to a 1.5-fold increase in saturation solubility compared to the micronized esculetin powder. A new nano-sized formulation with physical-chemical property changes was created. This approach has the potential to enable the development of innovative commercial products for the treatment of hyperuricemia.

Chapter 6 General discussion and conclusion

6.1 Discussion

In this thesis, we investigated TCM through extending the therapeutic scope of a heat-clearing and detoxifying herbal formula (Erding Formula (EF)) to hyperuricemia using modern pharmaceutical techniques.

6.1.1 TCM and modern pharmaceutical approaches

6.1.1.1 Extend the therapeutic application of EF to hyperuricemia/gout

Hyperuricemia was chosen as model disease which shows an abnormal high uric acid (UA) level in the blood. UA levels in the body are diagnosed using modern analytical technologies, so the hyperuricemia is a modern disease term. Long-term hyperuricemia can cause gout, an inflammatory form of arthritis that involves UA crystal deposition in tissues especially joints.

Generally, gout can be classified into two forms: acute gout attack and chronic tophaceous gout (40). Acute gout can be characterized by the sudden onset of pain associated with swelling, warmth, redness, and a decreased range of motion of the affected joints. Chronic gout is multiple severe attacks that occur within short intervals associated with significant UA tophi, joint destruction, and deformation. (40, 317)

According to “Criteria of diagnosis and therapeutic effect of diseases and syndromes in traditional Chinese medicine”, gout can be classified into four types: 1) accumulation and

coagulation of dampness-heat (湿热蕴结)；2) obstruction of blood stasis and heat（瘀热阻滞）; 3) obstruction of phlegm turbidity（痰浊阻滞）; 4) yin deficiency of liver and kidney（肝肾阴虚）(318). Based on the symptoms described in the criteria, the TCM type 1 gout should belong to acute gout and all other types belong to chronic gout. In this case, TCM practitioners treat acute gout mainly through clearing heat, alleviating dampness, and detoxifying as well as relieving pain and eliminating swelling (319-321). For chronic gout, a TCM treatment would focus on warming the spleen and kidney (温补脾肾), activating collaterals and relieving pain (活络止痛), and nourishing blood and harmonizing the ying level (养血和营) (321, 322).

As described in Section 2.7, heat is one of the climatic pathogens in TCM and it is a yang pathogen. Toxin in TCM refers to substances and/or waste products from the body's metabolic activities and/or environmental pollutants including microorganisms which upset the body out of balance and lead to illness. When it is rising and out of balance, heat toxin can lead to red faces, anger, irritability, fever, inflammation condition, sore throat, and dizziness. (323-325)

In order to re-harmonize the balance, clearing therapy which refers to the use of cold herbs to clear heat and purge fire, clear heat and nourish yin, clear heat and detoxify (25). This is a frequently used therapy to treat various heat syndromes. For heat-toxin syndromes, the treatment is heat clearing, detoxifying, alleviating dampness and combining with blood cooling, edema relieving and urination promoting (325).

EF is a formula consisted by Viola yedoensis Makino (Viola), Taraxacum mongolicum Hand.-Mazz. (Taraxacum), Lobelia chinensis Lour. (Lobelia), Root of Isatis indigotica Fort. (Isatidis) which are all cold herbs and have heat clearing and detoxifying properties. Hence, when the syndrome of gout is diagnosed as accumulation and coagulation of dampness-heat, EF can be used as the treatment.

In Chapter 3, modern pharmaceutical experiments were designed to investigate the efficacy of the formula to treat hyperuricemia. In the study, EF showed anti-hyperuricemic, anti-inflammatory and analgesic effects. The symptoms that can be relieved by EF in this study such as swelling and pain are similar to the symptoms of the type 1 gout. Hence, the results from Chapter 3 confirmed that hyperuricemia/acute gout can be a new indication of EF which is in agree with TCM.

When combining the results of Chapter 3 with TCM views, the interpretation of using EF to treat hyperuricemia/acute gout could be described as following: the high UA level is a toxin and it further results inflammation and pain. The property of heat clearing works as controlling the inflammation while pain and detoxifying works as lowering the UA levels.

6.1.1.2 Treating different diseases using the same formula

From the results of Chapter 3, EF showed a hypouricemic, anti-inflammatory and analgesic effects in the study. Originally, EF was used to treat furuncle, carbuncle, sore throat, and wind-burn-related eye inflammation (conjunctivitis) (39). Other researchers proved EF was

able to treat acute pharyngitis (syndrome of lung and stomach heat) and chronic bronchitis (326, 327). Researches also reported that EF has bacteriostatic, anti-inflammatory, immunomodulating and antiviral effects (328, 329).

All these are totally different disease and application in western medicine, while in TCM, they could be treated using the same formula. This is because TCM emphasizes “treatment based on syndrome differentiation” which aims to target the root of the illness as their essential principle to guide the treatment and selection of herbal formulas (330). Syndrome is a unique and key concept in TCM which reflects the essence of pathological changes at a certain stage during the disease and it is an outcome after analyzing the symptoms and signs. TCM believes that one disease may have different syndromes, and different diseases may be categorized by the same syndrome. In this case, TCM emphasizes one of its therapeutic principles is "treating different diseases using the same formula" (异病同治). (331, 332)

As shown in Figure 6.1, the diseases such as furuncles, sore throat, wind-burn-related eye inflammation (conjunctivitis) which are characterized by warmth, swelling, redness and pain. They are considered as a result of wind, heat and/or toxin (39, 325). As mentioned in section 6.1.1.1, the cause of the acute gout can be wind, dampness, and/or heat (Figure 6.1). When TCM diagnoses of diseases where heat and toxin are the cause, the herbal formulas with heat-clearing and detoxifying properties will be considered as the treatment (Figure 6.1). This is the reason why TCM practitioners might use EF to treat the gout in clinic. The

results from the chapter 3 confirmed that the EF can be used to treat hyperuricemia/acute gout which are totally different diseases from the original indications in the western medicine viewpoint.

To further confirm the concept of "treating different diseases using the same formula", additional studies should be conducted using other herbal formulas.

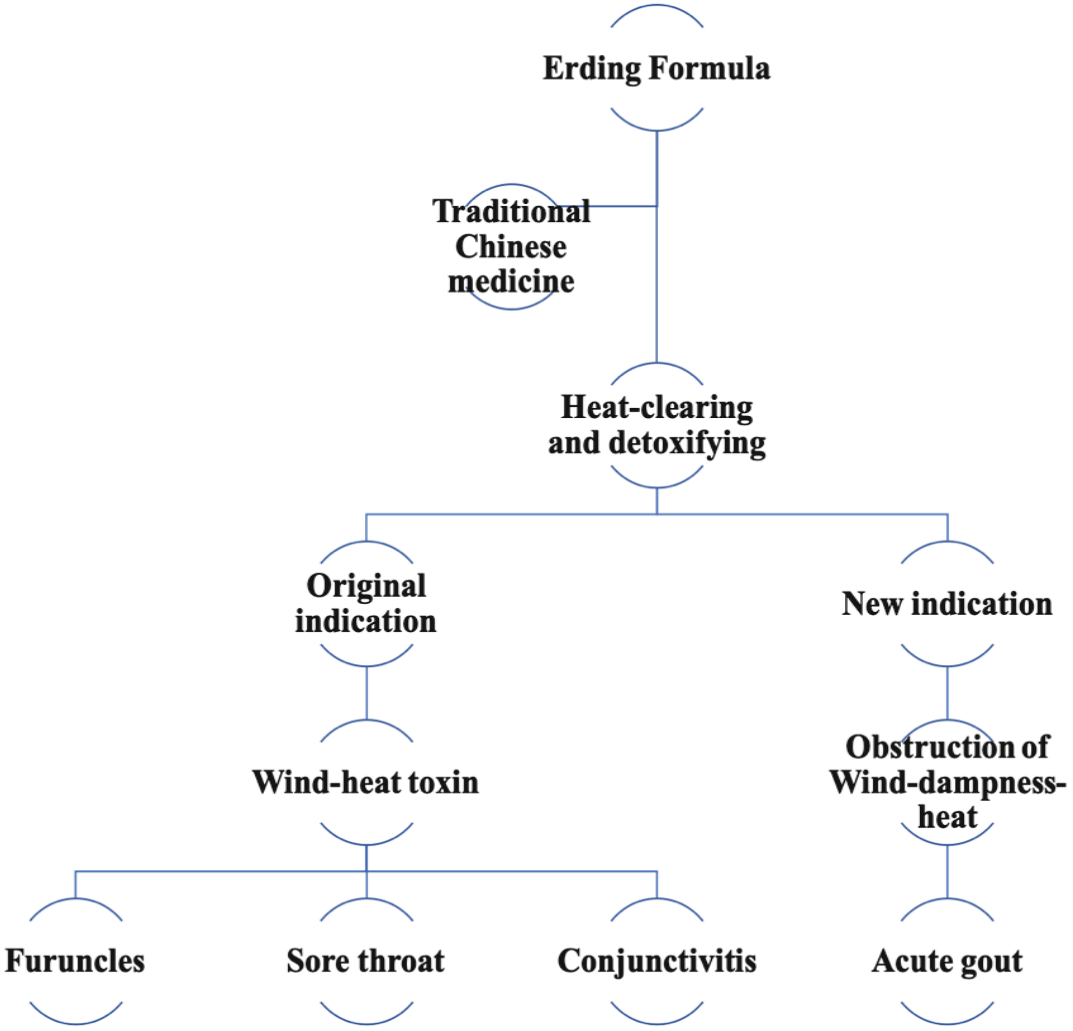

Figure 6. 1 Examples of "treating different diseases using the same formula" under TCM framework.

6.1.1.3 Preventive treatment of disease

The “preventive treatment of disease” which emphasizes "preventing before the occurrence of disease, preventing the further development and transmission to next stage of disease, and preventing the recurrent attacks” is another important principle in preventing and treating diseases in TCM (2). This is why sometimes TCM practitioners treat people who seem to be healthy or are not yet sick.

TCM considers the human body as a whole entity and focuses on removing the root cause of illness to promote healing and health, which is different from western medicine that treats symptoms. For the patient with extremely high UA levels but without symptoms, western doctors might not prescribe routine prophylactic urate lowering medicine (333). However, TCM practitioners may prescribe remedies to control UA levels and to prevent potential symptoms and/or disease that may resulted from high UA levels. Based on TCM, we investigated the anti-inflammatory and analgesic activity of EF in a preventive treated mouse model.

6.1.1.4 Clinical treatment of gout

In western medicine, the initial treatment of acute gout is to settle the symptoms with suggested indicators such as colchicine and non-steroidal anti-inflammatory drug (59, 334). The urate lowering therapy, such as allopurinol and uricosuric drugs, will not be initiated during the attacks due to the risk of aggravating or prolonging the attack (334) which is

also included in guidelines from European League Against Rheumatism (59). A recent published guideline from the American college of Rheumatology recommends to initiate urate lowering prophylaxis concurrent with anti-inflammatory agents to prevent recurrent attacks (335). TCM practitioners consider the original causes and prescribe herbs according to syndrome differentiation. It has been found in clinical trials that the Chinese herbal formulas were able to control serum UA level and inflammation severity for the patients with gout (336). The data in Chapter 3 also revealed that EF can control UA levels, pain and inflammation in mouse models.

6.1.1.5 Principle of compatibility

In TCM, the *"Jun, Chen, Zuo, Shi"* (君臣佐使) structure is the fundamental principle for herbal compatibility in a formula. From the TCM explanation of EF in hyperuricemia treatment, Viola is cold in nature which clears blood heat, removes toxicity, cools blood, and alleviates joint swelling pain. It is used as emperor herb in EF. Taraxacum and Lobelia can be considered as minister herbs because they clear dampness through diuresis to assist the emperor herb in detoxifying and eliminate swelling. Isatidis works as adjuvant herb to strength the activities of other herbs in clearing heat, removing toxicity, cooling blood, removing edema and pain.

In Chapter 3, Viola was determined as the emperor herb to treat hyperuricemia /acute gout because it was the only herb which has UA lowering effect. As Taraxacum, Lobelia and

Isatidis all presented anti-inflammatory and analgesic effects, it is difficult to determine their exact TCM role in EF based on the results in Chapter 3. However, Taraxacum, commonly known as Dandelion in western countries, its diuretic utility is well-known in both eastern and western cultures (337-342). This is in agree with the TCM description of Taraxacum activity which suggests that it works as minister herb in EF. Further studies are necessary to determine the TCM role of Lobelia and Isatidis in EF.

In general, compatibility is applied to reinforce mutual effects, enlarge the therapeutic scope, and avoid antagonism. As stated in the introduction: instead of random listing, the herbs in the formula are selected according to the diseases and herbal properties. This is also guided by certain considerations such as mutual reinforcement (相须，combine herbs with similar properties and efficacy to reinforce clinical effects), mutual assistance (相使，combine herbs with similar or different property and efficacy to treat the same syndrome), mutual restraint or mutual suppression (相畏/相杀，when combine two herbs, the toxicity of one herb can be reduced by another one) , mutual inhibition (相恶, when combine herbs, the medicinal efficacy can be reduced and/or neutralize)，and mutual antagonism (相反，when use two herbs together, can become toxic or reinforce toxicity) (15).

In order to understand the compatibility principle used for EF, additional experiments were conducted to investigate the effects of single herb and combined herbal groups on serum UA levels in hyperuricemic mice. EF is consisted of four different herbs: Viola, Taraxacum, Lobelia, Isatidis. Viola and Taraxacum are frequently used as a herbal pair (343). In this

case, three combinations (Viola + Taraxacum, Viola + Taraxacum + Lobelia, Viola + Taraxacum + Isatidis), were grouped and decocted following ChP protocols (39). In this case, the mice were randomly divided into 11 groups (n = 10): untreated (healthy), untreated disease, positive control (Benzbromarone, 20 mg/kg), EF extract, four individual plant extract groups (Viola, Taraxacum, Lobelia, and Isatidis), and three combination groups. All experiments were conducted and analyzed following the materials and methods in Chapter 3. The effects of each extract group on the UA levels in hyperuricemic mice are shown in Figure 6.2. Statistical analysis showed that the serum UA level in the untreated disease group was significantly increased compared with the untreated mice. The EF, Viola + Taraxacum + Lobelia, and Viola + Taraxacum + Isatidis groups significantly decreased UA levels ($P < 0.05$) compared with untreated disease mice. From the statistical results, the single herb group and the herbal pair (Viola + Taraxacum) group didn't significantly decrease the UA levels. However, when additional one/two more herbs were added to the pair, the combination was able to reduced UA levels in hyperuricemic mice. In summary, the herbal formulation showed a good efficacy, herbal compatibility was verified and the property of all four herbs in EF were heat-clearing and detoxifying, which was showed as UA lowering, anti-inflammatory and analgesic in the data of Chapter 3. The herbal combination in EF was prescribed under mutual reinforcement action.

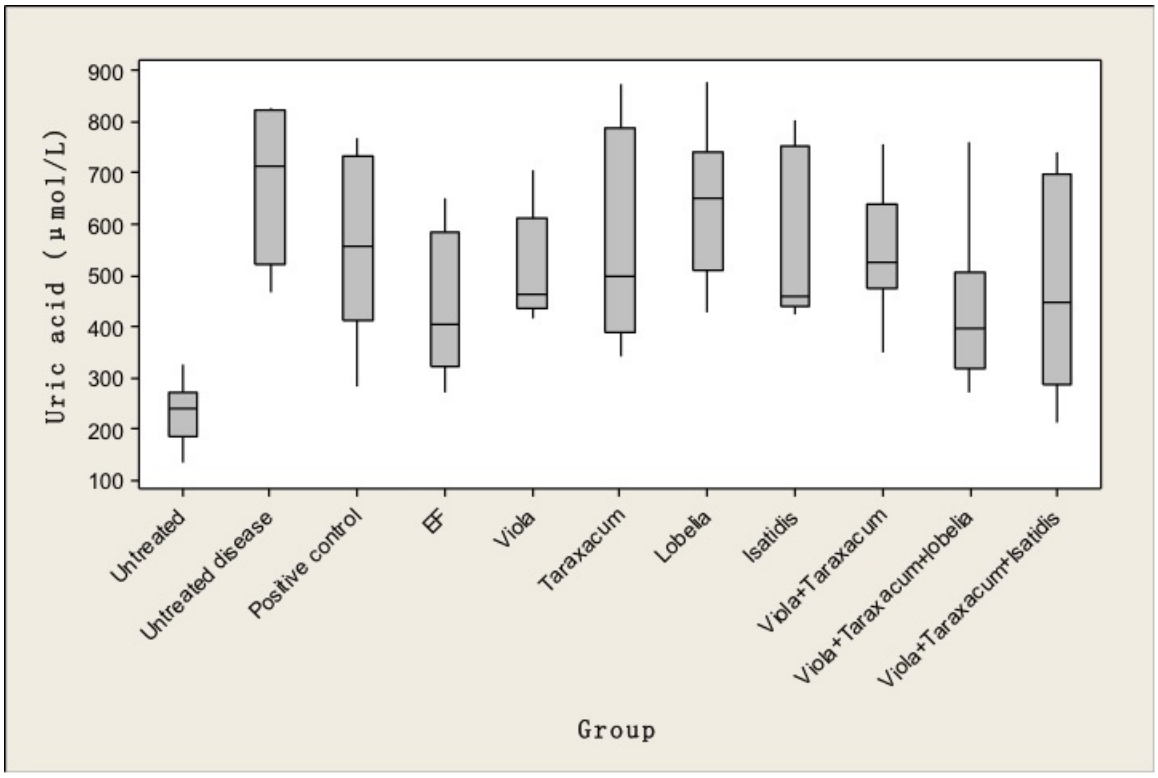

Figure 6. 2 Effects of the extract groups on the serum uric acid levels in hypoxanthine and potassium oxonate-induced consecutive hyperuricemic mice (n = 10). The box represents the data from the 25th to 75th percentiles, and the line in the middle of the box is the median. The end of bars represents the minimum and maximum values. Positive control, Benzbromarone; EF, Erding Formula; Viola, Viola yedoensis Makino; Taraxacum, Taraxacum mongolicum Hand.-Mazz.; Lobelia, Lobelia chinensis Lour.; Isatidis, root of Isatis indigotica Fort; Viola+Taraxacum: combination of Viola yedoensis Makino and Taraxacum mongolicum Hand.-Mazz; Viola+Taraxacum+Lobelia: combination of Viola yedoensis Makino, Taraxacum mongolicum Hand.-Mazz and Lobelia chinensis Lour.; Viola+Taraxacum+Isatidis: combination of Viola yedoensis Makino, Taraxacum mongolicum Hand.-Mazz and root of Isatis indigotica Fort.

6.1.2 Quality control of herbal formula

Quality control of herbal formulas is a challenge for the development of herbal preparations because of their complex composition. As stated before, TCM frequently uses the same herbal formula to treat different diseases which makes the quality control of herbal formula more difficult. The research question of Chapter 4 was: Is a pre-existing quality control marker of formula in the ChP suitable for the new indication of that herbal formula. Hence, esculetin, the marker used by the ChP monograph of Erding granules, was investigated for the hyperuricemica treatment.

As mentioned by Guo DA, the key issues for studying and establishing quality standards were described in four aspects: "*a) analysis and characterization of the chemical components in TCMs herbs and formulas; b) development of a comprehensive quality control model instead of single marker approach is necessary for the quality control of TCMs multiple component system; c) clarification of active or even effective components in TCMs; and d) elaboration of scientific, practical and feasible quality standards*."

In this case, some researches recommended to discover the effect-associated maker using an integrated multidiscipline based triarchic theory of "property-effect-component". The strategy includes the study of phytochemistry, analytical chemistry, computer-aided design, pharmacology, system biology, and pharmacodynamics (70). There are several cases which followed this strategy to determine the Q-marker. Zhang et al. confirmed the main

alkaloids as Q-marker of Corydalis Rhizoma through a specific biosynthesis pathway analysis of the chemical composition, pharmacodynamics, pharmacokinetics and network pharmacology studies. In their study, to further confirm a specific alkaloidal compound, the fingerprint method, the similarity analysis, and principle compound(s) analysis were conducted among 11 batches (344, 69). Yao et al. (345) and Da et al. (346) used a similar process to develop the quality standards of Panax Notoginseng Radix and Ganoderma lucidum, respectively (345, 346). A similar research strategy was also extended to herbal formulations. For example, in the Q-markers study of Yuanhu Zhitong Dropping Pill, identified 51 components from the formula by HPLC-MS/MS. Then the prototype components and metabolites were identified by HPLC-Q/TOF-MS and metabolomics. Lately, computer-aided design, pharmacodynamics, pharmacokinetics, network pharmacology approaches were employed to investigate the efficacy and mechanism of the formula and principle components. Finally, they determined d-corydaline, dl-tetrahydropalmatine, protopine, imperatorin, and isoimperatorin as the Q-markers for the formula (347).

However, when a herbal formula was used for different diseases, it's difficult to perform the above strategy to determine bioactive quality control marker for each indications that can be treated. An accurate and more practical strategy to discover bioactive quality control markers needs to be developed for each indication of a herbal formula.

6.1.3 Development of new TCM dosage form

The stability is one of the most important aspects for a nanocrystal formulation due to the size reduction which increases the surface energy. In our study, the selection of stabilizers was performed among common pharmaceutical excipients. However, during the screening, we experienced difficulties to find a suitable excipient which resulted a stable esculetin nanocrystal formulation. Recently, studies suggested the use of natural surfactants from plants as novel "friendly" stabilizers for nanocrystal preparations. For example, saponins, which are a widely distributed group of plant compounds. It has been reported that saponins are present in more than 100 plant families. (348) This group of compounds exhibits surfactant properties, such as detergent, wetting, emulsifying, and foaming properties, due to the lipid-soluble aglycone and water-soluble sugar component in their structure (349-352). These compounds are frequently used in the food industry as surface-active agents, as a "label friendly" alternative for synthetic ingredients (353-355). Xie, et al (356) and Chen, et al (357) used Panax Notoginseng saponins (PNS) and the triterpenoid saponin (glycyrrhizin) as stabilizers to prepare Baicalein nanocrystals and andrographolide nanocrystals, respectively. From their studies, both PNS and glycyrrhizin were not only able to maintain the dispersion of nanocrystals in suspension but were also able to prevent agglomeration during the drying process, given their interfacial properties, gel formation properties, and electrostatic effects. To date, only a few studies on the use of natural

compounds as stabilizers for nanocrystals have been reported (356, 357). Parallel to a guide herb in a TCM formula, saponins help (emulsify; stabilize) others (esculetin) to reach their targets and harmonize the properties (stabilize nanocryctals). The use of saponins derived from the EF or from the individual herbs as stabilizer for esculetin nanocrystals should be further investigated.

6.2 Conclusion

In this thesis, we presented an approach to apply a new indication, hyperuricemia, for a traditional used EF. First, we proved that EF could lower the UA levels, control inflammation and pain using modern pharmacological studies. At the same time, the study confirmed the advantage of the compatibility concept by comparing the efficacy of the herbal formula with the individual herbs from the formula in the treatment of hyperuricemia. The study also revealed a rational approach to determine a bioactive marker, esculetin, to ensure the therapeutic efficacy for patients when the same herbal formulation was applied to treat a different disease. Furthermore, the study presented an approach to develope a nanocrystal formulation of esculetin which is an active compound derived from the herbal formulation.

The *in vivo* studies concluded that the therapeutic scope of EF can be extended to hyperuricemia with esculetin as bioactive quality control marker. As well, the study presents the possibility to develop an innovative nanotechnological product of the active

substance derived from herbal TCM medicine. Our findings facilitate a better understanding of TCM terms and concept through mechanistic scientific experiments. This study revealed a potential pathway and an idea to modernize TCM without setting aside its unique concepts. This might increase the global acceptance of TCM products. Furthermore, the TCM concept might be useful in the development of multi-component drug products.

6.3 Future direction

In order to further confirm the effects of EF in acute gout treatment, a study should be conducted in a UA crystal induced gout arthritis mouse model. The effects of EF on enhancing UA excretion is reported in Chapter 3, while this pathway needs to be studied in more detail. The other pathway, production of UA also needs to be studied. Here the mechanism of suppressing xanthine oxidase activities needs to be evaluated for the EF. This may further confirm the advantage of compatibility concept in TCM. Additional studies to determine the mechanistic pharmacological activity and the TMC role of Taraxacum, Lobelia and Isatidis in EF for hyperuricemia treatment are necessary.

The TCM concept that “Using the same formula to treat different diseases” should be further investigated and confirmed using other formulas. To ensure the quality and efficacy, an accurate and practical strategy needs to be developed to discover bioactive quality control markers for each indication of a herbal formula.

Chapter 5 demonstrated that the created nanocrystal formulation increased the saturation solubility of esculetin, and the dosage form was robust and stable. The purpose to prepare esculetin nanocrystals was to enhance the bioavailability and eventually efficacy of esculetin. In this case, dissolution tests, cytotoxicity assessments and/or *in vivo* studies should be conducted to further investigate the viability of esculetin nanocrystals. The use the natural compounds derived from the plants as stabilizers for nanocrystal formulation should be considered in the future. The concept of multi-herb therapy in TCM might be a good model to apply to the development of multi-drug fixed dose combination therapies; this approach needs be investigated further.

References

1. Tang J, Liu B, Ma K. Traditional Chinese Medicine. Lancet. 2008;372(9654):1938-40.

2. Chai KF, Zhang QR. Fundamental theory of Traditional Chinese Medicine. 2nd ed. People's Medical Publishing House Co., LTD.: Beijing, China 2007.

3. Wang X, Zhang A, Sun H. Future perspectives of Chinese medical formulae: chinmedomics as an effector. OMICS. 2012; 16(7-8): 414-21.

4. Lu AP, Jia HW, Xiao C, Lu QP. Theory of traditional Chinese medicine and therapeutic method of diseases. World J Gastroenterol. 2004; 10(13):1854-6.

5. United Nations Educational, Scientific, and Cultural Oorganization. Full list of Reigistered Herit-age, Huang Di Nei Jing 《黄帝内经》 (Yellow Emperor's Inner Canon). Available at: http://www.unesco.org/new/en/communication-and-information/flagship-project-activities/memory-of-the-world/register/full-list-of-registered-heritage/registered-heritage-page-4/huang-di-nei-jing-yellow-emperors-inner-canon/ (Accessed March 2, 2015).

6. Cheung F. TCM: Made in China. Nature. 2011; 480: S82-S83.

7. Wang X, Sun H, Zhang A, Sun W, Wang P, Wang Z. Potential role of metabolomics apporoaches in the area of traditional Chinese medicine: as pillars of the bridge between Chinese and western medicine. J Pharm Biomedi Anal. 2011; 55(5): 859-68.

8. Wang M, Lamers R, Korthout H, van Nesselrooij JH, Witkamp R, van der Heijden R, et al. Metabolomics in the context of systems biology: bridge traditional Chinese medicine and molecular pharmacology. Phytother Res. 2005; 19(3):173-82.

9. Xue J. Discussion on the speciality of TCM term translation and the translating principles viewing from the concept of TCM term "qi". (从气概念谈中医名词术语翻译的特殊性和翻译原则) Zhongguo Zhong xi yi jie he za zhi 2008; 28(5): 471-2. (Article in Chinese)

10. Leung AY. Traditional toxicity documentation of Chinese Materia Medica--an overview. Toxicol Pathol. 2006;34(4):319-26.

11. Liu X, Wang Q, Song G, Zhang G, Ye Z, Williamson EM. The classification and application of toxic Chinese materia medica. Phytother Res. 2014;28(3):334-47.

12. Ekor M. The growing use of herbal medicines: issues relating to adverse reactions and challenges in monitoring safety. Front Pharmacol. 2013; 4: 177.

13. Calapai G. European legislation on herbal medicines: a look into the future. Drug Saf. 2008;31(5):428-31.

14. Yuan R, Lin Y. Traditional Chinese medicine: an approach to scientific proof and clinical validation. Pharmacol Ther. 2000;86(2):191-8.

15. Teng JL, Cui HJ. Chinese Materia Medica. People's Medical Publishing House Co., LTD: Beijing, China, 2007.

16. Li X, Zhang H. Synergy in natural medicines: implications for drug discovery. Trends Pharmacol Sci. 2008; 29(7): 331-2.

17. Wang S, Hu Y, Tan W, Wu X, Chen R, Cao J, et al. Compatibility art of traditional Chinese medicine: from the perspective of herb pairs. J Ethnopharmacol. 2012; 143(2): 412-23.

18. Wang S, Wu X, Tan M, Gong J, Tan W, Bian B, et al. Fighting fire with fire: poisonous Chinese herbal medicine for cancer therapy. J Ethnopharmacol. 2012; 140(1): 33-45.

19. Qiu J. 'Back to the future' for Chinese herbal medicines. Nat Rev Drug Discov. 2007; 6(7): 506-7.

20. Zhang M. A treatise on the standardization o prescription's name. In: Chang IM, editor. Experts Meeting for the Standardization of Titles of Chinese Prescriptions. Seoul: Natural Products Research Institute, Seoul National University, WHO Collaborating Center for Traditional Medicine: 1996, 33-9.

21. Qiu J. Traditional medicine: a culture in the balance. Nature. 2007; 448(7150): 126-8.

22. Yi Y, Chang I. An overview of traditional Chinese herbal formulae and a proposal of a new code system for expressing the formula titles. Evid Based Complement Alternat Med. 2004;1(2):125-32.

23. Fan TP, Yeh JC, Leung KW, Yue PY, Wong RN. Angiogenesis: from plants to blood vessels. Trends Pharmacol Sci. 2006;27(6):297-309.

24. Zhao X, Zheng X, Fan T, Li Z, Zhang Y, Zheng J. A novel drug discovery strategy inspired by traditional medicine philosophies. Science. 2015; 347(6219): S38–S40.

25. Chen DX, Zhu ZB. Formulas of Traditional Chinese Medicine. People's Medical Publishing House Co., LTD: Beijing, China, 2007.

26. Xu Q, Bauer R, Hendry BM, Fan T, Zhao Z, Duez P, et al. The quest for modernization of traditional Chinese medicine. BMC Complementary Alternative Med. 2013; 13:132.

27. Tu YY. The discovery of artemisinin (qinghaosu) and gifts from Chinese medicine. Nat Med. 2011; 17:1217-20.

28. Miller LH, Su X. Artemisinin: discovery from the Chinese herbal garden. Cell. 2011; 146:855–8.

29. Neill US. From branch to bedside: Youyou Tu is awarded the 2011 Lasker~DeBakey Clinical Medical Research Award for discovering artemisinin as a treatment for malaria. J Clin Invest. 2011; 121:3768–73.

30. Wall ME, Wani MC, Cook CE, Palmer KH, McPhail AT, Sim GA. Plant antitumor agents. I. The isolation and structure of camptothecin, a novel alkaloidal leukemia and tumor inhibitor from Camptotheca acuminata. J Am Chem Soc. 1966; 88:3888–90.

31. Wall M, Wani M. Camptothecin: Discovery to Clinic. Ann N Y Acad Sci. 1996; 803:1–12.

32. Stermitz FR, Lorenz P, Tawara JN, Zenewicz LA, Lewis K. Synergy in a medicinal plant: antimicrobial action of berberine potentiated by 5'-methoxyhydnocarpin, a multidrug pump inhibitor. Proc Natl Acad Sci USA. 2000;97(4):1433-7.

33. Junio HA, Sy-Cordero AA, Ettefagh KA, Burns JT, Micko KT, Graf TN, et al. Synergy-directed fractionation of botanical medicines: a case study with goldenseal (Hydrastis canadensis). J Nat Prod. 2011;74(7):1621-9.

34. Wang L, Zhou GB, Liu P, Song JH, Liang Y, Yan XJ, et al. Dissection of mechanisms of Chinese medicinal formula Realgar-Indigo naturalis as an effective treatment for promyelocytic leukemia. Proc Natl Acad Sci USA. 2008;105(12):4826-31.

35. Wagner H, Bauer R, Melchart D, Xiao PG. Staudinger A: Chromatographic fingerprint analysis of herbal medicines-Thin-layer and High Performance Liquid Chromatography of Chinese Drugs. Volume 1-2. Vienna: Springer-Verlag; 2011.

36. Stone R. Biochemistry. Lifting the veil on traditional Chinese medicine. Science. 2008; 319: 709-10.

37. Zhang X, Liu Y, Guo Z, Feng J, Dong J, Fu Q, et al. The herbalome - an attempt to globalize Chinese herbal medicine. Anal Bioanal Chem. 2012; 402:573-81.

38. Huang Y, Zhao Y, Liu F, Liu S. Nano traditional Chinese medicine: current progresses and future chanllges. Curr Drug Targets. 2015;16(13):1548-62.

39. State Pharmacopoeia committee. Chinese Pharmacopoeia, vol.1, Chemical Industry Press, Beijing, China, 2015.

40. Khanna D, Fitzgerald J, Khanna P, Bae S, Singh M, Neogi T, et al. 2012 American college of rheumatology guidelines for management of gout. Part 1: systematic nonpharmacologic and pharmacologic therapeutic approaches to hyperuricemia. Arthritis Care Res. Hoboken, 2013; 64: 1431-46.

41. Muluye RA, Bian Y, Alemu PN. Anti-inflammatory and antimicrobial effects of heat-clearing Chinese herbs: a current review. J Tradit Complement Med. 2014;4(2):93-8.

42. Franzblau SG, Cross C. Comparative in vitro antimicrobial activity of Chinese medicinal herbs. J Ethnopharmacol. 1986;15:279-88.

43. Geng L, Wang S. Progress in treatment of hyperuricemia with Chinese Medicine. (高尿酸血症中医药治疗进展). TCM Res. 2017, 30(2),68-72. (Article in Chinese)

44. Yin H, Zhou Y, Jiao J. Prospect of research and treatment of hyperuricemia in Chinese medicine. (高尿酸血症的中医药研究与治疗展望). Beijing Journal of Traditional Chinese Medicine. 2009;28(1):70-72. (Article in Chinese)

45. Vázquez-Mellado J, Hernández EA, Burgos-Vargas R. Primary prevention in rheumatology: the importance of hyperuricemia. Best Pract Res Clin Rheumatol. 2004; 18(2): 111-24

46. Neogi T. Clinical practice. Gout. N Engl J Med. 2011;364(5):443-52.

47. Terkeltaub R. Update on gout: new therapeutic strategies and options. Nat Rev Rheumatol. 2010;6(1):30–8.

48. Hao S, Zhang C, Song H. Natural products improving hyperuricemia with hepatorenal dual effect. Evid Based Complement Alternat Med. 2016, 7390504.

49. Ichida K, Matsuo H, Takada T, Nakayama A, Murakami K, Shimizu T, et al. Decreased extra-renal urate excretion is a common cause of hyperuricemia. Nat Commun. 2012; 3: 764.

50. Lai SW, Tan CK, Ng KC. Epidemiology of hyperuricemia in the elderly. Yale J Bio Med. 2001; 74: 151-7.

51. Jefferson JA, Escudero E, Hurtado ME, Kelly JP, Swenson ER, Wener MH, et al. Hyperuricemia, hypertension and proteinuria associated with high-altitude polycythemia. Am J Kidney Dis. 2002; 39(6): 1135-42.

52. Bove M, Cicero AF, Veronesi M, Borghi C. An evidence-based review on urate-lowering treatments: Implications for optimal treatment of chronic hyperuricemia. Vasc Health Risk Manag. 2017; 13:23-8.

53. Liu R, Han C, Wu D, Xia X, Gu J, Guan H, et al. Prevalence of hyperuricemia and gout in Mainland China from 2000 to 2014: A systematic review and meta-analysis. Biomed Res Int, 2015; 2015:762820.

54. Kanbay M, Jensen T, Solak Y, Le M, Roncal-Jimenez C, Rivard C, et al. Uric acid in metabolic syndrome: form an innocent bystander to a central player. Eur J Intern Med. 2016; 29: 3-8.

55. Choi HK, Ford ES. Prevalence of the metabolic syndrome in individuals with hyperuricemia. Am J Med. 2007; 120(5):442-7.

56. Liu C. Discussion draft of expert consensus of hyperuricemia. Proceedings of the 12th international endocrinology proceedings of Chinese Society of Endorinology, pp. 107-8, 2013.

57. Gliozzi M, Malara N, Muscoli S, Mollace V. The treatment of hyperuricemia. Int J Cardiol. 2016; 213: 23-7.

58. Jordan K, Cameron J, Snaith M, Zhang W, Doherty M, Seckl J, et al. British society for rheumatology and British health professionals in rheumatology guideline for the management of gout. Rheumatology. Oxford, 2007; 46: 1372-4.

59. Zhang W, Doherty M, Bardin T, Pascual E, Barskova V, Conaghan P, et al. EULAR evidence based recommendations for gout. Part II: management. Report of a task force of the EULAR standing committee for international clinical studies including therapeutics (ESCISIT). Ann Rheum Dis. 2006; 65(10):1312-24.

60. Hande KR, Noone RM, Stone WJ. Severe allopurinol toxicity: description and guidelines for prevention in patients with renal insufficiency. Am J Med. 1984; 76(1): 47-56.

61. Lu N, Rai SK, Terkeltaub R, Kim SC, Menendez ME, Choi HK. Racial disparities in the risk of Stevens-Johnson Syndrome and toxic epidermal necrolysis as urate-lowering drug adverse events in the United States. Semin Arthritis Rheum. 2016; 46(2):253-8.

62. Suresh E, Das P. Recent advances in management of gout. QJM. 2012; 105(5): 407-17.

63. Gustafsson D, Unwin R. The pathophysiology of hyperuricaemia and its possible relationship to cardiovascular disease, morbidity and mortality. BMC Nephrol. 2013; 14: 164.

64. Kydd A, Seth R, Buchbinder R, Edward C, Bombardier C. Uricosuric medications for chronic gout. Cochrane Database Syst Rev. 2014; 11:CD010457.

65. Sattui SE, Gaffo AL. Treatment of hyperuricemia in gout: current therapeutic options, latest developments and clinical implications. Ther Adv Musculoskel Dis. 2016; 8(4):145-59.

66. Gentry W, Dotson M, Williams B, Hartley M, Stafford K, Bottorff M, et al. Investigation of pegloticase-associated adverse events from nationwide reporting system database. Am J health Syst Pharm. 2014; 71(9): 722-7.

67. Hershfield M, Ganson N, Kelly S, Scarlett E, Jaggers D, Sundy J. Induced and pre-existing anti-polyethylene glycol antibody in a trial of every 3-week dosing of pegloticase for refractory gout, including in organ transplant recipients. Arthritis Res Ther. 2014; 16(2): R63.

68. Sundy J, Baraf H, Yood R, Edwards N, Gutierrez-Urena S, Treadwell E, et al. Efficacy and tolerability of pegloticase for the treatment of chronic gout in patients refractory to convetional treatment: two randomized controlled trials. JAMA. 2011; 306(7): 711-20.

69. Guo DA. Quality marker concept inspires the quality research of traditional Chinese medicines. Chinese Herbal Medicines. 2017;9(1):1-2.

70. Liu CX, Cheng YY, Guo DA, Zhang TJ, Li YZ, Hou WB, et al. A new concept on quality marker for quality assessment and process control of Chinese medicines. Chinese Herbal Medicines. 2017;9(1):3-13.

71. Jiang Y, David B, Tu P, Barbin Y. Recent analytical approaches in quality control of traditional Chinese medicines-a review. Anal Chim Acta. 2010; 657(1): 9-18.

72. Liang Y, Xie P, Chan K. Quality control of herbal medicines. J Chromatogr B. 2004; 812(1-2): 53-70.

73. Agapouda A, Booker A, Kiss T, Hohmann J, Heinrich M, Csupor D. Quality control of Hypericum perforatum L. analytical challenges and recent progress. J Pharm Pharmacol. 2017.

74. Pandey R, Rameshkumar KB, Kumar B. Ultra high performance liquid chromatography tandem mass spectrometry method for the simultaneous determination of multiple bioactive constituents in fruit extracts of Myristica fragrans and its marketed polyherbal formulations using a polarity switching technique. J Sep Science. 2015; 38(8): 1277–85.

75. Li S, Han Q, Qiao C, Song J, Cheng C, Xu H. Chemical markers for the quality control of herbal medicines: an overview. Chin Med. 2008; 3:7..

76. Huang X, Kong L, Li X, Chen X, Guo M, Zou H. Strategy for analysis and screening of bioactive compounds in traditional Chinese medicines. J Chromatogr B. 2004; 812(1–2): 71–84.

77. Li P, Qi L, Liu E, Zhou J, Wen X. Analysis of Chinese herbal medicines with holistic approaches and integrated evaluation models. TrAC. 2008; 27(1): 66-77.

78. Homma M, Oka K, Yamada T, Niitsuma T, Ihto H, Takahashi N. A strategy for discovering biologically active compounds with high probability in traditional Chinese herb remedies: an application of saiboku-to in bronchial asthma. Anal Biochem. 1992;202(1):179-87.

79. Xu W, Xing FJ, Dong K, You C, Yan Y, Zhang L, et al. Application of traditional Chinese medicine preparation in targeting drug delivery system. Drug Deliv. 2015; 22(2): 258-65.

80. Ma PY, Fu ZY, Su YL, Zhang JY, Wang WM, Wang H, et al. Modification of physicochemical and medicinal characterization of Liuwei Dihuang particles by ultrafine grinding. Powder Technology. 2009;191(1-2):194-9.

81. Manach C, Scalbert A, Morand C. Am J Clin Nutr. 2004;79:727–47.

82. Stella VJ, Rajewski RA. Cyclodextrins: their future in drug formulation and delivery. Pharm Res. 1997; 14(5): 556-67.

83. Nakano M. Places of emulsions in drug delivery. Adv Drug Deliv Rev. 2000;45(1):1-4.

84. Lawrence MJ, Rees GD. Microemulsion-based media as novel drug delivery systems. Adv Drug Deliv Rev. 2000; 45(1): 89-121.

85. Leuner C, Dressman J. Improving drug solubility for oral delivery using solid dispersions. Eur J Pharm Biopharm. 2000; 50(1): 47-60.

86. Merisko-Liversidge E, Liversidge G, Cooper ER. Nanosizing: a formulation approach for poorly-water-soluble compounds. Eur J Pharm Sci. 2003;18(2):113-20.

87. Food and Drug Administration. Guidance for Industry Considering Whether an FDA-Regulated Product Involves the Application of Nanotechnology. Rockville, MD: US Food and Drug Administration; 2014. http://www.fda.gov/RegulatoryInformation/Guidances/ucm257698.htm (Accessed on July 27, 2017).

88. Chen ML, John M, Lee SL, Tyner KM. Development considerations for nanocrystal drug products. AAPS J. 2017;19(3):642-51.

89. Yang XL, Xu HB, Wu JZ, Xie CS. Application of nano-technology in the research of Traditional Chinese Medicine. J Huazhong Univ Sci Tech. 2000;28(12):104-5. (Article in Chinese).

90. Rawat M, Singh D, Saraf S, Saraf S. Nanocarriers: promising vehicle for bioactive drugs. Biol Pharm Bull. 2006; 29(9):1790-8.

91. Duncan R. The dawning era of polymer therapeutics. Nat Rev Drug Discov. 2003; 2(5): 347-60.

92. Ferrari M. Cancer nanotechnology: opportunities and challenges. Nat Rev Cancer. 2005; 5(3):161-71.

93. Junghanns JUAH, Muller RH. Nanocrystals technology, drug delivery and clinical applications. Int J Nanomedicine. 2008; 3(3): 295–309.

94. Fakes MG, Vakkalagadda BJ, Qian F, Desikan S, Gandhi RB, Lai C, et al. Enhancement of oral bioavailability of an HIV-attachment inhibitor by nanosizing and amorphous formulation approaches. Int J Pharm. 2009;370(1-2):167-74.

95. Deng J, Huang L, Liu F. Understanding the structure and stability of paclitaxel nanocrystals. Int J Pharm. 2010; 390(2): 242-9.

96. Ghosh I, Bose S, Vippagunta R, Harmon F. Nanosuspension for improving the bioavailability of a poorly soluble drug and screening of stabilizing agents to inhibit crystal growth. Int J Pharm. 2011; 409(1-2): 260-8.

97. Bilgili E, Afolabi A. A combined microhydrodynamics-polymer adsorption analysis for elucidation of the roles of stabilizers in wet stirred media milling. Int J Pharm. 2012; 439(1-2):193-206.

98. Sinha B, Muller RH, Moschwitzer JP. Bottom-up approaches for preparing drug nanocrystals: formulations and factors affecting particle size. Int. J. Pharm. 2013; 453(1): 126-41.

99. Ghosh I, Schenck D, Bose S, Liu F, Motto M. Identification of critical process parameters and its interplay with nanosuspension formulation prepared by top down media milling technology—a QbD perspective. Pharm Dev Technol. 2013;18(3): 719-29.

100. Sun W, Mao S, Shi Y, Li L, Fang L. Nanonization of itraconazole by high pressure homogenization: stabilizer optimization and effect of particle size on oral absorption. J Pharm Sci. 2001;100(8): 3365-73.

101. Morakul B, Suksiriworapong J, Leanpolchareanchai J, Junyaprasert VB. Precipitation-lyophilization-homogenization (PLH) for preparation of clarithromycin

nanocrystals: influencing factors on physicochemical properties and stability. Int J Pharm. 2013;457(1): 187-96.

102. Moschwitzer JP. Drug nanocrystals in the commercial pharmaceutical development process. Int J Pharm. 2013; 453(1): 142–56.

103. Hu J, Johnston KP, Williams III RO. Nanoparticle engineering processes for enhancing the dissolution rate of poorly water-soluble drugs. Drug Dev Ind Pharm. 2004; 30(3): 233–45.

104. Food and Drug Administration. Guidance for industry: estimating the maximum safe starting dose in adult healthy volunteer. Rockville, MD: US Food and Drug Administration;2005. https://www.fda.gov/downloads/drugs/guidances/ucm078932.pdf (Accessed on August 9, 2017)

105. Nair AB, Jacob S. A simple practice guide for dose conversion between animals and human. J Basic Clin Pharm. 2016;7(2):27-31.

106. Kadam P, Bhalerao S. Sample size calculation. Int J Ayurveda Res. 2010; 1(1): 55–7.

107. Festing MF, Altman DG. Guidelines for the design and statistical analysis of experiments using laboratory animals. ILAR J. 2002; 43(4): 244-58.

108. Zuo J, Zheng Q, Jian H, Porttin T, Willson C, Misquita F, et al. Traditional Chinese Medicine for Managing Inflammatory Pain of Arthritis with Herbal Medicines. Current Traditional Medicine. 2016;2(2):80-93.

109. Robertson M. Translating breakthroughs in genetics into biomedical innovation: The case of UK Genetic Knowledge Parks. Technology Analysis and Strategic Management. 2007; 19(2):189-204.

110. Xue JM. Discussion on the speciality of TCM term translation and the translating principles viewing from the concept of TCM term "qi". Zhongguo Zhong xi yi jie he za zhi. 2008; 28(5): 471-2.

111. Men JZ, Guo L. A General Introduction to Traditional Chinese Medicine Preliminary Introduction to TCM Theory. CRC Press: Boca Raton, US 2009.

112. Wells K. Chinese medicine community split by language issue-language used with patients has sparked heated debate among Chinese medicine practitioners. CBC News. 2014. Available at: http://www.cbc.ca/news/health/chinese-medicine-community-split-by-language-issue-1.2595680 (Accessed March 3, 2015)

113. Wang S, Hu Y, Tan W, Wu X, Chen R, Cao J, et al. Compatibility art of traditional Chinese medicine: From the perspective of herb pairs. J Ethnopharmacol. 2012;143(2):412-23.

114. Ye HZ, Zheng CS, Xu XJ, Wu MX, Liu XX. Potential Synergistic and Multitarget Effect of Herbal Pair Chuanxiong Rhizome-Paeonia Albifora Pall on Osteoarthritis Disease: A Computational Pharmacology Approach. Chin J Integr Med. 2011; 17(9):698-703.

115. Wang M, Chen G, Lu C, Xiao C, Li L, Niu X, et al. Rheumatoid arthritis with deficiency pattern in traditional Chinese Medicine shows correlation with cold and hot patterns in gene expression profiles. Evid Based Complement Alternat Med. 2013;248650.

116. U. Viegener. Rheumatoid arthritis: Traditional Chinese Medicine preparation convinces in study, Pharmazeutische Zeitung. 2014. Available at: http://www.pharmazeutische-zeitung.de/index.php?id=51988 (Accessed March 30,2015)

117. Santosa A, Ng PS, Teng GG. Traditional Chinese medication for rheumatoid arthritis: more than what meets the eye. Rheumatol Int. 2015;35(2):383-4.

118. Centers for Disease Control and Prevention (CDC). Prevalence of doctor-diagnosed arthritis and arthritis-attributable activity limitation-United States, 2010-2012. MMWR Morb Mortal Wkly Rep 2013;62(44):869-73.

119. Arthritis Community Research and Evaluation Unit. Arthritis in Canada. 2013. Available at: https://www.arthritis.ca/document.doc?id=903 (Accessed June 13, 2015).

120. Health Canada. Life with arthritis in Canada : A personal and public health challenge. Chapter 3.2010 http://www.phac-aspc.gc.ca/cd-mc/arthritis-arthrite/lwaic-vaaac-10/5-eng.php (Accessed June 13, 2015)

121. Health Canada. Life with arthritis in Canada: A personal and public health challenge. Chapter 6. 2010 http://www.phac-aspc.gc.ca/cd-mc/arthritis-arthrite/lwaic-vaaac-10/8-eng.php (Accessed June 13, 2015)

122. Cisternas MG, Murphy LB, Yelin EH, Foreman AJ, Pasta DJ, Helmick CG. Trends in Medical Care Expenditures of US Adults with Arthritis and Other Rheumatic Conditions 1997 to 2005. J Rheumatol. 2009;36(11):2531-8.

123. Reginster JY. The prevalence and burden of arthritis. Rheumatology. 2002; 41(suppl.1):3-6.

124. Centers for disease control and prevention. Arthritis Types.Available at: http://www.cdc.gov/arthritis/basics/types.htm (Accessed June 13, 2015)

125. Krustev E, Rioux D, McDougall JJ. Mechanisms and Mediators That Drive Arthritis Pain. Curr Osteoporos Rep 2015;13(4):216-24.

126. Houard X, Goldring MB, Berenbaum F. Homeostatic mechanisms in articular cartilage and role of inflammation in osteoarthritis. Curr Rhematol Rep. 2013;15(11):375.

127. Burrage PS, Mix KS, Brinckerhoff CE. Matrix metalloproteinases: Role in arthritis. Front Biosci. 2006;11:529-43.

128. Chen C, Sun J, Li Y, Shen PA, Chen YQ. Action mechanisms of Du-Huo-Ji-Sheng-Tang on Cartilage Degradation in a Rabbit Model of Osteoarthritis. Evid Based Complement Alternat Med. 2011;571479.

129. Garner M, Alshameeri Z, Khanduja V. Osteoarthritis: genes, nature-nurture interaction and the role of leptin. Int Orthop. 2013;37(12):2499-505.

130. Blagojevic M, Jinks C, Jeffery A, Jordan KP. Risk factors for onset of osteoarthritis of the knee in older adults: a systematic review and meta-analysis. Osteoarthritis Cartilage. 2010;18(1):24-33.

131. Lee AS, Ellman MB, Yan D, Kroin JS, Cole BJ, Van Wijnen AJ, et al. A current review of molecular mechanisms regarding osteoarthritis and pain. Gene. 2013;527(2):440-7.

132. Muller-ladner U. Molecular and cellular interactions in rheumatoid synovium. Curr Opin Rheumatol. 1996; 8(3):210-20.

133. Pope RM. Apoptosis as a therapeutic tool in rheumatoid arthritis. Nat Rev Immunol. 2002;2(7):527-35.

134. Silman AJ, Hochberg MC. Epidemiology of the Rheumatic Diseases. 2nd ed. New York: Oxford University Press; 2001.

135. Helmick CG, Felson DT, Lawrence RC, Gabriel S, Hirsch R, Kwoh CK, et al. National Arthritis Data Workgroup. Estimates of the Prevalence of Arthritis and Other Rheumatic Conditions in the United States Part I. Arthritis Rheum 2008;58(1):15-25.

136. Scott DL, Wolfe F, Huizinga TW. Rheumatoid arthritis. Lancet 2010;376(9746):1094-108.

137. Schett G, Tohidast-Akrad M, Smolen JS, Schmid BJ, Steiner CW, Bitzan P, et al. Activation, differential localization, and regulation of the stress-activated protein kinases, extracellular signal-regulated kinase, c-JUN N-terminal kinase, and p38 mitogen-activated protein kinase, in synovial tissue and cells in rheumatoid arthritis. Arthritis Rheum. 2000;43(11):2501-12.

138. Westermarck J, Holmström T, Ahonen M, Eriksson JE, Kahari VM. Enhancement of fibroblast collagenase-1 (MMP-1) gene expression by tumor promoter okadaic acid is mediated by stress-activated protein kinases Jun N-terminal kinase and p38. Matrix Biol. 1998;17(8-9):547-57.

139. Yang CL, Or TC, Ho MH, Lau AS. Scientific basis of botanical medicine as alternative remedies for rheumatoid arthritis. Clin Rev Allergy Immunol. 2013;44(3):284-300.

140. Asano K, Matsuishi J, Yu Y, Kasahara T, Hisamitsu T. Suppressive effects of Tripterygium wilfordii Hook f., a traditional Chinese medicine, on collagen arthritis in mice. Immunopharmacology. 1998;39(2):117-26.

141. Zhang Y, Wang L, Bai L, Jiang R, Guo L, Wu J, et al. Anti-inflammatory effect of ebosin on rat collagen-induced arthritis through suppressing production of interleukin-1β, interleukin-6 and tumor necrosis factor-α. Cell Mol Immunol. 2015:1-9.

142. Sakurai H, Kohsaka H, Liu MF, Higashiyama H, Hirata Y, Kanno K, et al. Nitric oxide production and inducible nitric oxide synthase expression in inflammatory arthritides. J Clin Invest. 1995;96(5):2357-63.

143. Jang MH, Shin MC, Kim YJ, Kim CJ, Kim Y, Kim EH. Atractylodes japonica suppresses lipopolysaccharide-stimulated expressions of inducible nitric oxide synthase and cyclooxygenase-2 in RAW 264.7 macrophages. Biol Pharm Bull. 2004;27(3):324-7.

144. Saag KG, Teng GG, Patkar NM, Anuntiyo J, Finney C, Curtis JR, et al. American College of Rheumatology 2008 recommendations for the use of nonbiologic and biologic disease-modifying antirheumatic drugs in rheumatoid arthritis. Arthritis Rheum. 2008;59(6):762-84.

145. Sun PL, Vangermeersch L. Classification of bi syndrome. J Trad Chi Med 1995;47:8-14.

146. Zhang EQ. Bi Syndrome (Arthralgia Syndrome). J Tradit Chin Med. 2010;30(2):145-52.

147. Committee for Terms in TCM, China National Committee for Terms in Sciences and Technologies. Chinese Terms in Traditional Chinese Medicine and Pharmacy (中医药学名词).Science Press: Beijing, China 2004.

148. Shen T, Li GH, Wang XN, Lou HX. The genus Commiphora: a review of its traditional uses, phytochemistry and pharmacology. J Ethnopharmacol. 2012;142(2):319-30.

149. Shoemaker M, Hamilton B, Dairkee SH, Cohen I, Campbell MJ. In vitro anticancer activity of twelve Chinese medicinal herbs. Phytother Res. 2005;19(7):649-51.

150. Su S, Wang T, Duan JA, Zhou W, Hua YQ, Tang YP, et al. Anti-inflammatory and analgesic activity of different extracts of Commiphora myrrha. J Ethnopharmacol. 2011;134(2):251-8.

151. Racine P, Auffray B. Quenching of singlet molecular oxygen by Commiphora myrrha extracts and menthofuran. Fitoterapia. 2005;76(3-4):316-23.

152. Jiang P, Zhou LN. Analysis on Composing Principles of Prescriptions for Lijie Disease Based on The Prescription of Traditional Chinese Medicine Dictionary. Chinese Journal of Information on Traditional Chinese Medicine. 2015, 22(4):41-3. [Article in Chinese]

153. Chen CL, Zhang DD. Anti-inflammatory effects of 81 Chinese herb extracts and their correlation with the characteristics of Traditional Chinese Medicine. Evid Based Complement Alternat Med. 2014; 985176.

154. Li W, Tang Y, Chen Y, Duan JA. Advances in the chemical analysis and biological activities of chuanxiong. Molecules. 2012;17(9):10614-51.

155. Chawla AS, Singh M, Murthy MS, et al. Anti-inflammatory action of ferulic acid and its esters in carrageenan induced rat paw oedema model. Indian J Exp Biol. 1987;25(3):187-9.

156. Lv G, Cheng S, Chan K, Leung KS, Zhao Z. Determination of free ferulic acid and total ferulic acid in Chuanxiong by high-performance liquid chromatography for quality assessment. Zhongguo Zhong Yao Za Zhi 2010;35(2):194-8. [Article in Chinese]

157. Li Y, Lu DG, Lei YQ, Lei P, Liu S, Li XZ. Comparison of ferulic acid and paeoniflorin between traditional slice decoction and dispensing granule decoction of Siwu Tang. Zhong Yao Cai. 2008;31(1):125-8. [Article in Chinese]

158. Or TC, Yang CL, Law AH, Li JC, Lau AS. Isolation and identification of anti-inflammatory constituents from Ligusticum chuanxiong and their underlying mechanisms of action on microglia. Neuropharmacology. 2011;60(6):823-31.

159. Liu L, Ning ZQ, Shan S, Zhang K, Deng T, Lu XP, et al. Phthalide Lactones from Ligusticum chuanxiong inhibit lipopolysaccharide-induced TNF-alpha production and TNF-alpha-mediated NF-kappaB Activation. Planta Med. 2005;71(9):808-13.

160. Su S, Hua Y, Wang Y, Gu W, Zhou W, Duan JA, et al. Evaluation of the anti-inflammatory and analgesic properties of individual and combined extracts from Commiphora myrrha, and Boswellia carterii. J Ethnopharmacol. 2012;139(2):649-56.

161. Ammon HP. Modulation of the immune system by Bosweillia serrata extracts and boswellic acids. Phytomedicine. 2010;17(11):862-7.

162. Safayhi H, Mack T, Sabieraj J, Anazodo MI, Subramanian LR, Ammon HP. Boswellic acids: novel, specific, nonredox inhibitors of 5-lipoxygenase. J Pharmacol Exp Ther. 1992;261(3):1143-6.

163. McGuffin M, Hobbs C. American Herbal Products Association's Botanical Safety Handbook. CRC Press, New York, USA 1997.

164. Wu W, Xu X, Dai Y, Xia L. Therapeutic effect of the saponin fraction from Clematis chinensis Osbeck roots on osteoarthritis induced by monosodium iodoacetate through protecting articular cartilage. Phytother Res. 2010;24(4):538-46.

165. Mimaki Y, Yokosuka A, Hamanaka M, Sakuma C, Yamori T, Sashida Y. Triterpene saponins from the roots of clematis chinensis. J Nat Prod. 2004;67(9):1511-6.

166. Hsieh MS, Wang KT, Tseng SH, Lee CJ, Chen CH, Wang CC. Using 18F-FDG microPET imaging to measure the inhibitory effects of Clematis chinensis Osbeck on the pro-inflammatory and degradative mediators associated with inflammatory arthritis. J Ethnopharmacol. 2011;136(3):511-7.

167. Sun SX, Li YM, Fang WR, Cheng P, Liu L, Li F. Effects and mechanism of AR-6 in experimental rheumatoid arthritis. Clin Exp Med. 2010;10(2):113-21.

168. Tao X, Younger J, Fan FZ, Wang B, Lipsky PE. Benefit of an extract of Tripterygium Wilfordii Hook F in patients with rheumatoid arthritis. Arthritis Rheum. 2002; 46(7): 1735-43.

169. Bao J, Dai SM. A Chinese herb Tripterygium wilfordii Hook F in the treatment of rheumatoid arthritis: mechanism, efficacy, and safety. Rheumatol Int. 2011; 31(9):1123-9.

170. Liu Y, Tu S, Gao W, Wang Y, Liu P, Hu Y, et al. Extracts of Tripterygium wilfordii Hook F in the Treatment of Rheumatoid Arthritis: A Systemic Review and Meta-Analysis of Randomised Controlled Trials. Evil Based Complement Alternat Med. 2013; 410793.

171. Zheng JR, Fang JL, Gu KX, Yin YQ, Xu LF, Gao JW, et al. Screening of active anti-inflammatory-immunosuppressive and antifertile components from Tripterygium wilfordii. II. Screening of 5 monomers from total glucosides of Tripterygium wilfordii (TII). Zhongguo Yi Xue Ke Xue Yuan Xue Bao. 1987; 9(5):323-8. [Article in Chinese]

172. Chen BJ. Triptolide, a novel immunosuppressive and anti-inflammatory agent purified from a Chinese herb Tripterygium wilfordii Hook F. Leuk Lymphoma. 2001; 42(3):253–65.

173. Sylvester J, Liacini A, Li WQ, Dehnade F, Zafarullah M. Tripterygium wilfordii Hook f extract suppresses proinflammatory cytokine-induced expression of matrix metalloproteinase genes in articular chondrocytes by inhibiting activating protein-1 and nuclear factor-κB activities. Mol Pharmacol. 2001;59(5):1196–205.

174. Zhou HF, Niu DB, Xue B, Li FQ, Liu XY, He QH, et al. Triptolide inhibits TNF-α, IL-1β and NO production in primary microglial cultures. Neuroreport. 2003;14(7):1091–109.

175. Tao X, Ma L, Mao Y, Lipsky PE. Suppression of carrageenan-induced inflammation in vivo by an extract of the Chinese herbal remedy Tripterygium wilfordii Hook F. Inflamm Res. 1999;48(3):139–48

176. Lin N, Sato T, Ito A. Triptolide, a novel diterpenoid triepoxide from Tripterygium wilfordii Hook, f., suppresses the production and gene expression of pro-matrix metalloproteinases 1 and 3 and augments those of tissue inhibitors of metalloproteinases 1 and 2 in human synovial fibroblasts. Arthr Rheum. 2001;44(9):2193–200.

177. Lee GI, Ha JY, Min KR, Nakagawa H, Tsurufuji S, Chang IM, et al. Inhibitory effects of oriental herbal medicines on IL-8 induction in lipopolysaccharide-activated rat macrophages. Planta Med. 1995; 61(1):26–30.

178. Ye WH. Mechanism of treating rheumatoid arthritis with polyglycosides of Tripterygium wilfordii Hook (T II). III. Study on inhibitory effect of T II on in vitro Ig secreted by peripheral blood mononuclear cells from normal controls and RA patients. Zhongguo Yi Sue Ke Xue Yuan Xue Bao. 1990;12(3):217–222. [Article in Chinese]

179. Zhang P, Li J, Han Y, Yu XW, Qin L. Traditional Chinese medicine in the treatment of rheumatoid arthritis: A general review. Rheumatol Int. 2010;30(6):713-8.

180. Tao X, Cai JJ, Lipsky PE. The identity of immunosuppressive components of the ethyl acetate extract and chloroform methanol extract (T2) of Tripterygium wilfordii Hook.F. J Pharmacol Exp Ther. 1995;272(3):1305-12.

181. Su DF, Li RL, Sun YJ. Report of 270 patients with rheumatoid arthritis treated with ethyl acetate extract of Tripterygium wilfordii Hook F. Zhong Yao Yao Li Yu Lin Chuang. 1989;5:40-2. [Article in Chinese]

182. Yu DY. Clinical observation of 144 cases of rheumatoid arthritis treated with glycoside of radix Tripterygium wilfordii. J Tradit Chin Med. 1983;3(2):125-9.

183. Tao X, Cush JJ, Garret M, Lipsky PE. A phase I study of ethyl acetate extract of the chinese anti-rheumatic herb Tripterygium wilfordii hook F in rheumatoid arthritis. J Rheumatol. 2001;28(10):2160-7.

184. Goldbach-Mansky R, Wilson M, Fleischmann R, Olsen N, Silverfield J, Kempf P, et al. Comparison of Tripterygium wilfordii Hook F versus sulfasalazine in the treatment of rheumatoid arthritis: a randomized trial. Ann Intern Med. 2009;151(4):229-40, W49-51.

185. Hook IL. Danggui to Angelica sinensis root: are potential benefits to European women lost in translation? A review. J Ethnopharmacol. 2014;152(1):1-13.

186. Chen MP, Yang SH, Chou CH, Yang KC, Wu CC, Cheng YH, et al. The chondroprotective effects of ferulic acid on hydrogen peroxide-stimulated chondrocytes: inhibition of hydrogen peroxide-induced pro-inflammatory cytokines and metalloproteinase gene expression at the mRNA level. Inflamm Res. 2010; 59(8):587–95.

187. Zhang RX, Fan AY, Zhou AN, Moudgil KD, Ma ZZ, Lee DY, et al. Extract of the Chinese herbal formula Huo Luo Xiao Ling Dan inhibited adjuvant arthritis in rats. J Ethnopharmacol. 2009;121(3):366–71.

188. Magdalou J, Chen LB, Wang H, Qin J, Wen Y, Li XJ, et al. Angelica sinensis and osteoarthritis: a natural therapeutic link? Biomed Mater Eng. 2015;25(1 Suppl):179-86.

189. Lee WS, Lim JH, Sung MS, Lee EG, Oh YJ, Yoo WH, et al. Ethyl acetate fraction from Angelica sinensis inhibits IL-1β-induced rheumatoid synovial fibroblast proliferation and COX-2, PGE2, and MMPs production. Bio Res. 2014;47(1):41.

190. Chao WW, Kuo YH, Li WC, Lin BF. The production of nitric oxide and prostaglandin E(2) in peritoneal macrophages is inhibited by Andrographis paniculata, Angelica sinensis and Morus alba ethyl acetate fractions. J Ethnopharmacol. 2009;122(1):68-75.

191. Chao WW, Hong YH, Chen ML, Lin BF. Inhibitory effects of Angelica sinensis ethyl acetate extract and major compounds on NF-kappaB trans-activation activity and LPS-induced inflammation. J Ethnopharmacol. 2010;129(2):244-9.

192. Lu GH, Chan K, Leung K, Chan CL, Zhao ZZ, Jiang ZH. Assay of free ferulic acid and total ferulic acid for quality assessment of Angelica sinensis. J Chromatogr A. 2005; 1068(2):209-19.

193. Page RL, Lawrence JD. Potentiation of warfarin by dong quai. Pharmacotherapy. 1999;19(7): 870-6.

194. Heck AM, DeWitt BA, Lukes AL. Potential interactions between alternative therapies and warfarin. Am J Health-Syst Pharm. 2000; 57(13):1221-30.

195. Zhang W, Dai SM. Mechanisms involved in the therapeutic effects of Paeonia lactiflora Pallas in rheumatoid arthritis. Int Immunopharmacol. 2012;14(1):27-31.

196. He DY, Dai SM. Anti-inflammatory and immunomodulatory effects of paeonia lactiflora pall., a traditional chinese herbal medicine. Front Pharmacol. 2011 Feb 25;2:10.

197. Paeoniae Radix Alba (白芍). In Pharmacopoeia of the People's Republic of China 2010, vol.1 (中华人民共和国药典 2010 版一部). Chinese Pharmacopeia Commission. 2010: 96-7. [Chinese].

198. Zhang XJ, Chen HL, Li Z, Zhang HQ, Xu HX, Sung JJ, et al. Analgesic effect of paeoniflorin in rats with neonatal maternal separation-induced visceral hyperalgesia is mediated through adenosine A(1) receptor by inhibiting the extracellular signal-regulated protein kinase (ERK) pathway. Pharmacol Biochem Behav. 2009;94(1):88-97.

199. Wu H, Wei W, Song LH, Zhang LL, Chen Y, Hu XY. Paeoniflorin induced immune tolerance of mesenteric lymph node lymphocytes via enhancing beta2-adrenergic receptor desensitization in rats with adjuvant arthritis. Int Immunopharmacol. 2007;7(5):662-73.

200. Zhang LL, Wei W, Wang NP, Wang QT, Chen JY, Chen Y, et al. Paeoniflorin suppresses inflammatory mediator production and regulates G protein-coupled signaling in fibroblast-like synoviocytes of collagen induced arthritic rats. Inflamm Res. 2008;57(8): 388–95

201. Zhou H, Bian D, Jiao X, Wei Z, Zhang H, Xia Y, et al. Paeoniflorin protects against lipopolysaccharide-induced acute lung injury in mice by alleviating inflammatory cell infiltration and microvascular permeability. Inflamm Res. 2011;60 (10): 981–90.

202. Jiang D, Chen Y, Hou X, Xu J, Mu X, Chen W. Influence of Paeonia lactiflora roots extract on cAMP-phosphodiesterase activity and related anti-inflammatory action. J Ethnopharmacol. 2011;137(1): 914–20.

203. Chang Y, Zhang L, Wang C, Jia XY, Wei W. Paeoniflorin inhibits function of synoviocytes pretreated by rIL-1α and regulates EP4 receptor expression. J Ethnopharmacol. 2011;137(3):1275–82.

204. Chen G, Guo LX, Deng XH, Yin ZY, Jing JJ. Effects of total glucosides of paeony on nitric oxide and inducible nitric oxide synthase production in macrophages and its mechanism. Zhongguo Mian Yi Xue Za Zhi. 2008;24:345-7,351 [Article in Chinese]

205. Tsuboi H, Hossain K, Akhand AA, Takeda K, Du J, Rifa'i M, et al. Paeoniflorin induces apoptosis of lymphocytes through a redox-linked mechanism. J Cell Biochem. 2004; 93(1):162–72.

206. Zheng YQ, Wei W. Total glucosides of paeony suppressed adjuvant arthritis in rats and intervening cytokine-signaling between different types of synoviocytes. Int Immunopharmacol. 2005;5(10):1560–73.

207. Zhu L, Wei W, Zheng YQ, Jia XY. Effects and mechanisms of total glucosides of paeony on joint damage in rat collagen-induced arthritis. Inflamm Res. 2005;54 (5): 211–20.

208. Wang X, Zhang H, Chen L, Shan L, Fan G, Gao X. Liquorice, a unique "guide drug" of traditional Chinese medicine: a review of its role in drug interactions. J Ethnopharmacol. 2013; 150(3):781-90.

209. Wang YC, Yang YS. Simultaneous quantification of flavonoids and triterpenoids in licorice using HPLC. J Chromatogr B Analyt Technol Biomed Life Sci. 2007, 850; (1-2): 392–99.

210. Fu Y, Chen J, Li YJ, Zheng YF, Li P. Antioxidant and anti-inflammatory activities of six flavonoids separated from licorice. Food Chem. 2013;141(2):1063-71.

211. Zhang Q, Ye M. Chemical analysis of the Chinese herbal medicine Gan-Cao (licorice). J Chromatogr A. 2009;1216(11):1954-69.

212. Bao J, Li SM, Wang QJ. Literature Research of Chinese Medicine on Rheumatoid Arthritis. Journal of Emergency in Traditional Chinese Medicine. 2014;23(8):1446-50.[Article in Chinese]

213. Lv YB, Li L, Wang ZF, Zheng G, Guo HT, Jiang M, et al. The Medication Regularity of Traditional Chinese Medicine Against Rheumatoid Arthritis, Gout and Osteoarthritis. World Science & Technology. 2010;12(5):833-6. [Article in Chinese]

214. Kim KR, Jeong CK, Park KK, Choi JH, Park JH, Lim SS, et al. Anti-inflammatory effects of licorice and roasted licorice extracts on TPA-induced acute inflammation and collagen-induced arthritis in mice. J Biomed Biotechnol. 2010;709378.

215. Furuhashi I, Iwata S, Shibata S, Sato T, Inoue H. Inhibitionby licochalcone A, a novel flavonoid isolated from liquorice root, of IL-1b-induced PGE2 production in human skin fibroblasts. J Pharm Pharmacol. 2005;57(12):1661-6.

216. Saposhnikoviae radix (防风). In Pharmacopoeia of the People's Republic of China 2010, vol.1 (中华人民共和国药典 2010 版一部). Chinese Pharmacopeia Commission. 2010: 140. [Chinese]

217. Xue BY, Li W, Li L, Xiao YQ. A pharmacodynamics research on chromone glucosides of fangfeng. Zhongguo Zhong Yao Za Zhi. 2000;25(5):297-9. [Article in Chinese]

218. Tai J, Cheung S. Anti-proliferative and antioxidant activities of Saposhnikovia divaricata. Oncol Rep. 2007;18 (1):227-34

219. Dai J, Chen X, Cheng W, Liu X, Fan X, Shen Z, et al. A sensitive liquid chromatography-mass spectrometry method for simultaneous determination of two active chromones from Saposhnikovia root in rat plasma and urine. J Chromatogr B Analyt Technol Biomed Life Sci. 2008;868(1-2):13-9.

220. Gui Y, Tsao R, Li L, Liu CM, Wang J, Zong X. Preparative separation of chromones in plant extract of Saposhnikovia divaricata by high-performance counter-current chromatography. J Sep Sci 2011;34(5):520-26.

221. Kang J, Sun JH, Zhou L, Ye M, Han J, Wang BR, et al. Characterization of compounds from the roots of Saposhnikovia divaricata by high- performance liquid chromatography coupled with electrospray ionization tandem mass spectrometry. Rapid Commun Mass Spectrom. 2008;22(12):1899-1911.

222. Kong X, Liu C, Zhang C, Zhao J, Wang J, Wan H, et al. The suppressive effects of Saposhnikovia divaricata (Fangfeng) chromone extract on rheumatoid arthritis via

inhibition of nuclear factor-κB and mitogen activated proteinkinases activation on collagen-induced arthritis model. J Ethnopharmacol. 2013;148(3):842-50.

223. Peng HR. Grand Dictionary of Chinese medicinal formula (中医方剂大辞典). People's Medical Publishing House Co., LTD.: Beijing, China 2005. [Article in Chinese]

224. 凌锡森，王行宽，陈大舜。中西医结合内科学。中国中医药出版社: 北京，中国 2001。[Article in Chinese]

225. Ma Y, Cui J, Huang M, Meng K, Zhao Y. Effects of duhuojisheng tang and combined therapies on prolapse of lumbar intervertebral disc: a systematic review of randomized control trail. J Tradit Chin Med. 2013;33(2):145-55.

226. Zhao J, Zha Q, Jiang M, Cao H, Lu A. Expert consensus on the treatment of rheumatoid arthritis with Chinese patent medicines. J Altern Complement Med. 2013;19(2):111-8.

227. Lai JN, Chen HJ, Chen CC, Lin JH, Hwang JS, Wang JD. Duhuo Jisheng Tang for treating osteoarthritis of the knee: a prospective clinical observation. Chin Med. 2007;2:4.

228. Hsieh SC, Lai JN, Chen PC, Chen CC, Chen HJ, Wang JD. Is Duhuo Jisheng Tang containing Xixin safe? A four-week safety study. Chin Med. 2010;5 (1):6.

229. Chen MF, Jiang H. Research Progresses in Treatment of Knee Osteoarthritis Using Duhuo Jisheng Decoction. Journal of Liaoning University of Traditional Chinese Medicine. 2014;16(6):236-8. [Article in Chinese]

230. 程维, 张玉辉. 独活寄生汤对膝关节骨性关节炎患者关节液中 TNF-α、IL-6 及 MMP-3 的影响. 中医药导报 2012, 18(4):30-31.[Article in Chinese]

231. 万琦兵, 杨惠琴. 独活寄生汤对膝骨性关节炎患者关节液 hs-CRP 和 MMP-3 含量的影响. 放射免疫学杂志 2012, 25(5):531-532. DOI:10.3969/j.issn.1008-9810.2012.05.028. [Article in Chinese]

232. 詹宏钢, 林剑. 独活寄生汤对膝骨关节炎患者 Wnt/β-catenin-BMP 信号通路调控作用的临床研究. 中国中医药科技, 2013, 20(5):451-452. [Article in Chinese]

233. Graziose R, Lila MA, Raskin I. Merging traditional Chinese medicine with modern drug discovery technologies to find novel drugs and functional foods. Curr Drug Discov Technol 2010;7(1):2-12.

234. Fung FY, Linn YC. Developing traditional chinese medicine in the era of evidence-based medicine: current evidences and challenges. Evid Based Complement Alternat Med 2015;425037.

235. Health Canada. Natural Health Products Regulations. 2015. Available at: http://www.hc-sc.gc.ca/dhp-mps/prodnatur/index-eng.php. (Accessed June 23, 2015)

236. United States Pharmacopeia and National Formulary USP 37–NF 32. The United States Pharmacopeial Convention: Rockville, US 2014.

237. Food and Drug Administration.Dietary supplement. U.S. Department of Health and Human Services Food and Drug Administration Center for Drug Evaluation and Research. 2015. Available at: http://www.fda.gov/Food/DietarySupplements/QADietarySupplements/default.htm#what_is (Accessed June 23, 2015)

238. Zuo J, He H, Zuo Z, Bou-Chacra N, Loebenberg R. Erding Formula in hyperuricaemia treatment: unfolding traditional Chinese herbal compatibility using modern pharmaceutical approaches. J Pharm Pharmacol. 2018;70 (1):124-32.

239. Yan D, Ma Y, Shi R, Xu D, Zhang N. Pharmacokinetics of anthraquinones in Xiexin decoction and in different combinations of its constituent herbs. Phytother Res. 2009; 23(3): 317-23.

240. Tang D. Science of Chinese material medica. Publishing house of Shanghai University of traditional Chinese medicine, Shanghai, China, 2003.

241. Cai C, Chen Y, Zhong S, Zhang Y, Jiang J, Xu H, et al. Synergistic effect of compounds from a Chinese herb: compatibility and dose optimization of compounds from n-butanol extract of ipomoea stolonifera. Sci Rep. 2016;6:27014.

242. Mo SF, Zhou F, Lv YZ, Hu QH, Zhang DM, Kong LD. Hypouricemic action of selected flavonoids in mice: structure-activity relationships. Biol Pharm Bull. 2007;30(8):1551-6.

243. Feig DI, Kang DH, Johnson RJ. Uric Acid and Cardiovascular Risk, New Engl J Med. 2008; 359(17):1811-21.

244. Arafat OM, Tham SY, Sadikun A, Zhari I, Haughton PJ, Asmawi MZ. Studies on diuretic and hypouricemic effects of orthosiphon stamineus methanol extracts in rats. J Enthopharmacol. 2008;118(3):354-60.

245. Pascual E, Perdiguero M. Gout, diuretics and the kidney. Ann Rheum Dis. 2006; 65(8): 981-982.

246. Chen G, Tan ML, Li KK, Leung PC, Ko CH. Green tea polyphenols decreases uric acid level through xanthine oxidase and renal urate transporters in hyperuricemic mice. J Ethnopharmacol. 2015;175:14-20.

247. So A, Thorens B. Uric acid transport and disease. J Clin Invest. 2011;120(6):1791-9.

248. Li JM, Zhang X, Wang X, Xie YC, Kong LD. Protective effects of cortex fraxini coumarines against oxonate-induced hyperuricemia and renal dysfunction in mice. Eur J Pharmacol. 2011;666(1-3):196-204.

249. Zhou Q, Yu DH, Zhang C, Liu SM, Lu F. Total Saponins from discorea nipponica ameliorate urate excretion in hyperuricemic mice. Planta Med. 2014;80(15):1259-68.

250. Cao BJ, Meng QY, Ji N. Analgesic and anti-inflammatory effects of ranunculus japonicus extract. Planta Med. 1992;58(6):496-8.

251. Vilela FC, de Mesquita Padilha M, Dos Santos-E-Silva L, Alves-da-Dilva G, Giusti-Paiva A. Evaluation of the antinociceptive activity of extracts of Sonchus oleraceus L. in mice. J Ethnopharmacol. 2009;124(2):306-10.

252. Collier HO, Dinneen LC, Johnson CA, Schneider C. The abdominal constriction response and its suppression by analgesic drugs in the mouse. Brit J Pharmacol Chemoth. 1968;32(2): 295-310.

253. Wakuda H, Uchida S, Ikeda M, Tabuchi M, Akahoshi Y, Shinozuka K, et al. Is Hyperuricemia a Risk Factor for Arteriosclerosis? Uric Acid and Arteriosclerosis in Apolipoprotein E-Deficient Mice. Biol. Pharm. Bull. 2014;37(12):1866-1871.

254. Cheng LC, Murugaiyah V, Chan KL. Flavonoids and phenylethanoid glycosides from Lippia nodiflora as promising antihyperuricemic agents and elucidation of their mechanism of action. J Ethnopharmacol. 2015;176:485-93.

255. Carroll JJ, Coburn H, Douglass, Babson AL. A simplified alkaline phosphotungstate assay for uric acid in serum. Clin Chem. 1971; 17(3):158-60.

256. Zhan Y, Li TE, Huang WP, Jian H, Li Y, He MZ, et al. Simultaneous determination of caftaric acid, cichorigenin and chicoric acid in Erding Granules by HPLC. Chin Trad Pat Med. 2015;37:2190-3. (Article in Chinese)

257. Hong JL, Zhou HY, Zhu J, Li L, Shu P, Qin XY, et al. Comparative analysis of major constituents in Viola yedoensis Makino and different species from the Genus Viola by high-performance liquid chromatography with chemometrics methods. Journal of Medicinal Plant Research. 2011;5(21):5230-9.

258. Park SH, Sung YY, Nho KJ, Kim DS, Kim HK. Effects of Viola mandshurica on Atherosclerosis and Hepatic Steatosis in ApoE[Formula: see text] via the AMPK Pathway. Am J Chin Med. 2017;45(4):757-72.

259. Ma Y, Wink M. Lobeline, a piperidine alkaloid from Lobelia can reverse P-gp dependent multidrug resistance in tumor cells. Phytomedicine. 2008;15(9):754-8.

260. Hosoyamada M, Ichida K, Enomoto A, Hosoya T, Endou H. Function and localization of urate transporter 1 in mouse kidney. J Am Soc Nephrol. 2004;15(2): 261-8.

261. Chen H, Zheng S, Wang Y, Zhu H, Liu Q, Xue Y, et al. The effect of resveratrol on the recurrent attacks of gouty arthritis. Clin Rheumatol. 2016;35(5):1189-95.

262. Hirai A, Kumagai A. Animal model for gout. Jikken Dobutsu. 1982;31(2): 143-51.

263. Enomoto A, Kimura H, Chairoungdua A, Shigeta Y, Jutabha P, Cha SH, et al. Molecular identification of a renal urate anion exchanger that regulates blood urate levels. Nature. 2002; 417 (6887): 447-52.

264. Kou Y, Li Y, Ma H, Li W, Li R, Dang Z. Uric acid lowering effect of Tibetan Medicine RuPeng15 powder in animal models of hyperuricemia. J Tradit Chin Med. 2016; 36(2):205-210.

265. Zhao X, Zheng XH, Fan TP, Li ZJ, Zhang YY, Zheng JB. A novel drug discovery strategy inspired by traditional medicine philosophies. Science. 2015;347(6219):S38–S40.

266. Liang XM, Jin Y, Wang YP, Jin GW, Fu Q, Xiao YS. Qualitative and quantitative analysis in quality control of traditional Chinese medicines. J Chromatogr A. 2009; 1216: 2033-44.

267. Song Y, Zhang N, Shi S, Li J, Zhang Q, Zhao Y, et al. Large-scale qualitative and quantitative characterization of components in Shenfu injection by integrating hydrophilic interaction chromatography, reversed phase liquid chromatography, and tandem mass spectrometry. J Chromatogr A. 2015; 1407: 106-18.

268. Waldmann S, Almukainzi M, Bou-Chacra N, Amidon GL, Lee BJ, Feng J, et al. Provisional biopharmaceutical classification of some common herbs used in western medicine. Mol Pharm. 2012; 9: 815-22.

269. European Medicine Agency, 2009. Guideline on quality of combination herbal medicinal products / traditional herbal medicinal products. [Accessed on Nov 25, 2016.] Available from: http://www.ema.europa.eu/docs/en_GB/document_library/Scientific_guideline/2009/09/WC500003286.pdf,

270. Xie C, Wang Z, Wang C, Xu J, Wen Z, Wang H, et al. Utilization of gene expression signature for quality control of traditional Chinese medicine formula Si-Wu-Tang. AAPS J. 2013; 15: 884-92.

271. Wang L, Wang Z, Wo S, Lau CB, Chen X, Huang M, et al. A bio-activity guided in vitro pharmacokinetic method to improve the quality control of Chinese medicines, application to Si Wu Tang. Int J Pharm. 2011; 406: 99-105.

272. Zhu Y. Chinese Materia Medica: Chemistry, Pharmacology and Application. Boca Raton: CRC Press, 1998. p. 207-208.

273. Wang M, Xu X, Wu C, Gong Q, Zhang W, Jian H, et al. Pharmacodynamics study of Erding granule for gout. Pharmacology and Clinics of Chinese Materia Medica. 2016; 32: 125-8. (Article in Chinese)

274. Cai Y, Gao Y, Tan G, Wu S, Dong X, Lou Z, et al. 2013. Myocardial lipidomics profiling delineate the toxicity of traditional Chinese medicine Aconiti Lateralis radix praeparata. J Ethnopharmacol. 2013; 147: 349-56.

275. Xu T, Li S, Sun Y, Pi Z, Liu S, Song F, et al. Systematically characterize the absorbed effective substances of Wutou Decoction and their metabolic pathways in rat plasma using UHPLC-Q-TOF-MS combined with a target network pharmacological analysis. J Pharm Biomed Anal. 2017; 141: 95-107.

276. Hall IH, Scoville JP, Reynolds DJ, Simlot R, Duncan P. Substituted cyclic imides as potential anti-gout agents. Life Sci. 1990; 46: 1923-7.

277. Osada Y, Tsuchimoto M, Fukushima H, Takahashi K, Kondo S, Hasegawa M, et al. Hypouricemic effect of the novel xanthine oxidase inhibitor, TEI-6720, in rodents. Eur J Pharmacol. 1993; 241: 183-8.

278. Domagk GF, Schlicke HH. A colorimetric method using uricase and peroxidase for the determination of uric acid. Anal Biochem. 1968; 22: 219-24.

279. Gochman N, Schmitz JM. Automated determination of uric acid, with use of a uricase-peroxidase system. Clin Chem. 1971; 17: 1154-9.

280. Ding WJ, Deng Y, Feng H, Liu WW, Hu R, Li X, et al. Biotransformation of aesculin by human gut bacteria and identification of its metabolites in rat urine. World J Gastroenterol. 2009; 15: 1518-23.

281. Xie PS, Leung AY. Understanding the traditional aspect of Chinese medicine in order to achieve meaningful quality control of Chinese materia medica. J Chromatogr A. 2009; 1216: 1933-40.

282. Cos P, Ying L, Calomme M, Hu JP, Cimanga K, Van Poel B, et al. Structure-activity relationship and classification of flavonoids as inhibitors of xanthine oxidase and superoxide scavengers. J Nat Prod. 1998; 61: 71-6.

283. Nagao A, Seki M, Kobayashi H. Inhibition of xanthine oxidase by flavonoids. Biosci Biotechnol Biochem. 1999; 63: 1787-90.

284. Zhu JX, Wang Y, Kong LD, Yang C, Zhang X. Effects of Biota orientalis extract and its flavonoid constituents, quercetin and rutin on serum uric acid levels in oxonate-induced mice and xanthine dehydrogenase and xanthine oxidase activities in mouse liver. J Ethnopharmacol. 2004; 93: 133-40.

285. Lipinski CA. Drug-like properties and the causes of poor solubility and poor permeabilty. J Pharmacol Toxicol Methods. 2000;44(1):235-49.

286. Rabinow BE. Nanosuspensions in drug delivery. Nat Rev Drug Discov. 2004;3(9):785-96.

287. Kesisoglou F, Panmai S, Wu Y. Nanosizing-oral fomulation development and biopharmaceutical evaluation. Adv Drug Deliv Rev. 2007;59(7):631-44.

288. Hasa D, Voinovich D, Perissutti B, Grassi G, Fiorentino S, Farra R, Abrami M, Colombo I, Grassi M. Reduction of melting temperature and enthalpy of drug crystals: theoretical aspects. Eur J Pharm Sci. 2013;50(1):17-28.

289. Hasa D. Drug nanocrystals: theoretical background of solubility increase and dissolution rate enhancement. Chem Biochem Eng Q J. 2014;28(3):247-58.

290. Badawi AA, El-Nabarawi MA, El-Setouhy DA, Alsammit SA. Formulation and stability testing of itraconazole crystalline nanoparticles. AAPS Pharm Sci Tech. 2011;12(3):811-20.

291. Ochi M, Kawachi T, Toita E, Hashimoto I, Yuminoki K, Onoue S, et al. Development of nanocrystal formulation of meloxicam with improved dissolution and pharmacokinetic behavior. Int J Pharm. 2014;474(1-2):151-6.

292. Toziopoulou F, Malamatari M, Nikolakakis I, Kachrimanis K. Production of aprepitant nanocrystals by wet media milling and subsequent solidification. Int J Pharm. 2017;533(2):324-34.

293. Tuomela A, Hirvonen J, Peltonen L. Stabililzing agents for drug nanocrystals: effect on biovailability. Pharmaceutics. 2016:8(2):16.

294. Lourenço FR, Francisco FL, Ferreira MR, Andreoli Tde J, Löbenberg R, Bou-Chacra N. Design Space Approach for Preservative System Optimization of an Anti-Aging Eye Fluid Emulsion. J Pharm Pharm Sci. 2015;18(3):551-61.

295. International Council for Harmonisation, "Guidance for industry, Q8(R2) Pharmaceutical Development," rev.2, 2009. https://www.ich.org/fileadmin/Public_Web_Site/ICH_Products/Guidelines/Quality/Q8_R1/Step4/Q8_R2_Guideline.pdf (Accessed on Jan 28, 2018).

296. Hagedorn M, Bögershausen A, Rischer M, Schubert R, Massing U. Dual centrifugation - A new technique for nanomilling of poorly soluble drugs and formulation screening by an DoE-approach. Int J Pharm. 2017;530(1-2):79-88.

297. Iurian S, Bogdan C, Tomuta I, Szabo-Revesz P, Chvatal A, Leucuta SE, et al. Development of oral lyophilisates containing meloxicam nanocrystals using QbD approach. Eur J Pharm Sci. 2017; 104:356-65.

298. Hou Y, Shao J, Fu Q, Li J, Sun J, He Z. Spray-dried nanocrystals for a highly hydrophobic drug: increased drug loading, enhanced redispersity, and improved oral biovailability. Int J Pharm. 2017; 516(1-2):372-9.

299. Sahoo NG, Kakran M, Shaal LA, Li L, Muller RH, Pal M, et al. Preparation and characterization of quercetin nanocrystals. J Pharm Sci. 2011; 100(6):2379-90.

300. Bou-Chacra N, Melo KJC, Morales IAC, Stippler ES, Kesisoglou F, Yazdanian M4, et al. Evolution of Choice of Solubility and Dissolution Media After Two Decades of Biopharmaceutical Classification System. AAPS J. 2017; 19(4):989-1001.

301. The United States Pharmacopeial Convention. Reagents, indicators and solutions. In United States Pharmacopeia and National Formulary USP 36–NF 31. Rockville: The United States Pharmacopeial Convention; 2013. p. 1133-229.

302. Trinh TK, Kang LS. Response surface methodological approach to optimize the coagulation-flocculation process in drinking water treatment. Chem Eng Res Des. 2011; 89(7): 1126-35.

303. Wang Y, Zheng Y, Zhang L, Wang Q, Zhang D. Stability of nanosuspensions in drug delivery. J Control Release. 2013;172(3):1126–41.

304. Verma S, Kumar S, Gokhale R, Burgess DJ. Physical stability of nanosuspensions: investigation of the role of stabilizers on Ostwald ripening. Int J Pharm. 2011;406(1-2):145–52.

305. Freag MS, ElnaggarYS, AbdallahOY. Development of novel polymer-stabilized diosmin nanosuspensions: in vitro appraisal and ex vivo permeation. Int J Pharm. 2013;454(1):462–71.

306. Ali HS, York P, Ali AM, Blagden N. Hydrocortisone nanosuspensions for ophthalmic delivery: a comparative study between micro uidic nano- precipitation and wet milling. J Control Release. 2011;149(2):175–81.

307. Yuminoki K, Seko F, Horii S, Takeuchi H, Teramoto K, Nakada Y, et al. Preparation and evaluation of high dispersion stable nanocrystal formulation of poorly water-soluble compounds by using povacoat. J Pharm Sci. 2014;103(11):3772-81.

308. Mujumdar AS, Alterman DS. Drying in the pharmaceutical and biotechnology fields. In: Goldberg E (Ed). Handbook of downstream processing. Springer, Netherlands, Dordrecht, 1997; pp.235-60,6.

309. Bexiga NM, Bloise AC, Alencar AM, Stephano MA. Freeze-drying of ovalbumin-loaded carboxymethyl chitosan nanocapsules: Impact of freezing and annealing

procedures on physicochemical properties of the formulation during dried storage. Drying technology. 2018; 36(4): 400-17.

310. Fini A, Ospitali F, Zoppetti G, Puppini N. ATR/Raman and fractal characterization of HPBCD/progesterone complex solid particles. Pharm Res. 2008, 25(9):2030-40.

311. Lin S, Lin H, Chi Y, Hung R, Huang Y, Kao C, et al. Povacoat affecting solid-state polymorphic changes of indomethacin after co-evaporation from different types of solvents via conventional and microwave drying techniques. Asian J Pharm Sci. 2016;11(3):376-384.

312. Dwyer LM, Michaelis VK, O'Mahony M, Griffin RG, Myerson AS. Confined crystallization of fenofibrate in nanoporous sílica. CrystEngComm. 2015; 17(41):7922-9.

313. Shah DA, Patel M, Murdande SB, Dave RH. Influence of spray drying and dispersing agent on surface and dissolution properties of griseofulvin micro and nanocrystals. Drug Dev Ind Pharm. 2016;42(11):1842-50.

314. Wu W, Nancollas G. A new understanding of the relationship between solubility and particle size. J Solut Chem. 1998;27(6):521-31.

315. Barbosa SF, Takatsuka T, Tavares GD, Araujo GL, Wang H, Vehring R, et al. Physical-chemical properties of furosemide nanocrystals developed using rotation revolution mixer. Pharm Dev Technol. 2016;21(7):812-22.

316. Adams GDJ, Ramsay JR. Optimizing the lyophilization cycle and the consequences of collapse on the pharmaceutical acceptability of Erwinia L-Asparaginase. J Pharm Sci. 1996; 8606(12):1301-5.

317. Schlesinger N. Management of acute and chronic gouty arthritis. Drugs. 2004;64(21):2399-2416.

318. State administration of traditional Chinese medicine of the People's Republic of China. Criteria of diagnosis and therapeutic effect of diseases and syndromes in traditional Chinese medicine. (中华人民共和国中医药行业标准-中医病证诊断疗效标准). 1994, p50. (Article in Chinese).

319. ZhuYX, Xie QW. 陈秋教授痛风方治疗痛风小议. Journal of New Chinese Medicine. 2015; 47(2): 292-3. (Article in Chinese)

320. Liu HX, Feng XH. 冯兴华分期治疗痛风性关节炎经验. Journal of Traditional Chinese Medicine. 2012; 53(21): 1814-15, 30. (Article in Chinese)

321. Xia JL. 周福贻教授治疗痛风性关节炎的经验. Jiangsu Chinese Medicine. 2000;21(12):9. (Article in Chinese)

322. Xu F, Xiao HY, Zhou WQ, Shen JY, Peng JY. 中医对痛风的认识. Rheumatism and Arthritis. 2018;7(5):62-4. (Article in Chinese)

323. Lee D. How to flush out harmful toxins with TCM. http://www.asiaone.com/health/how-flush-out-harmful-toxins-tcm (Accessed on Dec 17, 2018)

324. Schoenbart B, Shefi E. Traditional Chinese Medicines causes of illness. https://health.howstuffworks.com/wellness/natural-medicine/chinese/traditional-chinese-medicine-causes-of-illness4.htm. (Accessed on Dec 17, 2018).

325. Yang YF. Chapter 3 Herbs that clear heat. In: Chinese herbal medicines: comparisons and characteristics. 2nd edition. Churchill livingstone, London, United Kingdom, 2010. Pp 41-62.

326. Ge L, Li Y. 二丁颗粒治疗急性咽炎胃肺实热证的疗效观察. Shanxi Chinese Medicine. 2010;31(9):1125-6. (Article in Chinese)

327. Zhang GY. 二丁颗粒治疗慢性支气管炎疗效观察。Hebei J TCM. 2011;33(6):911-2. (Article in Chinese)

328. Duan ZP. 二丁颗粒抗肠道病毒 71 型作用的体内外实验研究. Doctoral dissertation, Jinlin University, 2015. (Article in Chinese)

329. Jia HH, Yuan J, Gou J, Li DY. The bacteriostatic, anti-inflammatory and immunomodulating effects of Erding granule. Huaxi Yaoxue Zazhi. 2006(5):453-6. (Article in Chinese)

330. Jiang M, Lu C, Zhang C, Yang J, Yan Y, Lu AP, et al. Syndrome differentiation in modern research of traditional Chinese medicine. J Ethnopharmacol. 2012;140:634-42.

331. Ji Q, Luo YQ, Wang WH, Liu X, Li Q, Su SB. Research advances in traditional Chinese medicine syndromes in cancer patients. J Integr Med. 2016;14(1):12-21.

332. Yu F, Takahashi Y, Moriya J, Kawaura K, Yamakawa J, Kusaka K, et al. Traditional Chinese medicine and Kampo: a review from the distant past for the future. J Int Med Res. 2006;34(3):231-9.

333. Paul BJ, Anoopkumar K, Krishnan V. Asymptomatic hyperuricemia: is it time to intervene. Clin Rheumatol. 2017;36:2637-44.

334. Ruoff G. The treatment of gout. J Fam Pract. 2012; 61(6 Suppl): S11-5.

335. Khanna D, Khanna PP, FitzGerald JD, Singh M, Bae S, Neogi T. 2012 American college of rheumatology guidelines for management gout part II: therapy and anti-inflammatory prophylaxis of acute gouty arthritis.. Arthritis Care Res. 2012; 64(10):1447-61.

336. Li XX, Han M, Wang YY, Liu JP. Chinese herbal medicine for gout: a system review of randomized clinical trials. Clin Rheumatol. 2013;32:943-959.

337. Bensky D, Gamble A, Kaptchuk TJ. Chinese Herbal Medicine: Materia Medica. Rev. ed. Seattle, WA: Eastland Press, 1992.

338. Nadkarni KM, Nadkarni AK. Indian Materia Medica. 3rd ed. Bombay: Popular Book Depot, 1955.

339. European Scientific Cooperative on Phytotherapy. ESCOP Monographs, The Scientific Foundation for Herbal Medicinal Products. 2nd ed. Exeter, UK: European Scientific Cooperative on Phytotherapy, 2003.

340. Blumenthal M, Busse WR. Federal Institute for Drugs and Medical Devices; (Germany). The Complete German Commission E Monographs, Therapeutic Guide to Herbal Med- icines. Austin, TX: American Botanical Council; Integrative Medicine Communications, 1998.

341. Wichtl M. Herbal Drugs and Phytopharmaceuticals: A Handbook for Practice on a Scientific Basis. 3rd expanded and completely rev. ed. Stuttgart/Boca Raton, FL: Medpharm, CRC Press, 2004.

342. Clare BA, Conroy RS, Spelman K. The diuretic effect in human subjects of an extract of Taraxacum officinale Folium over a single day. J Altern Complement Med. 2009;15(8):929-34.

343. Lv JS. 施今墨对药. Fourth edition. Beijing, China: People's Military medical press; 2010, p. 86. (Book in Chinese)

344. Zhang TJ, Xu J, Han YQ, Zhang HB, Gong SX, Liu CX. Quality markers research on Chinese materia medica: quality evaluation and quality standards of Corydalis Rhizoma. Chin Tradit Herb Drugs. 2016; 47(9): 1458-67. (Article in Chinese)

345. Yao CL, Yang WZ, Wu WY, Da J, Hou JJ, Zhang JX, et al. Simultaneous quantitation of five Panax notoginseng saponins by multi heart-cutting two-dimensional liquid chromatography: Method development and application to the quality control of eight notoginseng containing Chinese patent medicines. J Chromtaogr A. 2015; 1402: 71-81.

346. Da J, Hou JJ, Long HL, Yao S, Yang Z, Cai LY, et al. Comparison of two officinal species of Ganoderma based on chemical research with multiple chromatographic and spectrographic technologies and chemometics analysis. J Chromatogr A. 2012; 1222: 59-70.

347. Zhang TJ, Xu J, Shen XP, Han YQ, Hu JF, Zhang HB, et al. Relation of "property-response-component" and action mechanism of Yuanhu Zhitong Dropping Pills based on quality marker (Q-Marker). Chin Tradit Herbal Drugs. 2016;47(13):2199-2211.

348. Hostettmann K, Marston A. Saponins. Cambridge University Press, Cambridge, New York. 1995.

349. Wang Z, Gu M, Li G.Surface properties of gleditsia saponin and synergisms of its binary system. J Disper Sci Technol. 2005; 26: 341– 7.

350. Sarnthein-Graf C, La Mesa C. Association of saponins in water and water-gelatine mixtures. Thermochim Acta. 2004; 418: 79–84.

351. Mitra S, Dungan SR. Micellar properties of quillaja saponin. 1. Effects of temperature, salt and pH on solution properties. J Agric Food Chem. 1997; 45: 1587–95.

352. Ibanoglu E, Ibanoglu S. Foaming behavior of liquorice (Glycyrrhiza glabra) extract. Food Chem. 2000; 70: 333–6.

353. San Martin R, Briones R. Industrial uses and sustainable supply of Quillaja saponaria (Rosaceae) saponins. Econ Bot. 1999; 53: 302–11.

354. Guclu-Ustundag O, Mazza G. Saponins: Properties, applications and processing. Crit Rev Food Sci Nutr. 2007; 47: 231–58.

355. Qian C, McClements DJ. Formation of nanoemulsions stabilized by model food-grade emulsifiers using high-pressure homogenization: Factors affecting particle size. Food Hydrocolloids. 2011; 25: 1000–8.

356. Xie Y, Ma Y, Xu J, Liu Y, Yue P, Zheng Q, et al. Panax notoginseng saponins as a novel nature stabilizer for poorly soluble drug nanocrystals: a case study with baicalein. Molecules. 2016;21(9):1149.

357. Chen Y, Liu Y, Xu J, Xie Y, Zheng Q, Yue P, et al. A natural triterpenoid saponin as multifunctional stabilizer for drug nanosuspensions powder. 2017;18(7):2744-53.

358. Zuo J, Gao Y, Bou-Chacra N, Löbenberg R. Evaluation of the DDSolver Software Applications. BioMed Res Int. vol. 2014, Article ID 204925, 9 pages, 2014.

359. Loebenberg R, Amidon GL. Modern bioavailability, bioequivalence and biopharmaceutics classification system. New scientific approaches to international regulatory standards. Eur J Pharm Biopharm. 2000; 50 (1): 3–12,

360. World Health Organization. Proposal to waive in vivo bioequivalence requirements for WHO model list of essential medicines—immediate-release, solid oral dosage forms. Fortieth report, annex 8. 2006, Geneva, Switzerland, pp. 391–438.

361. Costa P, Sousa Lobo JM. Modeling and comparison of dissolution profiles. Eur J Pharm Sci. 2001; 13(2): 123–33.

362. Singh B, Kaur T, Singh S. Correction of raw dissolution data for loss of drug and volume during sampling. Indian J Pharm Sci. 1997;59(4):196-9.

363. Zhang Y, Huo M, Zhou J, Zou A, Li W, Yao C, et al. DDSolver: an add-in program for modeling and comparison of drug dissolution profiles. AAPS J. 2010; 12(3):263–71.

364. Guidance for Industry: Immediate Release Solid Oral Dosage Forms. Scale-Up and Postapproval Changes: Chemistry, Manufacturing and Controls, In Vitro Dissolution Testing and In Vivo BE Documentation. US Department of Health and Human Services, Food and Drug Administration, Center for Drug Evaluation and Research (CDER), Rockville, Md, USA, 1995.

365. Guidance for Industry: Dissolution Testing of Immediate Release Solid Oral Dosage Forms. US Department of Health and Human Services, Food and Drug Administration, Center for Drug Evaluation and Research (CDER), Rockville, Md, USA, 1997.

366. Guidance for Industry: SUPAC-MR: Modified Release Solid Oral Dosage Forms. US Department of Health and Human Services, Food and Drug Administration, Center for Drug Evaluation and Research (CDER), Rockville, Md, USA, 1997.

367. Guidance for Industry: Waiver of In Vivo Bioavailability and Bioequivalence Studies for Immediate-Release Solid Oral Dosage Forms Based on a Biopharmaceutics Classification System. US Department of Health and Human Services, Food and Drug

Administration, Center for Drug Evaluation and Research (CDER), Rockville, Md, USA, 2000.

368. Committee for Proprietary Medicinal Products. Note for Guidance on the Investigation of Bioavailability and Bioequivalence, CPMP/EWP/QWP/1401/98. London, UK, 2010.

369. Committee for Proprietary Medicinal Products. Note for Guidance on Quality of Modified Release Products: A: Oral Dosage Forms, B: Transdermal Dosage Forms. Section I, (Quality), CPMP/QWP/604/96. London, UK, 1999.

370. Tandt LAGL, Stubbs C, Kanfer I. The use of dissolution rate data to account for differences in the absorption profiles of two controlled/modified-release capsule dosage forms of indomethacin in human volunteers. Int J Pharm. 1994; 104(1): 11-7.

371. Moore JW, Flanner HH. Mathematical comparison of dissolution profiles. Pharmaceutical Technology. 1996; 20(6): 64–74.

372. Tsong Y, Hammerstrom T, Sathe P, Shah VP. Statistical assessment of mean differences between two dissolution data sets. Drug Information Journal.1996; 30(4): 1105-12.

373. Siepmann J, Siepmann F. Mathematical modeling of drug delivery. Int J Pharm. 2008; 364(2): 328-43.

374. Siepmann J, Peppas NA. Modeling of drug release from delivery systems based on hydroxypropyl methylcellulose (HPMC). Adv Drug Deliv Rev. 2001; 48(2-3): 139–57.

375. Siepmann J, Goepferich A. Mathematical modeling of bioerodible, polymeric drug delivery systems. Adv Drug Deliv Rev. 2001; 48(2-3): 229-47.

376. Arifin DY, Lee LY, Wang CH. Mathematical modeling and simulation of drug release from microspheres: implications to drug delivery systems. Adv Drug Deliv Rev. 2006; 58(12-13): 1274–325.

377. Korsmeyer RW, Gurny R, Doelker E. Mechanisms of solute release from porous hydrophilic polymers. Int J Pharm. 1983; 15(1): 25-35.

378. Ritger PL, Peppas NA. A simple equation for desciption of solute release I. Fickian and non-Fickian release from non-swellable devices in the form of slabs, spheres, cylinders or discs. J Control Release. 1987; 5(1): 23-36.

379. Ritger PL, Peppas NA. A simple equation for description of solute release II. Fickian and anomalous release from swellable devices. J Control Release. 1987; 5(1): 37-42.

380. Wise DL. Handbook of Pharmaceutical Controlled Release Technology, CRC Press, 2000.

381. Kim H. Fassihi R. Application of binary polymer system in drug release rate modulation. 2. Influence of formulation variables and hydrodynamic conditions on release kinetics. J Pharm Sci. 1997; 86(3): 323-8.

382. Akaike H. A new look at the statistical model identification. IEEE Trans Automat Contr. 1974; 19(6): 716-23.

383. MicroMath, Scientist User Handbook. MicroMath, Salt Lake, UT, USA, 1995.

384. Gao Y, Zuo J, Bou-Chacra N, Pinto TD, Clas SD, Walker RB, et al. In vitro release kinetics of antituberculosis drugs from nanoparticles assessed using a modified dissolution apparatus. BioMed Res Int. 2013, Article ID 136590, 9 pages.

385. Shah VP, Tsong Y, Sathe P, Liu JP. In vitro dissolution profile comparison-statistics and analysis of the similarity factor, f2. Pharm Res. 1998; 15(6): 889-96.

386. Mendyk A, Pacławski A, Szlek J, Jachowicz R. PhEq bootstrap: open-source software for the simulation of distribution in cases of large variability in dissolution profiles. Dissolution Technol. 2013; 20(1): 13-7.

387. Ma MC, Wang BBC, Liu,JP, Tsong Y. Assessment of similarity between dissolution profiles. J Biopharm Stat. 2000; 10(2): 229-49.

388. Langer RS, Peppas NA. Present and future applications of biomaterials in controlled drug delivery systems. Biomaterials. 1981; 2(4): 201–14.

389. Langer R, Peppas NA. Chemical and physical structure of polymers as carriers for controlled release of bioactive agents: a review. Journal of Macromolecular Science, Part C. 1983; 23(1): 61-126.

390. Sinclair GW, Peppas NA. Analysis of non-fickian transport in polymers using simplified exponential expressions. J Memb Sci. 1984; 17(3): 329–31.

391. Nelder JA, Mead R. A simplex method for function minimization. Computer Journal. 1965; 7(4): 308–13.

392. Hixson AW, Crowell JH. Dependence of reaction velocity upon surface and agitation. Industrial & Engineering Chemistry. 1931; 23(8): 923–31.

393. Baker RW, Lonsdale HS. Controlled Release of Biologically Active Agents. John Wiley & Sons, Plenum Press, New York, NY, USA, 1974.

394. Silva AC, Lopes CM, Fonsecaa J, Soares ME, Santos D, Ferreira D. Risperidone release from solid lipid nanoparticles (SLN): validated HPLC method and modelling kinetic profile. Current Pharmaceutical Analysis. 2012;8(4):307-16.

395. Hopfenberg HB. Controlled Release Polymeric Formulations. vol. 33 of ACS Symposium Series, American Chemical Society, Washington, DC, USA, 1976.

396. Niebergall PJ, Milosovich G, Goyan JE. Dissolution rate studies. II. Dissolution of particles under conditions of rapid agitation. J Pharm Sci. 1963; 52: 236-41.

397. Katzhendler I, Hoffman A, Goldberger A, Friedman M. Modeling of drug release from erodible tablets. J Pharm Sci. 1997; 86 (1): 110-5.

398. Higuchi T. Rate of release of medicaments from ointment bases containing drugs in suspension. J Pharm Sci. 1961; 50: 874-5.

399. Higuchi T, Mechanism of sustained-action medication. Theoretical analysis of rate of release of solid drugs dispersed in solid matrices. J Pharm Sci. 1963; 52: 1145–9.

400. Zuo J, Gao Y, Bou-Chacra N, Löbenberg R. Challenges and Opportunities to Use Biowaivers to Compare Generics in China. AAPS PharmSciTech. 2014;15(5):1070-5.

401. World Health Organization. Country pharmaceutical situations: fact book on WHO level 1 indicators 2007. Geneva: WHO. 2009. http://apps.who.int/medicinedocs/documents/s16874e/s16874e.pdf Accessed 20 Nov 2012.

402. World Health Organization. Essential medicines and health product. 2012. http://www.who.int/medicines/en/ Accessed 20 Nov 2012.

403. Food and Drug Administration. Guidance for industry: waiver of in vivo bioavailability and bioequivalence studies for immediate-release solid oral dosage forms based on a biopharmaceutics classification system. U.S. Department of Health

and Human Services Food and Drug Administration Center for Drug Evaluation and Research. 2000. www.fda.gov/downloads/Drugs/GuidanceComplianceRegulatoryInformation/Guidances/ ucm070246.pdf. Accessed 20 Nov 2012.

404. World Health Organization. Multisource (generic) pharmaceutical products: guidelines on registration requirements to establish interchangeability. Annex 7 of WHO Expert Committee on Specifications for Pharmaceutical Preparations. Geneva: WHO Technical Report Series No.937, 2006; 40th report: p.347-90. http://apps.who.int/prequal/info_general/documents/TRS937/WHO_TRS_937__annex7_eng.pdf Accessed 20 Nov 2012.

405. World Health Organization. Proposal to waive in vivo bioequivalence requirements for WHO model list of essential medicines—immediate-release, solid oral dosage forms. Annex 8 of WHO Expert Committee on Specifications for Pharmaceutical Preparations. Geneva: WHO Technical Report Series No.937, 2006; 40th report: p.391-461. http://apps.who.int/prequal/info_general/documents/TRS937/WHO_TRS_ 937__annex8_eng.pdf Accessed 20 Nov 2012.

406. Williams RL, Chen ML, Hauck WW. Equivalence approaches. Clin Pharmacol Ther. 2002; 72: 229–37.

407. Food and Drug Administration. Orange book: approved drug products with therapeutic equivalence evaluations, 33rd ed. Rockville: U.S. Department of Health and Human Services Food and Drug Administration Center for Drug Evaluation and Research Office of Pharmaceutical Science Office of Generic Drugs. 2013. http://www.fda.gov/downloads/Drugs/ DevelopmentApprovalProcess/UCM071436.pdf Accessed 20 Apr 2013.

408. Spino M, Tsang YC, Pop R. Dissolution and in vivo evidence of differences in reference products: impact on development of generic drugs. Eur J Drug Metab Pharmacokinet. 2000; 25: 18–24.

409. Cameron A, Mantel-Teeuwisse AK, Leufkens HG, Laing RO. Switching from originator brand medicines to generic equivalents in selected developing countries: how much could be saved? Value Health. 2012; 15: 664–73.

410. GBI research. China pharmaceutical market outlook—government incentives, healthcare reform and a rapidly ageing population provide strong stimulus for growth. 2013. http://www.researchandmarkets. com/research/pgk2g8/china Accessed 20 Apr 2013.

411. Hirschler B. China seen as no. 2 drugs market by 2015. Reuters. 2010 Nov 8 http://uk.reuters.com/article/2010/11/08/us-summit- china-drugs-idUKTRE6A73SL20101108 Accessed 8 May 2013.

412. Deloitte China. The next phase: opportunities in China's pharmaceuticals market. 2012. http://www.deloitte.com/view/en_CN/cn/ind/lshc/723313bbb0943310VgnVCM3000001c56f00aRCRD.htm Accessed 20 Apr 2013.

413. Vesiongain. Chinese pharmaceutical market 2013–2023. 2013. http://www.visiongain.com/Report/1018/Chinese-Pharmaceutical-Market-2013-2023 Accessed 8 May 2013.

414. China Food and Drug Administration. Regulation on drug registration (《药品注册管理办法》) Order 28, 2007.Chinese. http://www.sfda.gov.cn/WS01/CL0053/24529.html Accessed 21 Apr 2013.

415. Database of pharmaceutical manufacturer (药品生产企业). China Food and Drug Administration, Beijing. 2013. Chinese. http://app1.sfda.gov.cn/datasearch/face3/dir.html Accessed 21 Apr 2013.

416. China Food and Drug Administration. Annual report of registration and approval of 2011(2011 药品注册审批年度报告). China Food and Drug Administration. 2012. Chinese. http://www.sda.gov.cn/WS01/ CL0050/75250.html Accessed 10 Feb 2013.

417. Uniformity of dosage units <905>. In United States Pharmacopeia and National Formulary USP 36–NF 31. Rockville: The United States Pharmacopeial Convention; 2013. p. 431–3.

418. Zhang Y, Huo M, Zhou J, Zou A, Li W, Yao C, et al. DDSolver: an add-in program for modeling and comparison of drug dissolution profiles. AAPS J. 2010; 12: 263–71.

419. Löbenberg R, Chacra NB, Stippler ES, Shah VP, DeStefano AJ, Hauck WW, et al. Toward global standards for comparator pharmaceutical products: case studies of amoxicillin, metronidazole, and zidovudine in the Americas. AAPS J. 2012; 14: 462–72.

420. World Health Organization. Guidance on the selection of comparator pharmaceutical products for equivalence assessment of interchangeable multisource (generic) products. Annex 11 of WHO Expert Committee on Specifications for Pharmaceutical Preparations. Geneva: WHO Technical Report Series No.902, 2002; 36th report: p.161-80. http://apps.who.int/medicinedocs/documents/s19641en/s19641en.pdf Accessed 20 Nov 2012.

421. Database of imported drug product (进口药品). China Food and Drug Administration, Beijing. 2013. Chinese. http:// app1.sfda.gov.cn/datasearch/face3/dir.html Accessed 20 Nov 2012.

422. Drug Product Database Online Query. Health Canada, Ottawa. 2012. http://webprod5.hc-sc.gc.ca/dpd-bdpp/index-eng.jsp Accessed 20 Nov 2012.

423. China Food and Drug Administration. Guideline of development of chemical generics with existing state standard (已有国家标准化 学药品研究技术指导原则). China Food and Drug Administration. 2007. Chinese. http://www.cde.org.cn/zdyz.do?method=largePage&id=2076 Accessed 1 May 2013.

424. Williams RL, Shah VP. Continuing equivalence: is there an end to the story? J Generic Med. 2008; 5: 297–304.

425. Wu Y, Fassihi R. Stability of metronidazole, tetracycline HCl and famotidine alone and in combination. Int J Pharm. 2005; 290: 1–13.

426. Amoxicillin capsules (阿莫西林胶囊). In Pharmacopoeia of the People's Republic of China 2010, vol. 2 (中华人民共和国药典 2010 版二部). Beijing: Chinese Pharmacopeia Commission. p. 403–4. Chinese.

427. Metronidazole tablets (甲硝唑片). In Pharmacopoeia of the People's Republic of China 2010, vol.2 (中华人民共和国药典 2010 版二部). Beijing: Chinese Pharmacopeia Commission. p. 153–4. Chinese.

428. Database of domestic drug product (国产药品). China Food and Drug Administration, Beijing. 2013. Chinese. http://app1.sfda.gov.cn/datasearch/face3/dir.html Accessed 21 Apr 2013.

429. Cyranoski D. Pharmaceutical futures: made in China? Nature. 2008; 455: 1168–70.

430. China Food and Drug Administration. View of reforming the drug approval process to encourage drug innovation (Draft) (关于深化药品审评审批改革进一步鼓励药物创新的意见) (征求意见稿). China Food and Drug Administration.2012. Chinese. http://www.sda.gov.cn/WS01/CL0778/77409.html Accessed 1 May 2013.

431. China Food and Drug Administration. Evaluation scheme of generic quality consistency(仿制药质量一致性评价工作方案). China Food and Drug Administration.2013. Chinese. http:// www.sfda.gov.cn/WS01/CL0844/78516.html Accessed 1 May 2013.

432. Washington C. Drug release from microdisperse systems: a critical review. Int J Pharm. 1990; 58(1): 1-12.

433. Souza SSD, DeLuca PP. Methods to assess in vitro drug release from injectable polymeric particulate systems. Pharm Res. 2006; 23(3), 460–74.

434. Bhardwaj U, Burgess DJ. A novel USP apparatus 4 based release testing method for dispersed systems. Int J Pharm. 2010; 388(1-2): 287-94.

435. Abdel-Mottaleb MMA, Lamprecht A. Standardized in vitro drug release test for colloidal drug carriers using modified USP dissolution apparatus I. Drug Dev Ind Pharm. 2011; 37(2): 178-84.

436. Langlois MH, Montagut M, Dubost JP, Grellet J, Saux MC. Protonation equilibrium and lipophilicity of moxifloxacin. J Pharm Biomed Anal. 2005; 37(2): 389-93.

437. Park HR, Kim TH, Bark KM. Physicochemical properties of quinolone antibiotics in various environments. Eur J Med Chem. 2002; 37(6): 443-60.

438. Becker C, Dressman JB, Junginger HE, Kopp S, Midha KK, Shah VP, et al., Biowaiver monographs for immediate release solid oral dosage forms: rifampicin. J Pharm Sci. 2009; 98(7): 2252-67.

439. Kreuter J, Mauler R, Gruschkau H, Speiser PP. The use of new polymethylmethacrylate adjuvants for split influenza vaccines. Exp Cell Biol. 1976; 44(1): 12-9.

440. Peppas NA. Analysis of Fickian and non-Fickian drug release from polymers. Pharm Acta Helv. 1985; 60(4): 110-1.

441. Azarmi S, Huang Y, Chen H, McQuarrie S, Abrams D, Roa W, et al. Optimization of a two-step desolvation method for preparing gelatin nanoparticles and cell uptake studies in 143B osteosarcoma cancer cells. J Pharm Pharm Sci. 2006; 9(1): 124-32.

442. Azarmi S, Tao X, Chen H, Wang Z, Finlay WH, Loebenberg R, et al. Formulation and cytotoxicity of doxorubicin nanoparticles carried by dry powder aerosol particles. Int J Pharm. 2006; 319(1-2): 155-61.

443. Al-Hallak KMHD, Azarmi S, Anwar-Mohamed A, Roa WH, Lobenberg R. Secondary cytotoxicity mediated by alveolar macrophages: a contribution to the total efficacy of nanoparticles in lung cancer therapy? Eur J Pharm Biopharm. 2010; 76(1): 112-9.

444. Zhang Y, Huo M, Zhou J, Zou A, Li W, Yao C, et al. DDSolver: an add-in program for modeling and comparison of drug dissolution profiles. AAPS J. 2010; 12(3):263–71.

445. Huang D, Yi F. Determination of moxifloxacin hydrochloride and dexamethasone acetate in compound moxifloxacin ear drops by HPLC. West China Journal of Pharmaceutical Sciences. 2009; 24(2): 188-9.

446. Wallis RS, Jakubiec W, Kumar V, Bedarida G, Silvia A, Paige D, et al. Biomarker-assisted dose selection for safety and efficacy in early development of PNU-100480 for tuberculosis. Antimicrob Agents Chemother. 2011; 55(2): 567-74.

447. Xu X, Khan MA, Burgess DJ. A two-stage reverse dialysis in vitro dissolution testing method for passive targeted liposomes. Int J Pharm. 2012; 426(1-2): 211-8.

448. Chidambaram N, Burgess DJ. A novel in vitro release method for submicron-sized dispersed systems. AAPS PharmSciTech. 1999; 1(3): 1-9.

449. Howes BD, Guerrini L, Sanchez-Cortes S, Marzocchi MP, Garcia-Ramos JV, Smulevich G. The influence of pH and anions on the adsorption mechanism of rifampicin on silver colloids. Journal of Raman Spectroscopy. 2007; 38(7): 859-64.

450. Pelizza G, Nebuloni M, Ferrari P, Gallo GG. Polymorphism of rifampicin. Farmaco, Edizione Scientifica. 1977; 32(7): 471-81.

451. Wang X, Wang S, Jiang T, Zhang X, Wang Z, Zheng W. Compatibility and stability of anti-tubercular fixed-dose combinations. Chinese Journal of Pharmaceutics.2009; 7(3): 154-60.

452. Kisich KO, Gelperina S, Higgins MP, Wilson S, Shipulo E, Oganesyan E, et al. Encapsulation of moxifloxacin within poly(butyl cyanoacrylate) nanoparticles

enhances efficacy against intracellular Mycobacterium tuberculosis. Int J Pharm. 2007; 345(1-2): 154-62.

453. Bhise SB, Mookkan SJ. Formulation and evaluation of novel FDCs of antitubercular drug. J Pharm Res. 2009; 2(3): 437-44.

454. Ziegler GR, Foegeding EA. The gelation of proteins. Adv Food Nutr Res. 1990; 34: 203-98.

455. Maksimenko OO, Vanchugova LV, Shipulo EV, Shandryuk GA, Bondarenko GN, Gel' perina SE, et al. Effects of technical parameters on the physicochemical properties of rifampicin-containing polylactide nanoparticles. Pharmaceutical Chemistry Journal. 2010; 44(3): 151-6.

456. Barbassa L, Mamizuka EM, Carmona-Ribeiro AM. Supramolecular assemblies of rifampicin and cationic bilayers: preparation, characterization and micobactericidal activity. BMC Biotechnology. 2011; 11(1): 40-7.

457. Bajpai AK, Choubey J. In vitro release dynamics of an anticancer drug from swellable gelatin nanoparticles. J Appl Polym Sci. 2006; 101(4): 2320-2332.

458. Agrawal S, Panchagnula R. Implication of biopharmaceutics and pharmacokinetics of rifampicin in variable bioavailability from solid oral dosage forms. Biopharm Drug Dispos. 2005; 26(8): 321-34.

459. Mariappan TT, Singh S. Regional gastrointestinal permeability of rifampicin and isoniazid (alone and their combination) in the rat. Int J Tuberc Lung Dise. 2003; 7(8): 797-803.

460. Kamat BP, Seetharamappa J. Mechanismofinteractionof vincristine sulphate and rifampicin with bovine serum albumin: a spectroscopic study. Journal of Chemical Sciences. 2005; 117(6): 649-55.

461. Arifin DY, Lee Ly, Wang CH. Mathematical modeling and simulation of drug release from microspheres: implications to drug delivery systems. Adv Drug Deliv Rev. 2006; 58(12-13): 1274-1325.

462. Zuo J, Gao Y, Almukainzi M, Löbenberg R. Investigation of the Disintegration Behavior of Dietary Supplements in Different Beverages. Dissolution Technol. 2013; 20(4): 6-9.

463. <2040> Disintegration and Dissolution of Dietary Supplements. In The United States Pharmacopeia and National Formulary USP 36–NF 31; The United States Pharmacopeial Convention, Inc.: Rockville, MD, 2013; pp 1111–6.

464. <701> Disintegration. In The United States Pharmacopeia and National Formulary USP 36–NF 31; The United States Pharmacopeial Convention, Inc.: Rockville, MD, 2013; pp 305–6.

465. Donauer N, Löbenberg R. A mini review of scientific and pharmacopeial requirements for the disintegration test. Int J Pharm. 2007; 345(1–2): 2–8.

466. Klute AS. Disintegration Testing: Strategy for Quality Control Testing of Immediate Release Dosage Forms in Exploratory Development. Am Pharm Rev. 2009; 12 (5): 90–3.

467. Fraser EJ, Leach RH, Poston JW. Bioavailability of digoxin. Lancet. 1972; 300(7776): 541.

468. Fraser EJ, Leach RH, Poston JW, Bold AM, Culank LS, Lipede AB. Dissolution and bioavailability of digoxin tablets. J Pharm Pharmacol. 1973; 25(12): 968–73.

469. Dietary Supplement Health and Education Act of 1994 (DSHEA); Public Law 103–417, Office of Dietary Supplements, National Institutes of Health, U.S. Government Printing Office: Washington, DC, 1994.

470. Almukainzi M, Salehi M, Bou-Chacra N, Löbenberg R. Investigation of the Performance of the Disintegration Test for Dietary Supplements. AAPS J. 2010; 12(4): 602–7.

471. Schmid K, Löbenberg R. Influence of the Changed USP Specifications on Disintegration Test Performance. Dissolution Technol. 2010; 17(1): 6–10.

472. Natural Health Products Regulations; SOR/2003-196. Justice Laws Website; Minister of Justice, Canada, 2013. http://laws-lois.justice.gc.ca/eng/regulations/ SOR-2003-196 (accessed Sept 25, 2013).

473. Dietary Supplements: New Dietary Ingredient Notifications and Related Issues; Draft Guidance for Industry; U.S. Department of Health and Human Services, Food and Drug Administration, Center for Food Safety and Applied Nutrition (CFSAN), U.S. Government Printing Office: Washington, DC, 2011. http://www.fda.gov/Food/GuidanceRegulation/ GuidanceDocumentsRegulatoryInformation/ DietarySupplements/ucm257563.htm (accessed Sept 25, 2013).

474. Bailey RL, Gahche JJ, Lentino CV, Dwyer JT, Engel JS, Thomas PR, et al. Dietary Supplement Use in the United States, 2003–2006. J Nutr. 2011; 141 (2): 261–266.

475. Natural Health Product Tracking Survey–2010 Final Report; Natural Health Products Directorate (NHPD), Health Canada, 2011. http://epe.lac-bac.gc.ca/100/200/301/pwgsc-tpsgc/por-ef/ health/2011/135-09/report.pdf (accessed Sept 25, 2013).

476. Waiver of In Vivo Bioavailability and Bioequivalence Studies for Immediate-Release Solid Oral Dosage Forms Based on a Biopharmaceutics Classification System; Guidance for Industry; U.S. Department of Health and Human Services, Food and Drug

Administration, Center for Drug Evaluation and Research (CDER), U.S. Government Printing Office: Washington, DC, 2000.

477. Fuchs J. The amount of liquid patients use to take tab- lets or capsules. Pharm Pract. 2009; 7(3): 170–4.

478. Anwar S, Fell JT, Dickinson PA. An investigation of the disintegration of tablets in biorelevant media. Int J Pharm. 2005; 290 (1–2): 121–7.

479. Washburn EW. The Dynamics of Capillary Flow. Phys Rev. 1921; 17(3): 273–83.

480. Radwan A, Amidon GL, Langguth P. Mechanistic investigation of food effect on disintegration and dis- solution of BCS class III compound solid formulations: the importance of viscosity. Biopharm Drug Dispos. 2012; 33(7): 403–16.

481. Chuong MC, Poirier B, Crosby SJ, Pidgeon C. A modified USP disintegration method to simulate a tablet disintegrated in the stomach when taken with cold beverage or with food. AAPS J. 2007; 9(S2): 1687.

482. Chuong MC, Taglieri CA, Crosby SJ, Ferullo JW, Ng P. Effect of Beverages on the In Vitro Disintegration of Immediate-Release Pain Medications. Dissolution Techonol. 2010; 17(1): 31–7.

483. Kalantzi L, Polentarutti B, Albery T, Laitmer D, Abrahamsson B, Dressman, J, et al. The delayed dissolution of paracetamol products in the canine fed stomach can be

predicted in vitro but it does not affect the onset of plasma levels. Int J Pharm. 2005; 296(1–2): 87–93.

484. Stellrecht P. Comparison of the viscosity of beverages; Application Note Physica Rheometers; Anton Paar Germany Gmbh: Ostfildern, 1999. http://www. bri-advantage.com/instrumentcms/pdf/mcrnote.pdf (accessed Sept 25, 2013).

485. Handbook of Chemistry and Physics, 93rd ed.; Haynes, W. M., Ed.; CRC Press: Boca Raton, FL, 2012.

486. Oberle RL, Chen TS, Lloyd C, Barnett JL, Owyang C, Meyer J, et al. The influence of the interdigestive migrating myoelectric complex on the gastric emptying of liquids. Gastroenterology. 1990; 99(5): 1275–82.

Appendix 1 Evaluation of the DDSolver Software Applications

This study has been published as Jieyu Zuo, Yuan Gao, Nadia Bou-Chacra, and Raimar Löbenberg. Evaluation of the DDSolver Software Applications in BioMed Research International. vol. 2014, Article ID 204925, 9 pages, 2014. Reference (358)

1. Introduction

Dissolution testing has been recognized as an important tool for both drug development and quality control because it determines the rate and extent of the drug release from orally administered pharmaceutical products. In addition, dissolution testing can also provide an in vitro prediction of the in vivo drug absorption in certain cases. Biowaivers utilize dissolution testing to assess similarity between two products, if proven to be equivalent, then bioequivalence studies are deemed to be unnecessary (359, 360). However, when a new oral dosage form is developed, one must ensure that the drug release occurs as desired by the product specification. Mathematical models can be applied to express the dissolution data as a function of parameters related to pharmaceutical dosage to characterize the in vitro drug release behavior (361).

A dissolution profile is a measurement of in vitro drug release from a preparation in a receptacle media over a period of time. Multiple samples are normally collected at several time points. The resulting curve represents the mean cumulative drug dissolved over time. The dissolution test procedure can be differentiated into two categories: (1) if the collected sample volume is not replaced with equal amount of receptacle media, both the receptacle volume and drug are lost during sampling, and the equation for drug release quantity is $F=\frac{C_t*[V_{or}-(n-1)V_s]}{Dose-\sum_1^{t-1} C_t*V_s}$; (2) if the collected sample volume is replaced with equal amount of receptacle volume, only the amount of drug removed must be considered, and the equation for drug release quantity at each time point is $F=\frac{C_t*V_{or}}{Dose-\sum_1^{t-1} C_t*V_s}$. In these equations F is the

quantity of drug release, Ct is the concentration at this time point, and Vor and Vs are original receptacle volume and the collected sample volume, respectively. As seen, the sample correction might be necessary and should not be omitted to achieve the actual dissolution profiles (362).

Dissolution data analysis is performed by comparing dissolution profiles statistically or using mathematical models to quantify or characterize the drug release from a pharmaceutical dose form. Most commercial statistical software programs which are used in pharmaceutical R&D are not designed for the statistical evaluation of dissolution profiles but evaluate pharmacokinetic parameters. To reduce the calculation time and to eliminate calculation errors, researchers designed the DDSolver program (363), which is a free and ready-to-use Excel plug-in program that allows the modeling of the dissolution data using 40 built-in dissolution models. In addition, this software allows a similarity analysis to be performed using well-established profile comparison approaches. The program provides an efficient data analysis report to summarize the dissolution data analysis.

This report aims to evaluate the application of the DDSolver program for analyzing dissolution data from different drug release systems. A particular focus is on the application of DDSolver to compare the dissolution profiles as described in leading regulatory guidelines (364–369). Similarities between the different dissolution profiles were investigated according two different aspects: (1) characterization of drug release, (2) in

vitro similarity of profiles for biowaivers applications (370). The similarity factor (f_2) (371) is a comparison method that is recommended by regulatory guidelines. As a simple measure of profile similarity, f_2 is obtained by comparing the mean percentage of the drug released at each sampling time point for two curves and is defined as the logarithmic reciprocal square root transformation of 1 plus the averaged squared mean differences as follows:

$$f_2 = 50 \cdot \log\left\{\left[1 + \frac{1}{n}\sum_{t=1}^{n}(R_t - T_t)^2\right]^{-0.5} \times 100\right\}$$

where n is the number of time points and Rt and Tt are the average percentage of active pharmaceutical ingredients (API) dissolved in the reference and test products, respectively, at time t. The value of f_2 falls between 0 and 100, and two profiles are considered to be similar when f_2 ranges between 50 and 100. The FDA guideline (365) suggests that f_2 could be used to compare dissolution profiles when the following criteria are satisfied: (1) sufficient sampling times are available with a minimum of 3 excluding t = 0; (2) the individual dosage unit for each product should be 12; (3) only a single sampling time should be considered when the percent drug release exceeds 85%; (4) the sampling times should be the same for the two products; and (5) the within-batch coefficient of variation (CV) should be below 20% for the early time points and below 10% for other time points. An f_2 comparison is unnecessary when both the test and reference products exceed 85% dissolved within 15 min. Products are considered to be similar because they meet the "very

rapidly dissolving" standards set by the European Medicines Agency (368). When the within-batch CV exceeds 15%, multivariate confidence region, procedures are recommended over f_2 (365, 372). This comparison approach is built into the DDSolver program as well; however, because our study does not feature any data with a CV above 15%, this approach is not discussed in this report.

Mathematical modeling of drug release can be used in optimizing the design of novel dosage forms, elucidate the underlying drug release mechanisms, and adequately estimate the required parameters and preparation procedures for different dosage forms (373). Many mathematical theories on dissolution behavior have been described in the literature (374-376). The DDSolver software features 40 models built into its library that can be used to directly calculate the parameters and the appropriateness of each model. Our report investigated the drug release mechanism for gelatin nanoparticles by fitting the dissolution data with the Korsmeyer-Peppas (K-P) (377) model and its modified forms using DDSolver.

The K-P model, the so-called power law, has frequently been used to describe the drug release phenomena of various modified-release pharmaceutical dosage forms. The following equation is used for the K-P model:

$$F = kt^n$$

where F is the cumulative quantity of drug released at time t, k is a constant that incorporates the structural and geometric characteristics of the device, and n is the release

exponent. The value of n helps to define the mechanism of drug release. The K-P model is a decision parameter to identify drug transport mechanism. The value of n is used to differentiate between the various drug release mechanisms (378, 379) as described in Table 1. The use of the n value as a criterion to discriminate dissolution mechanisms is influenced by the nature and geometries of the drug delivery system. Generally, an early portion of a release profile (F < 60%) is used in the model.

Table 1. Exponent n of the power law and drug release mechanism from polymeric controlled delivery systems of different geometries.

Exponent, n			Drug release mechanism
Thin film	Cylinder	Sphere	
0.5	0.45	0.43	Fickian diffusion
0.5<n<1.0	0.45<n<0.89	0.43<n<0.85	Anomalous transport
1.0	0.89	0.85	Case-II transport

According to Table 1, the drug release mechanism could be separated into three cases: (1) Fickian diffusion, which could be observed in nonswelling systems or in cases where the relative relaxation time of polymer is much shorter than the characteristic diffusion time in water with water transport controlled by a concentration gradient; (2) case II transport, which refers to the erosion of the polymer chain; and (3) anomalous transport, which is intermediate to Fickian and case II transport (380).

Two modified forms of the K-P equation are used to describe the late onset in the release rate (Tlag) at the beginning of the release profile (376) and the initial burst release effect (F0), respectively (381). The equations are modified in the following manner:

$$F = k(t - T_{lag})^n,$$

and

$$F = kt^n - F_0$$

Several issues should be considered when fitting the dissolution data to a suitable model. The theoretical calculations should be compared with the experimental results to perform a simulation adjustment of the model parameters. It is possible to obtain a good fit even if the model is inappropriate for the drug delivery system. In addition, if adequate experimental evidence is provided, one should use that evidence no matter how well theoretical models agree with the dissolution results (373). The selection of suitable criteria for fitting a model from a number of statistical criteria that are featured in the DDSolver program is critical. The three most important criteria for the selection of a dissolution model include the following: the adjusted coefficient of determination ($R^2_{adjusted}$) (361), the Akaike Information Criterion (AIC) (382), and the model selection criterion (MSC) (383). These criteria produce different values for assessing the appropriateness of a model. In addition, several other useful and efficient modules are built into the DDSolver program, including a dissolution sampling-volume correction and a calibration curve analysis. This report focuses on the analysis of dissolution data to evaluate the application of the DDSolver program to two dissolution studies: (1) the comparison of dissolution profiles between different products, (2) fitting of drug release data to the K-P model and its modifications.

2. Materials and Methods

The model data used in this paper were obtained from two recent research projects of the authors.

The data used to evaluate the dissolution profiles were obtained from the dissolution study of three different 250 mg amoxicillin capsules purchased from China, which are labeled A, B, and C. The test units were placed in a VK 7020 dissolution tester with six vessels, a VK 8000 autosampler station (Agilent Technologies, Carey, NC), and a USP apparatus 2. The Japanese Pharmacopeia Basket Sinkers (Quality Lab Accessories, Brigewater, NJ) which are compliant with USP were utilized. In the dissolution process, 1.25 mL sample was collected at 10, 15, 20, 30, 45, and 60 min without sample replacement from a 900 mL receptacle volume, respectively. The profiles after sample correction are shown in Figure 1 and used for profile comparison. Figure 2 shows profiles in the presences and absences of sample correction.

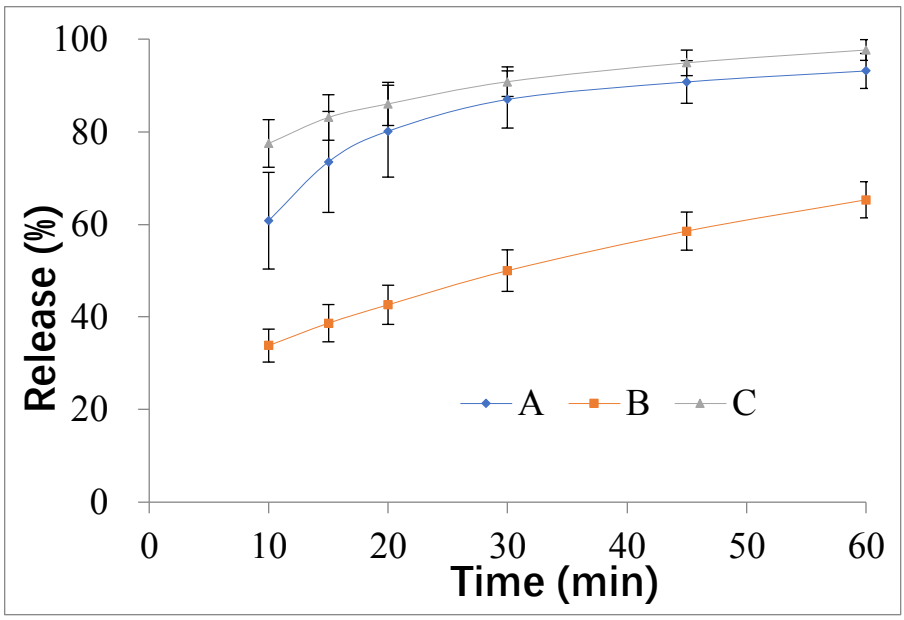

Figure 1. Dissolution behavior of three 250 mg amoxicillin products in simulated intestinal fluid.

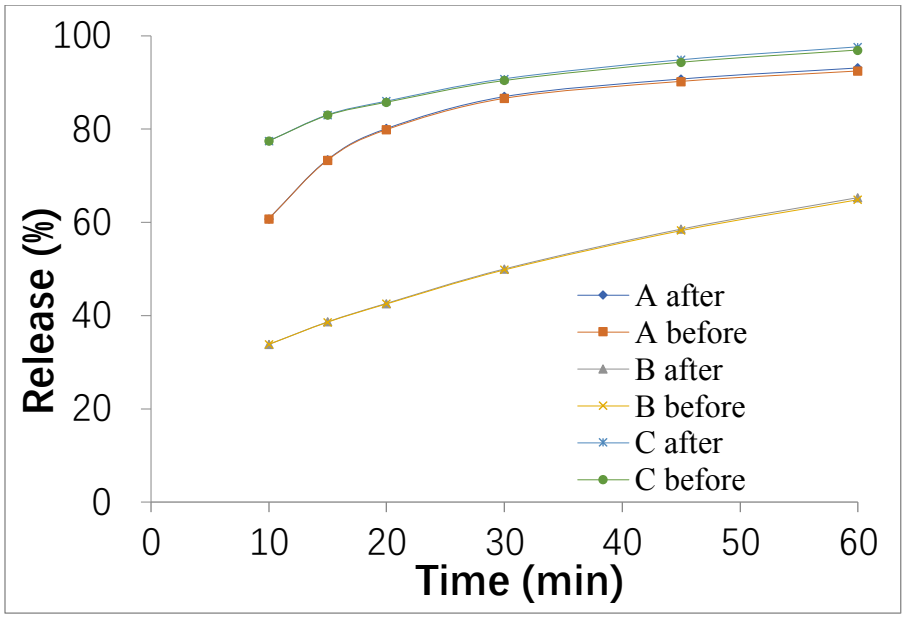

Figure 2. Dissolution profiles of three 250mg amoxicillin products in simulated intestinal fluid before or after sample correction.

Two groups of gelatin nanoparticle data were used to determine which K-P model provides the best fit. The detailed materials and methods of this study were published by Gao, et al. (384). In brief, the drug release from gelatin nanoparticles was determined in the presence of trypsin named as group 1, whereas in the second case, drug release from gelatin nanoparticles was measured in the absence of trypsin regarded as group 2, as shown Figure 3. All of the other conditions were held constant; it was expected to see different drug release from these nanoparticles because trypsin will cause a forced degradation of the nanoparticles. The cutoff values of the exponent n used to distinguish between the different drug release mechanisms were n = 0.43 and n = 0.85. An Excel (Microsoft Corporation, Redmond, WA, USA) worksheet was used as a control computing method for comparison with the results obtained using the DDSolver program. All data were entered into Excel according to the example format for each built-in module of the DDSolver. The relevant parameters were calculated following the equations step-by-step utilizing an Excel spreadsheet. The $R^2_{adjusted}$ value was used as the model selection criterion with the best model exhibiting the $R^2_{adjusted}$ value closest to 1.

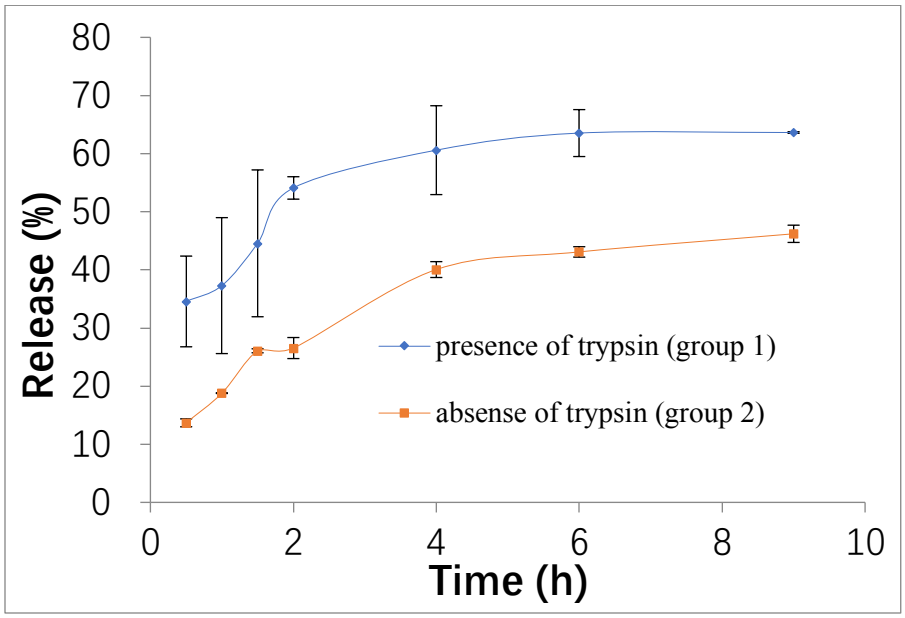

Figure 3. Dissolution profile of gelatin nanoparticles in the presence or absence of trypsin.

3. Results and Discussion

3.1. Sample Correction.

Figure 2 shows that slight differences will be observed in the presence or absence of sample correction which is expected. In general, the amount of sample volume removed without replacement impacts the dissolution result. The sample correction can be applied mathematically either to the raw concentration (obtained from sample analysis) or as percent released, as performed in this study.

3.2. Profile Comparison.

The profiles in Figure 1 were compared with $f2$ statistic in which only one drug release measurement of the tested product is allowed to exceed 85%. Therefore, the time points chosen for tested products, A and B, A and C, and B and C groups, were 10 to 30min, 10 to 20 min, and 10 to 20 min, respectively. The values of $f2$ were 23.21, 46.66, and 17.91

for these groups, respectively, which suggests that the three products were dissimilar. However, if all of the data points collected during the dissolution process were considered, values of 24.08, 52.81, and 19.67 were observed, which differs from those obtained using only one measurement over 85%. A comparison of the products A and C reveals that the dissolution results were similar. The same results were obtained with Excel and DDSolver. When using Excel to calculate the $f2$ value, the number of time points n used in the equation must be carefully accounted for, because n can vary among comparison groups and may not equal the number of time points collected during the experiment. Excel calculates the $f2$ value step-by-step using the equation and can thus only compare two products at once. Accordingly, with several different products, the calculations between each product may require a significant amount of time. Hence, when generating a profile comparison, the DDSolver program could reduce the errors and calculation time that are necessary with Excel.

$f2$ is actually insensitive to the shape of the dissolution profiles and is difficult to assess both type I and type II errors because there is no mathematical formula included for the statistical distribution of $f2$ (363, 385), which is the major drawback of $f2$ (386).

The bootstrap method is proposed as a tool to estimate the statistical distribution of the data and employ a confidence interval approach of $f2$ (385). Bootstrap of $f2$ generates a new population of dissolution profiles through random samples with replacement from 12 units of the test and reference batches, respectively (385, 386). It is possible to assess the

similarity of dissolution profiles with large variability if the data populations are identically distributed. Compared to $f2$, bootstrap-based $f2$ is more accurate in similarity comparison of dissolution profiles and especially important if the $f2$ value is less than 60 (387). Building the bootstrap based $f2$ module into DDSolver makes the similarity comparison of dissolution profiles convenient and accurate.

3.3. Model Fitting.

Most of in vitro kinetics of drugs released from nanoparticles under various conditions can be described by the K-P model.

The K-P and the modified K-P models were investigated to identify the most appropriate model to describe the in vitro drug release kinetics for the selected nanoparticle formulations. The tested drug delivery system was gelatin-nanoparticles in which gelatin was used as a hydrophilic carrier, which is bioerodible and can swell.

From the results, n values outputted by K-P, K-P Tlag, and K-P $F0$ models for group 1 (gelatin nanoparticles in the presence of trypsin) were 0.343, 2.942, and 2.291 with $R^2_{adjusted}$ were 0.812, 0.899, and 0.995, respectively. For group 2 (gelatin nanoparticles in the absence of trypsin), the K- P, K-P Tlag, and K-P $F0$ models that outputted the n as 0.392, 0.322, and 0.055 with $R^2_{adjusted}$ were 0.949, 0.958, and 0.968, respectively. The n value used to discriminate between diffusion, anomalous transport, and erosion was 0.43 and 0.85, respectively. According to the results, the K-P $F0$ model and drug release by erosion were appropriate for group 1, whereas the K-P Tlag model should be used for group

2. This is because $F0$ value of the model for group 2 is negative ($F0 = -199.0$), even if $R^2_{adjusted}$ is the most close to 1.

For group 1, with the presence of trypsin, the enzymatic degradation of nanoparticles should be taken into consideration. Generally, two erosion mechanisms exist: heterogeneous and homogeneous erosion of a polymer matrix. The heterogeneous erosion is surface erosion with degradation, which only happens at the surface of a polymer matrix. This erosion most likely takes place in hydrophobic polymers, as water is excluded. As hydrophilic polymers absorb water, they favor homogeneous erosion (bulk erosion) which is the result of degradation occurring through the polymer matrix (388, 389). As gelatin is a kind of hydrophilic polymers, the degradation of gelatin nanoparticles induced by trypsin could be defined as homogeneous erosion, and the dissolution behavior of group 1 can be characterized as having an initial burst release (373). Thus, the K-P $F0$ model exhibited drug release by erosion mechanism which is a more appropriate model for group 1.

For group 2, in the absence of trypsin, polymer swelling may play an important role in the control of drug release from the gelatin nanoparticles. Then polymer swelling should also be taken into consideration because it may increase the length of the diffusion pathways, decrease the drug concentration gradients, and potentially decrease the drug release rate (373). Therefore, the K-P Tlag model was found to be an appropriate model to describe the drug release from gelatin nanoparticles form group 2 as well as the statistical result obtained by DDSolver.

When Excel was used to obtain the n value for the K-P model, the experimental data were plotted on a logarithmic scale according to the equation, and the n value was determined using the slope (390). The DDSolver program uses the nonlinear least-squares curve-fitting technique to estimate such parameters by fitting the nontransformed dissolution data to the model. DDSolver employs the Nelder-Mead simplex algorithm, which is considered to be the most robust minimization algorithm (391), to minimize the objective functions, sum of squares or weighted sum of squares, and then obtain the best parameters.

The results for the two groups obtained by Excel using the K-P model were 0.309 and 0.794 and 0.437 and 0.963 for the n and $R^2_{adjusted}$ values, respectively. The results obtained using Excel differed slightly from those obtained using the DDSolver program. In particular, the n values in the K-P model estimated by Excel and DDSolver for group 2 were 0.437 and 0.392, respectively. Because the n value used to assess the drug release mechanism of the nanoparticles was 0.43, the difference in the n values indicated that the drug release mechanism of group 2 was either anomalous transport (according to Excel) or the Fickian diffusion mechanism (according to the DDSolver). As explained earlier, the different results from two methods are because when using Excel, the nonlinear data were first transformed to create a linear relationship and then were analyzed with linear regression while DDSolver used nonlinear optimization methods to facilitate the modeling of dissolution data (362). For nonlinear data, using nonlinear regression is more sensitive

than transforming the data to create a linear relationship because the transformation may distort experimental errors (360).

In addition, the use of Excel to estimate the modified K-P model parameters proved to be difficult. Future work has to focus on additional calculation approaches that can minimize the errors in the model parameter values while describing the dissolution behavior.

3.4. Model Selection.

Several other mathematical dissolution models are built into the DDSolver program to estimate the drug release mechanisms, such as the Hixson-Crowell (H-C) model (391, 392), Baker-Lonsdale (B-L) model (393, 394), and Hopfenberg model (395). Because the degradation of gelatin nanoparticles is characterized by a homogeneous erosion as mentioned above, the H-C model, which describes the release profile of drug particles with a diminishing surface area during dissolution (396), and the Hopfenberg model, which describes the heterogeneous erosion (397), cannot be applied. Thus, this report only discusses the B-L model.

The B-L model was developed from the Higuchi Model (398, 399) to describe drug release as a diffusion process based on the Fickian law. It can be represented by the following expression:

$$\frac{3}{2}\left[1-\left(1-\frac{F}{100}\right)^{\frac{2}{3}}\right]-\frac{F}{100}=\frac{3DC_s}{r_0^2C_0}t$$

where F is the cumulative quantity of drug released at time t, D is the diffusion coefficient, Cs is the saturation solubility, r_0 is the initial radius of a sphere, and C_0 is the initial drug loading in the matrix. DDSolver, uses kBL rather than $\frac{3DC_s}{r_0^2 C_0}$ in the equation. As these parameters are all constants, when using DDSolver to fit the data to the B-L model, it is not necessary to consider and input the value of these parameters and the output only provides the value of k_{BL}.

The $R^2_{adjusted}$ values obtained for group 1 (gelatin nanoparticles in the presence of trypsin) using the B-L model and B-L model were 0.376 and 0.798, respectively, and the values were 0.945 and 0.940 for group 2 as determined by DDSolver. The results showed that the B-L model did not provide a good fit for group 1, which means that it did not follow Fickian diffusion. In contrast, $R^2_{adjusted}$ value of the B-L model for group 2 (gelatin nanoparticles in the absence of trypsin) was nearly 1, which illustrated that this group may follow Fickian diffusion. Both of these findings were consistent with the kinetics of drug release from gelatin nanoparticles defined by the K-P model using case II transport and diffusion mechanisms, respectively.

3.5. Report Features in DDSolver.

Outputs of DDSolver are displayed for each analysis as text and graphic mode in Microsoft Excel dataset or as text only in Word which is very convenient for the user because it can be incorporated in customized reports. The copies of DDSolver reports of a spreadsheet for profile comparison and model selection are shown in Figures 4 and 5, respectively.

DDSolver 1.0 *In-vitro Dissolution Profile Comparison*

Time Unit	min	Analyst	Jieyu
Method	Similarity factor, f2	Date	########
		Time	23:24:26

Time (min)	Ref.1 F(%)	Mean	SD	RSD(%)
10	60.79	60.79		
15	73.48	73.48		
20	80.13	80.13		
30	86.97	86.97		

Time (min)	Test.1 F(%)	Mean	SD	RSD(%)
10	33.82	33.82		
15	38.66	38.66		
20	42.63	42.63		
30	50.01	50.01		

Similarity factor: f2

f2	Ref.1
Test.1	23.21

Overall Statistics

	Mean_R vs Individual_T Mean	SE	Mean_R vs Mean_T
f2	23.21		23.21
Is f2 ∈ [50,100] between Mean_R and Mean_T			No
Similarity of R and T			Reject

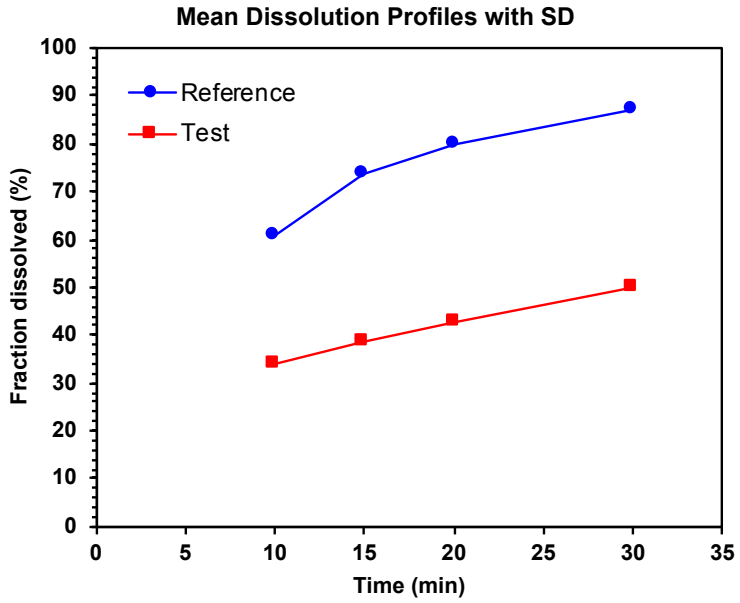

Figure 4. Example DDSolver report of profile comparison.

DDSolver 1.0 *Dissolution Data Modeling of Korsmeyer-Peppas Model*

Time Unit	h	Analyst	Jieyu
Model	Korsmeyer-Peppas	Date	2013-3-23
Equation	F=kKP*t^n	Time	23:50:21

Time (h)	No.1 F(%)	Mean	SD	RSD(%)
0.5	34.57	34.57		
1	37.30	37.30		
1.5	44.56	44.56		
2	54.10	54.10		

Time (h)	No.1 F(%)_Pre	Mean	SD	RSD(%)
0.5	31.93	31.93		
1	40.51	40.51		
1.5	46.56	46.56		
2	51.40	51.40		

Best-fit Values

Parameter	No.1	Mean	SD	RSD(%)
kKP	40.511	40.511		
n	0.343	0.343		

Secondary Parameter

Parameter	No.1	Mean	SD	RSD(%)
T25	0.245	0.245		
T50	1.845	1.845		
T75	6.009	6.009		
T80	7.252	7.252		
T90	10.218	10.218		

Goodness of Fit

Parameter	No.1
N_observed	4
DF	2
R_obs-pre	0.9357
Rsqr	0.8748
Rsqr_adj	0.8122
MSE	14.3114
MSE_root	3.7830
Weighting	1
SS	28.6227
WSS	28.6227
AIC	17.4168
MSC	1.0780

Figure 5. Example DDSolver report of model selection.

4. Conclusion

DDSolver is a free calculation and/or statistic program used to analyze dissolution data or fit drug release data. Because DDSolver can aid in reducing calculation errors and calculation time, it is a suitable tool for day-to-day comparisons of dissolution data. Researchers must understand each part of the program and the various models prior to using the program from both statistical and pharmaceutical aspects.

Appendix 2 Challenges and opportunities to use biowaivers to compare generics in China

This study has been published as Jieyu Zuo, Yuan Gao, Nadia Bou Chacra, Raimar Löbenberg. Challenges and Opportunities to Use Biowaivers to Compare Generics in China in AAPS PharmSciTech. 2014;15(5):1070-5.Reference (400)

Introduction

Most developing countries adopt national medical policies that (401) provide their residents access to essential medicines. The World Health Organization's (WHO) vision for essential drugs is (402) that people worldwide have the right to healthcare under the "principles of accessibility, availability, appropriateness, and assured quality to medical goods and services."

To achieve this goal, it is important to accelerate drug approval and make generics available. Usually, a generic manufacturer must conduct clinical bioequivalence testing of the generic product. This is done by comparing it with an innovator product and establishing therapeutic equivalence. These studies can be extremely expensive and time consuming. The United States (US) Food and Drug Administration (FDA) introduced biowaivers based on the biopharmaceutical drug classification system (BCS) in 2000 (403). Bioequivalence between products can be established using dissolution testing as surrogate (404). In 2006, the WHO published a proposal (405), which allows generic drug approval based on biowaivers. This proposal is based on the availability of innovator products or well-documented generics as reference products. However, many innovator products or their therapeutical equivalents are unavailable in many countries, particularly in developing countries. Generally, an interchangeable multisource (generic) product is therapeutically equivalent when exhibiting both pharmaceutical equivalence and bioequivalence to an innovator product (406). Moreover, a pharmaceutically equivalent product contains the

same active ingredients and salt form, requires the same dosage form and route of administration, and has the same strength as its comparator product (407).

Currently, governments worldwide struggle to offer high efficacy health-care services at affordable costs. For many countries, producing generic products instead of buying innovator products provides an efficient mechanism for reducing drug costs by approximately 50 to 89% (408, 409).

China is the world's largest developing country and accounts for 20% of the global population. The Chinese domestic drug market is growing rapidly. In 2011, China overtook Germany to become the third largest pharmaceutical market in the world, and it is predicted to overtake Japan by 2015 to become the second largest pharmaceutical market after the USA (410, 411). From 2013 to 2020, the Chinese market will continue to rapidly expand (410, 412-413). However, the size of the Chinese pharmaceutical market primarily results from its large population and increasing aging population rather than its maturity, as it is still an emerging market (410, 412).

A previous study suggested that if Chinese public hospitals exchange four different innovator products with their generic equivalents, they could reduce medical costs by US$370 million (409). Therefore, the use of generic products can reduce the cost of drug therapy. In the next 5 years, patents worth US$77 billion are estimated to expire for certain innovator products. This wave of patent expirations will significantly boost generic manufacturers and generic sales (412).

The centralized drug regulatory authority in China, the China Food and Drug Administration (CFDA), is responsible for supervising the regulations related to food, drugs, medical devices, and cosmetics in the provinces, autonomous regions, and municipalities. The CFDA correlates to the FDA in the USA. Specific to China, the CFDA classifies the generic products into the following categories: (1) generic products based on traditional Chinese medicines or natural drug injections, (2) generic chemical products, and (3) biosimilars (414). The presented research only focuses on generic chemical products. In fact, generic drugs are the mainstay of China's pharmaceutical market and are likely to remain so for a long time. There are 7,019 pharmaceutical companies in China (415), most of which produce generic drugs. China will most likely continue to rely upon the widespread prescription of generics through its public insurance plan to maintain overall healthcare expenditures (412). The CFDA approved 644 domestic drug registrations in 2011, 67.7% of which were for generic drugs (416). Thus, ensuring that large amounts of pharmaceutical products in the market are therapeutically equivalent is a challenge for the different level regulatory agencies in China. The practitioners have no knowledge which reference product was used to make a generic since no reference products are officially listed.

The objective of this study was to evaluate the performance of two widely used BCS I drug products, amoxicillin and metronidazole, which are marketed in China. The dissolution

behaviors of these products were compared to establish bioequivalence between products as used for biowaivers.

Methods

Chemicals

The amoxicillin (K0H332) and metronidazole (H0F263) reference standards (RS) were obtained from US Pharmacopeia (USP, Rockville, MD, USA). Acetonitrile HPLC Grade, potassium phosphate, potassium hydroxide, and sodium acetate were purchased from Caledon (Georgetown, ON). Hydrochloric acid, glacial acetic acid, sodium hydroxide, sodium chloride, and HPLC-grade phosphoric acid were purchased from Fisher Scientific (Fairlawn, NJ). All chemicals were USP grade except where specified.

Test Products and Media

All products were purchased from a pharmaceutical market in China and were tested prior to their expiration dates. The various strengths of the amoxicillin capsules and metronidazole tablets are listed in Tables I and II, respectively. The authors used three 250-mg amoxicillin products, A, B, and C and two 500-mg amoxicillin products, D and E, for the evaluation. Four metronidazole tablets were tested, A, B, C, and D. Simulated gastric fluid (SGF), acetate buffer (pH 4.5 USP), and simulated intestinal fluid (SIF) were prepared without enzymes according to the procedure for USP test solutions.

Table I. Amoxicillin capsules

Product	Manufacturer	Lot number	Expire Date	Approval Number
Amoxicillin 250mg	Liaoyuan Yulongyadong Pharmaceutical Co., Ltd.	120302	02/15	H22025159
Amoxicillin 250mg	Shijiazhuang Kanghewei Pharmaceutical Co., Ltd.	120310	02/15	H13020051
Amoxicillin 250mg	Hong Kong United Laboratories Co., Ltd.	18858	02/16	HC20090039
Amoxicillin 500mg	Zhuhai United Laboratories (Zhongshan) Co., Ltd.	20505011	04/16	H20003263
Amoxicillin 500mg	North China Pharmaceutical Group Corporation	1111203	10/14	H20043535

Table II. Metronidazole tablets

Product	Manufacturer	Lot number	Expire Date	Approval Number
Metronidazole 200mg	Feiyunling Pharmaceutical Co., Ltd.	120401	03/14	H52020150
Metronidazole 200mg	Shanxi Tongda Pharmaceutical Inc.	111201	11/14	H14022863
Metronidazole 200mg	Grand Pharm (China) Co., Ltd	120543	04/15	H42021947
Metronidazole 200mg	Huazhong Pharmaceutical Co., Ltd.	20120524	04/14	H42040388

Dissolution Test

A VK 7020 dissolution tester with six vessels, a VK 8000 auto-sampler station (Agilent Technologies, Carey, NC), and a USP apparatus 2 were used for the studies. For the capsule products, the Japanese Pharmacopeia Basket Sinkers (Quality Lab Accessories, Brigewater, NJ) which are compliant with USP were utilized. Preheated and degassed media (900 mL) were used to fill each vessel without the inclusion of air. The test was initiated at 75 rpm once the temperature was confirmed in all vessels. The medium (1.25 mL) was collected and filtered, and 1 mL was transferred into a vial from each vessel at 10, 15, 20, 30, 45, and 60 min. The remaining fluid was discarded, and the drug concentration was computationally corrected because the medium was not replaced after sampling.

HPLC Assay

The quantity of drug released from the products was determined using a high-performance liquid chromatography (HPLC) system. The flow rate was 1 mL/min, and the injected sample size was 10 μL. The run time for each drug was approximately 3–3.5 min. The retention time ranged from 2 to 2.5 min. A LiChrosphere RP 60 Select B column (12.5× 5 mm) (Merck, Darmstadt) with a guard column was used.

Amoxicillin

For the HPLC assay of amoxicillin, UV detection occurred at 219 nm. The mobile phase was 5% acetonitrile and a 95% pH 5.0 buffer. The pH 5.0 buffer was 6.8 g KH2PO4 in 900 mL water with the pH was adjusted to 5.0±0.1 to yield 45% KOH with an adjusted volume of 1,000 mL. The correlation coefficient of the calibration curve was at least 0.999 for each medium over the expected concentration range from 3.75 to 120% with a coefficient of variation (CV%) of 1.95 in SGF, 2.00 in pH 4.5 buffer, and 2.56 in SIF.

Metronidazole

The HPLC assay of the metronidazole utilized UV detection at 228 nm, and the mobile phase consisted of water/ acetonitrile (66:34). The calibration curve was linear for the concentration range between 3.75 and 120% with a correlation coefficient of at least 0.999 for each medium and CV%s of 1.73 in SGF, 2.02 in pH 4.5 buffer, and 1.59 in SIF.

Uniformity of Dosage Units

Weight variation was used to assess uniformity between test units; homogeneous drug distribution was assumed, and weight variation was used to link potential drug release

differences to weight differences of the test units. The weights of 18 to 36 capsules or tablets were recorded for each tested product. The weight variations were calculated as relative standard deviations (RSD) using the following equations:

$$s = \sqrt{\sum \frac{(X_i - \bar{X})^2}{n-1}} ,$$

$$\text{RSD } (\%) = \frac{100s}{\bar{X}} ,$$

in which s represents the standard deviation, Xi is the individual weight, $\bar{X}$ is the mean of all weights, and n is the number of samples measured (417). Generally, the RSDs are $\leqslant$ 6.0%.

Data Analysis

All dissolution data were evaluated using an Excel spreadsheet, and the results were plotted for each product. If two products both exhibited a drug release above 85% within 15 min, indicating a very rapidly dissolving product as defined by the WHO (404), then they were considered similar for that medium. Therefore, if the average drug release for six units of a drug product at 15 min was below 85%, an additional six samples were evaluated for that product, and the similarity factor (f_2) was calculated for two products which were compared with each other using DDSolver, an Excel-plug-in module (418). The *in vitro* equivalence among the various test products was established when the dissolution profiles were similar in all three test media according to the f_2 evaluation.

Results

Amoxicillin

No innovator product could be identified for the Chinese market. Therefore, the available products were compared only to each other.

The 250-mg amoxicillin capsules varied in weight between 369.3 and 388.5 mg, with an observed RSD between 1.0 and 2.6%. The mean weights of the two 500-mg amoxicillin products were 693.6 and 684.4 mg, with RSDs of 0.7 and 1.7%, respectively.

The drug release profiles of the three 250-mg amoxicillin capsules are shown in Figure 1. Figure 2 presents the dissolution behavior of the 500-mg amoxicillin products. Both figures indicate that the amoxicillin is chemically unstable in SGF, which is consistent with the findings of Loebenberg et al. (419) who studied amoxicillin products in the Americas.

As shown in Figure 1, the 250-mg amoxicillin products A, B, and C dissolved rapidly in SGF only. All three products were less than 85% dissolved in 15 min in the pH 4.5 buffer and in SIF. All three products failed their f_2 comparisons in SIF (f_2 = 23.21, 46.66, and 17.91). In the pH 4.5 buffer, product B was unlike products A and C (f_2 = 24.12 and 20.27), whereas product A was similar to C (f_2 = 60.84).

Figure 2 provides the drug release profile of the 500-mg amoxicillin product E, which rapidly dissolved in all three media. The 500-mg product D dissolved rapidly only in SGF with a drug release of less than 85% after 15 min in the pH 4.5 buffer and SIF. The two 500-mg products were also different.

Therefore, the 250- and 500-mg amoxicillin capsules were not equivalent to the other products of the same strength *in vitro*.

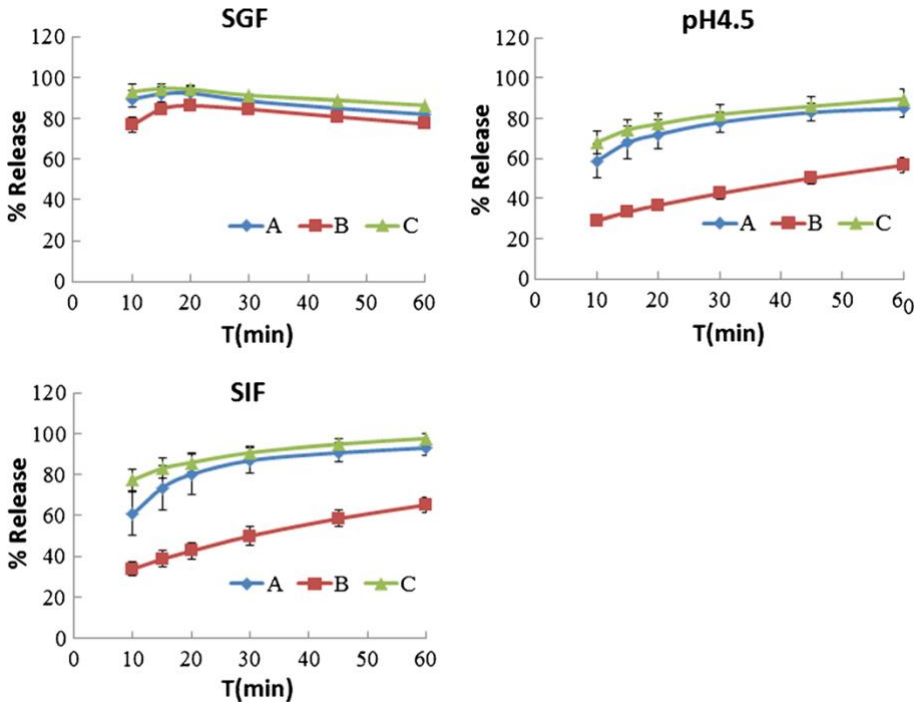

Figure 1. Dissolution behavior of 250-mg amoxicillin capsules.

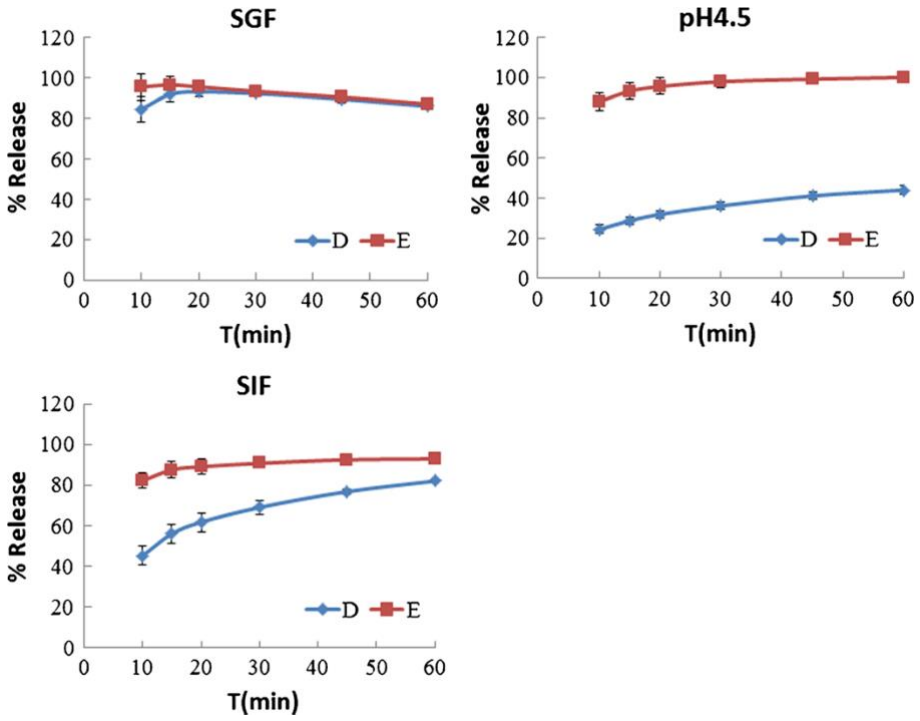

Figure 2. Dissolution behavior of 500-mg amoxicillin capsules

Metronidazole

The variations in the weights of all tested metronidazole tablets ranged from 249.2 to 289.9 mg, with an RSD ranging from 1.1 to 3.5%. The *in vitro* drug release behavior of the 200-mg metronidazole tablets is presented in Figure 3. Products B, C, and D dissolved very rapidly in all three media, and they were considered equivalent to each other *in vitro*. Product A dissolved rapidly only in the pH 4.5 buffer and SIF, with less than 85% dissolved after 15 min in SGF. Therefore, the drug release profile of product A was unlike the other three products.

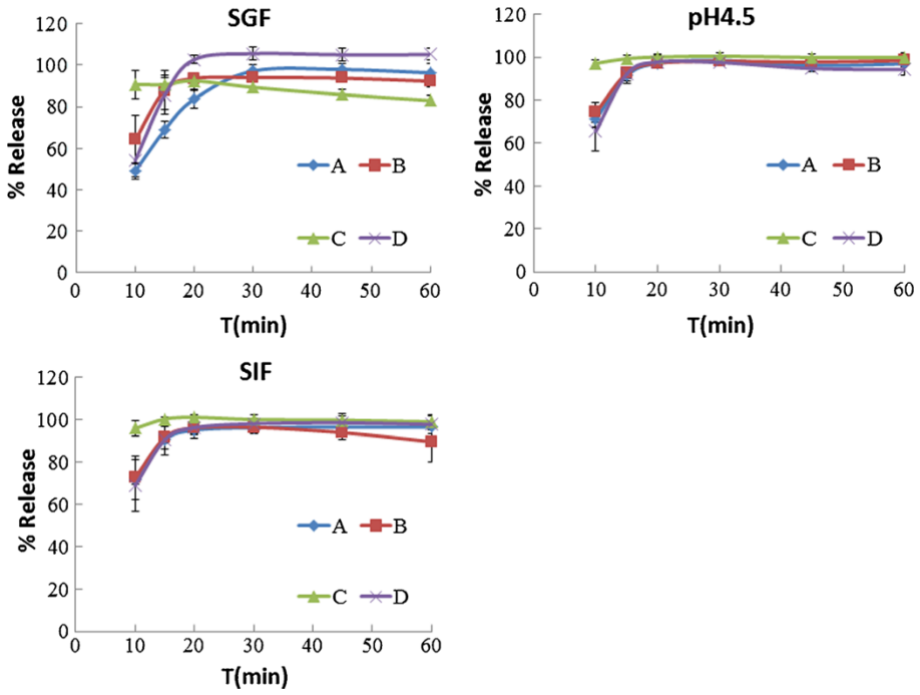

Figure 3. Dissolution behavior of metronidazole tablets

Discussion

For amoxicillin, neither an amoxicillin comparator pharmaceutical product (CPP) listed in the WHO Guidance on the selection of comparator pharmaceutical products for

equivalence assessment of interchangeable multisource (generics) products (420), Amoxil from SmithKline Beecham, nor the listed reference drug in the FDA's Orange Book (407), Amoxicillin from TEVA, was available on the pharmaceutical market in China (421) or Canada where the study was undertaken (422). For metronidazole, the strength of the metronidazole purchased from China is 200 mg, different to the strength of 250 mg that sold in North America. According to the WHO guidance (420), the innovator product for metronidazole cannot be identified and no specific CPP exists. In 2007, the CFDA defined that the reference products used for generics development in China should be innovator products if they are available on the domestic market; otherwise, market-leading products can be used instead (423). Identifying market-leading products as reference products for generics remains challenging when the innovator products are discontinued or unavailable in a country's pharmaceutical market (424). Therefore, this study can only determine whether the tested products are *in vitro* equivalents to each other.

Based on the results, none of the amoxicillin products were *in vitro* equivalents at the same dose and dosage form tested. To ensure the therapeutic equivalence of these products, an *in vivo* study must be performed despite the possibility to request a biowaiver.

All of the tested products were approved by the regulatory agency, and they are presumably bioequivalent *in vivo*. However, our results illustrate that the *in vitro* behaviors of various amoxicillin brands were not similar. If an innovator product is discontinued or is unavailable on the Chinese market, then it is impossible to know for the practitioner which

reference product was used. Furthermore, it is not known whether different reference products exist and whether these products are bioequivalent to each other.

Figure 3 also indicates that product A of metronidazole dissolves slower in SGF than in the pH 4.5 buffer and SIF, which is surprising because metronidazole is a weak base with a maximum dissolution at approximately pH $\leqslant$ 2.0 (425). This result may depend on the excipients used in the formulation.

Generally, establishing a reference product and applying a biowaiver for equivalence assessment simplify the approval process for several generic products, aid generic manufacturers in reducing their drug development costs, and eliminate the ethical question raised by hundreds of bioequivalence studies necessary if biowaivers are not used.

According to the Regulation on the Drug Registration promulgated by the CFDA in 2007 (414), once the drug quality is controlled by defined processes and standards, 18–24 subjects are typically required for each chemical generic product in a bioequivalence study. According to the Pharmacopoeia of the People's Republic of China, there are three different strengths (125, 250, and 500 mg) of amoxicillin capsules (426) and three different strengths (100, 200, and 250 mg) of metronidazole tablets (427) sold in China. Therefore, as expected, the CFDA lists 372 types of amoxicillin capsules and 692 types of metronidazole tablets marketed in China from different manufacturers with different strengths (428). For each product, the overall approval process may take 1 to 2 years. Even if the cost of clinical testing performed in China is only half or one fifth of that in the USA

(429), for the massive amount of generic products marketed in China, the overall cost of clinical trials remains large. These costs could be saved by establishing the reference products and *in vitro* equivalences to waive the *in vivo* bioequivalence studies for qualifying generic drug products.

During this study, the CFDA released (December 2012) a recommendation that suggested reforming the drug approval review process by enhancing its efficiency (430), providing more effective and safe medical services, and ensuring citizen rights to high-quality health care. Based on this initial statement, the CFDA (February 2013) issued a scheme to evaluate generic quality consistency and establish a standard to reevaluate and control the quality of the essential generic products that were approved prior to 2007 (431). In this scheme, the CFDA will define the standard *in vitro* evaluation methods of generics by 2015, identify the universal standard reference products, and allow biowaiver studies. All essential generic products that were approved prior to 2007 will be reevaluated according to the new regulations. After being reevaluated, the generic approval time in China will decrease 8 to 12 months.

Therefore, establishing a reference product is valuable for the development of pharmaceutical manufacturers in China. This benefits both the government, which may reduce the approval processing time, and the manufacturers, who may reduce their development costs. These reference products may also aid the regulatory agencies in overseeing the quality of various product batches.

Conclusion

Three of the four tested metronidazole tablets exhibited *in vitro* equivalence, whereas none of the amoxicillin products tested exhibited *in vitro* equivalence. To determine the bioequivalence of these amoxicillin products, clinical trials must be performed. Compared with clinical trials, the *in vitro* equivalence studies are a less time-consuming and a lowercost method of ensuring bioequivalence of between drug products. The difficulty in identifying a reference product on the Chinese domestic market may result in the use of different reference products by different generic manufacturers. It is not known whether such reference products are bioequivalent to each other. Establishing a universal reference product for interchangeable multisource products is valuable and may aid governments in providing high-quality generics. Establishing nationally or even globally accepted reference products may also provide the regulatory agencies with an efficient mechanism for approving high-quality generics.

Appendix 3 In vitro release kinetics of anti- tuberculosis drugs from nanoparticles assessed using a modified dissolution apparatus

This study has already been published as Yuan Gao, Jieyu Zuo, Nadia Bou-Chacra, Terezinha de Jesus Andreoli Pinto, Sophie-Dorothee Clas, Roderick B. Walker, and Raimar Löbenberg. In Vitro Release Kinetics of Antituberculosis Drugs from Nanoparticles Assessed Using a Modified Dissolution Apparatus in BioMed Research International. vol. 2013, Article ID 136590, 9 pages, 2013. Reference (384)

1 Introduction

Over the past decade, NPs have received significant attention as drug delivery systems, due to significant advantages, including increased drug solubility and bioavailability, reduced toxicity and ability to behave as a drug depot in addition to providing a delivery system using targeting vectors. However, there are no standard methods for the evaluation of the *in vitro* release behaviour of molecules loaded into NPs.

A variety of methods have been reported for *in vitro* drug release evaluation for colloidal drug carriers (432, 433). Also several methods have been tried to standardized the *in vitr*o release test such as a modified USP Apparatus 4 (flow through cell) equipped with a dialysis adapter (434) and a modified USP Apparatus 1 (basket) fixed with a glass cylinder cell to investigate ibuprofen NPs (435). The data reported for these methods have low standard variations and show different release profiles for different formulations.

In this study, to further investigate the applicability of the modified USP Apparatus 1 that was equipped with a membrane diffusion cylinder, we have assessed *in vitro* release of RIF an MX and the mechanism of drug release from the drug loaded NPs using this method (Figure 1). Gelatin B and PBCA were selected as the model nanocarriers, respectively. MX is a modified fluoroquinolone antibiotic that is amphoteric with two protonation sites (Figure 2A). The pKa values are 6.25 for the carboxylic acid group and 9.29 for the piperazine moiety and it has an isoelectric point of 7.9 (436). The presence of

both a carboxyl and the amine functional group indicates that the molecule will exhibit pH sensitive attributes (437). RIF is one of the first line antituberculosis agents that also exhibits pKa values at 1.7 (hydroxyl group at position C8) and 7.9 (protonation at the piperazine moiety at position N4). The isoelectric point occurs at a pH of 4.8 (438) (Figure 2B). Gelatin B is a protein with both carboxylic and amine functional groups with its isoelectric point between pH 4.6 and pH 5.2. PBCA NPs are the oldest known pharmaceutical NPs (439) and possess a negative charge on their surface. They undergo enzymatic hydrolysis to yield a primary alcohol, butanol, and water-soluble, poly (2-cyanoacrylic acid).

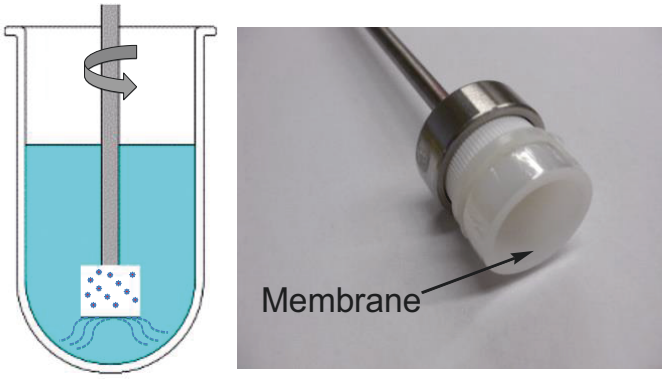

Figure 1 Modified dissolution apparatus for NPs.

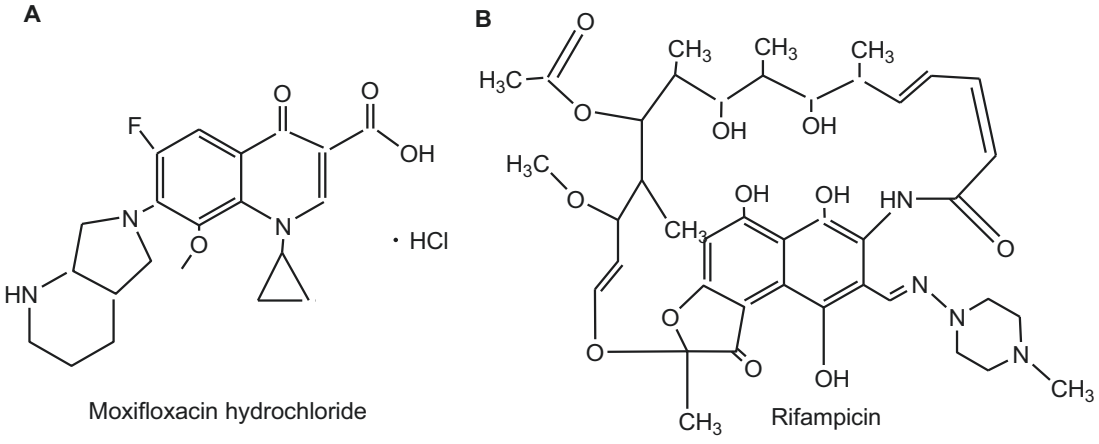

Figure 2 Structures of MX (A) and RIF (B).

The aim of this study was to investigate whether the use of the modified cylinder approach permits discrimination between different *in vitro* release patterns and mechanisms of release of RIF and MX. Drug release was assessed in media of different pH and enzymatic degradation of gelatin NPs was induced with trypsin. The resultant drug release profiles were fitted to the Korsmeyer-Peppas model (440) to establish the predominant drug release mechanisms.

2 Materials and methods

2.1 Materials

Gelatin B (225 Bloom), glutaraldehyde (25% w/w aqueous solution) and trypsin were obtained from Sigma-Aldrich (Ontario, Canada). N-butyl cyanoacrylate monomer was a gift from Loctite Ltd. (Dublin, Ireland). RIF was obtained from PCCA (Ontario, Canada) and MX from Wanquan Pharmaceuticals (Beijing, China). Dialysis membranes were from Spectrum Laboratories Inc. (Rancho Dominguez, CA, USA). All chemicals were of analytical grade.

2.2 Preparation of drug loaded gelatin NPs

MX loaded gelatin NPs (MX-Gel-NPs) and RIF loaded gelatin NPs (RIF-Gel-NPs) were manufactured following a two-step desolvation process as has been previously described (441). In brief, 1.25 g gelatin was dissolved in 25 mL double distilled water

(ddH_2O) under constant heating in the temperature range 30-40 °C. A 25 mL aliquot of acetone was added to the gelatin solution as a desolvating agent to precipitate the gelatin. The supernatant was discarded and the gelatin was redissolved by adding 25 mL ddH_2O and stirring at 600 rpm under constant heating. The pH of the gelatin solution was adjusted to 2.5. Acetone (75 mL) was added dropwise to facilitate the formation of NPs. Approximately 10 mg of MX or 5 mg RIF was dissolved in acetone at concentration of 1 mg/mL or 2 mg/mL, respectively, and was added to the NPs after 1 h. At the end of the process, 250 μL of 25% w/w glutaraldehyde solution was added to the solution as a cross-linking agent, and the mixture was stirred for 12 h at 600 rpm. Acetone was removed by evaporation using a rotary evaporator (IKA, Staufen, Germany). The resultant NPs were purified by centrifugation at 8000 rpm for 30 min (Beckman L8-M ultra-centrifuge, CA, USA) and washed three times with ddH_2O. The NPs were collected and filtered through a hydrophilic 0.45 μm polyvinylidene fluoride filter (Millipore, Billerica, MA, USA), followed by lyophilization for 24 h at -50 °C and 45 Pa.

2.3 Preparation of drug loaded PBCA NPs

MX loaded PBCA NPs (MX-PBCA-NPs) and RIF loaded PBCA NPs (RIF-PBCA-NPs) were manufactured by anionic polymerization as previously described (442). Briefly, a 1% v/v solution of n-butyl-2-cyanoacrylate was added dropwise to a 1% m/v dextran in 0.01 N HCl solution with constant stirring at 600 rpm for 30 min after which drug was

added to the mixture. After 3 h of exposure the reaction was stopped by neutralization with 0.1 N NaOH. The particles were purified by centrifugation at 8000 rpm for 30 min and washed three times with ddH_2O. The NPs were collected and filtered through a 0.45 μm filter prior to lyophilization at -50 °C and 45 Pa and further studies.

2.4 Drug loading

MX-Gel-NPs or RIF-Gel-NPs powders were dispersed in 5 mL of a trypsin solution (0.2 mg/mL) in a 10 mL flask and shaken until a clear colorless solution formed, indicating that complete digestion of the gelatin NPs and release of all MX or RIF encapsulated in the matrices of the NPs had been achieved. Methanol was added to the flask and the solution was made up to volume, filtered through a 0.45 μm filter and analyzed using a validated HPLC method.

For the PBCA NPs, the drug loading was calculated as the difference between the initial drug concentration and the drug concentration found in the supernatant of unwashed NPs suspension using HPLC (443).

The drug loading of the MX-Gel-NPs, MX-PBCA-NPs and RIF-PBCA-NPs was, 6.622 ± 0.1124% w/w, 50.41 ± 2.323% w/w, 5.157 ± 1.231% w/w, respectively and that of the RIF-Gel-NPs was 21.60 ± 1.861% w/w and 56.71 ± 1.280% w/w.

2.5 In vitro drug release using the modified cylinder method and dialysis bag technique

Two methods based on membrane separation techniques were used to evaluate the *in vitro* release of RIF and MX from the NPs formulations. One approach was the use of the modified cylinder method and the other the use of dialysis.

The modified cylinder method required that 5 mg of NPs were suspended in 2 mL of release media and placed into a flat-bottom cell (internal diameter 2 cm) with the opening covered using dialysis membrane (MWCO: 12-14 kDa). The *in vitro* release study was performed using USP dissolution Apparatus 1 by fixing the modified cylinder onto a basket shaft and operating the apparatus at 100 rpm. A 100 mL aliquot of release media was used at 37 °C. At designated time intervals, 1 mL of samples were collected and the withdrawn media was replaced with fresh media. The release media were phosphate buffer solution (PBS) of pH 7.4, acetate buffer of pH 4.0, and HCl buffer of pH 1.2, respectively. The drug concentrations were measured using a validated HPLC assay.

The dialysis bag technique entails dispersing 5 mg of the NPs in 2 mL of the release medium and placing in a dialysis bag (MWCO: 12-14 kDa, surface area of 22.5 cm^2), which was then submerged in a conical flask that contained 100 mL of the test media maintained at 37 °C and that was stirred at 100 rpm. At designated time intervals, 1 mL aliquots were collected and replaced with fresh media. The drug concentrations were determined using a validated HPLC assay.

2.6 Drug diffusion behaviour through the dialysis membrane

Solutions of MX and RIF as free drug were prepared in different release media of pH 1.2, 4.0, and 7.4. Solutions of drug containing an equivalent dose to that in the NPs (2.6 mg MX, 1.1 mg RIF or 2.9 mg RIF) were placed in the modified cylinder apparatus. The dialysis membranes of MWCO 12–14, 25 and 50 kDa have been used for the experiment. The diffusion experiments were performed in 100 mL of the specific release media maintained at 37 °C and agitated at 100 rpm. At pre-determined time intervals, 1 mL samples were withdrawn and analyzed using a validated HPLC assay to determine the amount of drug that had been released.

2.7 Kinetic analysis of drug release profiles

The drug release data were computed using DDSolver, which is an Excel-plugin module (444) and the resultant data were fitted to the Korsmeyer-Peppas exponential equation (1) to establish the mechanism of drug release.

$$Q = k\, t^n \qquad (1)$$

Where Q is the percentage of drug released at time t and k is a constant incorporating the structural and geometric characteristics of the device under investigation. The diffusional exponent n is an important indicator of the mechanism of drug transport from the dosage form. A value of $n \leqslant 0.43$ indicates that drug release is controlled by Fickian diffusion, whereas a value of $n \geqslant 0.85$ suggests that drug release is dominated by an erosion

mechanism. For values $0.43 < n < 0.85$, the release is described as anomalous, implying that a combination of diffusion and erosion contributes to the control of drug release.

2.8 HPLC analysis

The concentration of MX and RIF was determined by reversed-phase HPLC using a LiChrocart–LiCrospher® 100 RP-18, 5 μm stationary phase (Merck, Darmstadt, Germany). The mobile phase consisted of a mixture of methanol and 0.3% v/v triethylamine-0.02 M PBS (pH 3.0) (40:60 v/v) for the analysis of MX and a 20 μL sample was injected at a flow rate of 0.9 mL/min with UV detection at 295 nm as reported (445). In 0.1 N HCl buffer with pH 1.2, acetate buffer with pH 4.0 and PBS with pH 7.4, the linear regression equations obtained were: $A = 94.48\ C + 31.29$ ($r^2 = 0.9996$, n = 5), $A = 90.31\ C - 62.53$ ($r^2 = 0.9994$, n = 5) and $y = 84.69\ C - 16.35$ ($r^2 = 0.9997$, n = 5), respectively. A is the absorbance and C (μg/mL) is the concentration.

The mobile phase used for the analysis of RIF comprised of a mixture of methanol and 10 mM ammonium acetate (60:40 v/v) as previously reported (446). The RIF samples were analyzed at a flow rate of 0.9 mL/min with UV detection at 337 nm. The linear regression equation was: $A = 28.25\ C + 15.17$ ($r^2 = 0.9990$, n = 5).

3 Results and discussion

3.1 Diffusion rate of free drug solutions using the modified cylinder method

The advantage of using dialysis membranes is that they can be used to separate the dialyzed solution containing drug from NPs matrices. However dialysis membranes may limit drug release (447, 448) and therefore, to prevent the impact of the membrane on drug diffusion, a large pore size dialysis membrane should be selected. Thus, the diffusion of MX and RIF from solution through the membrane with MWCO of 12-14, 25 and 50 kDa in different media was tested. As shown in Table 1, only a very slightly but not significantly increase of t50% was observed for MX and RIF upon increasing the membrane pore size ($p > 0.01$). When membrane of MWCO of 12-14 kDa was used, t50% of the free MX solution in different release media of pH1.2, 4.0 and 7.4 was achieved within 7-9 min. t50% values of free RIF solution in media of pH 7.4 and 4.0 were within 13-16 min. The results confirm that dissolved drug molecules readily pass freely through the dialysis membrane. This may be because the molecular weight of the MX and RIF was much smaller than the pore sizes of membrane (435, 447). Accordingly, MWCO of 12-14 kDa membranes were selected for all future release tests. In addition, the maximum concentration in the dialysate of free RIF solution in medium of pH 1.2 reached 52.82 % at 2 h, which maybe due to the formation of an ion pair between RIF and Cl^- when the pH is $\leqslant$ 2.6 (449). Another reason for this observation may be due to degradation of RIF in acid (450, 451). Similar results were reported by Abdel-Mottaleb and Lamprecht (435).

Table 1 Comparison of t50% for free drug diffusion through dialysis membranes with different MWCO in media.

Free drug/t50%	MWCO of membrane (kDa)		
	12-14	25	50
MX	7-9 min	5-7 min	5-7 min
RIF	13-16 min	12-14 min	11-13 min

3.2 In vitro release of MX from MX-Gel-NPs

The release of MX from MX-Gel-NPs was performed in buffers of different pH in the presence or absence of the enzyme, trypsin at 37 °C. The MX release profiles over time are shown in Figure 3A at different pH values in the absence of trypsin. Approximately 26–44% MX is released within 1 h. In contrast, the release of MX in media containing 0.05% w/w trypsin increases significantly ($p < 0.05$), with more than 80% of MX releases after 1 h in all media. The forced degradation of NPs using digestive enzymes produces a significant increase in the extent of MX released in both media. In addition, as shown in Figure 3A, the drug release tends to be lower at high pH values. This may in part be due to the lower solubility of MX at this pH. Langlois et al. reported that MX is most lipophilic at pH 7.4 due to the presence of neutral and zwitterions forms, which may explain the slow dissolution rate observed (436).

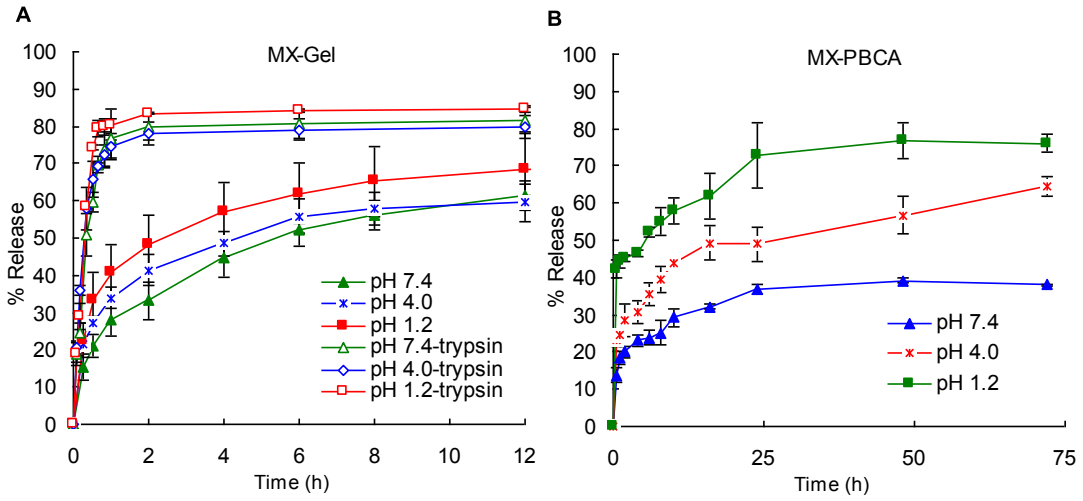

Figure 3 *In vitro* release curves of MX-NPs in media with different pH using the modified cylinder method. A) MX-Gel-NPs in the presence and absence of trypsin; B) MX-PBCA-NPs. Data shown is the mean ± S.D. (n = 4).

3.3 In vitro release of MX from MX-PBCA-NPs

All *in vitro* release profiles from MX-PBCA-NPs show an initial burst release within the first 10 minutes (Figure 3B), which may be associated with the distribution of MX on the surface of PBCA NPs. The location of the drug on the surface of the particles permits instantaneous dissolution when it comes in contact with the dissolution medium. Surface adsorption seems to be a predominant interaction between this fraction of MX and surface of PBCA particles. The remaining fraction is located inside the NPs matrix and is released slowly which supports reports that PBCA NPs exhibit a biphasic release pattern with an initial burst effect followed by a sustained release of the drug contained in the particle (452).

3.4 In vitro release of RIF from RIF-Gel-NPs

The *in vitro* release profiles of RIF from RIF-Gel-NPs over time in different media are shown in Figure 4A and 4B. In the absence of trypsin, RIF is released extremely slowly when compared to the release profiles observed when digestive enzymes are present in the dissolution medium. It is also established that the release of RIF is also dependent on drug loading (Figure 4C). A higher drug loading results in a slower rate of drug release. In addition RIF release is found to be pH dependent. As shown in Figure 4A, the higher extent of drug release is observed in buffer of pH 7.4 with a lower amount of drug release occurring in a medium of pH 4.0. The concentration of RIF in medium of pH 1.2 in which trypsin is omitted is below the limit of detection and approximately 1-5% RIF is released from RIF-Gel-NPs when trypsin is present (Data not shown), which is similar to the results reported by Bhise and Mookkan (453).

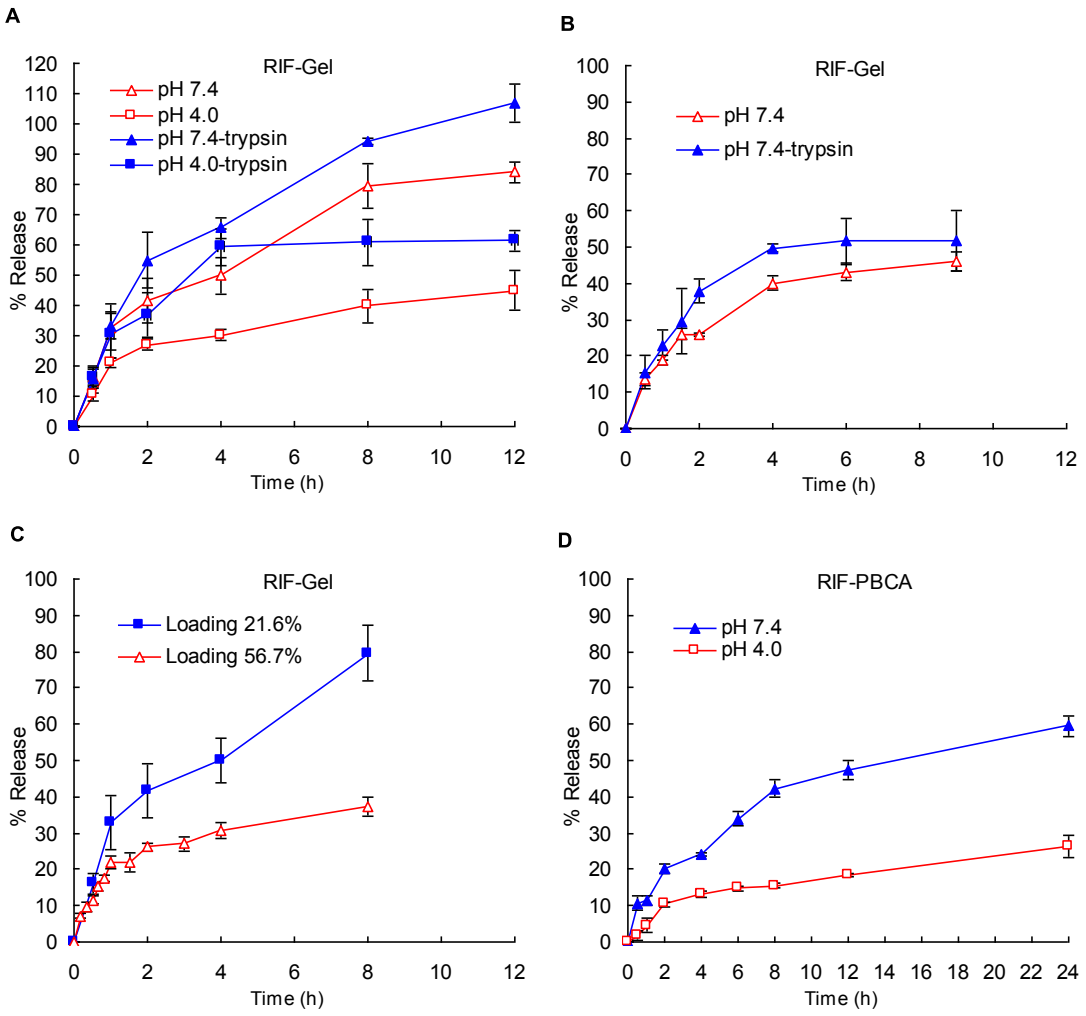

Figure 4 *In vitro* release curves of RIF-NPs using the modified cylinder method. A) RIF-Gel-NPs with drug loading of 21.6% w/w in the presence and absence of trypsin; B) RIF-Gel-NPs with drug loading of 56.7% w/w in the presence and absence of trypsin; C) RIF-Gel-NPs with different loadings in PBS with pH 7.4; D) RIF-PBCA-NPs in buffers with different pH values. Data shown is the mean ± S.D. (n = 3).

The loading efficiency of NPs is dependent on the properties of the polymer used and the physicochemical characteristics of the drug to be incorporated into the particles. The interaction of RIF with gelatin NPs is dependent on three factors, namely, hydrogen

bonding, electrostatic interaction and hydrophobic forces (454, 455). Firstly, hydrogen bonding occurs in the presence of hydroxyl functional groups of the RIF molecule and carboxyl groups of gelatin B. Secondly, there are electrostatic interactions between molecules (namely, molecules of the gelatin B and molecules of RIF). Gelatin exhibits a net negative charge at a pH of 7.4 due to the predominance of negative $-COO^-$ functional groups which repel the partly anionic RIF at this pH (456). Therefore electrostatic repulsion may facilitate a greater extent of drug release in these solutions. Similar results were reported by Bajpai and Choubey (457). The greater solubility of RIF at pH 7.4 than that at pH 4.0 may also explain the higher dissolution rate observed from RIF-Gel-NPs at this pH. Due to the fact that the molecule exhibits two pKa values, a biphasic solubility curve is expected. The solubility of RIF has been reported as 125–127.2 mg/mL at pH 1.0–1.4 (458), 3.35 mg/mL at pH 7.4 and 0.99 mg/mL at pH 4.0 (459). However, the slowest rate of RIF release is observed at a pH of 1.2 despite its relatively high solubility at this pH. Part of the reason for this observation may be due to degradation of RIF in acid. Another possible explanation for this behaviour may be that RIF and Cl^- form an ion pair when the pH is $\leqslant$ 2.6 (459). This effect seems to play a significant role in respect of drug release in a solution of pH 1.2. Finally, hydrophobic forces might also impact drug release and it has been reported that hydrophobic forces were responsible for binding of RIF to bovine serum albumin (460). In our study, the high drug loading w/w is accompanied with slow drug

release and this might be due to the presence of hydrophobic interactions between RIF and gelatin.

3.5 In vitro release of RIF from RIF-PBCA-NPs

The release profiles of RIF released from RIF-PBCA-NPs are shown in Figure 4D. The rate of drug release is slower when compared to that observed for the gelatin NPs and this may be due to the hydrophobic interactions of RIF with the PBCA matrix leading to a slower and lower extent of drug release.

The pH dependent release of RIF from RIF-PBCA-NPs can be explained by a similar mechanism as that proposed for RIF release from RIF-Gel-NPs. At pH 1.2, RIF is able to form an ion pair with Cl^- ions, which in turn decreases the extent of drug release from PBCA NPs. The higher solubility observed at pH 7.4 compared to pH 4.0 contributes a higher drug release of RIF at this pH. In addition, the zwitterionic RIF molecule (~ 40% anionic) is repelled from the anionic PBCA matrix, which increases the drug release rate at pH 7.4.

3.6 Comparison of dialysis bag technique for release from MX-Gel-NPs and RIF-Gel-NPs

The pH dependent dissolution behaviours of MX and RIF are similar using both methods of drug release that were investigated (Figure 5A and 5B). However when the modified cylinder method was used, a much slower drug and no burst release was observed. This might be caused by the relatively smaller release area compared to dialysis bags.

Similar results were reported by Abdel-Mottaleb and Lamprecht (435). The release profiles of MX-Gel-NPs (Figure 6A) and RIF-Gel-NPs (Figure 6B) in buffers with or without trypsin using the dialysis bag technique are shown in Figure 6. It is clear that use of the dialysis bag technique does not permit differentiation between studies in which trypsin was included (forced) in the dissolution medium or not (non-forced) for MX-Gel-NPs.

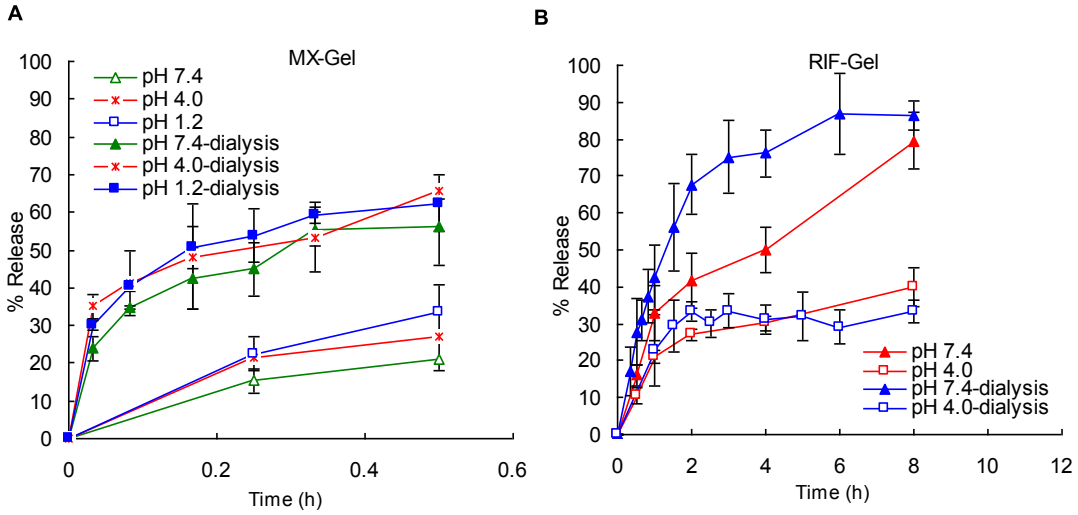

Figure 5 *In vitro* release curves of gelatin NPs using the modified cylinder method and the dialysis bag technique. A) MX-Gel-NPs; B) RIF-Gel-NPs with drug loading of 21.6% w/w.

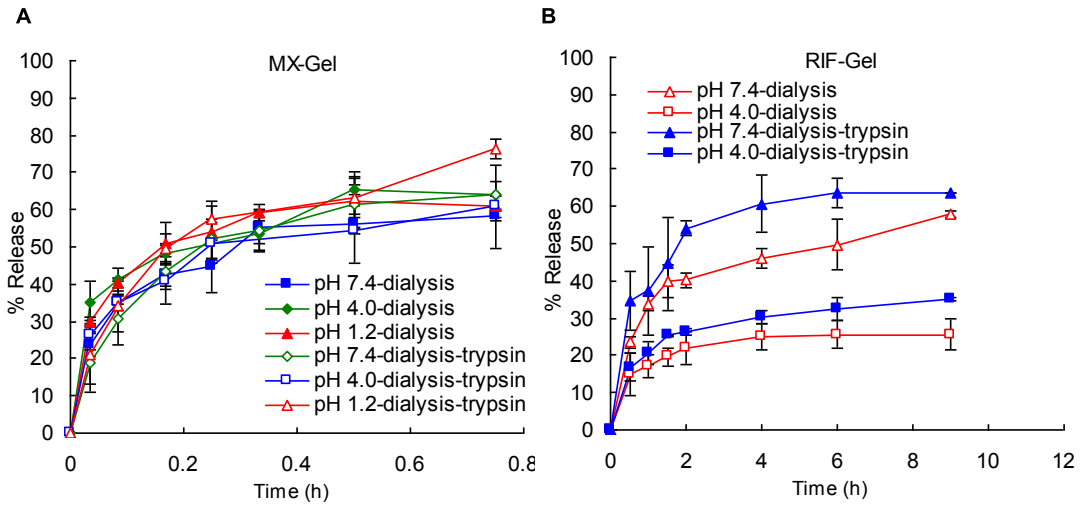

Figure 6 *In vitro* release curves of gelatin NPs in the presence and absence of trypsin. A) MX-Gel-NPs using dialysis bag; B) RIF-Gel-NPs with drug loading of 56.7% w/w. Data shown is the mean ± S.D. (n = 3).

3.7 Kinetic assessment and release mechanisms

The regression coefficients (*r*-values) generated following fitting of drug release data to the Korsmeyer-Peppas model equation are summarized in Tables 2-4 for all formulations tested. As observed in Table 2, the release data of MX-Gel-NPs without trypsin using the modified cylinder method is fitted to the Korsmeyer-Peppas equation with a Fickian release exponent (n= 0.2538–0.3640), suggesting that the drug release from the NPs occurs primarily via diffusion. The significant MX release observed in the presence of trypsin at pH 4.0 and pH 7.4 are best described by an anomalous transport mechanism (n= 0.6910–0.6918) and the release at pH 1.2 is described by a Case II transport process (n= 0.8966).

This transport is characterized by polymer relaxation due to polymer erosion when enzymatic degradation occurs (461).

The release data observed for the RIF-Gel-NPs manufactured using different drug loading fit well to the Korsmeyer-Peppas equation with an *n* value of from 0.3543 to 0.4254, which suggest that a Fickian diffusion process is predominant (Table 3). In the presence of trypsin, RIF release from RIF-Gel-NPs is best described as anomalous transport (*n*= 0.5432–0.5728) due to the erosion of the gelatin matrix by enzymatic degradation.

From above, the use of the modified cylinder method permits differentiation between the presence and absence of trypsin in the cases of the MX-Gel-NPs (Table 2) and RIF-Gel-NPs (Table 3). However, the use of the dialysis bag technique results in poor differentiation between forced and non-forced drug release studies in all the cases. The release of MX from gelatin NPs using the dialysis bag is best fitted to a Fickian diffusion model in both cases (*n*= 0.1899–0.3902) (Table 2) and there is no obvious difference in the release profiles in the presence or absence of trypsin (Figure 6A). Though the release profiles of RIF from gelatin NPs with high drug loading using dialysis bag can be differentiated in the presence or absence of trypsin for RIF-Gel-NPs (Figure 6B), their kinetics mechanism can only be described by Fickian diffusion (*n*= 0.2555–0.2994) in both cases (Table 3).

The release mechanisms of MX-PBCA-NPs and RIF-PBCA-NPs are summarized in Table 4. The release of MX-PBCA-NPs is found to be Fickian diffusion controlled (*n*=

0.1054–0.2256) for the first 10 mins after which sustained release is observed. Furthermore, the mechanism of RIF release from RIF-PBCA-NPs is best described by an anomalous transport mechanism (n= 0.4531–0.4612). This is different to the release observed for the RIF-Gel-NPs which exhibit Fickian diffusion. The different release mechanism of RIF from gelatin NPs and PBCA NPs may be due to hydrophobic interactions between the two nanocarrier matrices and RIF.

Table 2 Kinetic assessment of release data of MX-Gel-NPs in diverse buffers (Q < 0.6)

Methods	Media	Korsmeyer-Peppas	
		n [b]	R^2 [a]
Modified cylinder method	pH 7.4	0.3640	0.9956
	pH 4.0	0.2538	0.9765
	pH 1.2	0.2944	0.9631
	pH 7.4-trypsin	0.6918	0.9503
	pH 4.0-trypsin	0.6910	0.9979
	pH1.2-trypsin	0.8966	0.9780
Dialysis bag technique	pH 7.4	0.3032	0.9875
	pH 4.0	0.1899	0.9893
	pH 1.2	0.2891	0.9863
	pH 7.4-trypsin	0.3902	0.9825
	pH 4.0-trypsin	0.2678	0.9824
	pH 1.2-trypsin	0.3614	0.9122

[a] Squared correlation coefficient

Table 3 Kinetic assessment of release data of RIF-Gel-NPs in diverse buffers (Q < 0.6)

Method	Drug loading (w/w)	Media	Korsmeyer-Peppas	
			n [b]	R^2 [a]
Modified cylinder method	21.6%	pH 7.4	0.4254	0.9541
		pH 4.0	0.3543	0.9478
		pH 7.4-trypsin	0.5501	0.8854
		pH 4.0-trypsin	0.5728	0.9636
	56.7%	pH 7.4	0.3911	0.9245
		pH 7.4-trypsin	0.5432	0.9774
Dialysis bag technique	21.6%	pH 7.4	0.6764	0.9721
		pH 4.0	0.5472	0.9760
	56.7%	pH 7.4	0.2779	0.9397
		pH 4.0	0.2555	0.9842
		pH 7.4-trypsin	0.2994	0.9098
		pH 4.0-trypsin	0.2744	0.9772

[a]Squared correlation coefficient and [b] diffusional exponent

Table 4 Kinetic assessment of release data of MX-PBCA-NPs and RIF-PBCA-NPs in diverse buffers (Q < 0.6)

Model drug	Media	Korsmeyer-Peppas	
		n [b]	R^2 [a]
MX	pH 7.4	0.2256	0.9697
	pH 4.0	0.2165	0.9653
	pH 1.2	0.1054	0.8442
RIF	pH 7.4	0.4531	0.9762
	pH 4.0	0.4612	0.9510

[a]Squared correlation coefficient and [b] diffusional exponent

3.8 Advantages of the modified cylinder method

To evaluate the *in vitro* release mechanisms of pharmaceutical dosage forms, a dissolution system should operate under sink conditions and be able to discriminate release characteristics that may be a consequence of variation in formulation composition. Ideally the *in vitro* release profiles should mimic the *in vivo* release mechanisms as much as possible. The modified cylinder method described and used in our study is able to discriminate and facilitate the elucidation of the *in vitro* release mechanism of drug from NPs formulation in different media, whereas the dialysis bag technique is not useful in this respect in these cases. In addition, the standard deviation of the release data using the modified cylinder method is tighter compared to that observed for the dialysis bag technique (Figure 5A and 5B). These findings may be attributed to the constant surface area as well as constant hydrodynamic conditions that exist at the surface of the membrane used in the modified cylinder apparatus. The hydrodynamic conditions at the surface of dialysis bags might vary slightly when the bags are stirred and use of the modified cylinder in standard dissolution equipment may also be an advantage.

4 Conclusions

The drug release profiles observed for the different NP formulations manufactured in these studies exhibited different mechanisms of release. The dialysis bag technique was compared to a modified cylinder method using a standard dissolution apparatus. The use of the modified cylinder method facilitated identification of the release kinetics of the two

model drugs depending on their pH dependent solubility, electrostatic interaction with the nanocarriers and the impact of hydrophobic forces. In addition the impact of enzymatic degradation on drug release was readily observed. Use of the dialysis bag technique did not permit differentiation between forced and non-forced drug release from gelatin NPs in these cases. Though the modified cylinder method has not yet used to mimic *in vivo* conditions, it offers an alternate evaluation tool to investigate *in vitro* drug release from NPs. This approach and apparatus can be considered and used as a performance test for quality control testing of nanosized delivery systems. The utility of this new method to establish *in vitro / in vivo* relationships needs to be further investigated.

Appendix 4. Investigation of the Disintegration Behavior of Dietary Supplements in Different Beverages

This study has already been published as Jieyu Zuo, Yuan Gao, May Almukainzi, Raimar Löbenberg. Investigation of the Disintegration Behavior of Dietary Supplements in Different Beverages in Dissolution Technologies. 2013; 20(4):6-9. Reference (462)

Introduction

Disintegration is a prerequisite for dissolution of immediate-release oral dosage forms. The disintegration test is often used to determine whether tablets or capsules disintegrate within the desired time when placed into a liquid medium at given experimental conditions (463, 464). This test is a useful tool for quality control and can be a critical parameter for drug release in certain scenarios like highly soluble drugs (465, 466). However, disintegration is not a universal surrogate for dissolution as shown in the 1970s for drugs like digoxin. At that time, disintegration was the only required performance test for oral solid dosage forms. Several studies showed that tablets with similar disintegration times failed bioequivalence tests due to different dissolution behaviors of the drug (467, 468). However, these early studies showed the value of disintegration and dissolution testing.

Dietary supplements that contain a specific dietary ingredient or ingredients are designed to supplement the diet and enhance nutritional supply. Dietary supplements may include vitamins, minerals, herbs or other botanicals, amino acids, and substances such as enzymes, organ tissues, glandular tissues, metabolites, or probiotics (469).

United States Pharmacopeia (USP) General Chapter <2040> is devoted to dietary supplements, and it divides dietary supplement dosage forms into three categories: vitamin–mineral dosage forms, botanical dosage forms, and other dosage forms (463). The products used in this project included vitamin–mineral dosage forms and botanical dosage forms. The only difference between these two dosage forms is in the use or omission of

disks for the disintegration tests (463). Previous studies conducted by Almukainzi et al. (470) and Schmid et al. (471) found that the disintegration time was sensitive to the change of the disintegration apparatus conditions. Both studies contributed to the update of USP General Chapter <2040>.

Due to the variety of the excipients and the formulation procedures, different disintegration phenomena may be observed for various dietary supplements. This may lead to differences in the bioavailability of the active ingredients. However, very few comprehensive studies are available that show the bioavailability of dietary supplements linked to the biopharmaceutical properties of the dosage form. From a scientific point of view, it is clear that the contents of a dosage form can dissolve and get absorbed to be bioavailable only if it disintegrates. Therefore, disintegration is the most basic step to ensure bioavailability, but as mentioned before, it is not a universal surrogate for bioavailability.

It is well established that drugs should be taken with a glass of water, while many dietary supplements do not give any further instructions except for the units per serving. No beverage (e.g., water) is specified, and it can be assumed that any available beverage, including pop, juices, and alcoholic beverages, might be used for the administration of dietary supplement dosage forms.

The aim of this study was to investigate the impact of beverages, particularly beverages containing different concentrations of alcohol, on the disintegration time of commercially

available dietary supplements and to evaluate the effect of beverage temperature on the disintegration behaviors.

Materials and methods

Materials

This study investigated the influence of beverages on the three commercial tablets: calcium citrate (Kirkland, Lot# 398597-01, exp. 09/14), Ester-C (American Health, Lot# 306041-01, exp. 11/13), Boswellia serrata extract (The Vitamin Shoppe, Lot# 121674, exp. 05/15), and cinnamon extract (The Vitamin Shoppe, Lot# 108010, exp. 08/13).

Media

All tests were performed with six test beverages including alcoholic beverages, regular Pepsi-Cola, and orange juice (Minute Maid) compared with water, which is the USP reference medium for tablets. The alcoholic beverages were prepared by diluting 95% ethanol to different concentrations (40%, 20%, 10%, and 5%) to mimic commercial spirits (liquor, wine, and beer). The tests were performed in 750 mL of the various liquids with six units.

Methods

A disintegration tester (model ED-2 L, Electrolab, Betatek, Ontario) was used with Apparatus A without disks for botanical tablets smaller than 18 mm and Apparatus B with disks for vitamin–mineral tablets larger than 18 mm (464). Beakers (1000 mL) with an inside diameter of 102 ± 0.5 mm (PYREX, No. 1003) were used, satisfying the USP beaker

specification for disintegration in Chapter <701>, which states that the inside diameter of beakers should range from 97 to 115 mm when assessing the effects of media on the disintegration time of dosage forms. The evaluated beverage temperatures were 37 ± 2 °C (USP) and 5 ± 1 °C (simulating a refrigerated beverage) with a bath temperature at 37 ± 2 °C.

Statistical Analysis

Individual disintegration times were noted and reported as the mean ± SD. Minitab was used to perform the statistical analysis. The Bartlett test (normal distribution) was used to test the data that were normally distributed for equal variance. When the conditions of normality and equal variance were met, a one-way ANOVA with an α-level of 0.05 was used for the group data analysis. For data with unequal variance, the Kruskal–Wallis rank-sum test was chosen. The independent t-test and Mann–Whitney test were used for two-group data analyses with normally distributed data and data with unequal variance, respectively. The statistical tests were conducted between different immersion media or different temperatures in the same immersion medium.

Results

The study investigated four tablet formulations of dietary supplements: calcium citrate, Ester-C, Boswellia serrata, and cinnamon extract.

The disintegration times of calcium citrate in different buffers at different temperatures are shown in Figure 1A. Both the beverages and the low temperature delayed the disintegration

time of the calcium citrate. The mean disintegration times of calcium citrate in different buffers ranged from 1.6 ± 0.2 to 6.0 ± 0.8 min versus 1.4 ± 0.2 min in water at 37 °C ($p < 0.05$) with the exception of 5% alcohol ($p = 0.092$). Additionally, low temperature at 5 °C delayed the mean disintegration times of calcium citrate in all buffers ($p < 0.05$).

The disintegration of the Ester-C tablets differed from that of the calcium citrate tablets. As shown in Figure1B, the mean disintegration times of the Ester-C tablets ranged from 27.6 ± 2.1 min in cola to 49.8 ± 6.4 min in 40% alcohol (Figure 1B) compared with 23.4 ± 1.5 min in water. The disintegration time was significantly influenced by the test beverages at the same temperature, with the exception of 5% alcohol at 37 °C ($p = 0.6889$). In addition, although temperature had no significant effect on the Ester-C disintegration time in water ($p = 0.0927$), orange juice ($p = 0.2298$), and 40% alcohol ($p = 0.1735$), it did significantly affect the disintegration time in the remaining beverages ($p < 0.05$).

Figure 1C shows the disintegration time of cinnamon tablets in different buffers at different temperatures. Orange juice (93.8 ± 7.3 min), cola (72.9 ± 1.3 min), and 40% alcohol (70.6 ± 7.8 min) significantly affected the disintegration time of cinnamon tablets when compared with water (58.4 ± 6.8 min) at 37 °C, while the other test beverages (5%, 10%, and 20% alcohol) had no significant impact on the disintegration time ($p > 0.05$). In addition, temperature did not influence the disintegration time of cinnamon tablets in the beverages with the exception of cola and 10% alcohol ($p < 0.05$).

The Boswellia serrata extract tablets did not disintegrate during the 3-h testing period in any of the tested media including water at different temperatures.

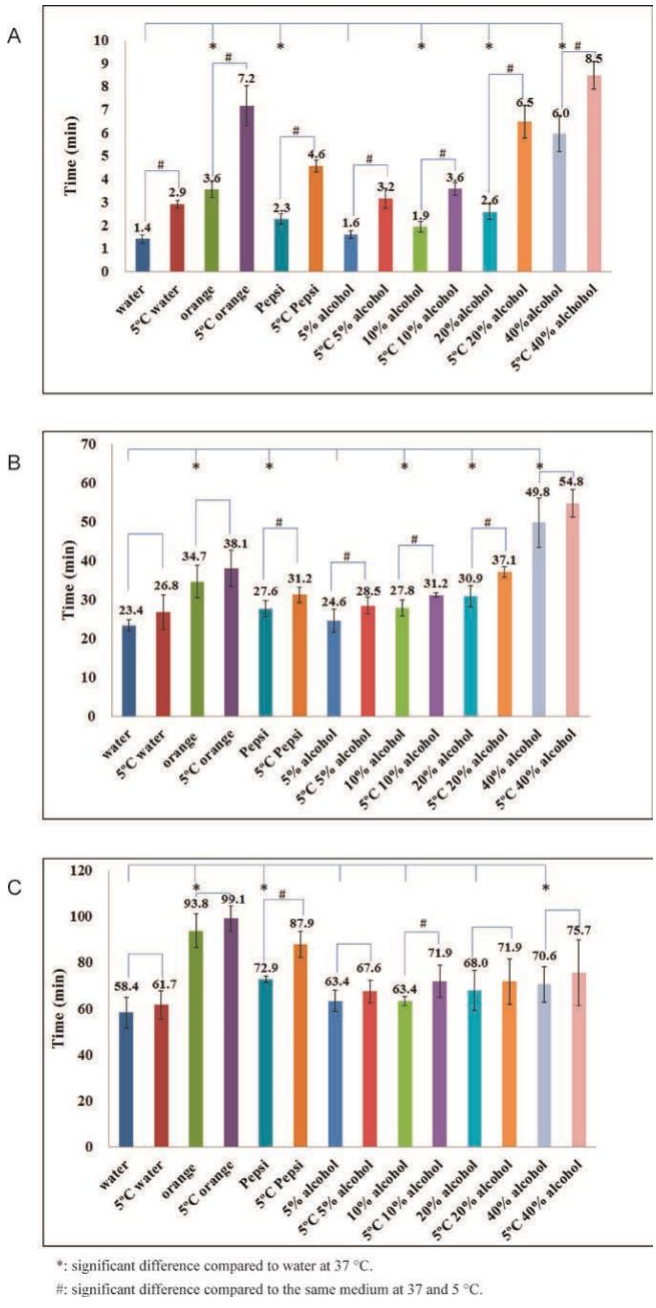

Figure 1. Disintegration times for (A) calcium citrate, (B) Ester C, and (C) cinnamon extract in beverages and water at different temperatures (n = 6).

Discussion

Dietary supplements are regulated differently in different regions of the world. For instance, they are regulated as Natural Health Products (NHP) in Canada, and disintegration is the only required performance test according to the Natural Health Product Regulation for immediate- release dosage forms (472). Dietary supplements are regulated as foods in the United States, and the FDA guidance does not require performance testing (473). The use of dietary supplements has increased over the years. In the United States, 49% of the population ingests a dietary supplement on a daily basis (474), while 73% of Canadians regularly take NHPs according to a survey in 2010 (475).

Previous studies showed that the disintegration test can be a valuable performance test for oral dosage forms (467); however, the apparatus setup and the volume of the immersion medium must be considered because they impact the test results (470, 471). It is further well established that oral solid dosage forms of drugs should be taken with 250 mL of water (476). However, a study showed that most patients do not follow this recommendation when they take medications such as capsules and tablets. A study by Fuchs (477) showed that the average water intake for oral drug administration is 115 mL; 15.4 % of patients took less than 60 mL, 20.6% between 61 and 100 mL, and the remaining 64% more than 101 mL. This behavior indicates poor compliance of patients with the recommendation of 250 mL for oral drug administration. Extrapolating the lack of compliance to dietary supplements raises the question of what impact the nature of the beverage might have on the disintegration of dietary supplements taken as dosage forms. To our best knowledge,

no data is available to answer this question. Therefore, the study investigated different popular beverages and their impact on the disintegration behavior of dietary supplements. Mechanistically, the first step of the disintegration process is water uptake. A good correlation between the penetration rate of a fluid into a tablet and the disintegration time results from viscosity, contact angle, and surface tension as described by Anwar et al. (478). This relationship can be explained by the Washburn equation (479), which is $v^2 = r\gamma \cos\theta t$, where v is the volume of liquid penetrating 2η at time t, γ is the surface tension, θ is the contact angle, η is the viscosity, and r is the capillary radius. Increasing media viscosity has been shown to cause a profound delay of drug disintegration time (478). Radwan et al. (480), Chuong et al. (481,482), and Kalantzi et al. (483) have shown that product disintegration is delayed in milk. The penetration rates for milk are also slow, which may be a reflection of its relatively high viscosity and low surface tension (478). The viscosity of orange juice is 4.9 MPa·s, whereas the viscosity of water is 1.0 MPa·s at 20 °C (284). At 25 °C, the viscosities of ethanol and water are 1.074 and 0.89 MPa·s, respectively (485). However, for most liquids, viscosity increases with decreasing temperature (485). Therefore, the delay in the disintegration time caused by the test beverages in our study may be associated with those factors.

Although the impact of the beverages on the disintegration time of tablets that disintegrate in a short time was statistically significant, these results may not have a major clinical impact because their disintegration times were less than 15 min, which is the average

gastric emptying time when fluid is taken with a dosage form in the absence of food (486). However, for tablets that disintegrate slowly, the results may have clinical relevance because of a significant increase in disintegration time (up to 35.4 min), which was observed between water and other beverages. While this study did not investigate bioavailability, it is obvious that a delay in disintegration will result in a delayed dissolution and absorption and consequently will affect bioavailability.

This study only focused on the effect of the beverages on the disintegration time of the dietary supplements.

Conclusion

Disintegration is the most basic process that is required for the release of the contents of a dosage form into the body. The results of this study suggest that water may be the best beverage to be used for the administration of dietary supplements and that cola, orange juice, and high alcoholic beverages should be avoided due to their impact on the disintegration of dosage forms. The increasing use of dietary supplements and their different regulatory status in different regions of the world make it necessary to implement appropriate performance testing for these products. However, further studies on the interaction between beverages and dietary supplement are warranted.